

GUIDEBOOK 1

**GUIDEBOOK TO PERMAFROST AND QUATERNARY GEOLOGY
ALONG THE RICHARDSON AND GLENN HIGHWAYS
BETWEEN FAIRBANKS AND ANCHORAGE, ALASKA**

Edited by

T.L. Péwé
Arizona State University

and

R.D. Reger
Alaska Division of Geological & Geophysical Surveys

First Edition 1983
Reprinted Edition 1993

Fourth International Conference on Permafrost
July 18-22, 1983
University of Alaska
Fairbanks, Alaska, U.S.A.

Cover photo: Oblique aerial view southwest of Trident Glacier in the northcentral Alaska Range, Mt. Hayes Quadrangle, Alaska. Photograph 512RT-55RT-M864-55SRW-9M58 by U.S. Air Force, August 29, 1949.



STATE OF ALASKA
Walter J. Hickel, *Governor*

DEPARTMENT OF NATURAL RESOURCES
Glenn A. Olds, *Commissioner*

DIVISION OF GEOLOGICAL & GEOPHYSICAL SURVEYS
Thomas E. Smith, *State Geologist*

Address mail orders to the Fairbanks office. DGGs publications may be inspected at the following locations.

Alaska Division of Geological & Geophysical Surveys
794 University Avenue, Suite 200
Fairbanks, Alaska 99709-3645

Department of Natural Resources
Public Information Center
3601 C Street, Suite 200
Anchorage, Alaska 99110

This publication, released by the Division of Geological & Geophysical Surveys, was produced and printed in Fairbanks, Alaska, by Graphics North Printing Co. at a cost of \$12 per copy. Publication is required by Alaska Statute 41, "to determine the potential of Alaskan land for production of metals, minerals, fuels, and geothermal resources; the location and supplies of groundwater and construction materials; the potential geologic hazards to buildings, roads, bridges, and other installations and structures; and shall conduct such other surveys and investigations as will advance knowledge of the geology of Alaska."

FOREWORD

This document inaugurated a new series of publications by the State of Alaska Division of Geological & Geophysical Surveys (DGGS) and was the first in a collection of international guidebooks that describes outstanding localities in diverse regions of northwestern North America. The series includes not only guides to Alaska, but also descriptions of routes and sites in neighboring Canada. These guidebooks represent the cooperative efforts of scientists from the United States and Canada who have labored hard—in some cases for several years—to compile and field check guidebook information, organize it into a logical sequence, and prepare comprehensive manuscripts.

The stimulus for this series was the Fourth International Conference on Permafrost, which was held in Fairbanks during July 1983. It was especially fitting that this gathering of internationally known scientists and engineers specializing in frozen-ground phenomena was held in Fairbanks, near the center of the zone of discontinuous permafrost in Alaska. The Fairbanks area is an outstanding natural laboratory that invites inquiry and research on many aspects of the subarctic environment, but especially on permafrost. High points of the conference were the field trips, during which visitors saw many excellent examples of problems and features related to frozen ground.

DGGS was pleased to support the Fourth International Conference on Permafrost by sponsoring publication of these field guides. The wealth of information they provide should enrich the experience of all who have travelled so far to visit the areas described.

Because of the widespread popularity of Guidebook 1, DGGS stocks have been depleted in the past 10 years. Since numerous requests continue to be received, we have decided to reprint the 1983 report.

*Thomas E. Smith
State Geologist*

CONTENTS

	<u>Page</u>
Introduction.....	1
General statement.....	1
Organization and acknowledgments.....	1
Selected references.....	3
Middle Tanana River valley.....	5
Résumé of the permafrost and Quaternary geology.....	5
Road log and locality descriptions.....	12
Selected references.....	42
Delta River area, Alaska Range.....	47
Résumé of the permafrost and Quaternary geology.....	47
Road log and locality description.....	50
Trans-Alaska Pipeline System.....	67
Thawing problems.....	67
Construction modes.....	69
Conventional burial.....	71
Special burial.....	71
Conventional elevated and anchor support.....	72
Selected references.....	130
Copper River basin.....	137
Résumé of Quaternary geology.....	137
Road log and locality description.....	139
Gakona section.....	150
Richardson Highway.....	152
Simpson Hill roadcut.....	153
Copper River Bluff section.....	155
Glenn Highway.....	160
Selected references.....	172
Overview of the Matanuska Glacier.....	177
Selected references.....	182
Upper Cook Inlet region and the Matanuska Valley.....	185
Introduction.....	185
Physiography and geology.....	185
Upper Cook Inlet region.....	185
Matanuska Valley.....	185
Climate.....	187
Vegetation.....	189
Soils.....	189
Résumé of Quaternary geology.....	190
General statement.....	190
Late Pliocene-early Pleistocene glaciations and inter- glaciations.....	190
Mt. Susitna Glaciation.....	191
Mt. Susitna-Caribou Hills interglaciation.....	191
Caribou Hills Glaciation.....	191
Late Pleistocene glaciations and interglaciations.....	194
Caribou Hills-Eklutna interglaciation.....	194
Eklutna Glaciation.....	194
Eklutna-Knik interglaciation.....	195

	<u>Page</u>
Knik Glaciation.....	195
Knik-Naptowne nonglacial interval.....	198
Naptowne Glaciation.....	198
Early Holocene Glaciations.....	204
Middle to Late Holocene events.....	204
Alaskan Glaciation.....	204
Tustumena advances.....	205
Tunnel advances.....	205
Other events.....	205
Road log and locality descriptions.....	206
Selected references.....	252
Appendix A - Radiocarbon dates related to late Quaternary events in the Upper Cook Inlet region, Alaska.....	261

FIGURES

Figure 1. Index map showing field-trip route from Fairbanks to Anchorage.....	2
2. Index map of the middle Tanana River valley showing field-trip stops.....	6
3. Generalized permafrost map of the Fairbanks area.....	8
4. Schematic composite cross section of stratigraphic relationships of Quaternary deposits in creek valley near Fairbanks.....	9
5. Map showing distribution of ice wedges and permafrost in Alaska and field-trip route.....	10
6. Index to U.S. Geological Survey topographic maps (1:63,360) used with road log.....	13
7. Map of the Chena River Lakes Flood Diversion Project, showing levee, dam, and floodway.....	14
8. Oblique aerial view of the flooding Chena River, August 15, 1967, at Fairbanks.....	15
9. Aerial photograph of the Tanana River flood plain and former drainage channels near Eielson Air Force Base...	16
10. Sketch map of Harding Lake and vicinity.....	19
11. Bathymetric map of Harding Lake.....	21
12. Schematic drawing of bottom profiles of Birch and Harding Lakes.....	22
13. Sketch map of Birch Lake and vicinity.....	24
14. Oblique aerial view of Birch Lake and the Yukon-Tanana Upland.....	25
15. Sketch of longitudinal (centerline) profile of peat test section and amounts of settlement after 4 yr (1973-1977), Mile 300.7, Richardson Highway.....	26
16. Sketch of the view from Shaw Creek bluff of the Alaska Range, glacial moraines, and the broad, braided Tanana River.....	31
17. Map showing the distribution and types of eolian deposits in the Big Delta area in relation to the Delta Glaciation.....	34

	<u>Page</u>
18. Map showing the distribution and types of eolian deposits in the Big Delta area in relation to the Donnelly Glaciation.....	35
19. Photograph of stabilized sand-dune complex north of Shaw Creek Flats between Rosa and Keystone Creeks, Big Delta B-5 Quadrangle.....	36
20. Photograph of roadcut that exposes loess, eolian sand, ventifacts, and solifluction deposits over bedrock, Shaw Creek bluff.....	37
21. Sketch of exposure of a solifluction layer with ice-wedge casts of sand overlain by an extensive ventifact layer in a borrow pit at Mile 0.6 (1 km) on Shaw Creek Road.....	38
22A. Photograph of exposure of ice-shoved rampart on the southwest side of Quartz Lake.....	41
22B. Photograph of sand-blasted, faceted, and grooved cobbles of rock types from the Alaska Range in glacial outwash from ice-shoved ridge on the southwest side of Quartz Lake.....	42
23. Photograph of Bert and Mary's Roadhouse, Richardson Highway.....	43
24. Photograph of elevated crossing of the Tanana River by the Trans-Alaska Pipeline System, Big Delta A-4 Quadrangle.....	44
25. Index map of the Delta River area, Alaska Range, showing field-trip stops.....	48
26. Oblique aerial view of Gillam Glacier, Hess Mountain, and Mount Deborah, north-central Alaska Range, Healy Quadrangle.....	49
27. Photograph of an elongate sand dune (late Donnelly age) covered with a forest of white spruce.....	50
28. Photograph of the Alaska Range, with Donnelly Dome in the middle ground and Donnelly-age outwash plain in the foreground.....	52
29. Diagrammatic cross section of probable permafrost and ground-water distribution in the Big Delta area.....	53
30. Photograph of the northeast flank of the central Alaska Range from the FAA station along the Richardson Highway.....	55
31. Oblique aerial view of clouds of silt transported by wind from the Delta River flood plain near Donnelly Dome....	56
32. Oblique aerial view of the outwash plains and moraines of Donnelly age near Donnelly Dome, with the Delta River and Alaska Range in the distance.....	58
33. Comparison of glacial chronologies in the east-central Alaska Range and vicinity.....	60
34. Photograph of deeply weathered granite boulders on Delta-age moraine 1 mi (1.6 km) north of Donnelly Dome and 1 mi (1.6 km) west of Mile 250 on the Richardson Highway.....	61
35. Oblique aerial view of large-scale patterned ground in outwash gravel in the Donnelly Dome area.....	63

	<u>Page</u>
36. Plane-table map of large-scale polygons, Donnelly Dome area.....	64
37. Diagrammatic sketch of ice-wedge cast, Donnelly Dome area...	65
38. Infrared photograph of surface of Donnelly moraine looking north from Mile 244 on the Richardson Highway.....	68
39. Oblique aerial view of Mt. Hayes in the Alaska Range, with the Delta River in the distance.....	69
40. Index map of Alaska indicating route of the Trans-Alaska Pipeline System.....	70
41. Diagrammatic sketch of different construction modes used in construction of the Trans-Alaska Pipeline System....	71
42. Photograph of the refrigerated crossing beneath the Richardson Highway by the Trans-Alaska Pipeline System at Mile 243.5, Richardson Highway, Mt. Hayes D-4 Quadrangle.....	73
43. Landform map of part of the Delta River valley in the vicinity of the Yardang Site, central Alaska Range.....	75
44. Stratigraphy of the Yardang Site (Mt. Hayes 252), Mile 243.8, Richardson Highway, central Alaska Range.....	76
45. Photograph of the Richardson Highway under construction (1951) at Mile 231.8, looking southwest up the Darling Creek alluvial fan.....	78
46. Photograph of the Delta River and terminus of the Black Rapids Glacier.....	79
47. Photographs of the terminus of Black Rapids Glacier in 1937 and 1951.....	81
48. Photograph of Hidden Lake on the east side of the Delta River valley near Black Rapids Glacier, Mt. Hayes C-4 Quadrangle.....	83
49. Photograph of reddish-yellow pod of remolded outwash incorporated into till of the earliest known Holocene advance of Black Rapids Glacier, Mile 226.7, Richardson Highway.....	84
50. Landform map of Holocene glacial deposits at the terminus of Black Rapids Glacier, central Alaska Range.....	87
51. Index map of the central Alaska Range showing major glaciers in the vicinity of the Richardson Highway.....	88
52. Comparison of <u>Rhizocarpon geographicum</u> growth curves initially developed for the central Alaska Range by Reger and Péwe and for the St. Elias Mountains by Denton and Karlén.....	89
53. Map showing relationship of maximum-diameter <u>Rhizocarpon geographicum</u> thalli to Holocene moraines of Black Rapids Glacier, central Alaska Range.....	91
54. Oblique aerial view of the Richardson Highway, the TAPS Route, and the termini of Canwell and Castner Glaciers in the central Alaska Range.....	92
55. Map showing relation of major faults in Alaska to the TAPS route, Richardson and Glenn Highways, and Stop 16.....	94

	<u>Page</u>
56. Oblique aerial view along the trace of the McKinley strand of the Denali fault in the drainage of Augustana Creek between the Delta River and Black Rapids Glacier, Mt. Hayes B-4 Quadrangle.....	95
57. Photograph of the special-design crossing of the Denali fault zone by the Trans-Alaska Pipeline System, Mt. Hayes B-4 Quadrangle.....	96
58. Map showing relationship of maximum-diameter <u>Rhizocarpon geographicum</u> thalli to Holocene moraines of Canwell Glacier, central Alaska Range.....	97
59. Oblique aerial view of the Rainbow Mountain area near the crest of the Alaska Range, Mt. Hayes B-4 Quadrangle....	99
60. Photograph of an active rock glacier on the west flank of Rainbow Mountain from Mile 206.8 on the Richardson Highway in the upper Delta River area.....	100
61. Block diagram of the Gulkana-College Glaciers area, south-central Alaska Range.....	103
62. Map of Gulkana Glacier, central Alaska Range, showing accumulation and ablation areas, principal ice streams and icefalls, transverse profiles along which motion and ice-thickness surveys were made, and 1960 and 1961 firn lines.....	104
63. Comparison of ice balance-altitude curves for Gulkana Glacier and other representative Alaskan glaciers.....	105
64. Yearly surface velocity (1960-61) and subsurface topography of Gulkana Glacier, central Alaska Range.....	106
65. Map showing approximate variations of Holocene terminal positions of Gulkana and College Glaciers relative to their 1962 termini.....	107
66. Map showing relationship of maximum-diameter <u>Rhizocarpon geographicum</u> size ranges to Holocene moraines and 1962 ice limits of Gulkana and College Glaciers, central Alaska Range.....	108
67. Photographs of the terminal zone of Gulkana Glacier in 1910 and 1952.....	111
68. Photograph from Summit Lake of the snow-covered south-central Alaska Range and Gulkana Glacier.....	112
69. Map of glacial deposits in the headwaters area of the Delta River, Amphitheater Mountains.....	113
70. Oblique aerial view of Round and Long Tangle Lakes and Sugarloaf Mountain with ice-stagnation deposits in the foreground, Mt. Hayes A-5 Quadrangle.....	116
71. Physiographic diagram of the Mt. Hayes A-5 Quadrangle.....	118
72. Oblique aerial view of Whistler Ridge cryoplanation-terrace site and the Denali Highway, Mt. Hayes A-5 Quadrangle.....	121
73. Map of the bedrock and surficial geology in the vicinity of the Phalarope Lake and Whistler Ridge cryoplanation study sites.....	122

	<u>Page</u>
74. Plane-table map and topographic profile of the Whistler Ridge cryoplanation-terrace site, Mile 29.5, Denali Highway, Mt. Hayes A-5 Quadrangle.....	124
75. Photograph of frost-sorted stone rings in till of late Wisconsinan age, Mile 32.2, Denali Highway.....	127
76. Plane-table map and topographic profile of the Phalarope Lake cryoplanation-terrace site, Mile 35, Denali Highway, Mt. Hayes A-5 Quadrangle.....	128
77. Photograph of palsa sectioned during construction of the Denali Highway in the Maclaren River valley, Mt. Hayes A-5 Quadrangle.....	129
78. Index map of the Copper River basin showing field-trip stops.....	138
79. Photograph of shore of a typical thaw (thermokarst) lake about 40 mi (64 km) northwest of Glennallen, Alaska....	139
80. Photograph from Mile 179.7, Richardson Highway, with Paxson Mountain in the background.....	141
81. Photograph from Mile 171.5, Richardson Highway, of drainage of proglacial stream from a glacier occupying Paxson Lake trough during Wisconsinan time.....	142
82. Photograph of well-developed gravel terraces of Wisconsinan age at north end of Meier Lake.....	143
83. Oblique aerial view showing Meier Lake, the Richardson Highway, and frost-rived blocks of granite on hill in foreground.....	144
84. Photograph from Mile 155.4, Richardson Highway, of the snow-covered Wrangell Mountains and the floor of the Copper River basin.....	145
85. Photograph of access road at Mile 147.5, Richardson Highway, showing severe differential settlement caused by disturbing the ground surface and the resultant thawing of the underlying ice-rich permafrost.....	147
86. Cross section of permafrost table and geology at Mile 130, Richardson Highway.....	149
87. Generalized stratigraphic section of Pleistocene deposits in the east-central part of the Copper River basin.....	151
88. Map showing the location of mud volcanoes and mineral springs in the southeastern Copper River basin.....	153
89. Photograph of Lower Klawasi Mud Volcano.....	154
90. Comparison of certain physical characteristics of mud volcanoes in the Copper River basin.....	155
91. Photograph of slump block of fine-grained highway fill material at Simpson Hill, near Mile 112 on the Richardson Highway.....	159
92. Photograph of abandoned roadcut on Simpson Hill showing successive slumps that destroyed the old road surface..	160
93. Photograph of Simpson Hill near Mile 112, Richardson Highway, showing new roadcut and site of old roadcut where serious slumping problems occurred.....	161

	<u>Page</u>
94. Photograph of high bluff exposing thick section of Pleistocene deposits on west side of the Copper River near Mile 112.5, Richardson Highway.....	162
95. Photograph of the Trans-Alaska Pipeline elevated above the ground on steel vertical-support members (VSMs) to prevent thawing of the underlying ice-rich permafrost..	163
96. Diagrammatic sketch of piling- and cable-installation plan for Alaska Department of Highway apartment house at Glennallen.....	164
97. Photograph of schoolhouse in Glennallen built in 1952-53 on ice-rich permafrost.....	165
98. Index map of the upper Matanuska Valley and Nelchina River area showing field-trip stops.....	169
99. Oblique aerial photograph on the Glenn Highway west from Mile 109.5 to 105 showing the Matanuska River flowing west past the mouth of Caribou Creek to Lion Head, beyond which it flows along the terminus of the Matanuska Glacier.....	173
100. Oblique aerial photograph of the terminus of the Matanuska Glacier.....	178
101. Map of the Matanuska Glacier and vicinity.....	179
102. Vertical aerial photograph of part of the western terminus of the Matanuska Glacier.....	180
103. Sketch of the spatial distribution of depositional processes in relation to the ice-margin position and topographic slope, where the ice-cored moraine slopes toward the active ice.....	182
104. Sketch of the spatial distribution of depositional processes in relation to the ice-margin position and topographic slope, where the ice-cored moraine slopes away from the active ice.....	183
105. Map showing the major physiographic subdivisions of south-central Alaska relative to the field-trip route.....	186
106. Tentative comparison of late Quaternary glacial chronologies in the upper Cook Inlet region with other areas in southern Alaska.....	193
107. Sketch map of the present terminus of Matanuska Glacier and vicinity showing former terminal positions.....	207
108. Oblique aerial view of Pinochle Creek and Pinochle Creek spillway, Anchorage D-3 Quadrangle.....	208
109. Oblique photograph of the middle Matanuska Valley showing bedrock ridges differentially scoured by glaciation, Anchorage Quadrangle.....	211
110. Aerial photograph of Castle Mountain, Anchorage D-4 and D-5 Quadrangles.....	214
111. Oblique aerial photograph of the Granite Creek fan, Anchorage Quadrangle.....	216
112. Oblique aerial photograph of the high-level outwash terrace and esker complex west of Moose Creek, Anchorage C-6 Quadrangle.....	220

	<u>Page</u>
113. Sketch of stratigraphic sections of eolian deposits in the Palmer area.....	221
114. Isopach map of the eolian silt and sand blanket in the Palmer area.....	222
115. Map showing percentage of sand in eolian deposits of the Palmer area.....	223
116. Isopach map of loess in the vicinity of Palmer.....	225
117. Map showing percentage of clay in loess in the vicinity of Palmer.....	226
118. Map showing variation in the sorting coefficient for loess in the vicinity of Palmer.....	227
119. Oblique aerial photograph of the Palmer area on a calm day when no loess is deflating from flood plain of the Knik River, Anchorage Quadrangle.....	228
120. Oblique aerial view of loess being deflated by the 'Knik wind' from the Knik River flood plain, Anchorage Quadrangle.....	229
121. Oblique aerial photograph of large gravel-extraction operations in pitted 'Palmer terrace' near McLeod Lake, Anchorage C-6 SW Quadrangle.....	232
122. Oblique aerial photograph of the esker and crevasse-fill-ridge complex west of Palmer, Anchorage Quadrangle.....	233
123. Oblique aerial photograph of gravel-mining operation in the crevasse-fill-ridge complex near Canoe and Irene Lakes, Anchorage C-6 SW Quadrangle.....	234
124. Photograph of cross sections through crevasse filling of late Elmendorf (Naptowne) age, Anchorage C-7 SE Quadrangle.....	235
125. Aerial photograph of the Twin Peaks area, western Chugach Mountains front, Anchorage B-6 Quadrangle showing highest levels of Eklutna, Knik, and Naptowne Glaciations.....	240
126. Illustration of a representative electric cone-penetration test (CPT) through sediments at Stop 37.....	241
127. Map showing the location of former Lake George, Knik Glacier, and the Knik River relative to Stop 37.....	242
128. Map showing annual outburst cycle of Lake George from 1918 through 1966, except 1963.....	243
129. Bar graph showing maximum daily average discharge for outburst and nonoutburst floods of the Knik River prior to 1967.....	244
130. Oblique aerial photograph of high-level surface (west of Mount Eklutna) glaciated in Caribou Hills time, Anchorage B-7 Quadrangle.....	246

TABLES

Table 1. Physical properties of eolian sand exposed at Shaw Creek Flats and near Shaw Creek bluff, central Alaska.....	40
2. Rates of deposition of Holocene loess along rivers in central Alaska.....	57

	<u>Page</u>
3. Comparison of physiographic and sedimentologic parameters of Delta- and Donnelly-age moraines in the type area.....	59
4. Results of tree-ring counts on cores collected in 1951 from trees growing on Holocene moraines and outwash surfaces of Black Rapids Glacier.....	86
5. Mean values for physical parameters of engineering-geologic facies in the Bootlegger Cove Formation, Government Hill area, Anchorage, Alaska, based on analyses of several hundred samples.....	251

PLATE
[In pocket]

Plate 1. Physiographic map and field-trip localities of the Upper Cook Inlet area, Alaska

GUIDEBOOK TO PERMAFROST AND QUATERNARY GEOLOGY
ALONG THE RICHARDSON AND GLENN HIGHWAYS
BETWEEN FAIRBANKS AND ANCHORAGE, ALASKA

Edited by
Troy L. Pêwè¹ and Richard D. Reger²

INTRODUCTION

General Statement

Permafrost and marine, fluvial, lacustrine, glacial, eolian, and periglacial deposits of Quaternary age that are widespread in the central and southern parts of Alaska are forming today. Glaciers are common in mountainous areas, and the forces of glacial action that formerly shaped much of the world's land area can be directly observed today in southern Alaska. Geological processes active in cold regions---periglacial processes such as solifluction, cryoplanation, and the formation of permafrost---are known throughout much of the area. Dust is blown from active valley trains and outwash fans and is deposited as loess on the adjacent terrain.

Five major areas are considered (fig. 1): a) the middle Tanana River valley, b) the Delta River area of the Alaska Range, including the eastern Denali Highway, c) the Copper River basin, d) the Matanuska Glacier, and e) the upper Cook Inlet region and Matanuska Valley. The middle Tanana River valley is typical of the unglaciated interior of Alaska, with its extensive eolian deposits, widespread perennially frozen ground, and silt-choked glacial streams near major moraines.

The Delta River area of the Alaska Range and the Denali Highway are characterized by numerous glaciers and deposits that record more extensive glaciation in the past. The Copper River basin has an interesting record of alternating glacial and lacustrine deposits. Lake deposits are perennially frozen and present serious problems to utilization by man. In the upper Cook Inlet region and Matanuska Valley---including the Matanuska Glacier---extensive evidence of multiple glaciation and numerous landslides generated by the Good Friday Earthquake of March 27, 1964, are present. The Trans-Alaska Pipeline System parallels the highway for 300 mi (483 km) through the three northernmost areas covered by this guidebook.

Organization and Acknowledgments

This guidebook is an updated, enlarged, and better-illustrated version of the 1965 'Central and South-central Alaska Guidebook F' for the Seventh INQUA Conference. The organizer of the two field trips and editor of the earlier guidebook is T.L. Pêwè. Pêwè and R.D. Reger are responsible for sections of this guidebook dealing with the middle Tanana River valley and the Delta River area of the Alaska Range. L.A. Viereck, Research Botanist, Northern Forest Experiment Station, U.S. Forest Service, University of Alaska (Fairbanks), contributed all discussions of vegetation north of the Alaska Range.

¹Department of Geology; Arizona State University; Tempe, Arizona 85281.

²DGGS, 794 University Avenue, Suite 200, Fairbanks, Alaska 99709-3646.

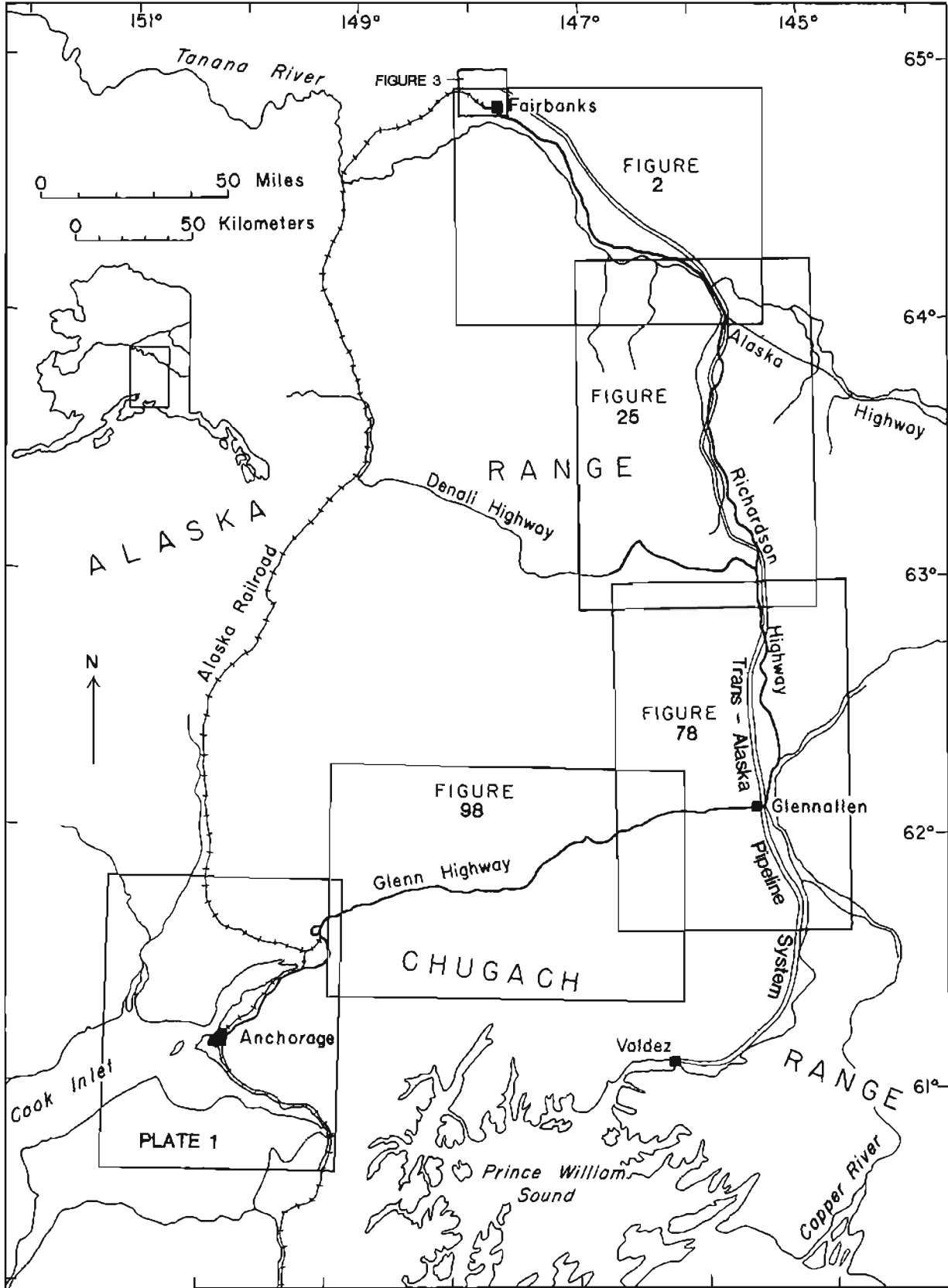


Figure 1. Index map showing field-trip route from Fairbanks to Anchorage.

The section on the Copper River basin is updated by the original authors, O.J. Ferrians, Jr., D.R. Nichols, and J.R. Williams. D.E. Lawson prepared the section dealing with the Matanuska Glacier.

The section on the upper Cook Inlet region and Matanuska Valley (by R.D. Reger and R.G. Updike) is considerably recast from the 1965 edition. J.R. Williams provided a very helpful review of this section.

D.R. Reger reviewed all sections related to archeology and offered extremely helpful comments. He and C.E. Holmes provided unpublished information on the 1977 collection of artifacts from Ruby Creek (Yardang Site).

James C. Walters provided recent information on frost-sorted features in the vicinity of the Denali Highway.

The authors appreciate the efficient cartographic support provided by Susan Selkirk (Arizona State University), Duncan Hickmott (DGGs), Dave Vogel (DGGs), and Karen Pearson (DGGs). Cheri Daniels (DGGs) edited the guidebook.

References used in compiling résumés and road logs are listed in the general bibliography and in bibliographies at the end of individual sections. References are generally not inserted in the text, except where controversial points are discussed.

All radiocarbon dates are given in years before present (B.P.) with appropriate laboratory numbers.

Selected References

- Burrows, R.L., Emmett, W.W., and Parks, Bruce, 1981, Sediment transport in the Tanana River near Fairbanks, Alaska, 1977-1979: U.S. Geological Survey Water Resources Investigations Report 81-20, 56 p.
- Coulter, H.W., Hopkins, D.M., Karlstrom, T.N.V., Péwé, T.L., Wahrhaftig, Clyde, and Williams, J.R., 1965, Extent of glaciations in Alaska: U.S. Geological Survey Miscellaneous Geologic Investigations Map I-415, scale 1:2,500,000, 1 sheet.
- Hopkins, D.M., Karlstrom, T.N.V., and others, 1955, Permafrost and ground water in Alaska: U.S. Geological Survey Professional Paper 264-F, p. 113-146.
- Johnson, P.R., and Hartman, C.W., 1969, Environmental atlas of Alaska: Fairbanks, University of Alaska Institute of Water Resources, 111 p.
- Karlstrom, T.N.V., and others, 1964, Surficial geology of Alaska: U.S. Geological Survey Miscellaneous Geologic Investigations Map I-357, scale 1:1,584,000, 1 sheet.
- Lutz, R.J., 1956, Ecological effects of forest fires in the interior of Alaska: U.S. Forest Service Technical Bulletin 133, 121 p.
- Matthews, J.V., Jr., 1970, Quaternary environmental history of interior Alaska: Pollen samples from organic colluvium and peats: Arctic and Alpine Research, v. 2, no. 4, p. 241-251.
- _____, 1974, Wisconsin environment of interior Alaska: Pollen and macro-fossil analysis of a 27-meter core from the Isabella basin (Fairbanks, Alaska): Canadian Journal of Earth Sciences, v. 11, no. 6, p. 828-841.

- Mertie, J.B., Jr., 1937, The Yukon-Tanana region, Alaska: U.S. Geological Survey Bulletin 872, 276 p.
- Naeser, N.D., Westgate, J.A., Hughes, O.L., and Pêwé, T.L., 1982, Fission-track ages of late Cenozoic distal tephra beds in Yukon Territory and Alaska: Canadian Journal of Earth Sciences, v. 19, no. 11, p. 2167-2178.
- Pêwé, T.L., 1958, Geology of the Fairbanks (D-2) Quadrangle: U.S. Geological Survey Geologic Quadrangle Map GQ-110, scale 1:63,360, 1 sheet.
- _____, 1969, The periglacial environment, past and present: Montreal, McGill-Queen's University Press, 487 p.
- _____, 1975a, Quaternary stratigraphic nomenclature in unglaciated central Alaska: U.S. Geological Survey Professional Paper 862, 32 p.
- _____, 1975b, Quaternary geology of Alaska: U.S. Geological Survey Professional Paper 835, 145 p.
- _____, 1975c, Permafrost: Challenge of the Arctic, in 1976 yearbook of science and the future: Chicago, Encyclopedia Britannica, p. 90-105.
- _____, 1976, Permafrost, in Yearbook of science and technology: New York, McGraw-Hill, p. 30-47.
- _____, 1982, Geologic hazards of the Fairbanks area, Alaska: Alaska Division of Geological and Geophysical Surveys Special Report 15, 109 p.
- Pêwé, T.L., Ferrians, O.J., Jr., Karlstrom, T.N.V., Nichols, D.R., 1965, Guidebook for field conference F, central and south-central Alaska, International Association for Quaternary Research, 7th Congress, Fairbanks, 1965: Lincoln, Nebraska Academy of Science, 141 p. (reprinted 1977, College, Alaska Division of Geological and Geophysical Surveys).
- Pêwé, T.L., and Reger, R.D., 1972, Modern and Wisconsinan snowlines in Alaska: International Geological Congress, 24th, Montreal, 1972, Proceedings, v. 12, p. 187-197.
- Pêwé, T.L., Wahrhaftig, Clyde, and Weber, F.R., 1966, Geologic map of the Fairbanks Quadrangle, Alaska: U.S. Geological Survey Miscellaneous Geologic Investigations Map I-455, scale 1:250,000, 1 sheet.
- Pêwé, T.L., Westgate, J.A., and Naeser, N.D., 1983, The mid-Pleistocene Ester Ash Bed in central Alaska: Geological Society of America Bulletin [in press].
- Viereck, L.A., 1970a, Forest succession and soil development adjacent to the Chena River in interior Alaska: Arctic and Alpine Research, v. 2, no. 1, p. 1-26.
- _____, 1970b, Soil temperatures in river bottom stands in interior Alaska, in Ecology of the subarctic regions---Proceedings of the Helsinki symposium: UNESCO, p. 223-233.
- _____, 1973, Wildfire in the taiga of Alaska: Quaternary Research, v. 3, no. 3, p. 465-495.
- Viereck, L.A., and Little, E.L., Jr., 1972, Alaska trees and shrubs: U.S. Forest Service Agriculture Handbook 410, 265 p.

MIDDLE TANANA RIVER VALLEY

By
Troy L. Péwé³ and Richard D. Reger⁴

Résumé of the Permafrost and Quaternary Geology

The middle Tanana River valley in central Alaska is located approximately 100 mi (161 km) south of the Arctic Circle (fig. 1). The area has a continental climate characterized by an extreme range between summer and winter temperatures. The mean annual temperature is 26.1°F (-3.3°C) and the mean annual precipitation is 11.7 in. (29.7 cm). The Richardson Highway alternately traverses the north side of the broad Tanana River valley and the southern hills of the Yukon-Tanana Upland (fig. 2).

The Tanana River valley is a large structural basin, and much of its bedrock floor is below sea level. Quaternary deposits 300 to 700 ft (91 to 230 m) thick are in large part an accumulation of fluvial and glaciofluvial sediments from the rising Alaska Range. Deposition of this material pushed the Tanana River northward against and near the Yukon-Tanana Upland. Thick sediments bury a fairly rugged bedrock topography, but hilltops of bedrock form small knobs above the alluvial plain. An apron of well-drained coalescing fans 30 mi (50 km) long flanks the Alaska Range.

In this section of Guidebook 1, we discuss permafrost and the Quaternary geology along the north side of the Tanana River valley from Fairbanks to Big Delta, a distance of approximately 90 mi (150 km) (fig. 2). The Tanana River is 230 mi (379 km) long and has an average discharge of 35,000 ft³ per s (100 m³ per s) in August at Big Delta. Upstream from Birch Lake, it is joined by several sediment-charged proglacial streams and is extensively braided. The stream gradient is 6 to 7 ft per mi (1 to 1.2 m per km) between Birch Lake and the Delta River, and the river becomes less braided and more meandering near Fairbanks. A 6-yr (1974-1979) study of the Tanana River sediment load in the vicinity of Fairbanks demonstrated that the average annual load was 18,800,000 to 21,800,000 tons (20,700,000 to 24,000,000 metric tons) of suspended sediment (silt to very fine sand) and 271,000 to 290,000 tons (298,000 to 321,000 metric tons) of bedload (fine sand to coarse gravel). During this period, annual mean discharge of the river ranged from 16,720 to 21,578 ft³ per s (475 to 613 m³ per s) and averaged 19,008 ft³ per s (540 m³ per s). Downstream from Fairbanks, the Tanana River meanders widely across its flood plain and contains few islands compared to reaches upstream from Fairbanks.

Except for small cirque glaciers in local mountainous highlands, central Alaska has not been glaciated, but glaciers from the Alaska Range approached within 50 mi (80 km) of Fairbanks during extensive glacial expansions, and heavily laden rivers deposited several hundred feet of silt, sand, and gravel in the Tanana River valley, forcing streams heading in the adjacent Yukon-Tanana Upland to aggrade their lower valleys. More than 400 ft (120 m) of sediment was deposited in creek valleys of the southern upland near Fairbanks. Silt that was blown from the flood plain of the glacier-derived Tanana River

³Department of Geology; Arizona State University; Tempe, Arizona 85281.

⁴DGGS, 794 University Avenue, Suite 200, Fairbanks, Alaska 99709-3645.

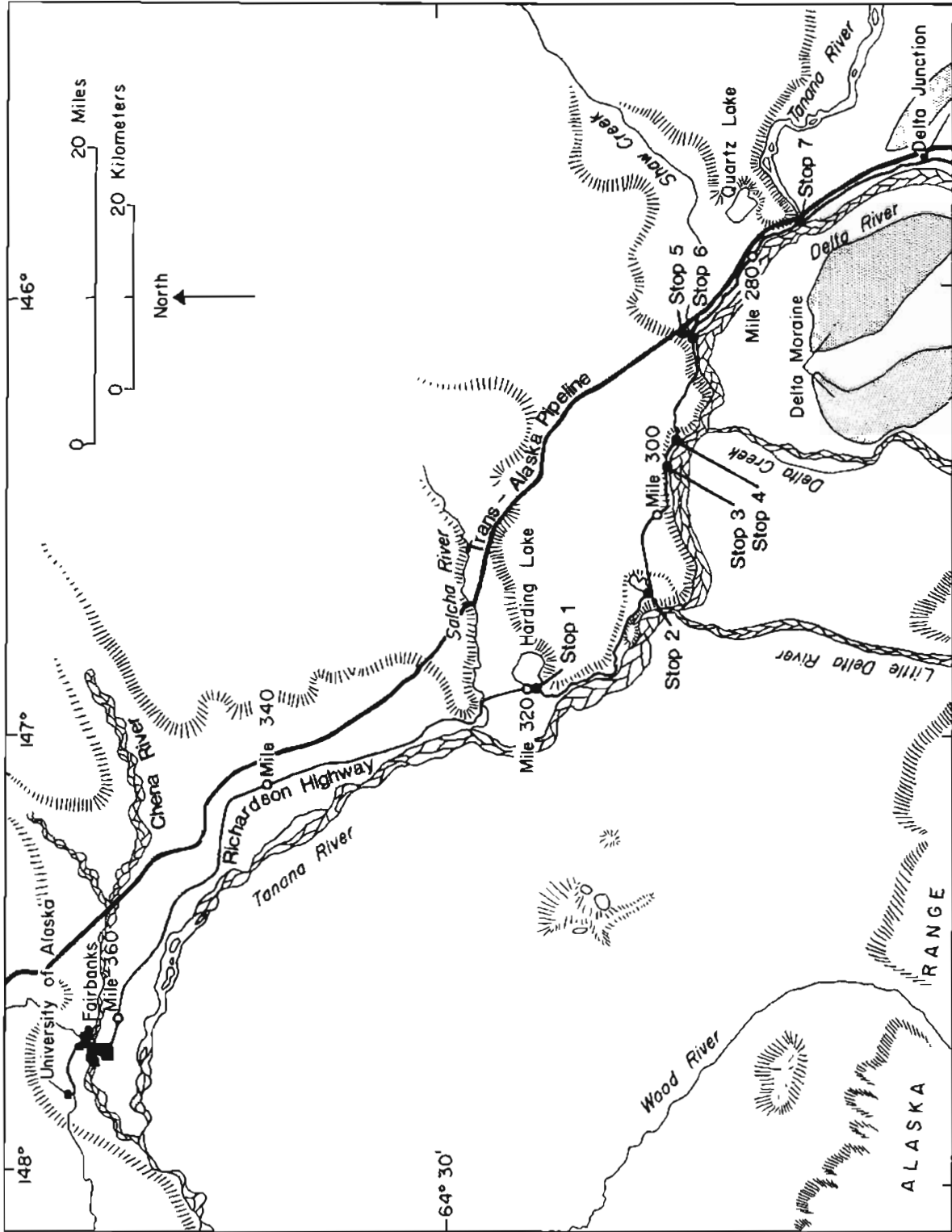


Figure 2. Index map of the middle Tanana River valley, Alaska, showing field-trip stops.

was deposited as loess that blanketed ridges of the southern upland in thicknesses from a few inches on summits to more than 150 ft (45 m) on middle slopes (fig. 3).

Quaternary deposits in the middle Tanana River valley, especially near Fairbanks, document a complex record of alternating cycles of silt and gravel deposition and erosion, and formation and destruction of permafrost. Climatic fluctuations ranged from climates warmer than now to climates colder than now. Both climatic changes and geologic processes, including permafrost formation, are related to glacial expansion and recession in the Alaska Range south of the middle Tanana River valley.

In late Pliocene or early Pleistocene time (or both), gold placers formed in upland creek valleys north of the middle Tanana River valley; later, thick accumulations of coarse, angular, locally derived alluvial gravel were deposited in these valleys in response to alluviation of the Tanana River valley. In the Fairbanks area, at least two cycles of gold and gravel deposition are recorded (fig. 4). Gravel deposits of the younger cycle are probably early Pleistocene in age because they contain tusks and large bones of mammoths and other megafauna. The poorly sorted, angular gravel grades into, and in some instances overlies, solifluction deposits that probably originated under rigorous climatic conditions. North of the middle Tanana River valley, the oldest known Quaternary event is a cold period recorded by solifluction deposits. These deposits, which are thought to be pre-Illinoian(?) in age, lie on weathered bedrock under eolian sediments in numerous exposures from Fairbanks to Big Delta (fig. 2) and contain ice-wedge casts.

In late Quaternary time, an advance of glaciers from the Alaska Range caused rapid aggradation of the Tanana River, which affected south-flowing streams in the Yukon-Tanana Upland. Unvegetated outwash-plain and valley-train surfaces were exposed to wind action, which deposited sand and silt as sand dunes or as a blanket of sand and loess on the low hills flanking the Tanana River valley. Sand is more common in the Delta River section of the middle Tanana River valley, but thins and disappears to the northwest, where loess predominates. Ventifacts formed at this time on bluffs facing the Tanana River near its junction with the Delta River and downstream as far as Harding Lake.

In the Fairbanks area (fig. 3), some windblown silt was retransported to creek-valley bottoms, incorporated considerable organic debris (including vertebrate remains), and became perennially frozen. The maximum age of these silt deposits is unknown, but they are older than 56,000 yr and younger than about 450,000 yr (fig. 4). Additional indications of loess antiquity include joints that were heavily stained and locally cemented by iron oxides before the deposit became perennially frozen and ice-wedge casts, which indicate that perennially frozen silt was subsequently thawed and refrozen.

With the end of the Delta Glaciation, downcutting by proglacial streams resulted in partial removal of the Tanana River valley fill, leaving terraces perched along valley sides. As the local base level was lowered, much of the eolian sediment on valley walls and retransported silt in creek-valley bottoms was gullied and carried away.

During the subsequent Donnelly Glaciation, the Tanana River again aggraded as glaciers advanced from the Alaska Range toward the Yukon-Tanana Up-

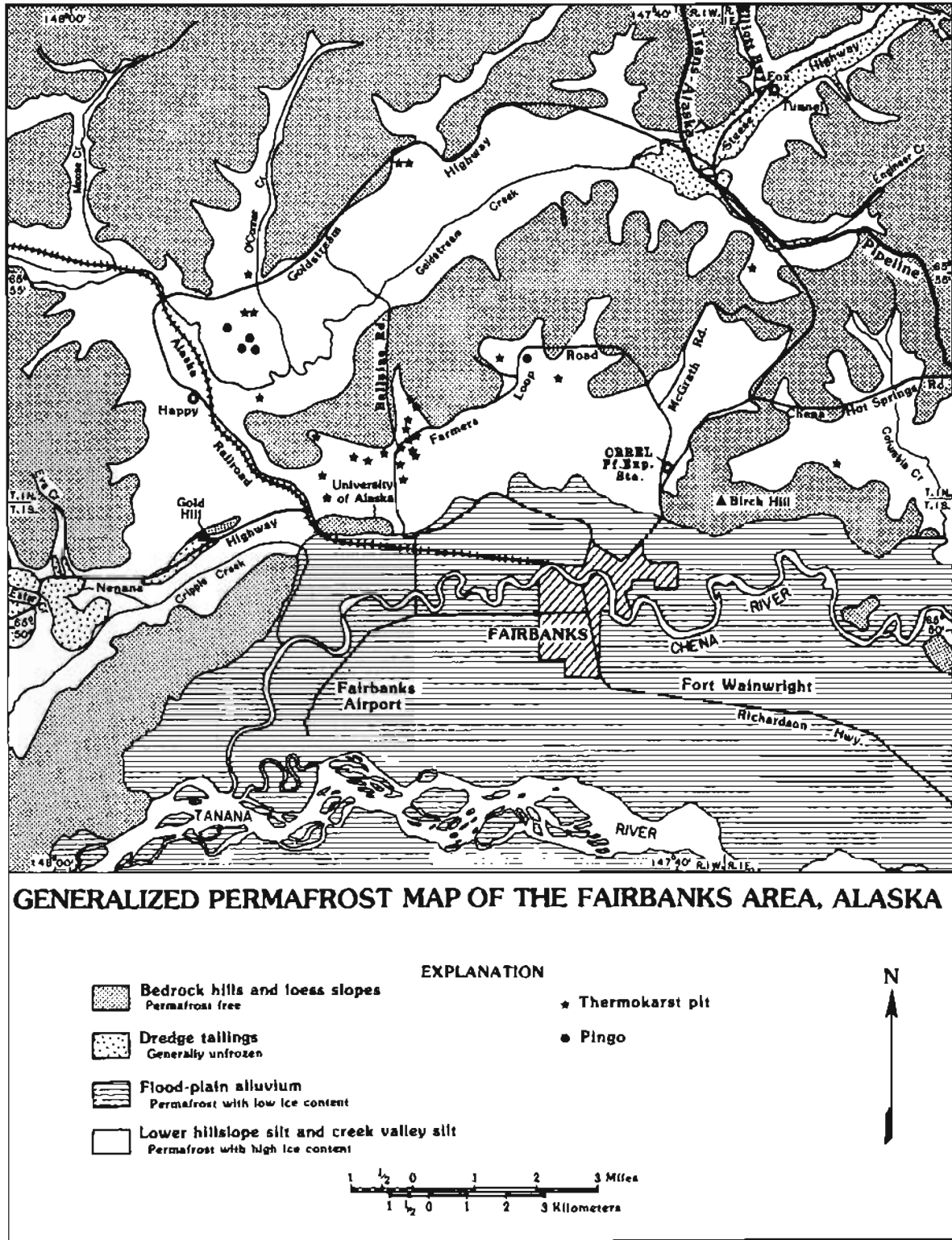


Figure 3. Generalized permafrost map of the Fairbanks area, Alaska (updated from Pêwê, 1958).

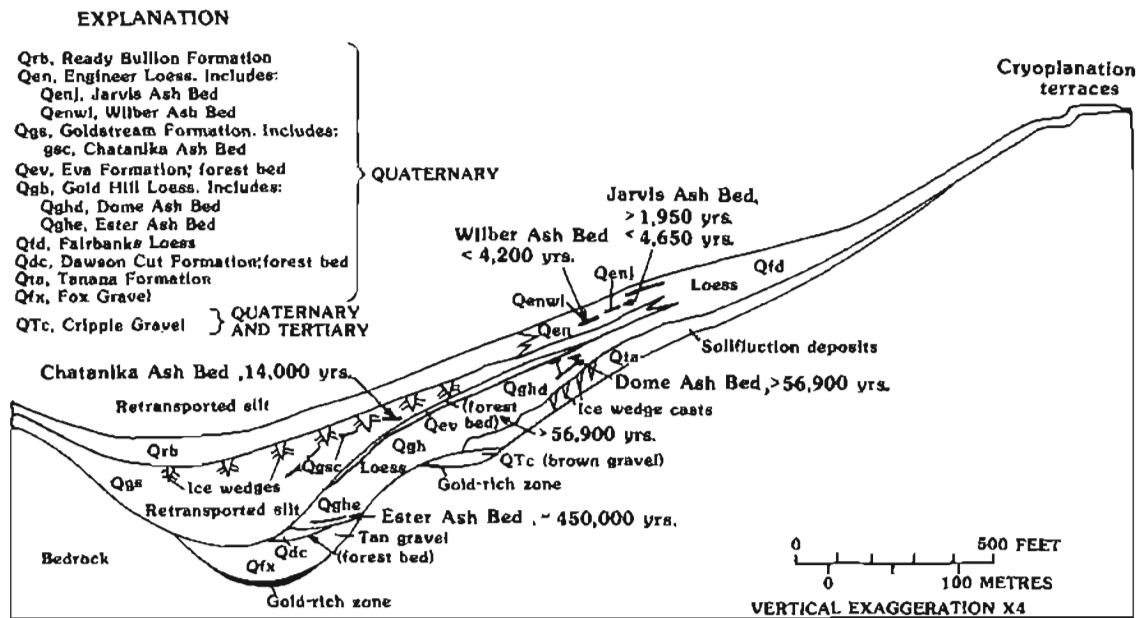


Figure 4. Schematic composite cross section of stratigraphic relationships of Quaternary deposits in creek valley near Fairbanks, central Alaska.

land. Windblown silt was again deposited on valley walls, and sand dunes formed on lowlands adjacent to the Delta and Tanana Rivers.

During the Donnelly Glaciation, loess was retransported to valley bottoms to form an organic-rich, fetid, perennially frozen deposit---locally termed 'muck.' This retransported loess of Wisconsinan age is 10 to 150 ft (3 to 46 m) thick and contains abundant vertebrate and plant fossils, including partial carcasses of vertebrates that were entombed in silt and perennially frozen. Typical vertebrate remains (from most to least abundant) include bison, mammoth, and horse. The retransported silt, which contains many ice wedges 1 to 10 ft (0.3 to 3 m) wide and up to 30 ft (10 m) high (fig. 3), is more than 56,000 yr old at the base and 10,000 yr old at the top.

Tree line was 1,500 to 1,800 ft (450 to 550 m) lower, and trees were limited mainly to creek and valley bottoms during the Donnelly Glaciation. The lower tree line is substantiated by the great reduction of tree pollen, the concurrent increase in pollen of tundra species, and the presence of fossils of alpine animals that lived in the Fairbanks area at that time.

The Fairbanks area is in the discontinuous-permafrost zone of Alaska (fig. 5), and perennially frozen ground is widespread, except beneath hilltops and moderate to steep, south-facing slopes (fig. 3). Since 1903, fires and disturbances of vegetation by land development have increased the depth to permafrost by 25 to 40 ft (8 to 12 m) in many places, although much of the ground refroze after the surface was revegetated. Sediments beneath the flood plain are perennially frozen as deep as 265 ft (81 m). Permafrost frequently occurs as multiple layers of varying thickness, and in many areas permafrost is not present. Unfrozen areas occur beneath existing or recently abandoned river channels, sloughs, and lakes. Elsewhere, layers of frozen sand and silt are intercalated with unfrozen beds of gravel. Depth to permafrost in undis-

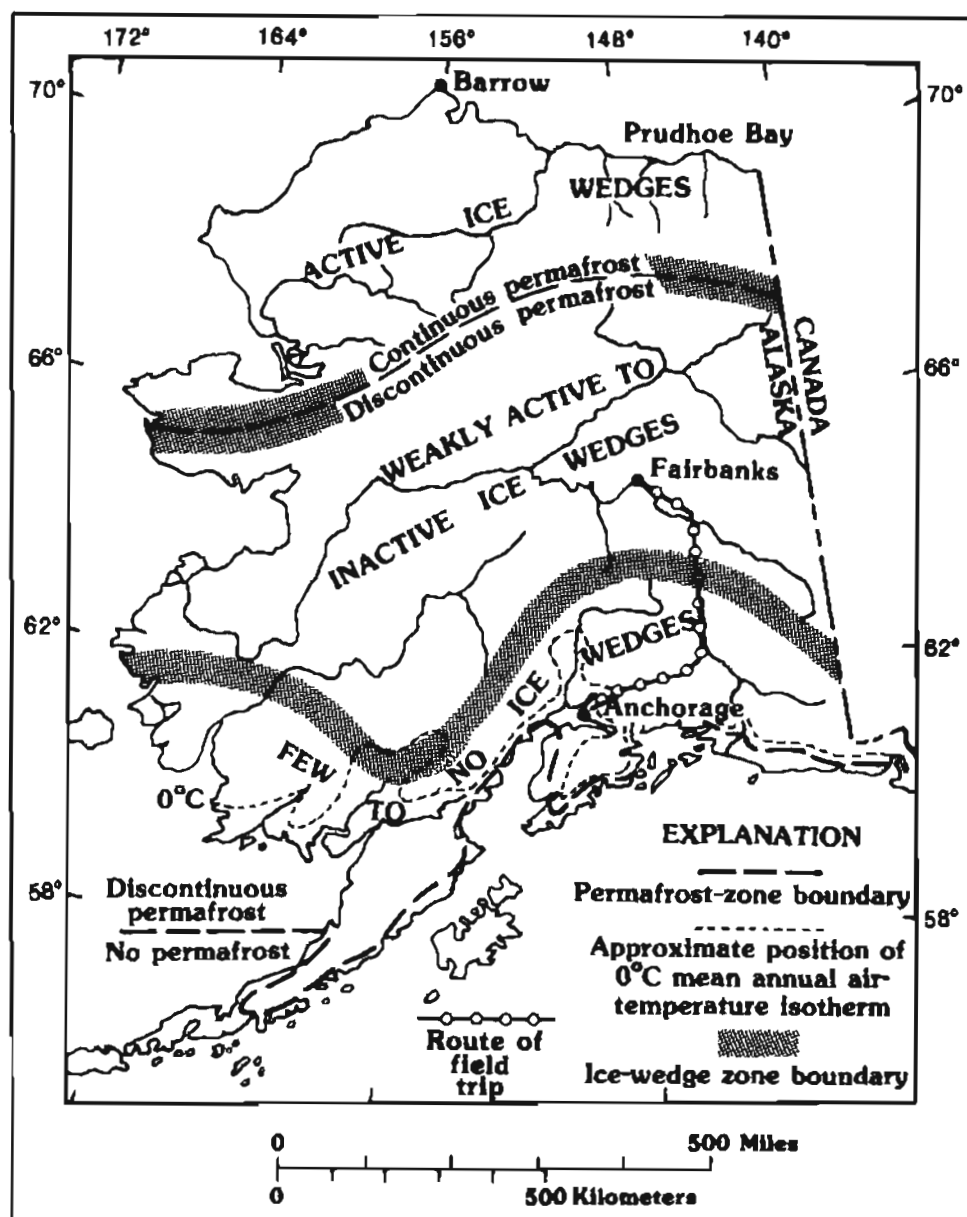


Figure 5. Distribution of ice wedges and permafrost in Alaska and field-trip route (from Péwé, 1966, fig. 3).

turbed areas varies from 2 to 3 ft (0.6 to 0.9 m) and is more than 4 ft (1.2 m) on the slip-off slopes of rivers. Ice in perennially frozen sediments beneath the flood plain consists of granules that cement grains. Large ice masses are absent.

Permafrost in the retransported valley-bottom silt in creek valleys and on lower slopes is thickest at lower elevations---up to at least 175 ft (76 m) near the flood plain of the Tanana-Chena Rivers. Perennially frozen ground does not exist beneath steep, south-facing slopes but extends nearly to the summit of north-facing slopes. Permafrost in these sediments contains large

masses of clear ice in the form of horizontal to vertical sheets, wedges, and saucer- and irregular-shaped masses. The ice masses are foliated (ice wedges) and range from less than 1 ft to more than 15 ft (0.3 to 15 m) in length. Much of the ice is arranged in a polygonal or honeycomb network that encloses silt polygons 10 to 40 ft (3 to 12 m) in diameter.

The temperature of permafrost in the Fairbanks area at a depth below the level of seasonal-temperature fluctuations [30 to 50 ft (8 to 15 m)] is about 31°F (-0.5°C). If the vegetation cover is removed, the relatively warm, sensitive permafrost thaws (degrades). Thawing of permafrost in flood-plain alluvium with low ice content results in little or no subsidence of the ground, but in creek-valley bottoms and on lower slopes, thawing of ice-rich retransported loess (muck) results in considerable differential subsidence of the ground surface.

Although much permafrost in the area is probably relict (from colder Wisconsinan-age conditions), it also forms today under favorable circumstances. Pre-Wisconsin permafrost probably disappeared during the widespread thawing in Sangamon time.

Vegetation in the Fairbanks area is a complex mosaic resulting from a long history of repeated or periodic forest fires, from differences in slope exposure and parent material, and from a complicated pattern of permafrost. On well-drained upland soils where permafrost is lacking or is deeper than 4 ft (1.2 m), large areas are covered by relatively young stands of paper birch (Betula papyrifera) and quaking aspen (Populus tremuloides) that have developed directly after forest fires or cutting. An understory of scattered young white spruce (Picea glauca) in many of the aspen and birch stands indicates that they will eventually be replaced by successional stands of white spruce. The white spruce and the white spruce-paper birch forests are widespread on well-drained upland soils that have not been burned in the past 200 yr. Associated with white spruce is a sparse shrub layer of high bush-cranberry (Viburnum edule), prickly rose (Rosa acicularis), alder (Alnus spp.), and willows (Salix spp.), and a thick moss layer of Hylocomium splendens, Pleurozium schreberi, and Rhytidiadelphus triquetrus.

Upland areas underlain by shallow permafrost are usually vegetated by black spruce (Picea mariana) in either open or dense stands. In these areas, black spruce often seed after fire, but may be preceded by stands of alder or paper birch. Associated with black spruce are the shrubs Labrador-tea (Ledum groenlandicum), bog blueberry (Vaccinium uliginosum), and resin birch (Betula glandulosa). Ground cover consists of lingenberry (Vaccinium vitis-idaea), Sphagnum spp. and other mosses, and lichens (especially Cladonia, Lycopodium, and Peltigera spp.). In such areas, frozen ground is usually within 1 to 3 ft (0.3 to 1 m) of the surface, even during late summer.

On the flood plains, stands of willow (Salix spp.), balsam poplar (Populus balsamifera), and white spruce grow on the youngest alluvial surfaces, especially on slip-off slopes where there is no permafrost. These locations are relatively protected from fire by rivers and sloughs, and some of the most extensive stands of commercial white spruce in interior Alaska grow along these rivers. In most older alluvial deposits, permafrost is close to the surface, and vegetation consists of slow-growing black spruce and larch (Larix laricina) or sedge and Sphagnum bogs.

Permafrost forms in alluvial deposits partly as a result of the insulating effect of vegetation. White-spruce stands develop a thick surface layer of mosses that insulate the ground more efficiently during hot summers when the moss is dry than during cold winters when the moss is frozen and saturated. As a result, the soil becomes progressively colder and eventually becomes perennially frozen. The presence of shallow permafrost creates wet, cold conditions that are more suitable for black spruce than for white spruce, and white spruce is replaced by black spruce as older trees die. Wet surface conditions promote the replacement of forest mosses by the more water-tolerant Sphagnum mosses and sedges, and eventually black spruce may be replaced by either Sphagnum or sedge bogs. The importance of the insulating effect of the vegetation is clearly shown by rapid lowering of the permafrost table after clearing or other disturbance of vegetation.

The relationship between vegetation and permafrost is fairly clear in the Fairbanks area, and vegetation can be used as a general indicator of permafrost conditions. Black spruce, larch, and bogs nearly always indicate the presence of permafrost within less than a foot of the surface. White spruce and aspen usually indicate an area free of permafrost or an area in which the active layer is several feet thick. Paper birch occurs on sites that are free of permafrost or where the active layer has temporarily deepened as a result of burning or clearing.

Road Log and Locality Descriptions

363.8.⁵ Start in Fairbanks D-2 Quadrangle.⁶

Richardson Highway and Airport Way, Fairbanks. Mileposts are on the left going toward Anchorage. The highway is on the flood plain of the Tanana River. From Fairbanks to Mile 330, the flood plain is a flat surface with meandering streams and a complex network of shallow swales. The surface layer of silt is 1 to 20 ft (0.3 to 6 m) thick and the total thickness of alluvium is 300 to 700 ft (91 to 230 m). Shallow swales are filled with about 30 ft (9 m) of clayey silt. Permafrost is discontinuous and there are many unfrozen lenses, layers, and vertical zones. The ground-ice content of permafrost is low, and no large ice masses are known.

Drainage is excellent and permeability is high, except locally in silt or where the ground is perennially frozen. Depth to the water table is about 10 to 15 ft (3 to 4.5 m) where permafrost is absent. The soils in this area support good crops if they are fertilized. The city of Fairbanks and military reservations are on the flood plain.

Because of present aggradation by the Tanana River and the wide, braided nature of the stream, large areas along the river and on islands are in various stages of recolonization by vegetation. Extensive stands of willow (Salix alaxensis, S. bebbiana, and Salix spp.) and alder (Alnus crispa) exist between Fairbanks and Big Delta. Large stands of balsam poplar range in age from 30 to 100 yr. Later stages in plant succession, especially white-spruce

⁵Miles from Valdez on the Richardson Highway.

⁶U.S. Geological Survey topographic quadrangle map, scale 1:63,360. Names and locations of quadrangle maps used on field-trip route are indicated on figure 6.

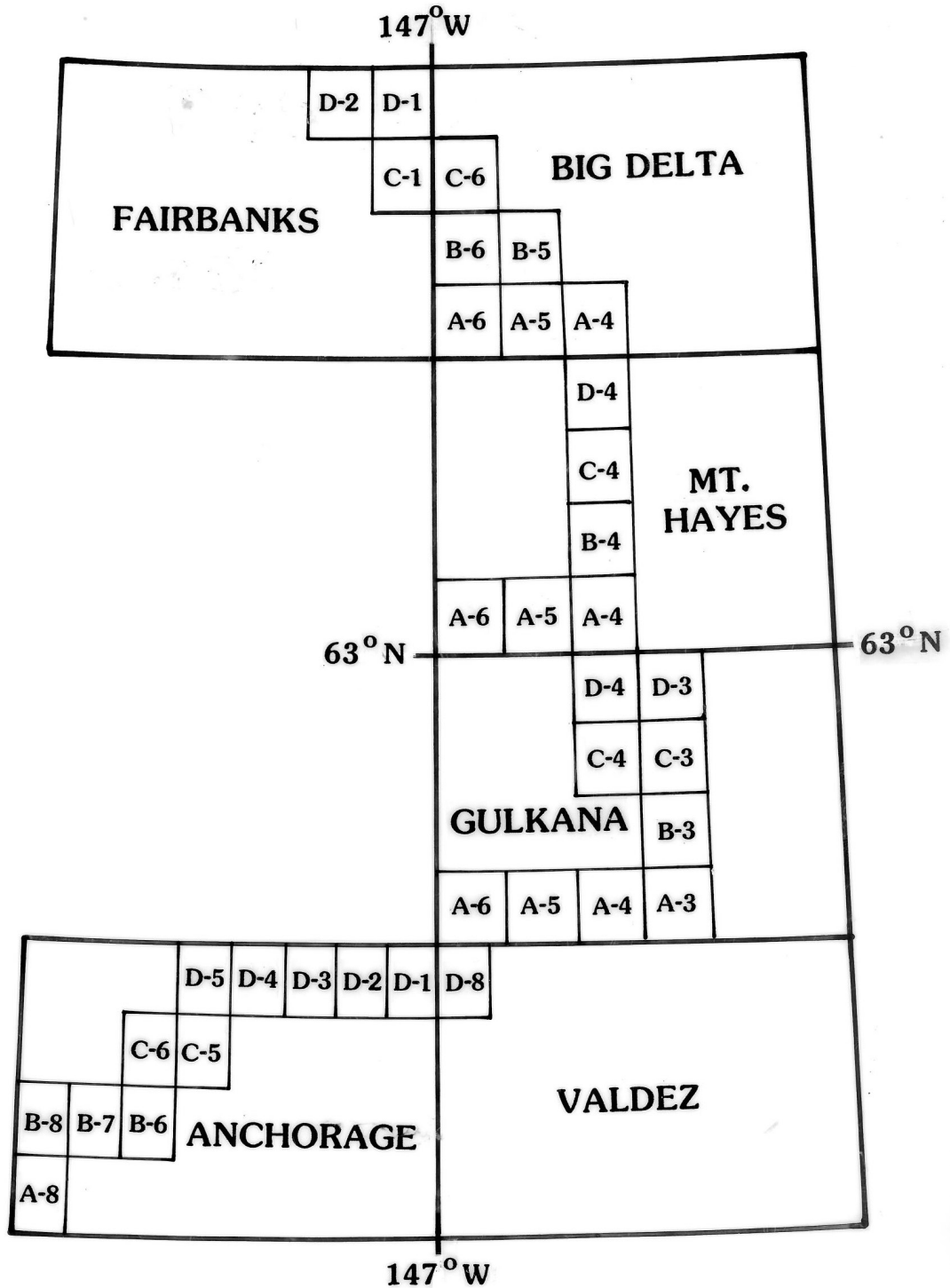


Figure 6. Index to U.S. Geological Survey topographic maps (1:63,360) used with road log.

stands of all ages, occur along the flood plain adjacent to the highway. Black spruce, larch, and bogs are conspicuous at many points along the river, but are absent where the river adjoins hills of the Yukon-Tanana Upland.

362.2 to 347.2. Most vegetation along the first 25 mi (49 km) of the highway is a result of recent disturbance and fire. Nearly all stands are successional, and because of poor drainage, stands of willow, black spruce, larch, and paper birch are most common.

355. Enter Fairbanks D-1 Quadrangle.

356.1. To the right, telephone poles heaved by seasonal freezing of the ground are braced at the base, but not successfully.

353.8. On the right is the low dike of the Chena River Lakes Flood Diversion Project. Fairbanks citizens have fought spring and summer flooding of the Chena, Little Chena, and Tanana Rivers for 50 yr. After the disastrous flood of 1967---when the entire flood plain was covered with water, locally to a depth of 5 ft (1.8 m)---the U.S. Army Corps of Engineers outlined an impressive flood-control project (fig. 7). This plan, called the Chena River Lakes Flood Diversion Project, resulted in the building of a levee system along the Tanana River and provided reservoir storage in the Chena River and its tributaries by construction of a long earth-filled dam. This \$165-million plan provides protection for Fairbanks and adjacent Fort Wainwright from a flood of 250,000 ft³ per s (7,102 m³ per s) on the Tanana River and 85,000 ft³ per s (2,415 m³ per s) on the Chena River. During the 1967 flood, peak discharge of the Chena River at Fairbanks was 74,400 ft³ per s (21,136 m³ per s), more than three times the previous maximum discharge of 24,200 ft³ per s (688 m³ per s) recorded on May 21, 1948.

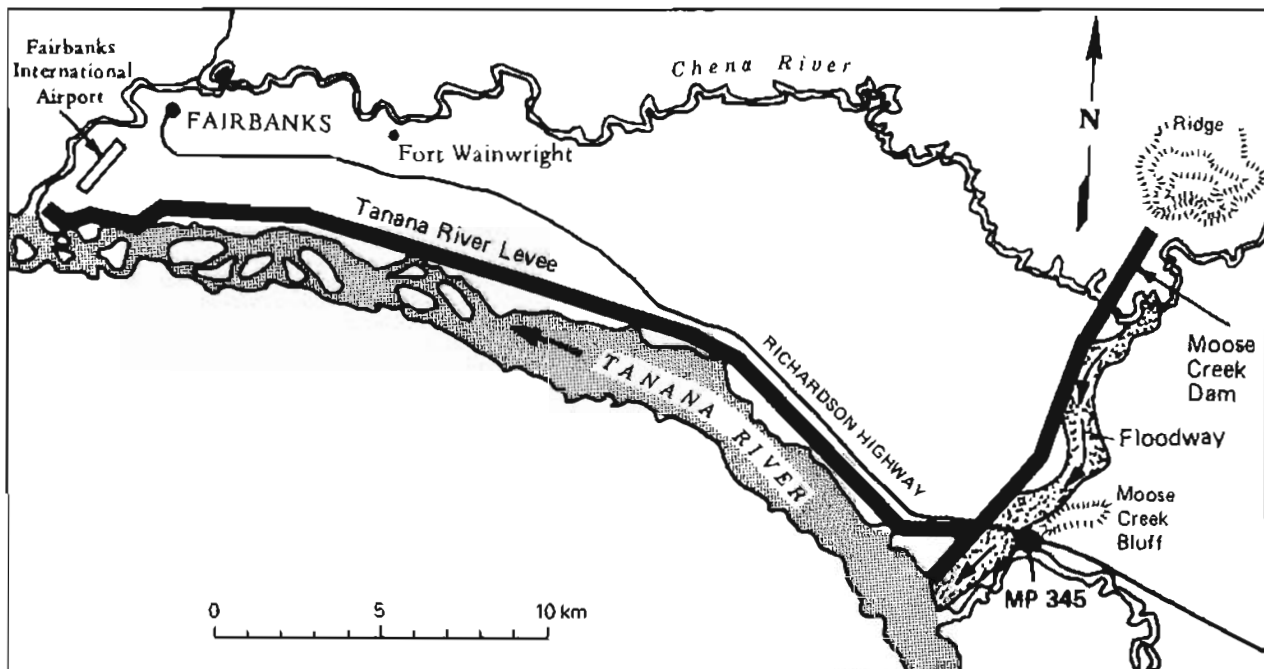


Figure 7. The Chena River Lakes Flood Diversion Project showing levee, dam, and floodway.

The 1977 peak discharge of the Chena River at Fairbanks was 2.2 times the peak discharge estimated for the 50-yr flood. In fact, it was greater than the magnitude of the 100-yr flood, the 'flood of the century' (fig. 8).



Figure 8. Oblique aerial view (to the west) of the flooding Chena River, August 15, 1967, at Fairbanks. Water was 3.9 ft (1.2 m) deep in the downtown area and inundated the Cushman Street bridge. Photograph courtesy of the Alaska Railroad.

A unique feature of the Chena River Lakes Flood Diversion Project is the floodway, an extensive cleared area upstream of the 7-mi-long (11.3 km) dam. In the event of flooding in the Chena River drainage, the outlet will divert excess water through the floodway south into the Tanana River. Construction of the floodway necessitated relocating sections of the Alaska Railroad and Richardson Highway under which floodwaters will pass.

352.6. To the right, a water well penetrated 265 ft (81 m) of permafrost, the thickest permafrost recorded beneath the Tanana River flood plain.

349.7. Enter Fairbanks C-1 Quadrangle.

348.6. Village of North Pole. Site of an oil refinery that was built in 1977. Using oil from the North Slope, this facility refines a small amount of jet and heating fuels.

346.2. Crest of main dike diverting floodwaters of the Chena River into the Tanana River.

345. End of dike. Moose Creek bluff is a bedrock hill of Cretaceous granite that pokes through the alluvial fill of the Tanana River valley. Cliff-head dunes of Holocene age cap the knob.

340. Typical flood plain of the Tanana River with modern sloughs and a myriad of scars of older sloughs and other drainage lines (fig. 9).



Figure 9. Aerial view (to the northwest) of the Tanana River flood plain and former drainage channels near Eielson Air Force Base. Photograph 1466 ATC-5M12-8(2) by U.S. Army Air Corps, about 1943.

337.7. Former south entrance of Eielson Air Force Base. South of this point, a 1964 statistical study of the prominent transverse frost cracks in the highway over a distance of 1 mi (1.6 km) showed that the cracks are spaced an average of 105 ft (32 m) apart. These are thermal-contraction cracks in seasonally frozen ground (seasonal-frost cracks). A recent study by McHattie (1980) showed that the spacing of cracks is strongly related to climate. He hypothesized that the problem relates most directly to thermal-expansion coefficients and frozen tensile-strength properties of upper-layer soils. McHattie indicated that in an area with 2,000 degree-days of freezing⁷ annually, there are about 10 cracks per mi, but an area with 3,000 degree-days of freezing has about 25 cracks per mi, and with 4,000 degree-days there are about 55 cracks per mi. The average number of degree-days of freezing each year in Fairbanks, based on U.S. Weather Bureau air temperatures, is 5,042; based on temperatures on an asphalt pavement, it is 3,630.

Cracking of seasonally frozen ground in interior Alaska occurs only in certain restricted environments. According to present theory, cracking occurs only in areas that are vegetation free or snow free during winter (or both), such as roads and pathways near Fairbanks. In seasonally frozen ground, cracks that traverse roads and paths rapidly narrow and disappear in areas covered by vegetation and unpacked snow. Because the highway is unprotected by vegetation and snow cover, it is subject to cracking that results from contraction stresses created by low temperatures and rapid cooling of the ground.

Most ice wedges that exist today in perennially frozen ground in central Alaska formed under a more rigorous climate. Very locally, in favorable microclimatic environments, small ice wedges are growing in interior Alaska. The average diameter of the polygons formed by thermal-contraction cracking of permafrost in central Alaska is approximately 100 ft (30 m).

336.1. A cryoplanation terrace is on the skyline to the east in the Big Delta C-6 Quadrangle.

336. The road passes through an extensive stand of black spruce and larch that developed about 45 yr ago after a fire.

330. Bedrock hill of schist. On the steep, dry, unstable south-facing slopes at this location and elsewhere along the highway, two species of sagebrush, Artemisia frigida and A. krushiana, grow. Aspen and white spruce are common on stabilized slopes. Several stands of river-bottom white spruce are visible along this section of the highway.

The high-water level of the August 1967 flood can be seen as a discolored zone (recently repainted) on the log cabin to the right.

329.2. Enter Big Delta C-6 Quadrangle.

328.9. Loess-capped bedrock bluff on left. Local slumping of this bluff blocked the highway during the June 21, 1967 earthquake.

⁷ A degree-day of freezing is 1 day with a mean temperature of 1 Fahrenheit degree colder than 32° F. A mean daily temperature of -2°F yields 34 degree-days of freezing.

328.1. The Richardson Highway parallels the scarp of a low terrace on the right. Two river terraces exist along the right limit of the Tanana River from near the junction of the Little Salcha River and the Tanana River, upstream for about 50 mi (80 km). The upper terrace ranges from 45 to 80 ft (13.6 to 24.2 m) above the Tanana River and extends upstream to the mouth of Canyon Creek; the lower terrace is 10 to 25 ft (3 to 7.6 m) above the river and has been mapped upstream to the mouth of Shaw Creek. Terraces on the right limit are obvious remnants of abandoned flood plains of the Tanana River. However, on the left limit of the Tanana River, one or more terraces with scarps that have been clearly cut by the Tanana River are probably not underlain by material deposited by the Tanana River. These terraces are probably the distal ends of truncated outwash fans of tributaries to the Tanana River from the Alaska Range to the south.

Sediments of the upper terrace on the north side of the Tanana River are considerably more weathered than sediments of the lower terrace. Also, sediments in the upper terrace contain ice-wedge casts and involutions. Ventifacts occur locally on the upper terrace, but none are known on the lower terrace.

Logically, terrace surfaces on the right limit of the Tanana River can be correlated to outwash-plain surfaces extending north from the Alaska Range. At this time, two terraces are correlated with the two prominent, late Pleistocene glacial advances in the Delta River valley. The upper terrace is associated with the Delta Glaciation and the lower with the Donnelly Glaciation. The age of the Delta Glaciation is controversial---some scientists believe the glaciation is Illinoian in age and others believe it is early Wisconsinan in age. We discuss this controversy in the Delta River section of the guidebook.

327.2. Crossing the clear water of the Little Salcha River, a small stream incised in the lower terrace of the Tanana River.

327.1. Rise onto lower terrace of the Tanana River. The top of the terrace in this locality (including the silt overburden) is about 15 ft (4.5 m) (average) above the modern flood plain of the Tanana River. At the scarp, this terrace is underlain by rounded, moderate- to well-sorted sandy gravel capped with up to 8 ft (2.5 m) of frozen silt. This silt thickens eastward and may have buried the upper terrace of the Tanana River.

327.1 to 326.1. The road is built on ice-rich, perennially frozen silt as thick as 12 ft (3.6 m).

326.2. Enter Big Delta B-6 Quadrangle.

326. Salcha School. The lower terrace is about 10 ft (3 m) above the modern flood plain.

325.8. To the left is a bluff of schist. The Tanana River is on the right. Terraces are absent. Several successional stands of willow, alder, and balsam poplar are present along the river.

325 to 324. The highway traverses the modern flood plain near the confluence of the Tanana and Salcha Rivers. Terraces are absent or concealed

by overlying alluvial silt fans issuing from the hills to the north.

324. Salcha River bridge.

323.3 to 320.2. The road is on the higher of the two terraces (fig. 10) on the northeast side of the Tanana River valley in the Big Delta B-6 Quadrangle. The Salcha River is graded to the Tanana River, and similar terrace sets are recognized along both rivers. Studies of lithology and sedimentary structures indicate that the material underlying the highway was deposited by the Salcha River. About 1 to 1.5 mi (1.6 to 2 km) to the west, the gravel is of Tanana River origin.

The upper terrace is mantled with from a few inches to 6 ft (1.8 m) of silt, probably loess. Several ice-wedge casts occur in the gravel of the upper terrace, but none are recognized in the lower terrace.

324 to 323.3. Modern flood plain of the Salcha River. The Richardson Highway is occasionally inundated during high water.

323.3. Scarp of lower terrace of the Salcha River (fig. 10).

323.2. Scarp of upper terrace of the Salcha River.

320.1. In the borrow pit on the left, gravel of the upper terrace is exposed and, although partially stripped, is mantled by several feet of sand and silt. Silty sediments are firmly cemented by iron oxides and display excellent involutions. Imbricate structures of the pebbles in near-surface

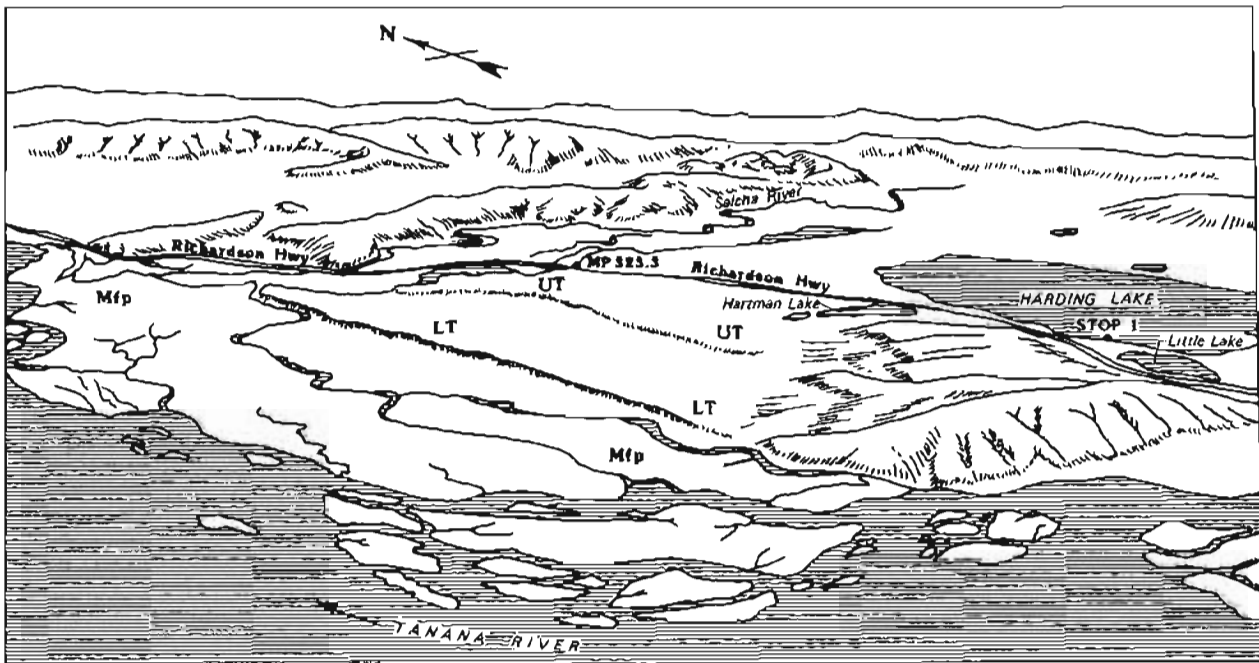


Figure 10. Harding Lake and vicinity, central Alaska. UT, upper terrace; LT, lower terrace; Mfp, modern flood plain; MP, milepost (modified from Blackwell, 1965, fig. 11).

deposits are similar to those found in modern ice-pushed ridges around Harding Lake, which suggests that an arm of Harding Lake may have occupied this area. The borrow pit on the right exposes an ice-wedge cast extending several feet into gravel of the upper terrace.

319. STOP 1. HARDING LAKE (named after the 29th President of the United States, who visited Alaska in 1923).

Aggradation of the Tanana River and its major tributaries apparently dammed several valleys in the Yukon-Tanana Upland during late Quaternary time. This damming may have produced several lakes on the north side of the Tanana River valley, including Harding, Birch, and Quartz Lakes (fig. 2), and perhaps a dozen others farther upstream.

Most lakes 50 to 150 mi (80 to 240 km) upstream from the Delta River are apparently below the level of the Tanana River at flood stage. Lakes downstream from the Delta River occur on the north edge of the aggradation surface of glaciofluvial material in reentrants in the Yukon-Tanana Upland (figs. 2 and 10) and are separated from the Tanana River by a terrace scarp.

Harding Lake is 142 ft (42.8 m) deep (fig. 11), 2 mi (3.5 km) in diameter, and about 50 ft (15 m) above the Tanana River. The bottom of the lake is 65 ft (20 m) below the level of the river. Harding Lake is unique among lakes on the north side of the Tanana River because its maximum depth exceeds, by a factor of three to four, the maximum depth of the other lakes. Also, the bottom of Harding Lake shows considerable relief, whereas the bottom profile of the other lakes is generally smooth (figs. 10 and 11). For comparison, a typical profile of Birch Lake (Stop 2) is included (fig. 12).

Ice-pushed ridges (ice-shoved ramparts) are well developed along the shores of Harding Lake. Along the north shore, up to seven distinct ridges, which average about 3 ft (1 m) in height, have been counted. The sharpness of these ridges suggests they are only a few hundred years old.

Ventifacts of quartz exposed near the edge of Harding Lake at low-water level have orangish-yellow surface staining from lake waters, which indicates they are not being faceted; however, they could have been cut during periods of low water after the lake initially formed.

A detailed bathymetric survey of Harding Lake in 1964 (Blackwell, 1965) revealed that submerged beach features (ice-pushed ridges and wave-built terraces) are also present. Analyses of the depth of these features indicate that the west margin of Harding Lake has been depressed up to 6 ft (2 m) relative to the east shore.

Harding Lake formed on the upper-terrace level, perhaps in part by aggradation of the Tanana River. Recent tilting of the lake---and its exceptional depth---strongly suggest that tectonism has had at least a minor effect on its history (fig. 12). Since 1900, at least 16 earthquakes of Richter magnitude 5 or more have occurred within a 25-mi (40 km) radius of Harding Lake.

A 2-ft-long (6 m) core was collected in 1979 from the deepest part of the lake (fig. 11) by Japanese and U.S. Geological Survey scientists. A radio-

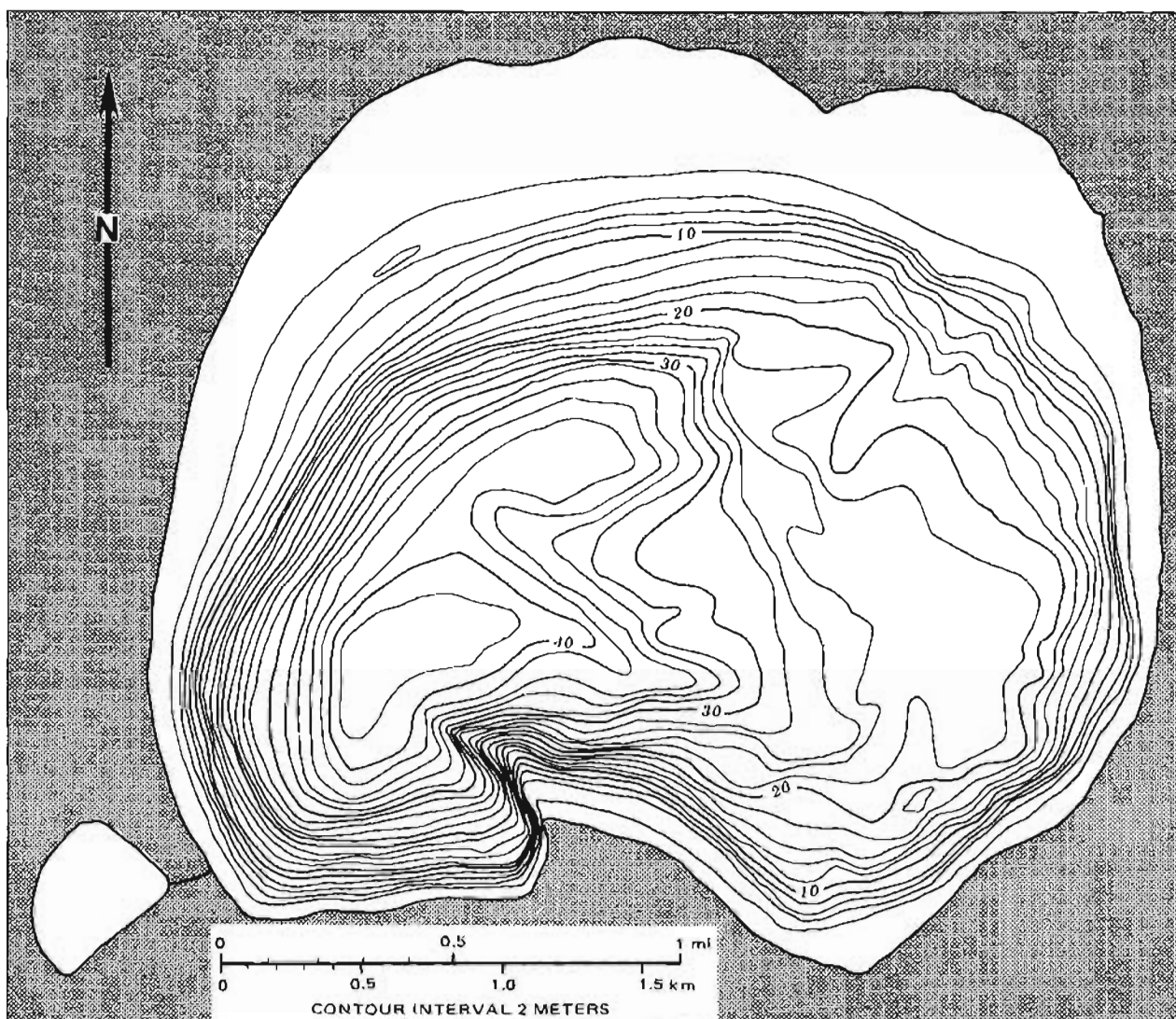


Figure 11. Bathymetric map of Harding Lake, Alaska (from Nakao and others, 1980, fig. 1).

carbon date of 25,000 to 40,000 yr B.P. is reported for material near the bottom of the core. Pollen analyses of sediments in the lake revealed that the lake varied from a bog to a shallow lake to a deep lake over this time span; the high-level lake is about 8,000 yr old. The maximum lake age may represent the time of deposition of the upper-terrace sediments or the lake may have formed as the terrace surface locally subsided, thereby postdating the terrace.

Extensive stands of paper birch, often with an understory of white or black spruce, surround the lake. These stands are about 100 yr old and began growing during a time when fires seem to have been especially extensive in the Tanana River valley. Many upland stands between here and Big Delta are about this age.

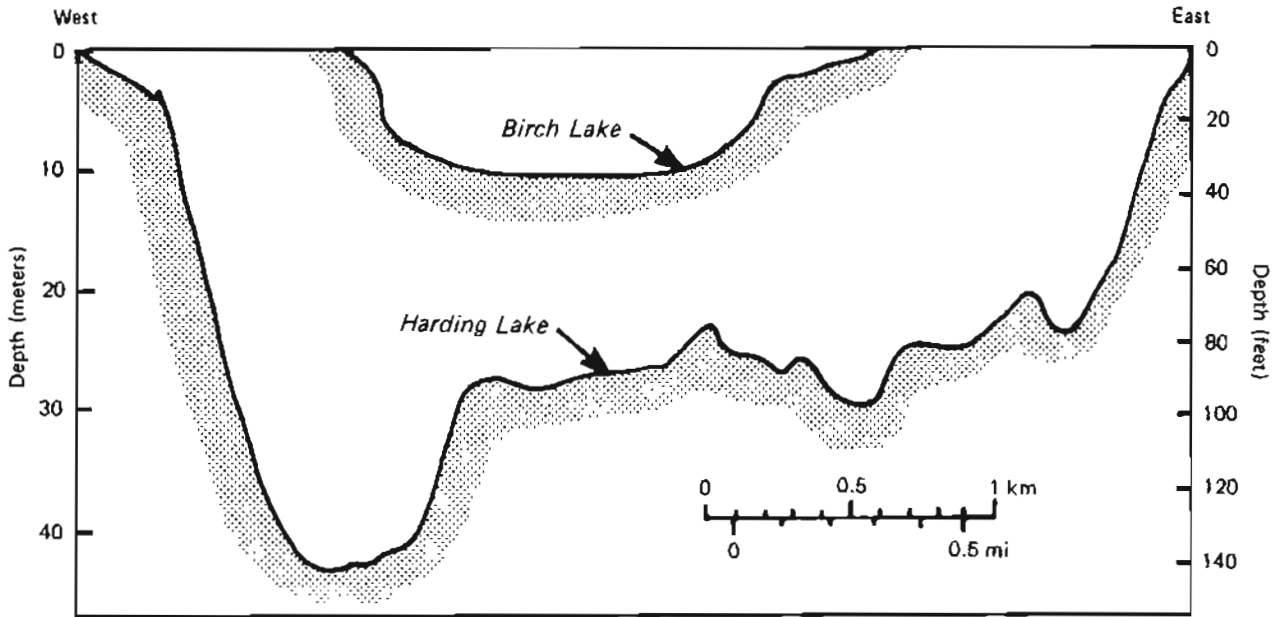


Figure 12. Bottom profiles of Birch and Harding Lakes, Alaska (from Blackwell, 1965, fig. 23).

318. Excellent view of Mt. Hayes, 13,832 ft (4,219 m) in elevation, and peaks of the central Alaska Range.

317.9. Road descends to the lower terrace of the Tanana River. This terrace, which is 10 ft (3 m) above river level at this locality, is underlain by moderately well-sorted sandy gravel overlain by 2 to 4 ft (about 1 m) of silt.

316.8. To the right, the road parallels the edge of a 10- to 15-ft-high (3 to 5 m) terrace scarp. The scarp of the upper terrace can be seen 1,000 ft (300 m) to the left.

316.7. Road descends to modern flood plain of the Tanana River. Gravel exposed here includes typical Tanana River sediments with clasts of gneiss, quartz diorite, schist, and volcanic rocks. Schist clasts are weathered and friable.

316.5. Scarp of the upper terrace is 800 ft (250 m) to the left. This terrace is 15 to 18 ft (4.5 to 5.5 m) above the lower terrace and is covered by about 3 ft (1 m) of silt at the scarp. This silt mantle thickens rapidly to the east.

314.4. Ventifacts of quartz occur on the west slope of the hill 1 mi (1.6 km) east of the road and 400 ft (120 m) above the present level of the Tanana River. They are buried by 2.5 ft (0.8 m) of loess.

313.7. Descend from lower terrace to the modern Tanana River flood plain. The terrace scarp is rock defended at this point.

313. South-facing bedrock slopes are covered by sagebrush (Artemesia frigida). Loess and sand cover the lower slope and overlie polymictic Tanana River gravel in a strath-terrace remnant that is 13 ft (3.9 m) above the present river level. Undiagnostic waste flakes and one crude scraper manufactured from a stream cobble were found low in the loess and sand section and are between 6,000 and 8,000 yr old. The youngest extinct elk (Cervus elaphus) bones found in Alaska, (identified by R.D. Guthrie, vertebrate paleontologist, University of Alaska, Fairbanks) were recovered from the section and are slightly less than 3,000 yr old.

312.8. To the left are basalt dikes and faults in schist.

312.7. To the left is a landslide, probably inactive, in loess and colluvium on the steep slope.

310.8 to 308.8. The road overlies ice-rich permafrost in colluvial silt from the loess-covered hill to the right. The roadway is consequently in poor condition. Stands of black spruce, larch, and paper birch along this section of road are good indicators of permafrost.

308.4. To the right, bedrock is coarse-grained granite and quartz monzonite that is weathered to a depth of more than 20 ft (6 m). A borrow pit in this weathered zone reveals a well-developed, 5-ft-thick (1.5 m) layer of grus that has moved downslope by solifluction. This layer is overlain by 1 to 5 ft (0.3 to 1.5 m) of loess.

308.3. Descend to lower terrace of the Tanana River.

308.3 to 308. Black spruce (Picea mariana) forest on left is growing on frozen, organic-rich silt overlying gravel of the lower terrace. Depth to permafrost is 1 ft (0.3 m) or less.

307.4. Ascend to upper terrace of the Tanana River (fig. 13). Borrow pit on right is in Tanana River gravel. A ventifact was found near the surface of the upper terrace under the 4-ft-thick (1.2 m) silt cover near the southwest end of Birch Lake.

307. This very rough stretch of road passes through a dense stand of black spruce that is about 90 yr old and underlain by permafrost as shallow as 2 in. (5 cm).

306. On the right side of the road at Birch Lake, a sharp unconformity between the bedrock and overlying loess is exposed. Mineralogical studies indicate that the silt is compositionally distinct from the quartz monzonite bedrock, thus excluding the possibility that the silt may be residual in origin, and not loess, as postulated by Taber (1943).

305.9. STOP 2. BIRCH LAKE.

Birch Lake lies in a reentrant of the Yukon-Tanana Upland and is dammed on the west side by sediments of the Tanana River (fig. 14). The lake has a maximum depth of 36 ft (12 m) and a diameter of 1 mi (1.75 km). Blackwell (1965, fig. 8) indicated that the surface of the lake is about 30 ft (10 m)

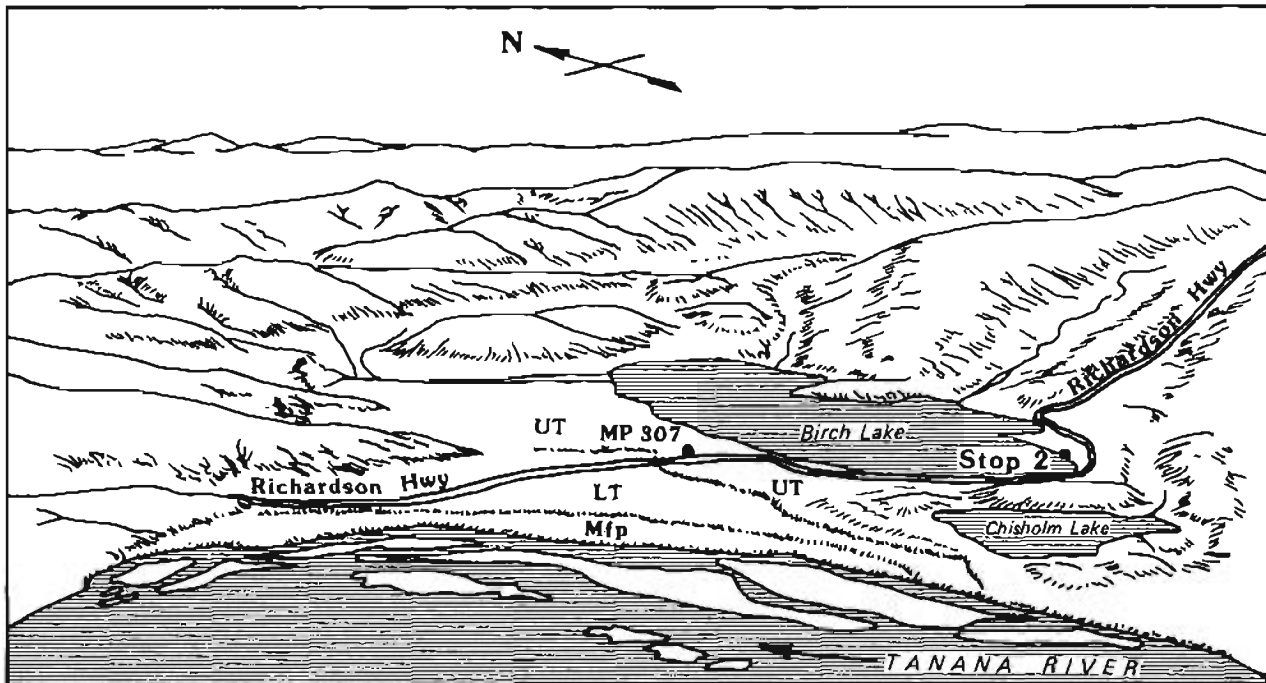


Figure 13. Birch Lake and vicinity, central Alaska. UT, upper terrace; LT, lower terrace; Mfp, modern flood plain; MP, mile post (modified from Blackwell, 1965, fig. 12).

above the level of the Tanana River and about 10 ft (3 m) below the surface of the upper terrace.

In the 1950s and 1960s, it was suggested that the lakes on the north side of the Tanana River may hold a complete late Quaternary pollen record. In the 1970s, the pollen record of Birch Lake was investigated by T.A. Ager, who found that sediments near the lake bottom are about 16,000 yr old and that a herbaceous tundra environment was present about 15,000 yr B.P.. At about that time, the water level began to rise in the boglike environment and eventually formed a lake similar to the modern lake. The herbaceous tundra environment evolved to shrub-tundra vegetation about 14,000 yr B.P., and by about 9,000 yr B.P., the spruce-birch forest had replaced the shrub tundra over much of the region, at least in the lowland.

Birch Lake probably formed near the top of the upper terrace in the past 10,000 to 15,000 yr because Tanana River gravel floors much of the lake bottom. Ice-shoved ramparts of Tanana River gravel are built up around the lake, especially on the west side. Ager's data show that the earlier interpretation that the lake was formed by Tanana River aggradation in Delta time is no longer valid because of the youthfulness of the lake.

305.7. Many finished stone tools and flakes of slate and chert were found 6 to 18 in. (15.2 to 45.7 cm) below the surface in loess when borrow pits in the grus were opened in 1947.

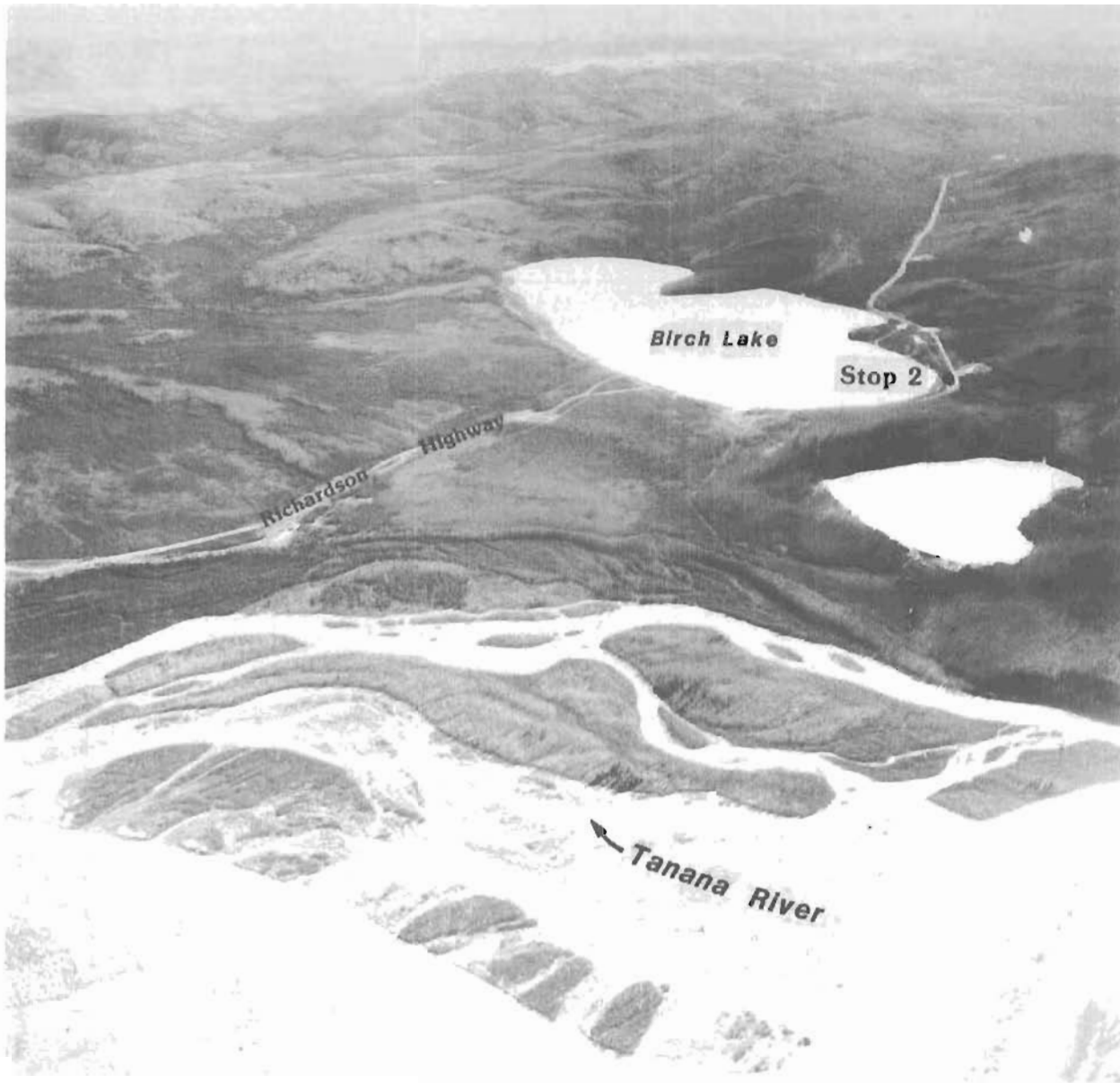


Figure 14. Oblique aerial view (to the northeast) of Birch Lake and the Yukon-Tanana Upland, Alaska. Photograph 179 LT 72 PL-M-8M107-72RS by U.S. Air Force, August 20, 1948.

304.8. To the left is a borrow pit in weathered quartz monzonite overlain by 4 ft (1.3 m) of loess.

303.9. On the left side of the road are tors, which are residual bedrock pillars left by differential stripping of the deeply weathered quartz monzonite.

300.7. Enter Big Delta B-5 Quadrangle. The Richardson Highway traverses a 587-ft-long (178 m) test section that was constructed in the fall of 1973 in perennially frozen, ice-rich silt and sand. About 387 ft (117 m) of the test

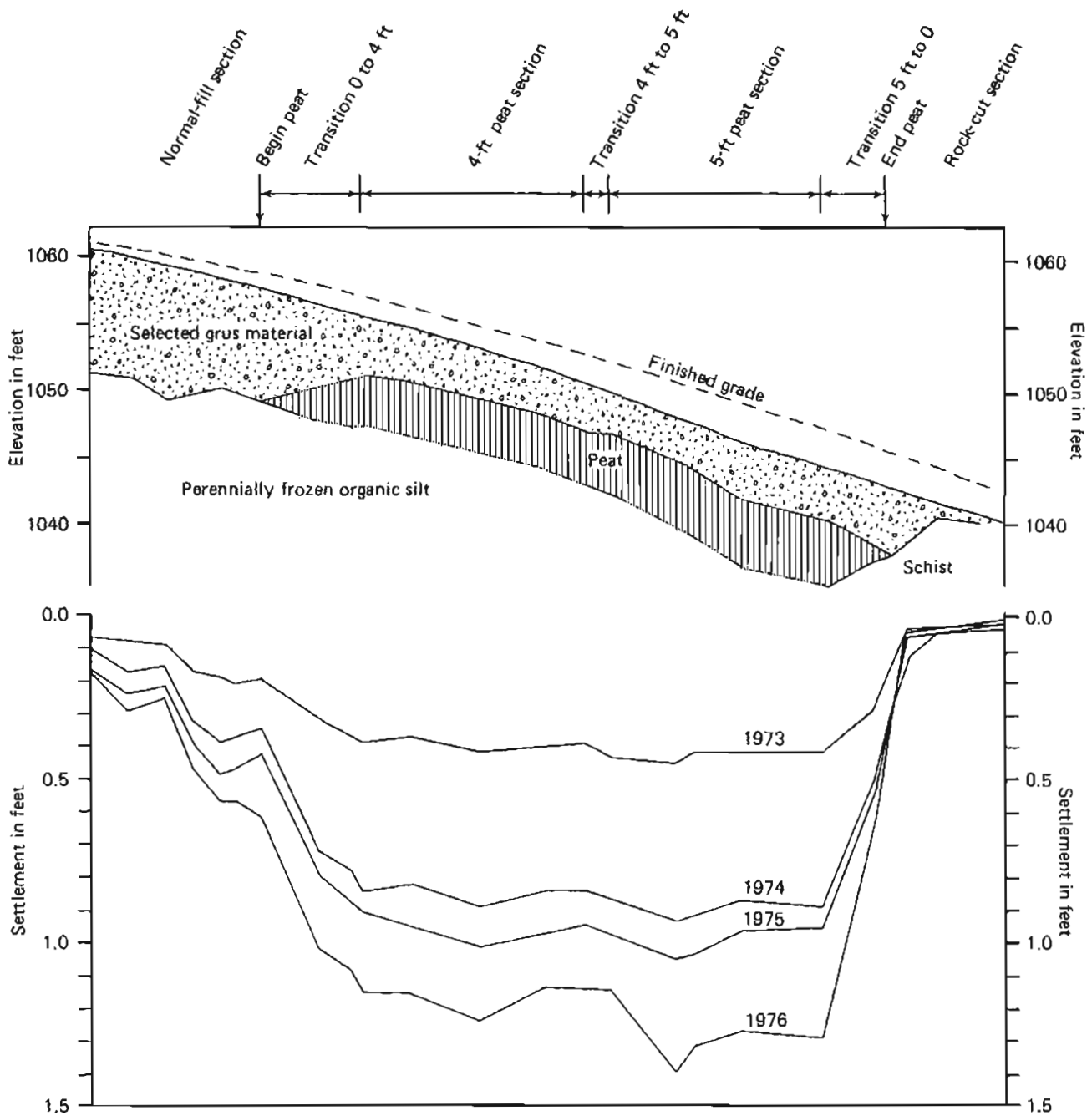


Figure 15. Comparison of longitudinal (centerline) profile of peat test section and amounts of settlement after 4 yr (1973-1977), Mile 300.7, Richardson Highway, Alaska (modified from Esch and Livingston, 1978, figs. 6 and 27).

section were designed to evaluate the thermal effects of laying 4- (1.3 m) and 5-ft (1.5 m) thicknesses of frozen peat beneath normal road fill (fig. 15).

Climatic measurements at the test site indicate that the mean annual air temperature is about 25°F (-3.9°C), with seasonal temperature extremes of 95°F

(35°C) and -60°F (-51.1°C). Annual precipitation averages about 12 in. (30.5 cm), and there is about 70 in. (1.8 m) of snowfall. Snow covers the ground from late September until middle to late April and generally reaches maximum thickness [about 27 in. (68.6 cm)] in February. The temperature of permafrost below the level of seasonal temperature variation beneath a nearby undisturbed site is 30.6°F (-0.8°C).

Four years of observations indicate that the test section freezes much sooner than other sections of the road each year and that the permafrost beneath the peat fill annually chills much colder than other sections. From 1973 through 1977, the 4-ft (1.3 m) test section settled 2 ft (0.6 m) in response to thawing and draining of ice-rich peat that was frozen when emplaced; in the 5-ft (1.5 m) test section, all but 0.8 ft (0.2 m) of peat thawed and 1.9 ft (0.6 m) of consolidation occurred (fig. 15).

The preliminary performance of this test section indicates that in interior Alaska, 2.5 ft (0.8 m) of prethawed and preconsolidated peat placed beneath a 5-ft-thick (1.3 m) layer of road fill and paving is adequate to prevent thawing of underlying permafrost. However, collection of runoff water in ditches and warming of cut slopes result in progressive thawing of permafrost beneath ditches and behind cut slopes. In normal roadways, seasonal thawing occurs beneath 10 ft (3 m) of gravel.

300. Mouth of Canyon Creek. The two gravel terraces of the Tanana River apparently converge near here. The lower terrace [mantled by 17 ft (4.3 m) of silt] is only 3 ft (1 m) above the present level of the river, whereas the upper terrace, represented by scattered patches of calcium-carbonate-coated cobble gravel, is 17 ft (4.3 m) above the river. A log at the base of silt overlying the lower terrace gravel has been dated at 3,000 ± 75 yr B.P. (GX-0277).

Weber and others (1981) described the roadcut exposure of eolian sediments, solifluction deposits with ventifacts, ice-wedge casts, and radiocarbon-dated vertebrate fossils at the mouth of Canyon Creek. The section was well exposed from 1974 to 1978. Local arkosic gravel and sand with a few angular fragments of volcanic ash (evidently washed into the deposit) are located on top of the Tanana River gravel. This material is 50 ft above the modern Tanana River and probably part of the upper Delta-age terrace; it is overlain by colluvium with ventifacts that are overlain by eolian sand covered with a thin loess layer.

Most mammal remains were recovered from the lower part of the section in the arkosic gravel and sand, and a collagen date of 39,360 ± 1,740 yr B.P. (SMU-640) was obtained on the bones. The fauna is a typical Wisconsinan vertebrate assemblage from central Alaska that is stratigraphically controlled and radiometrically dated. Megafauna remains include woolly mammoth, arctic ass, western camel, bison, mountain sheep, wolf, and others. Some of the mammals, such as the mountain sheep, indicate a lower tree line than now.

Weber and others (1981) believed the section indicates that the Tanana River terrace gravels are at least in part of early Wisconsinan age. Overlying sediments are 40,000 yr old (late Wisconsinan age). An alternate interpretation is that the basal terrace gravels are older than early Wisconsinan and are simply overlain by dated sediments of the late Wisconsinan

cold period. John Westgate (personal commun., October 19, 1982) correlated retransported volcanic ash exposed in this section with volcanic ash collected by Péwé from Sheep Creek in the Fairbanks area. The ash from Sheep Creek is in the Gold Hill Loess, which underlies the Goldstream and Eva Formations of Wisconsinan age (the base of the Eva Formation is more than 56,900 yr old). Thus, the ash in the Canyon Creek section may be pre-Wisconsinan in age.

299.3. Gravel of the upper terrace overlies schist. The gravel is 3.5 ft (1.1 m) thick and is covered by 5 in. (13 cm) of fine sand and 4.5 ft (1.4 m) of loess. This gravel is sporadically exposed on the left for a distance of a few hundred yards beyond Canyon Creek. Fine-grained sand usually overlies the gravel, but farther to the east [0.3 mi (0.5 km) beyond Canyon Creek], the sand lies directly on bedrock. This gravel is probably part of the upper Tanana River terrace.

296.5. STOP 3. TANANA RIVER OVERLOOK.

The river is 1.5 m (2 km) wide. The gradient of the braided stream here is 6 ft per mi (1 m per km). Most successional stands of vegetation along the river are dominantly alder and willow. An extensive white-spruce stand can be seen in the distance south of the river.

295.9. To the left, a borrow pit exposes a solifluction layer of bedrock debris that is capped by retransported silt and sand.

295.6. To the right, an open-system pingo occurs in forest 100 ft (30 m) from road.

295.5. Banner Creek. From 1 to 10 ft (0.3 to 3 m) of silt overlie creek gravel. Banner Creek gravel may correspond to the lower terrace gravel of the Tanana River. A log from 4 ft (1.2 m) below the top of the Banner Creek gravel, 220 ft (67 m) downstream from the highway bridge, has been dated at $3,920 \pm 75$ yr B.P. (GX-0257).

295. Richardson Roadhouse, first established in 1907 after the gold strike on Tenderfoot Creek, was moved three times eastward toward the base of the hill because of lateral erosion by the Tanana River. The structure was destroyed by fire in 1982. The Richardson mining district is well known for its deep fluvial placers and high-level eluvial placers. From 1907 through 1977, total production of gold and silver was about 95,000 oz (2,954,500 g) and 24,000 oz (746,400 g), respectively. As of 1982, about 103,000 oz (3,203,300 g) of gold and 2,500 oz (77,750 g) of silver were extracted from the district. Fineness values for the gold are some of the lowest in Alaska, ranging from 650 to 790.⁸

An iron-stained, well-stratified, poorly sorted, angular to subrounded creek gravel with pebbles and cobbles 1 to 6 in. (2.5 to 15 cm) in diameter is exposed in a borrow pit near the site of the former Richardson Roadhouse. No detailed study has been made of this exposure, but ice-wedge casts and a

⁸ Expressed as parts of gold per thousand parts of metal, that is, a nugget with a fineness of 650 contains 65 percent gold and 35 percent other metals or alloys. Other common impurities include silver and copper.

weathered mammoth tusk are reported.

The gravel differs in size, sorting, roundness, and lithology from the Tanana River gravel at the base of the nearby bluff. The creek gravel in the pit contains many angular fragments of porphyritic rhyolite that crops out nearby in Banner Creek valley. A study of pebble orientations reveals that the direction of transport of the gravel was southwest, the present direction of flow of Banner Creek.

A preliminary interpretation of this exposure is that the gravel represents a high-level creek gravel of perhaps mid-Pleistocene age that is capped by loess of late Pleistocene to Holocene age. The relationship of the section to the terraces of the Tanana River is unknown.

292.6. STOP 4. SOUTH WALL OF ROADCUT AT TOP OF HILL.

The elevation here is 1,350 ft (422 m), about 450 ft (137 m) above the modern flood plain of the Tanana River. Bedrock is intercalated chlorite-muscovite schist and muscovite-chlorite schist of the greenschist facies. White to clear, discontinuous quartz veins and boudins parallel schistosity. Bedrock is weathered to a depth of over 25 ft (7.6 m), and the upper 3 ft (0.9 m) is especially well weathered and deformed by downslope movement. Capping this rounded ridge is a particularly interesting section that documents at least part of the complex permafrost history of this area. The top 3 to 5 ft (0.9 to 1.5 m) of the section is tan loess, which is probably of Holocene and Donnelly age and perhaps, in part, of Delta age. Beneath this loess cap is a thin [up to about 12-in.-thick (30.5 cm)], discontinuous layer of gray eolian silty sand, probably of Delta age. Mixed into the sand layer are hundreds of white to buff, pebble- to cobble-size quartz ventifacts that form a lag gravel. The composition of the wind-modified stones indicates they are derived from local bedrock.

The ventifact lag gravel is locally deformed downward to form casts in cavities left by melting of ice wedges that formerly grew in the weathered bedrock. These ice wedges may have been of Delta age or younger, but they obviously melted after the quartz ventifacts formed and the gray eolian sand layer was deposited. Nearby, the ventifact lag gravel cuts across ice-wedge casts of gray eolian sand that formed by melting of ice wedges and infilling of the resulting cavities before formation of the quartz ventifacts and deposition of the eolian-sand layer in Delta time. It is not known if these two episodes of ice-wedge melting were climatically induced or were the results of local wildfires.

292. Placer gold was discovered in the valley of Tenderfoot Creek in 1905. In the Richardson mining district, a system of northwest-trending lineaments apparently controls the distribution of mineralized, Cretaceous quartz-potassium feldspar (rhyolite) porphyries that are probably the source of the gold. Former production shafts, associated tailings piles, and open-pit workings are concentrated along, downslope, and downstream from the main or Richardson lineament on Tenderfoot, Buckeye, and Banner Creeks in Hinkley Gulch and near the head of Junction Creek downstream from the point of its beheading. Placer gold was recovered by drift and open-pit methods. Tailings piles can be seen in the trees on the left in the valley bottom. Where the Richardson Highway crosses perennially frozen, ice-rich, retransported silt, thawing of permafrost produces a very irregular highway surface.

288.7. Turn off to STOP 5. SHAW CREEK BLUFF.

About 1.5 mi. (2 km) along the old Richardson Highway on the left is a section exposing 4 ft (1.2 m) of loess overlying clean, gray, cross-bedded eolian sand with sharp contact. (This is an excellent place to sample the eolian sand). Physical characteristics of the sand are listed under the discussion for Mile 282.5.

STOP 5. SHAW CREEK BLUFF.

To the south is the panorama of the Alaska Range and the broad Tanana River valley (fig. 16). The braided, silt-laden Tanana River lies at the base of the bluff 100 ft (30 m) below. From this spot, evidence of the mid- to late Quaternary history of the area can be viewed (figs. 17, 18, and 19).

In Delta (Illinoian?) time, a piedmont glacier from the Alaska Range pushed north along the Delta River and formed a terminal moraine 8 mi (13 km) south of Shaw Creek bluff. Broad gravel plains extended north from the glacier to Shaw Creek bluff and into the Shaw Creek Flats to the southeast. The braided Tanana River and associated outwash streams wandered over these plains. Winds blowing over the outwash plain picked up sand that cut ventifacts on the plain (Jack Warren Road and Quartz Lake) and cut and polished ventifacts on the south-facing bedrock slopes and hilltops from Shaw Creek bluff west for at least 20 mi (32 km) (fig. 17). Ventifacts were formed from river level to hilltops at least 650 ft (200 m) above the river.

Probably throughout the Delta Glaciation, sand and silt were blown from the plains north and west onto the hills. Sand dunes formed on the south-facing slopes of the hills north and west of Shaw Creek Flats (fig. 19). Some dunes that migrated over the low hills now lie on the north side of the hills. Approximately 40 mi² (100 km²) of sand dunes were formed at that time.

The sand facies of the eolian deposits covers an 800-mi² area (2,000 km²) north of the Tanana River and thins away from the Shaw Creek bluff area. About 15 to 20 mi (25 to 30 km) from the former ice front, windblown silt dominates. In the Fairbanks area 60 mi (96.5 km) away, no sand facies of Delta age is known, but thick deposits of Delta-age silt are present.

After the Delta Glaciation, the glaciers retreated, tree line rose, eolian deposition decreased, and base level was probably lowered as the Tanana River cut into its valley fill. The sand cover on the lower hills and loess in the Fairbanks area were gullied.

The Donnelly Glaciation occurred in late Quaternary (Wisconsinan) time, and valley glaciers again pushed north from the Alaska Range to the Tanana River valley. In the Delta River area, the glacier terminated near Donnelly Dome. Strong winds again blew sand and silt from valley trains and outwash plains to cut ventifacts. Ventifacts formed during this glaciation occur much farther south than those associated with the more extensive Delta Glaciation and are within 1 to 5 mi (1.6 to 8 km) of the Donnelly ice front. Sand dunes were limited to areas near the Delta River (fig. 18), but windblown silt was abundant, and areas north of the Donnelly glacier were blanketed with loess. Near Shaw Creek bluff and Shaw Creek Flats, thin loess covered the sand dunes and gullied sand blanket of the hillslopes. In post-Wisconsinan time, additional loess blanketed dunes and moraines of Wisconsinan age.

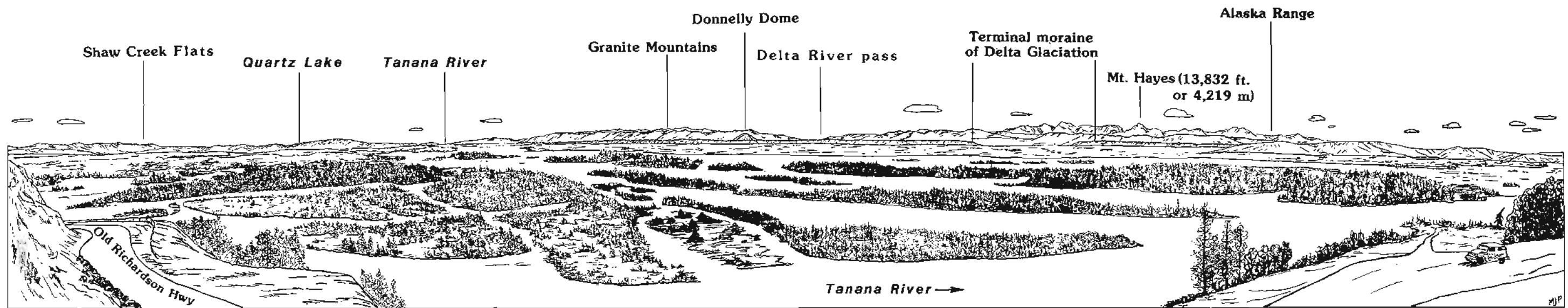


Figure 16. Panoramic view from Shaw Creek bluff of the Alaska Range, glacial moraines, and the broad, braided Tanana River. The terminal moraine of the Delta Glaciation is represented by a 200-ft-high (60 m) ridge on the south side of the Tanana River 8 mi (13 km) south of Shaw Creek bluff. The glacier that deposited this moraine emerged from the Delta River valley in the Alaska Range (sketch by M.J. Pêwé).

Unconsolidated sediments overlying the schist in the road cut at Shaw Creek bluff illustrate, in part, the geologic history of the area (fig. 20). Silt and sand that cover the hillside thicken downslope. Overlying the schist is a 1- to 2-ft-thick (0.3 to 0.6 m) calcareous solifluction layer with no ventifacts and rare pods of gray sand. Overlying the solifluction debris is a gray, coarse- to medium-grained sand layer a few inches thick on the upslope end of the exposure that thickens to more than 5 ft (1.5 m) downslope. Many ventifacts were incorporated during retransportation of the sand downslope. The ventifacts are cut and polished and are from 0.3 in. (0.6 cm) to more than 12 in. (30.5 cm) in diameter. The ventifacts have a 0.1-in.-thick (1 mm) calcium-carbonate coating on their lower sides.

Overlying the sand with a fairly sharp break is loess less than 1 ft (0.3 m) thick upslope but thickening to 5 ft (1.5 m) downslope. A Subarctic Brown Forest soil profile about 10 in. (51 cm) thick is present on the loess. No ventifacts occur in the loess.

The solifluction layer may indicate a cold period and glacial advance during pre-Delta time. The ventifacts and sand are of Delta age. In the warm period that followed sand deposition and ventifact formation, the ground was not perennially frozen, and downward-percolating surface water deposited calcium carbonate on the ventifacts. In Donnelly time, the sand and ventifacts were buried by a loess blanket deposited on the hills. An alternative interpretation is that the earlier cold period occurred during Delta time, and thus the ventifacts and sand are of Donnelly age.

296.7. STOP 6. SHAW CREEK ROAD.

About 0.6 mi (1 km) from the Richardson Highway north on the Shaw Creek Road [on the bluffs on the west side of Shaw Creek Flats at an elevation of 950 ft (289.2 m)], only 50 ft (15.2 m) above the present level of the Tanana River, a borrow pit cuts across two low ridges and exposes a 170-ft-long (51.8 m) section of sediments of mid- to late Quaternary age (fig. 21). A calcareous layer of solifluction debris that is from 0.5 ft (0.15 m) to more than 4 ft (1.2 m) thick and composed of weathered and fractured bedrock has been transported a short distance down the gentle bedrock surface toward Shaw Creek Flats and unconformably overlies augen gneiss bedrock.

Wedges and pockets of unbedded, medium-grained sand mixed with smaller rock fragments and measuring 1 to 4 ft (0.3 to 1.2 m) long by 0.5 to 1 ft (0.2 to 0.3 m) wide occur as ice-wedge casts in the solifluction material. This sand fill contains no ventifacts, is more poorly sorted, and is more silty than the overlying bedded sand. The solifluction deposit is complex in the shallow valley between the two ridges, and there appears to be a gully filled with solifluction debris and large pockets and masses of pebbly sand with weathered rock fragments. Several stream pebbles of dark, fine-grained mafic rock (unlike the bedrock of the exposure) are also evident. The pebbles are polished but not cut by windblown sand.

A well-developed and extensive ventifact layer 1 to 4 in. (2.5 to 10 cm) thick unconformably overlies bedrock, the solifluction layer, and the sand wedges and pockets. Ventifacts of vein quartz from the bedrock are well faceted and polished. They form an almost continuous horizontal sheet and

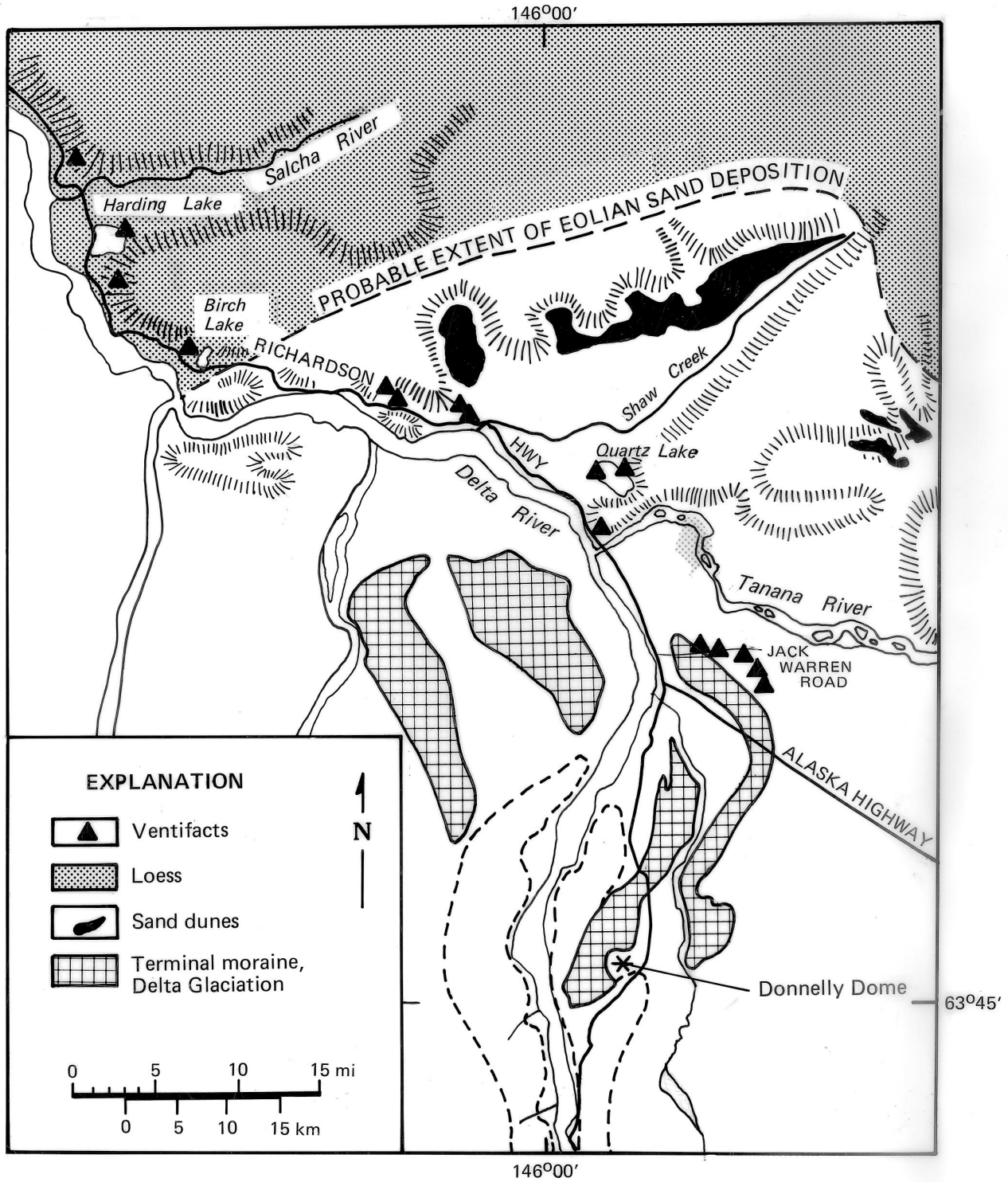


Figure 17. Distribution and types of eolian deposits in the Big Delta area, Alaska, in relation to the Delta Glaciation (from Pêwê, 1965, fig. 4-19).

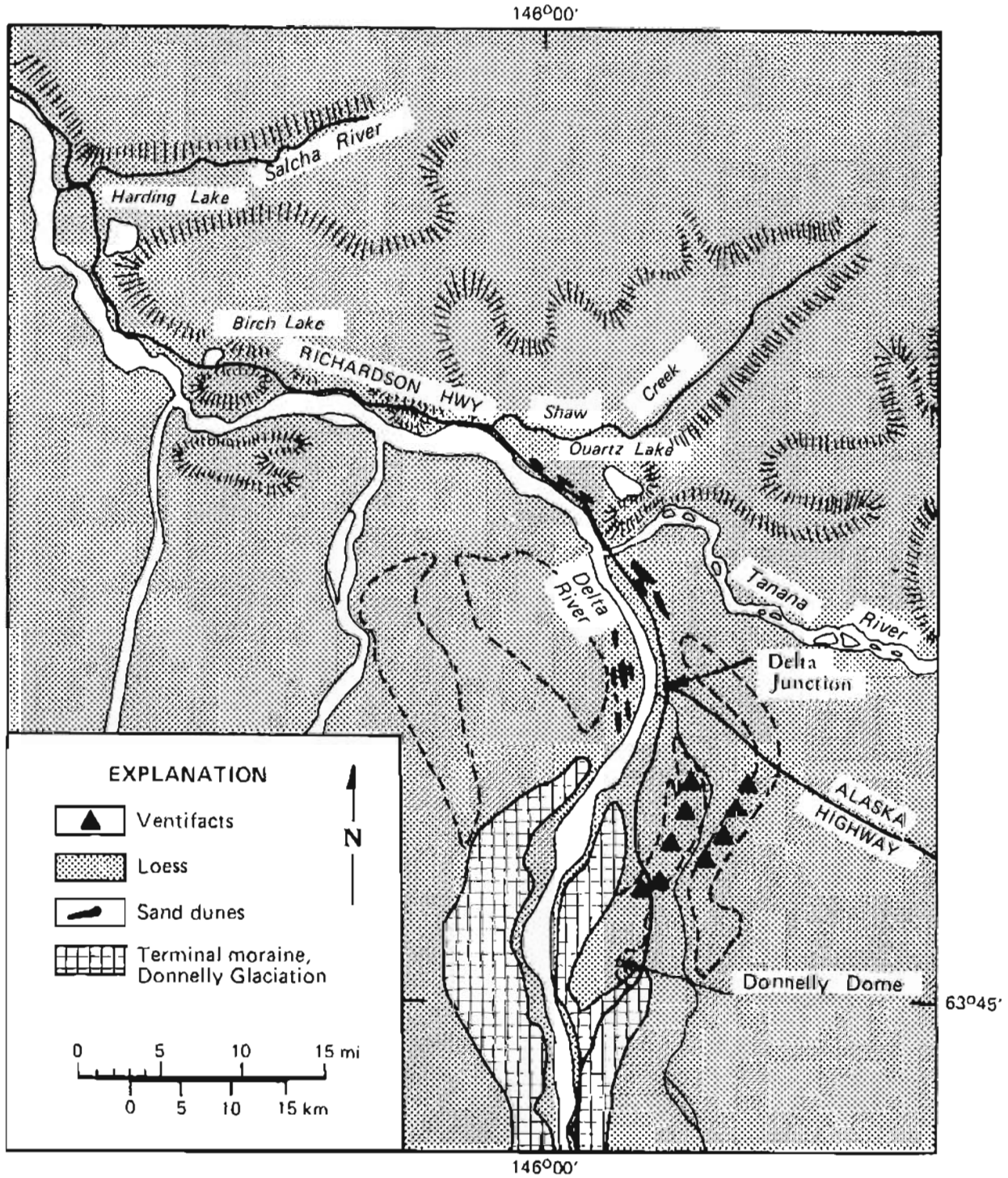


Figure 18. Distribution and types of eolian deposits in the Big Delta area, Alaska, in relation to the Donnelly Glaciation (from Péwé, 1965, fig. 4-20).



Figure 19. View (to the east) of stabilized sand-dune complex north of Shaw Creek Flats between Rosa and Keystone Creeks, Big Delta B-5 Quadrangle, Alaska. Note very steep, north-facing slip slopes that are up to 200 ft (60 m) high. Photograph 54-2 by R.D. Reger, September 15, 1976.

range from 0.5 to 6 in. (0.2 to 15.2 cm) in diameter. The largest and most striking ventifact is also the only one of exotic lithology; it is a 6-in.-diameter (15.2 cm) ventifact of black chert found in the gully area overlying pebbles of transported mafic rock. Ventifacts and rock fragments in the solifluction layer and fractured bedrock are coated with calcium carbonate coated on their lower sides.

Overlying the ventifact layer in the center of the exposure is a well-sorted, medium-grained, cross-bedded, gray eolian sand that is a few tenths of an inch thick in the shallow valley and as much as 3.5 ft (9.3 m) thick under the ridges (fig. 21). Several sand- or sand- and loess-filled burrows of Citellus undulatus are present in the sand. Near one burrow, Richard Péwé found a ground-squirrel skull that was identified as Citellus undulatus by R.D. Guthrie, who noted that the mature skull was smaller than skulls of mature modern ground squirrels.

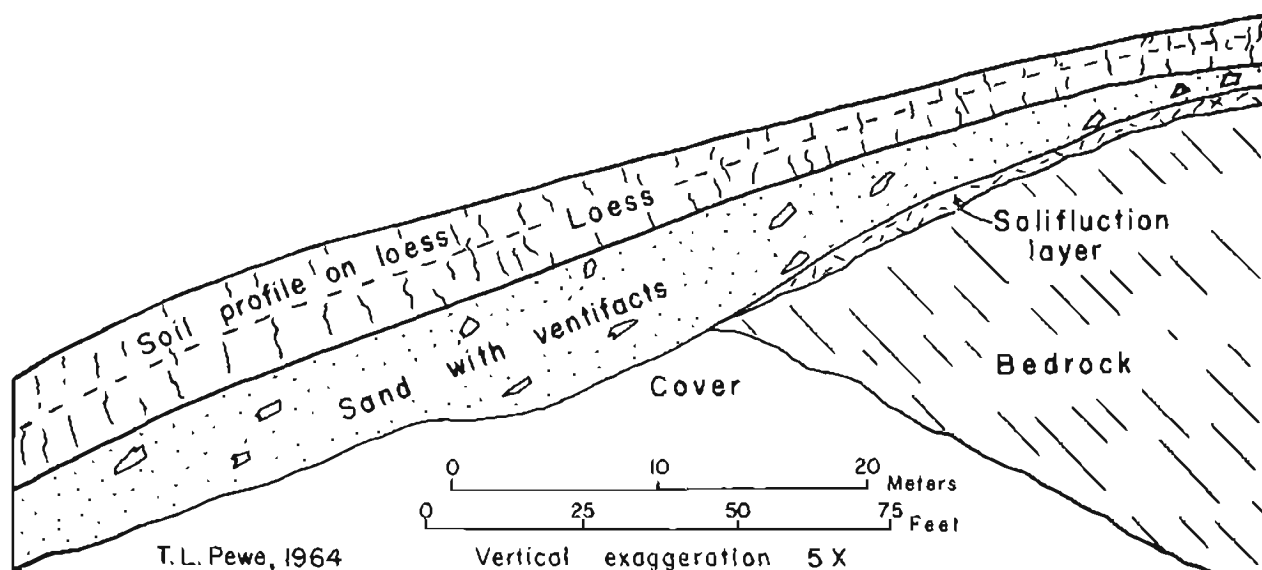


Figure 20. Roadcut that exposes loess, eolian sand, ventifacts, and solifluction deposits over bedrock, Shaw Creek bluff, 20 mi (32 km) northwest of Delta Junction, Alaska (from P \acute{e} w \acute{e} , 1965, fig. 4-21).

A 4-ft-thick (1.2 m) blanket of loess unconformably covers sand, ventifacts, and bedrock. A well-developed, 24-in.-thick (61 cm) Subarctic Brown Forest soil is developed in the loess. The loess maintains a vertical face that is perforated by holes of bank swallows. About 2 ft (0.6 m) below the surface at the south end of the section is a thin [0.3-in.-thick (0.6 cm)] charcoal layer dated at $2,565 \pm 290$ yr B.P. (GX-0254).

A record of alternating periods of cold and warmer climates from mid-Quaternary time to the present is represented by sediments in this exposure. Solifluction deposits were formed under a rigorous climate in mid(?)-Quaternary time at the present elevation of 905 ft (289 m), if the area has been tectonically stable. Today, solifluction deposits are actively forming at elevations as low as 3,000 to 3,500 ft (910 to 1,070 m) in the Yukon-Tanana Upland. Ice wedges that formed in the solifluction deposits may have formed during the latter part of the cold period or during a separate cold period after the solifluction deposits were stabilized. In either instance, the mean annual air temperature was probably at least 3°C to 4°C colder than now.

Evidently, some sand was deposited on the hills in the latter part of the cold period. Streams cut in the small gully in the center of the section, and rocks foreign to the area were brought in from upslope.

The cold period was followed by a warmer period, as indicated by the melting of ice wedges and filling of voids by overlying sand and solifluction material (from the collapsing sides of the voids). Residual fragments of vein quartz formed a thin blanket on the surface as the result of a long period of weathering.

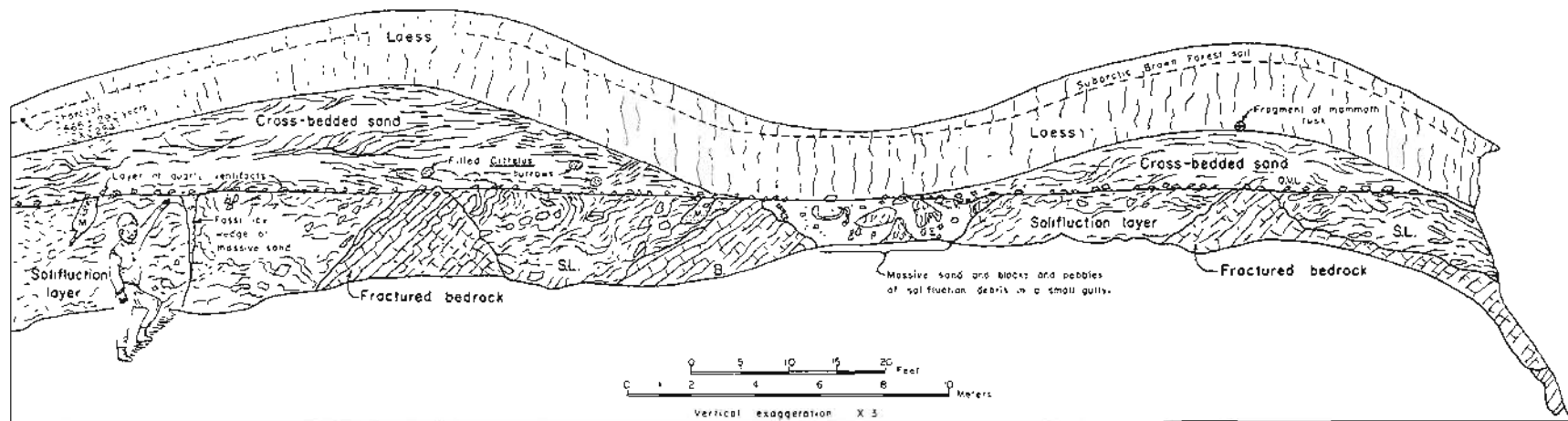


Figure 21. Exposure of a solifluction layer with ice-wedge casts of sand overlain by an extensive ventifact layer in a borrow pit at Mile 0.6 (1 km) on Shaw Creek Road, central Alaska. The ventifacts are overlain by eolian sand, which is blanketed by 4 ft (1.2 m) of loess. QVL, quartz-ventifact layer; SL, solifluction layer; B, fractured bedrock; CV, well-developed chert ventifact; E, stream pebbles of basic dike rock, wind polished but not cut; M, massive unbedded sand. Boy is pointing to layer of quartz ventifacts (from Péwé, 1965, fig. 4-22).

With the return of a more rigorous climate (a cold period probably associated with the Delta Glaciation), sand was blown against the bluff, cutting and polishing the rock fragments. The cutting and polishing is especially well preserved on quartz fragments and other resistant rocks. Eventually, accumulating sand in the form of dunes and a sand blanket covered the bedrock and terminated most ventifact development. Ground squirrels that were abundant at this time indicate near tree-line conditions.

With climatic amelioration, glaciers retreated and sand deposition ceased or greatly decreased. The sand blanket was gullied and in part removed by erosion. In the absence of permafrost, downward-percolating water deposited calcium carbonate on ventifacts and other clasts. Ground squirrels moved to other areas as tree line rose.

Deposition of the loess layer is probably associated with the advance of glaciers during Donnelly time, when outwash plains and valley trains were less vegetated. In the last few thousand years, as the glaciers withdrew and the climate warmed, loess deposition was reduced and a well-developed Subarctic Brown Forest soil formed. Radiocarbon dates indicate the upper layers of loess are relatively young. The sand and loess deposition and ventifact formation may have occurred in Donnelly time.

286.6 to 278. Except for sand dunes near the river, the poorly drained Shaw Creek Flats is underlain by permafrost at shallow depths. Beneath the surface of the Shaw Creek Flats, the Tanana River gravel is overlain by 3 to 9 ft (1 to 3 m) of silty fluvial sand and 3 to 5 ft (1 to 1.5 m) of organic silt (lowland loess). Extensive stands of larch (Larix laricina) and black spruce (Picea mariana) cover much of the terrace. In the center of the flats is a nearly treeless bog, which appears to be a stabilized strangamoor or string fen. Fen vegetation consists mainly of cottongrass tussocks (Eriophorum vaginatum), sedges (Carex spp.), resin birch (Betula glandulosa), and leather-leaf (Chamadaphne calyculata). From the air, distinct patterns of ridges and depressions (palsas) are evident. A few charred stumps indicate that at least the edges of the fen have burned. Most black spruce and larch near the highway are from 50 to 100 yr old.

285. Enter Big Delta A-3 Quadrangle.

283. Enter Big Delta A-4 Quadrangle.

282.5. Sand dunes of late Wisconsinan and Holocene age. For the next 5 mi (8.1 km) (Miles 282.5 to 277.7), the road follows a discontinuous string of 'cliff-head' sand dunes along the edge of a low terrace next to the Tanana River (fig. 18). The dunes are covered by 1 to 5 ft (0.3 to 1.5 m) of loess, but the sand is well exposed in roadcuts.

Physical properties of the tan sand exposed here and the gray sand of Delta age exposed at Mile 287.5 near Shaw Creek bluff (Stop 6) are listed in table 1.

Sand dunes along the edge of the Tanana River were deposited more than 8,000 yr B.P., probably in late Wisconsinan time. They represent the northernmost sand-dune area associated with the Donnelly glacial advance in the lower Delta River area (fig. 17).

Table 1. Physical properties of eolian sand exposed at Shaw Creek Flats and near Shaw Creek bluff, central Alaska.

	Shaw Creek Flats (Mile 282.5, Richardson Highway)	Near Shaw Creek bluff (Mile 296.7, old Richardson Highway)
Mineralogy	73% quartz	63% quartz
Roundness	Approximately 75% angular to subangular grains	Approximately 75% angular to subangular grains
Sphericity	32% of grains have high sphericity	75% of grains have high sphericity
Luster	89% of grains have dull luster	75% of grains have dull luster
Sorting	Well sorted	Well sorted
Mean diameter	1.47 mm	2.27 mm
Color	Tan	Gray

278.9. About 2 mi (3.2 km) northeast (left) is Quartz Lake (fig. 2), which is similar to Harding, Birch, and other lakes on the north side of the central Tanana River valley, because it probably formed on the upper gravel terrace in late Quaternary time. Quartz Lake is a shallow [40-ft-deep (12 m)] lake dammed on the west side by alluvium of the Tanana and Delta Rivers (fig. 2). Examination of the gravel alluvium in ice-shoved ramparts around the lake reveals numerous cobbles of quartz, diorite, granite, and other rocks of the Alaska Range; these cobbles are up to 6 in. (15 cm) in diameter and are wind faceted, grooved, and polished (fig. 22A, B). The presence of wind-cut cobbles of Alaska Range rock types at this location suggests that in Delta time the outwash plain from the glacier extended as far as the present lake. The cobbles were cut by windblown sand when the broad outwash plain was scantily vegetated and sand was easily transported. These wind-cut cobbles are probably the same age as ventifacts examined at earlier stops in the vicinity of Shaw Creek bluff. No detailed work has been done on the origin and age of Quartz Lake, and much work, especially pollen analysis, is necessary to provide more evidence of origin and age.

278.1. To the left is the U.S. Army pumping station for the 10-in.-diameter (25.4 cm) fuel line from Haines to Fairbanks. To the right, the section in the river-terrace scarp exposes late Quaternary sediments:

Top

0 to 4 ft 1.2 m)	Loess with forest-fire layers. Radiocarbon date on (0 to charcoal near base of loess is 8,040 ± 190 yr B.P. (GX-0255).
4 to 9 ft (1.2 to 2.7 m)	Tan, fine-grained, cross-bedded eolian dune sand.
9 to 13 ft (2.7 to 4 m)	Buff, fluvial sandy silt.



Figure 22A. Exposure of ice-shoved rampart on the southwest side of Quartz Lake, middle Tanana River valley, central Alaska. Removal of forest cover has revealed outwash gravel that contains many cobbles that have been faceted by the wind. Photograph 574 by T.L. Pêwé, July 27, 1951.

13 to 19 ft Rounded pebble gravel from Tanana River.

(4.0 to 5.8 m)

277.7. End of sand dunes of Donnelly age along river.

275.7. To the left is the former location of Bert and Mary's Roadhouse, which was built in 1949. For 15 yr, a large log lodge (deformed by thawing of permafrost) existed at this spot (fig. 23). The roadhouse was torn down in 1964.

275.5. To the right, a hill of schist is covered by a cap of Wisconsin loess that has slumped.

275.3. STOP 7. TANANA RIVER BRIDGE.

Confluence of the braided Delta River and the Tanana River and crossing of the Tanana River by the elevated Trans-Alaska Pipeline System (TAPS) (fig. 24).



Figure 22B. Sand-blasted, faceted, and grooved cobbles of rock types from the Alaska Range in glacial outwash from ice-shoved ridge on the southwest side of Quartz Lake, middle Tanana River valley, central Alaska. Photograph 577 by T.L. Pêwê, July 27, 1951.

Selected References

- Ager, T.A., 1972, Surficial geology and Quaternary history of the Healy Lake area, Alaska: Fairbanks, University of Alaska, M.S. thesis, 127 p.
- _____, 1975, Late Quaternary environmental history of the Tanana River valley, Alaska: Columbus, Ohio State University, Ph.D. thesis, 117 p.
- _____, 1983, Holocene vegetational history of Alaska, *in* Wright, H.E., Jr., ed., *Holocene environments of the United States*: Minneapolis, University of Minnesota Press [in press].
- Blackwell, J.M., 1965, Surficial geology and geomorphology of the Harding Lake area, Big Delta Quadrangle, Alaska: Fairbanks, University of Alaska, M.S. thesis, 91 p.
- Bundtzen, T.K., and Reger, R.D., 1977, The Richardson lineament--A structural control for gold deposits in the Richardson mining district, interior Alaska, *in* Short notes on Alaskan geology - 1977: Alaska Division of Geological and Geophysical Surveys Geologic Report 55, p. 29-34.
- Esch, D.G., and Livingston, H.R., 1978, Performance of a roadway with a peat underlay over permafrost: Alaska Department of Transportation Division of Research and Development Report AK-RD-78-1, 62 p.



Figure 23. Bert and Mary's Roadhouse, Richardson Highway, 80 mi (133 km) southeast of Fairbanks, Alaska. This large log cabin with a full concrete basement was built in 1949 on ice-rich loess typical of the southern Yukon-Tanana Upland. A furnace in the front of the building (in the basement) provided heat, but the attached front porch and rear service building were not heated. The front of the heated structure subsided the most and the fastest. The porch and utility buildings did not subside immediately, but were dragged down as the rest of the building settled. In 1964, the entire building was razed. Photograph 2073 by T.L. Pêwê, May 29, 1962.

- Hudson, Travis, and Weber, F.R., 1977, The Shaw Creek fault, east-central Alaska, *in* Blean, K.M., The U.S. Geological Survey in Alaska: Accomplishments during 1976: U.S. Geological Survey Circular 751-B, p. B33-B34.
- Krieg, R.A., and Reger, R.D., 1982, Air-photo analysis and summary of landform soil properties along the route of the Trans-Alaska Pipeline System: Alaska Division of Geological and Geophysical Surveys Geologic Report 66, 149 p.
- McHattie, R.B., 1980, Highway pavement cracks---an Alaskan overview: *The Northern Engineer*, v. 12, no. 4, p. 17-21.
- Nakao, Kinshiro, LaPerriere, J., and Ager, T.A., 1980, Climatic changes in the interior of Alaska, *in* Nakao, Kinshiro, ed., Report of the Alaskan Paleolimnology Research Project, 1977/78/79: Laboratory of Hydrology, Department of Geophysics, Hokkaido University, p. 16-23.
- Pêwê, T.L., 1955a, Middle Tanana River valley, *in* Hopkins, D.M., Karlstrom, T.N.V., and others, Permafrost and ground water in Alaska: U.S. Geological Survey Professional Paper 264-F, p. 126-130.
- _____, 1955b, Origin of the upland silt near Fairbanks, Alaska: *Geological Society of America Bulletin*, v. 66, p. 699-724.

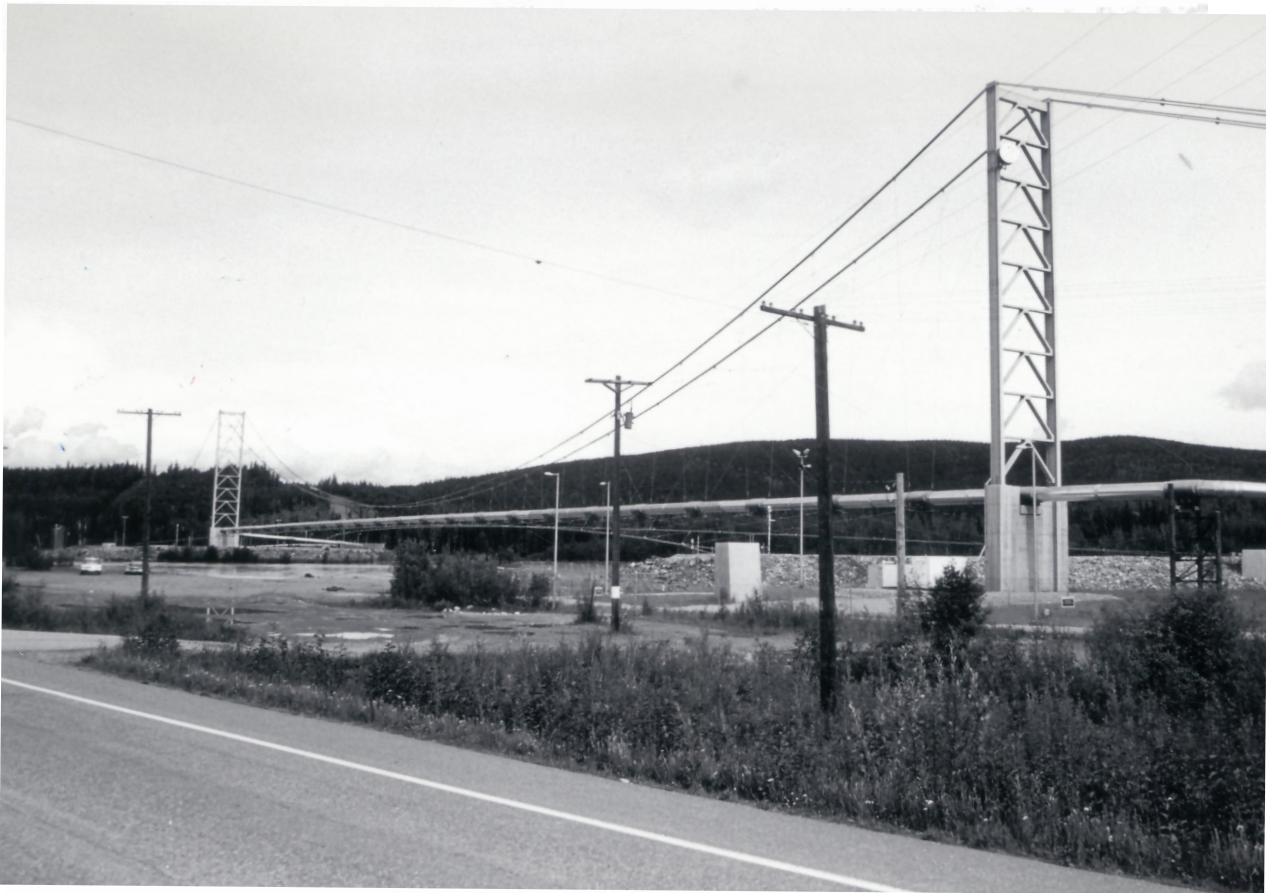


Figure 24. View (to the northeast) of elevated crossing of the Tanana River by the Trans-Alaska Pipeline System (TAPS), Big Delta A-4 Quadrangle, Alaska. Photograph 83-14 by R.D. Reger, July 20, 1981.

Péwè, T.L., 1958, Geology of the Fairbanks (D-2) Quadrangle, Alaska: U.S. Geological Survey Geologic Quadrangle Map GQ-110, scale 1:63,360, 1 sheet.

_____, 1965, Middle Tanana River valley, in Péwè, T.L., Ferrians, O.J., Jr., Karlstrom, T.N.V., and Nichols, D.R., Guidebook for field conference F, central and south-central Alaska, International Association for Quaternary Research: 7th Congress, Fairbanks, 1965: Lincoln, Nebraska Academy of Science, p. 36-54 (reprinted 1977, College, Alaska Division of Geological and Geophysical Surveys).

_____, 1975a, Quaternary stratigraphic nomenclature in central Alaska: U.S. Geological Survey Professional Paper 862, 32 p.

_____, 1975b, Quaternary geology of Alaska: U.S. Geological Survey Professional Paper 835, 145 p.

Péwè, T.L., and Bell, J.W., 1975a, Map showing distribution of permafrost in the Fairbanks (D-1 SW) Quadrangle, Alaska: U.S. Geological Survey Miscellaneous Field Studies Map MF-671A, scale 1:24,000, 1 sheet.

_____, 1975b, Map showing distribution of permafrost in the Fairbanks (D-2 SE) Quadrangle, Alaska: U.S. Geological Survey Miscellaneous Field Studies Map MF-669A, scale 1:24,000, 1 sheet.

- Péwé, T.L., Bell, J.W., Forbes, R.B., and Weber, F.R., 1976, Geologic map of the Fairbanks (D-2 SE) Quadrangle, Alaska: U.S. Geological Survey Miscellaneous Geologic Investigations Map I-942, scale 1:24,000, 1 sheet.
- Péwé, T.L., Burbank, Lawrence, and Mayo, L.R., 1967, Multiple glaciation of the Yukon-Tanana Upland, Alaska: U.S. Geological Survey Miscellaneous Geologic Investigations Map I-507, scale 1:500,000, 1 sheet.
- Skarland, Ivar, and Giddings, J.L., Jr., 1948, Flint stations in central Alaska: *American Antiquity*, v. 14, p. 116-120.
- Taber, Stephen, 1943, Perennially frozen ground in Alaska: Its origin and history: *Geological Society of America Bulletin*, v. 54, p. 1433-1548.
- Weber, F.R., Foster, H.L., Keith, T.E.C., and Dusel-Bacon, Cynthia, 1978, Preliminary geologic map of the Big Delta Quadrangle, Alaska: U.S. Geological Survey Open-file Report 78-529A, scale 1:250,000, 1 sheet.
- Weber, F.R., Hamilton, T.D., Hopkins, D.M., Repenning, C.A., and Haas, Herbert, 1981, Canyon Creek: A late Pleistocene vertebrate locality in interior Alaska: *Quaternary Research*, v. 16, no. 2, p. 167-180.

DELTA RIVER AREA, ALASKA RANGE

By
Troy L. Péwé⁹ and Richard D. Reger¹⁰

Résumé of the Permafrost and Quaternary Geology

The Alaska Range is a glacially sculptured, arcuate mountain wall extending west and southwest 620 mi (1,000 km) from the Canadian border to the Aleutian Range. It is composed of a core of Precambrian or lower Paleozoic schist and gneiss, and the higher mountains are supported by granitic intrusions of Mesozoic age. The range is flanked by and in part made up of sedimentary and volcanic rocks of Paleozoic and Mesozoic age. On the lower flanks of the range and underlying adjoining lowlands are weakly consolidated, coal-bearing conglomerate, sandstone, and claystone of Tertiary age. The range is extremely rugged and includes Mt. McKinley [20,300 ft (6,195 m) elevation], the highest mountain on the North American continent. In the central Alaska Range, Mt. Hayes, Mt. Deborah, Mt. Hess, and Mt. Kimball are prominent peaks. The Delta River originates on the south side of the range in the Tangle Lakes and flows north. The Richardson Highway (fig. 25) crosses the range through the Delta River valley.

The Alaska Range is characterized by spectacular valley glaciers 1 to 40 mi (1.6 to 65 km) long (fig. 26). The glaciers are largest and most numerous on the south side of the range, where they are nourished chiefly by air masses moving north to northeast from the northern Pacific Ocean. On the south-central side of the range, modern snowline is at about 5,500 ft (1,670 m) elevation; on the north side it is 6,500 ft (1,980 m) elevation.

At least four Quaternary glaciations, each apparently less extensive than the previous, are recorded in the Delta River area of the central Alaska Range. Glaciers pushed south and north from the crest of the range, and some of the ice on the south side exited north through the Delta River valley. On the north side, the glaciers largely remained in mountain valleys, spreading terminal bulbs onto the lowland of the Tanana River valley. On the south side, glaciers coalesced to form large piedmont ice sheets that covered the lowlands and pushed south into the Copper River basin.

The earliest recognized glacial advance is the Darling Creek Glaciation of early Quaternary age. It is identified from patches of drift 2,000 to 3,000 ft (610 to 920 m) above the floor of the Delta River valley and from isolated erratics up to 15 ft (4.6 m) in diameter in the Amphitheater Mountains on the south side of the Alaska Range. The succeeding glacial advance was the Delta Glaciation, recognized by fairly well-preserved breached moraines on the north side of the range. On the south side, the glaciers of this mid- to late Quaternary advance did not cover all small peaks of the foothills and extended well into the Copper River basin.

The next two glacial advances occurred in late Quaternary (Wisconsinan) time and are closely related in extent and age. On the north side of the

⁹Department of Geology; Arizona State University; Tempe, Arizona 85281.

¹⁰DGGS; 794 University Avenue, Suite 200; Fairbanks, Alaska 99709-3645.

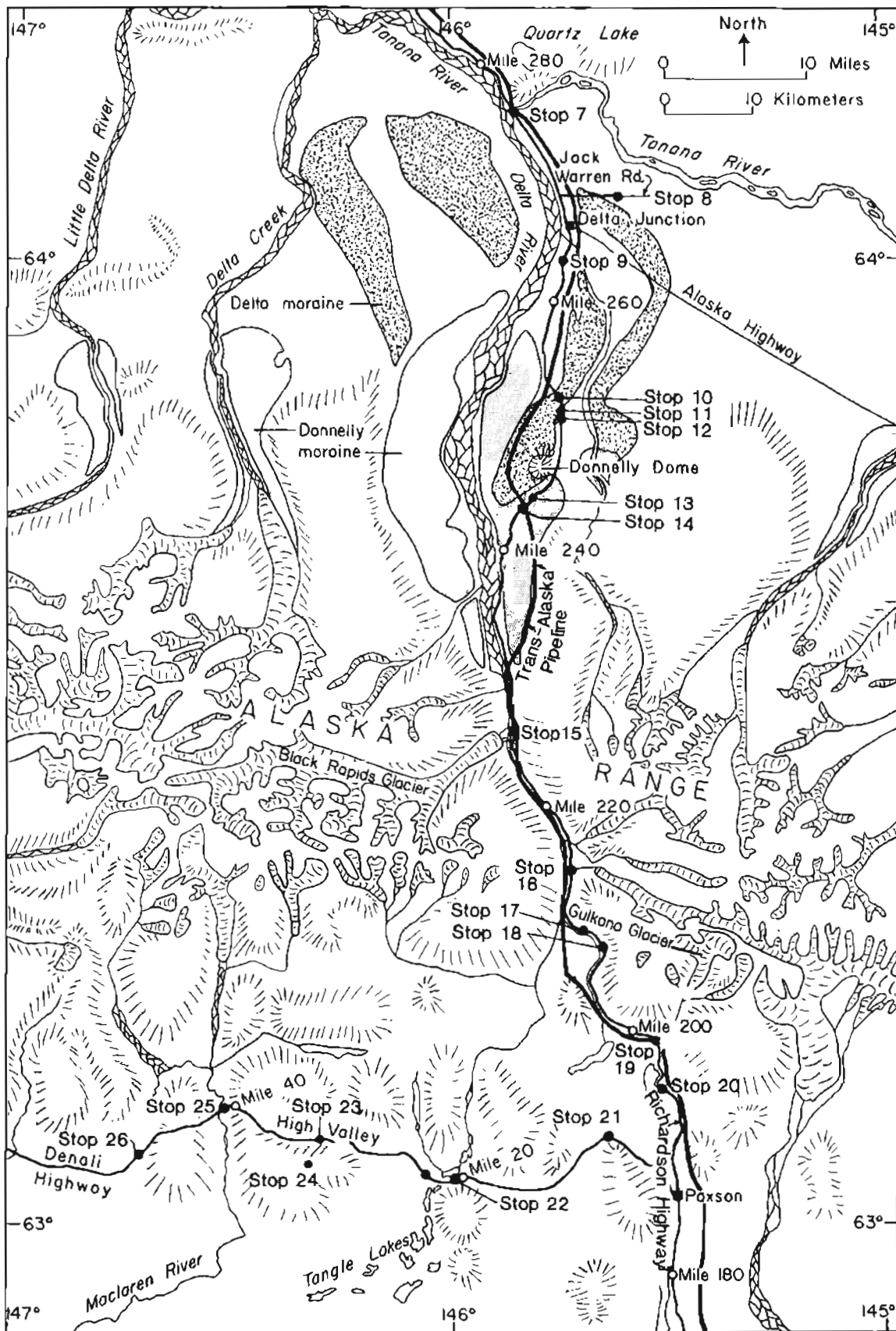


Figure 25. Index map of the Delta River area, Alaska Range, showing field-trip stops.



Figure 26. Oblique aerial view (to the south) of Gilliam Glacier, Hess Mountain [11,940 ft (3,618 m)], and Mount Deborah [12,339 ft (3,739 m)], north-central Alaska Range, Healy Quadrangle, Alaska. Photograph 665LT-55RT-M864-55SRW-9M58 by the U.S. Air Force, August 29, 1949.

Alaska Range, they have been grouped into one broad glaciation, termed the Donnelly Glaciation; on the south sides they have been named the Denali I and Denali II Glaciations. On both sides of the range, these deposits are characterized by fresh knob-and-kettle topography. On the south side, especially in the vicinity of Tangle Lakes, are hundreds of square miles of fresh ice-contact features formed when broad sheets of the ice stagnated.

In Holocene time, a small glacial advance that is especially well represented on the south side of the range occurred. Glacial advances of the last

few centuries have left morainal loops within a few hundred yards to a few miles of the present glaciers.

Road Log and Locality Description

273.¹¹ Outwash fan of Donnelly Glaciation, the bulk of which was deposited before 18,000 to 20,000 yr B.P. Elongate sand dunes 1 to 1.5 mi (1.6 to 2.4 km) long that occur on the outwash fan 0.5 to 1 mi (0.8 to 1.6 km) east of the Richardson Highway are dated at about 19,000 yr B.P. (figs. 18 and 27). The dunes are about 30 ft (9.8 m) high and 100 ft (30 m) wide at the base and



Figure 27. View down an elongate sand dune (late Donnelly age) covered with a forest of white spruce. Depth to permafrost in the sand dune is more than 5 ft (1.5 m). On each side of the dune, a black-spruce forest grows with a 12-in.-thick mat (0.3 m) of *Sphagnum* on silt. Permafrost occurs immediately under the moss in the silt. This dune (one of a series) is located 1 mi (1.2 km) east of the Richardson Highway at Mile 273.1 (sec. 15, T. 9 S., R. 10 E.), Big Delta A-4 Quadrangle. Photograph 572 by T.L. Péwé, June 26, 1951.

¹¹Miles from Valdez on the Richardson Highway.

covered with 3.5 ft (1 m) of loess. They are composed of brown, well-sorted, fine sand.

268.3. STOP 8. JACK WARREN ROAD 1.3 MI (2 KM) EAST OF RICHARDSON HIGHWAY.

In front of the Delta-age terminal moraine is an outwash plain with well-developed ventifacts (fig. 18) under a thin cover of eolian silt and sand.

267. An abandoned channel of Jarvis Creek that, by radiocarbon dating, is older than 380 yr and younger than 3,400 yr B.P. At this locality, the abandoned channel is used as an airfield.

266. Delta Junction. End of the Alaska Highway, Mile 1422. Delta Junction is built on coarse alluvium deposited by Jarvis Creek and inset into Donnelly outwash. Radiocarbon dates indicate the upper part of the sand and gravel is younger than 3,400 yr B.P.

The Delta Junction area has a high frequency of strong winds compared to other places in interior Alaska, especially in the winter. A 20-yr record of wind data from the Federal Aviation Administration (FAA) station 3.3 mi (5.3 km) south of Delta Junction indicates that the mean wind velocity is about 9.3 mi per hr (4.2 m per s), compared to 5 mi per hr (2.2 m per s) at Fairbanks. During winter, strongest winds prevail from the east and winds blow from the eastern quadrant more than 90 percent of the time. Annually, calm periods occur only 13 percent of the time. During summer and fall, when sand and silt are available for entrainment by winds sweeping across river bars, strongest winds blow from southern and eastern quadrants, particularly from the east-southeast and south-southwest. From 1977 through 1979, strongest summer winds measured 34.2 mi per hr (15.4 m per s) from the south (May 19, 1977). The strong directional preference of winds at Delta Junction results from its close proximity to the upper Tanana River valley, which trends east-southeast, and the Delta River valley, which is south-southwest of town. Both valleys serve as conduits relieving strong pressure gradients developed north and south of the Alaska Range.

264.8. Jarvis Creek. On windy days, dust is blown from this small flood plain. A loess ridge that is several feet high has been built on the north side of the creek.

The vegetation successional stages are somewhat different on the Delta River and its tributaries than on the finer alluvial deposits of the Tanana River. Early successional stages are longer and include both the dwarf and narrow-leaved fireweed (Epilobium latifolium and E. angustifolium), several legumes, the most conspicuous of which are Hedysarum spp., Astragalus spp., and Oxytropis spp., the avens Dryas drummondii and D. octopetala, buffaloberry (Shepherdia canadensis), and several species of willow. This early pioneer stage is often replaced by a nearly continuous cover of forbs and grasses, of which Festuca spp., Elymus inovatus, and Agropyron spp. are the most common. These early successional stages are an important source of food for the buffalo herd that was introduced in the Big Delta area in the 1920s. The original herd of 15 bison has increased to more than 500 animals.

Balsam poplar invades and replaces the meadow stage, and the poplar is succeeded by white spruce. On most coarse-gravel surfaces, white spruce may persist indefinitely or may be eventually replaced by black spruce in a manner similar to that described for the Fairbanks area.

Directly to the south, Donnelly Dome can be seen 10 mi (16 km) away (fig. 28).

264.6. Edge of outwash plain from the main lobe of the Donnelly-age ice advance.



Figure 28. View (to the south) of the Alaska Range, with Donnelly Dome in the middle ground and Donnelly-age outwash plain in the foreground. Jarvis Creek passes near Ft. Greely in the foreground. Photograph by U.S. Army Air Corps.

263.2. Enter Mt. Hayes D-4 Quadrangle. (Refer to Péwé and Holmes, 1964).

Permafrost is sporadic in the broad, gently sloping outwash plain from the moraine south of Ft. Greely to the Tanana River 12 mi (19.2 km) north of Ft. Greely (fig. 29). Isolated masses of frozen ground exist in places from 3 to 40 ft (1 to 13 m) below the ground surface; the base of permafrost ranges from 10 to 118 ft (3.1 to 35 m) in depth. Drilling at Ft. Greely indicates the permafrost is in sandy gravel 10 to 40 ft (3.1 to 12 m) below the surface. Most permafrost lies above the present water table. The abandoned channel of Jarvis Creek west of Delta Junction is probably free of permafrost.

Between Delta Junction and the Tanana River, the silt cover thickens to 10 ft (3 m). The lower part of the silt is perennially frozen, as is the underlying gravel, to depths of 20 to 30 ft (1.8 to 10.2 m). In isolated areas north of Delta Junction---where the microclimate is exceptionally cold for this area---small, active ice wedges are present in the silty sand of the outwash fan.

The depth to the water table beneath this sloping outwash plain ranges from 180 ft (54 m) at Ft. Greely to 80 ft (24.5 m) at Delta Junction [5 mi (8 km) north] to 10 ft (3.1 m) at Big Delta at the Tanana River (fig. 29). Annual fluctuation of the water-table depth ranges from 50 to 60 ft (15.5 to 20.4 m) in the Fort Greely area to 2 to 3 ft (0.7 to 1 m) at Big Delta.

Ground water is apparently recharged in late spring and early summer when ground thawing permits penetration of meltwater from the mountains. Some water moving northward in the outwash gravel emerges as springs in the scarp on the south side of the Delta River. A perennial spring flow keeps some creeks and part of the Tanana River unfrozen during winter.

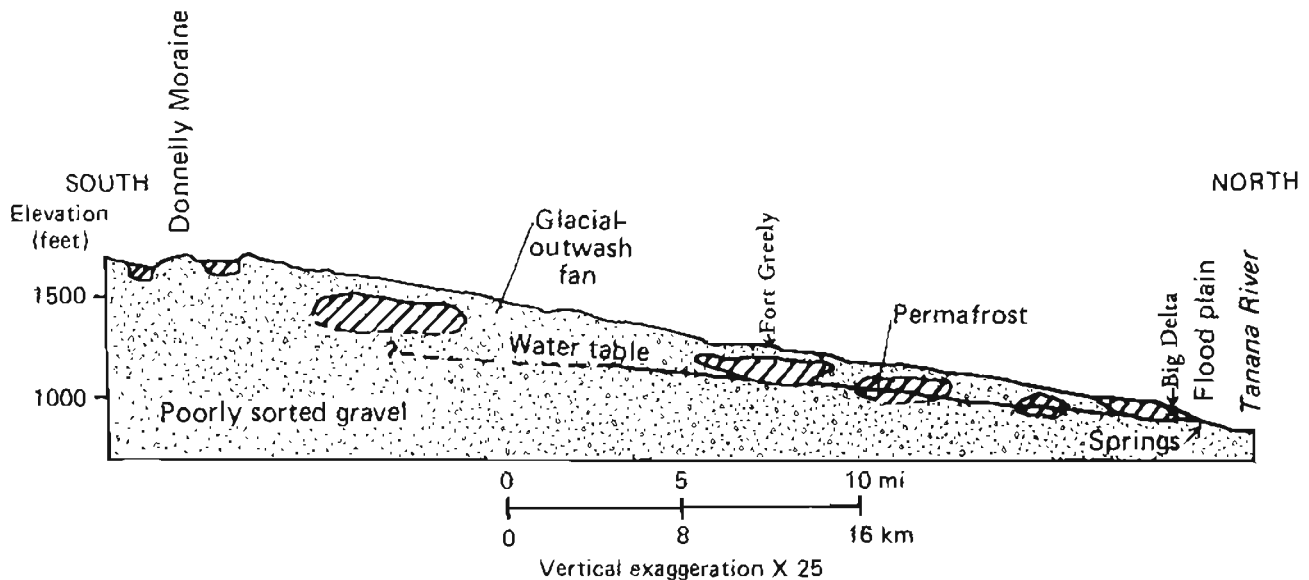


Figure 29. Diagrammatic cross section of probable permafrost and ground-water distribution in the Big Delta area, Alaska (from Péwé, 1955, fig. 9).

262.7. STOP 9. FAA STATION OVERLOOK.

To the south is a panorama of the Alaska Range; Mt. Hayes is the most prominent peak (fig. 30). Where the braided Delta River comes into view, it has cut through the terminal moraine of the Donnelly Glaciation. Directly west of the overlook, the subdued moraine of Delta age forms the skyline.

261.8. To the left is the entrance to Ft. Greely.

258.8. The gradient of the outwash plain from Ft. Greely south to the Donnelly terminal moraine is 55 ft per mi (10.5 m per km). Outwash sediments range in size from cobbles 4 to 6 in. (10 to 15 cm) in diameter at the end of the outwash plain (Mile 264.4) to boulders 1 or 2 ft (0.3 to 0.6 m) in diameter at the front of the moraine (Mile 256.5).

In this section of outwash, nearly continuous stands of balsam poplar and aspen---in many places with an understory of white spruce---are later replaced by white-spruce stands similar to the area just north of Delta Junction.

257.5. To the right is Meadows Road, which leads to outcrops of loess more than 40 to 50 ft (12 to 15 m) thick along the edge of the Delta River flood plain. Radiometric dates of approximately 7,000 yr B.P. were obtained on wood at the base of the loess.

Deposition of loess along most braided glacial streams in Alaska continues, most notably along the Delta River (fig. 31), along the Knik and Matanuska Rivers, and near the junction of the Tanana and Yukon Rivers. Measurement of loess thicknesses and radiocarbon dating of enclosed stumps and logs yield rates of loess accumulation at various locations (table 2). Assuming no erosion of the accumulating loess during the measured intervals, the rate of accumulation is 0.2 to 2 mm per yr, which Péwé considers valid because the area of accumulation is flat to almost flat and heavily vegetated.

256.5. Front of the Donnelly-age moraine, with a good view of Granite Mountain to the left.

254. Start climbing the subdued moraine of Delta age.

252.7. STOP 10. DELTA MORaine (fig. 32).

The roadcut exposes light-yellowish-brown silty gravel composed of cobbles and boulders of gneiss, granite, diorite, and dark volcanic rocks, with some limestone and schist.

Correlations of glaciations in the eastern and central Alaska Range have been controversial for many years because, until recently, few radiometric dates were available and correlations depended on much less reliable relative-age criteria. The ages of the Delta and Donnelly Glaciations are still vigorously debated. Initially, Péwé (1953) related the Delta Glaciation to early Wisconsinan ice expansions in the mid-continental United States and related the Donnelly Glaciation to late Wisconsinan events. Later, based primarily on relative-age criteria (table 3) and a lack of significant radiocarbon dates, he and his colleagues revised their chronology, correlated the Delta Glaciation with the Illinoian Glaciation of the north-central United



Figure 30. View (to the southwest) of the northeast flank of the central Alaska Range from the FAA station along the Richardson Highway at Mile 262.7. MH, Mt. Hayes, 13,832 ft (4,216 m); MM, Mt. Moffitt, 13,020 ft (3,968 m); D, terminal moraine of Donnelly advance; OW, edge of scarp of outwash plain extending from the Donnelly terminal moraine; DR, Delta River; DE, terminal moraine of the Delta Glaciation. Infrared photograph 409A by T.L. Péwé, August 4, 1949.



Figure 31. Oblique aerial view (to the north) of clouds of silt transported by wind from the Delta River flood plain near Donnelly Dome, central Alaska (from Péwé, 1951, pl. 1-A).

States, and correlated the Donnelly Glaciation with the entire Wisconsin Glaciation (fig. 33).

Attempts by others to map Delta- and Donnelly-age moraines elsewhere along the north flank of the east-central Alaska Range have been frustrated because the type area of these glaciations (the lower Delta River valley) is unique among valleys in the region. First, the Delta River valley cuts across

Table 2. Rates of deposition of Holocene loess along rivers in central Alaska (from P  w  , 1968, table 1).

Area	Location	Source	Measured thickness (m)	Duration accumulation (radiocarbon yr)	Rate of accumulation (mm/yr)
East side of Delta River	Adjacent to east side of flood plain 32-80 km south of Big Delta on terraces and alluvial fans	P��w�� and others 1965, p. 362; Reger and others, 1964, p. 95-96	2.4	1,950±150 (L-163K)	1.14-1.33
			3.8	4,650±250 (L-137Q)	0.78-0.86
			14.0	7,000±275 (L-462)	1.93-2.07
			5.2	5,900±250 (I-646)	0.85-0.92
			3.7	2,300±180 (I-647)	1.49-1.75
North side of Tanana River	Adjacent to north side of river near junction with Delta River a) On south-east-facing slope 1 km from river b) On low terrace at river edge	P��w��, 1965a, p.48-49, 53	a)0.61	2,565±290 (GX-0254)	0.21-0.27
			b)1.2	8,040±190 (GX-0255)	0.15
Fairbanks	Gold Hill 70 m above and 5.4 km north of present Tanana River	P��w��, 1965b, p. 16, 20	6.0	4,020±200 (W-183)	1.40-1.57

the entire Alaska Range. It served as a conduit for ice flowing north from vigorous sources on the south side of the Alaska Range. Thus, the relative extents of Delta- and Donnelly-age glaciers were much different in the Delta River valley than in typical north-flank valleys, which received less precipitation and were less active producers of glacial ice. Second, the Delta River valley is in a transitional zone between terrain to the east, where valleys have obviously been considerably elevated by tectonic activity and deeply dissected in late Quaternary time, and terrain to the west, where the effects of uplift and dissection, although obvious, are less dramatic. Like many valleys in the eastern Alaska Range, no evidence has been found in the Delta River valley or in the adjacent Yukon-Tanana Upland for glaciation that was more extensive than the Delta Glaciation, even though P  w   and his associates have searched the area for many years. Perhaps pre-Delta glaciations



Figure 32. Oblique aerial view (to the southwest) of the outwash plains and moraines of Donnelly age near Donnelly Dome, with the Delta River and Alaska Range in the distance. Field-trip stops are indicated along the Richardson Highway. Photograph 21ORT-55RT-M864-55SRW-MM58 by U.S. Air Force, August 29, 1949.

were less extensive than the Delta Glaciation, or the evidence was destroyed by slope processes or buried by subsequent valley filling. Many valleys west of the Delta River valley contain numerous erratics and glacier-scoured surfaces resulting from pre-Delta glaciations. Third, the lower Delta River valley is subject to heavier eolian deposition than other valleys along the north flank of the Alaska Range. A thick blanket of eolian sand and silt that covers much of the outer Delta moraine in the type area, especially west of the Delta River, masks morainal topography, beyond the thick eolian blanket,

Table 3. Comparison of physiographic and sedimentologic parameters of Delta- and Donnelly-age moraines in the type area (Holmes and Benninghoff, 1957; Pêwê and Holmes, 1964; Pêwê, 1965).

<u>Parameter</u>	<u>Delta moraines</u>	<u>Donnelly moraines</u>
Frontal slope characteristics		
Range of relief (ft)	25-225	50-175
Median of relief (ft)	75	125
Range of slope (%)	1-20	5-33
Median of slope (%)	6.5	13
Morainal width		
Range (mi)	0.7-2.7	0.7-1.9
Mean (mi)	1.36	1.25
Total number of kettles	76	212
Kettles/mi ²	3	16
Closure ^a of kettles (%)		
Less than 25 ft	71	77
25 to 50 ft	29	19
50 to 75 ft	0	4
Total number of bogs and marshes	53	12
Bogs/mi ²	2	1
Average depth of surface- weathering profile (ft)	5-7	1.5-2.5
Content of schist clasts in weathering profile (%)	1-10	25-35
Thickness of silt cover (ft)	0-1.8	0-1.9
Median grain size		
Range (mm)	0.2-21	0.7-10
Mean (mm)	4.1	2.6
Number of samples	39	29
Sorting coefficient		
Range	2-33	2.7-18.4
Mean (mm)	7.9	9.1
Number of samples	32	28
Sand content (dry-wt %)	43	45
Silt and clay content		
Range (dry-wt %)	0-38	5-32
Mean (dry-wt %)	14	17
Number of samples	59	38
Clay content ^c		
Range (dry-wt %)	0-8	0-8
Mean (dry-wt %)	1	2
Number of samples	59	38

^aVertical distance between floor of kettle and highest closed contour line in depression

^bParticles passing through No. 200 mesh sieve

^cParticles less than 0.005 mm in diameter

appear very subdued. However, to the west, beyond the thick eolian blanket, the type-Delta moraine has a form very much like the nearby type-Donnelly moraine. This similar morphology is typical of Delta and Donnelly moraines in

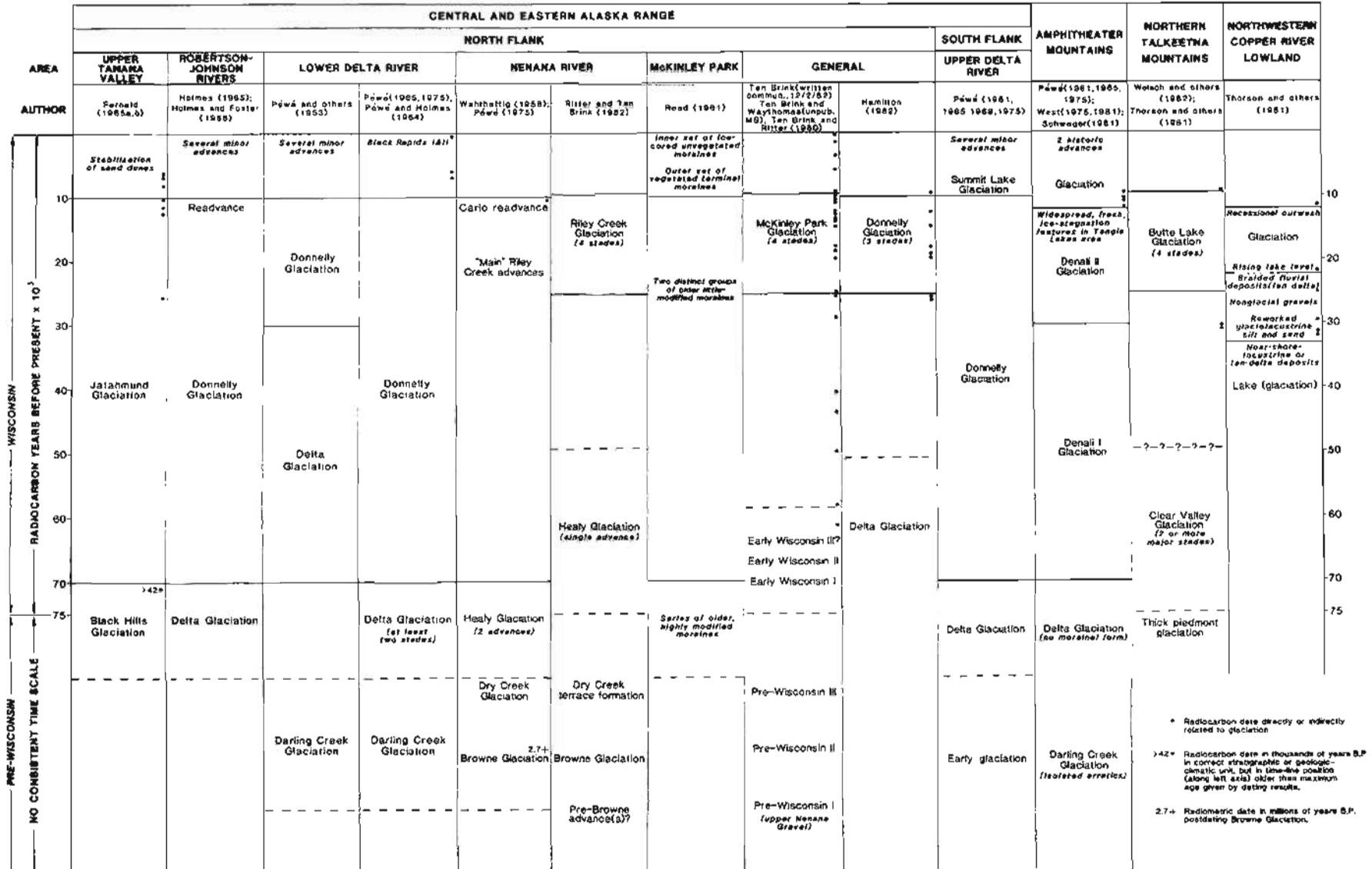


Figure 33. Comparison of glacial chronologies in the east-central Alaska Range and vicinity, Alaska.

most valleys along the north flank of the Alaska Range.

The most dependable criterion for separating Delta and Donnelly moraines is the difference in their weathering profiles (table 3). Delta till is commonly pinkish to light yellowish brown in the weathering zone, which is generally 5 to 7 ft (1.5 to 2.1 m) thick, and schist clasts are less common than in weathered Donnelly till (table 3). Donnelly till is generally light gray, but weathers to light yellowish brown or light olive brown in profiles that average 1.5 to 2.5 ft (0.5 to 0.7 m) in depth (table 3). On Delta moraines, boulder counts are relatively low, and many large boulders are weathered into pinnacled masses (fig. 34). Boulder counts are higher on Donnelly moraines, and clast surfaces are less affected by granular disintegration than on Delta moraines.



Figure 34. Deeply weathered granite boulders on Delta-age moraine 1 mi (1.6 km) north of Donnelly Dome and 1 mi (1.6 km) west of Mile 250 on the Richardson Highway. Photograph 1194 by T.L. Péwé, July 20, 1955.

During the past decade, the age of the Donnelly Glaciation has been well documented by a series of radiocarbon dates related directly or indirectly to this regional event. Samples collected by N.W. Ten Brink and T.D. Hamilton and their colleagues clearly demonstrate that the Donnelly Glaciation began about 25,000 yr B.P. and ended by 9,500 yr B.P. (fig. 33). However, Ten Brink and Hamilton disagree on the number of stades involved in the Donnelly Glaciation. Péwé did not subdivide Donnelly moraines, but has for many years been aware that this glaciation was a multistadial event and still considers it to have spanned all of Wisconsinan time.

The age of the Delta Glaciation remains unsettled (fig. 33). The most recent work by Ten Brink and Hamilton has convinced them that this major ice expansion is early Wisconsinan. However, because soil profiles are much deeper on Delta moraines than on Donnelly moraines, because many Delta moraines appear to be considerably modified by slope processes, and because firm radiocarbon evidence is lacking, Péwé believes the Delta Glaciation pre-dates the last major (Sangamon) interglaciation (fig. 33) and correlates it with deposition of the Gold Hill Loess in the Fairbanks area. In the type area, inner and outer morainal belts document at least two stades within the Delta Glaciation.

251.5. STOP 11. EDGE OF THE DELTA MORaine AND OUTWASH OF DONNELLY AGE (fig. 32).

To the south is a broad lowland of Donnelly-age outwash gravel that slopes north-northeast at a gradient of 93 ft per mi (17.4 m per km) from the terminal moraine of a lobe of the Donnelly-age glacier that stood at the base of Donnelly Dome [4 mi (6.4 km) to the south] about 20,000 yr B.P. The highway ascends the front of this terminal moraine in the distance. To the right, extending from the east shoulder of Donnelly Dome, is a Delta-age moraine (fig. 34) that is continuous with the moraine at this stop (fig. 32). In Delta time, the glacier completely surrounded Donnelly Dome, which formed a nunatak 700 ft (214 m) above the glacial ice. Donnelly Dome is composed of Precambrian or early Paleozoic schist and is a stream- and glacier-modified fault block that lies on the upthrown side of a fault that extends from the 'Dome' eastward into the Granite Mountain area (fig. 32). Granite Mountain is a fault block of quartz monzonite and associated metamorphic rocks. The fault scarp along the front of Granite Mountain is quite prominent and cuts Donnelly-age moraines that were deposited at the base of the mountain by small glaciers originating in short mountain valleys (Péwé and Holmes, 1964). The low-relief surface across the top of Granite Mountain is probably an exhumed erosional surface covered by Tertiary gravel and coal-bearing deposits.

During Wisconsinan time, strong winds blew across the unvegetated outwash plain south of this locality and carried sand that cut, grooved, and polished boulders and cobbles to form ventifacts along the southern flank of the Delta-age moraine. Many of these ventifacts occur on the moraine from this spot north to Ft. Greely (fig. 18).

251.2. STOP 12. POLYGONAL GROUND AND ICE-WEDGE CASTS. Refer to Péwé and others (1969) for a discussion of the origin and paleoclimatic significance of large-scale patterned ground in the Donnelly Dome area.

Large-scale polygons on the outwash plain of Wisconsinan age (Donnelly Glaciation) are outlined by a network of intersecting, trenchlike depressions 1 to 3 ft (0.3 to 0.9 m) deep and 3 to 6 ft (0.9 to 1.8 m) wide. Lichens grow where there is little or no silt in the center of the polygons. Most mixed evergreen-deciduous scrub and shrub vegetation grows in troughs at the edges of the polygons where the silt is thickest. The difference in vegetation types between the polygon centers and troughs delineates the polygonal pattern. The polygons are 80 to 130 ft (24.4 to 39.6 m) in diameter and three to six sided; most are four sided (figs. 35 and 36).

Wedge-shaped masses of fine-grained sediments underlie the slight surface depressions that mark polygon boundaries (fig. 35) and crosscut the massive outwash gravel. These wedges have a wide upper part, a narrow middle section, and an extremely irregular lower part. They extend from 3 to 9 ft (0.9 to 2.7



Figure 35. Oblique aerial view of large-scale patterned ground in outwash gravel in the Donnelly Dome area, Alaska. Vegetation cover is mixed evergreen-deciduous scrub and shrub. Photograph 2021 by T.L. Pêwê, July 14, 1961.

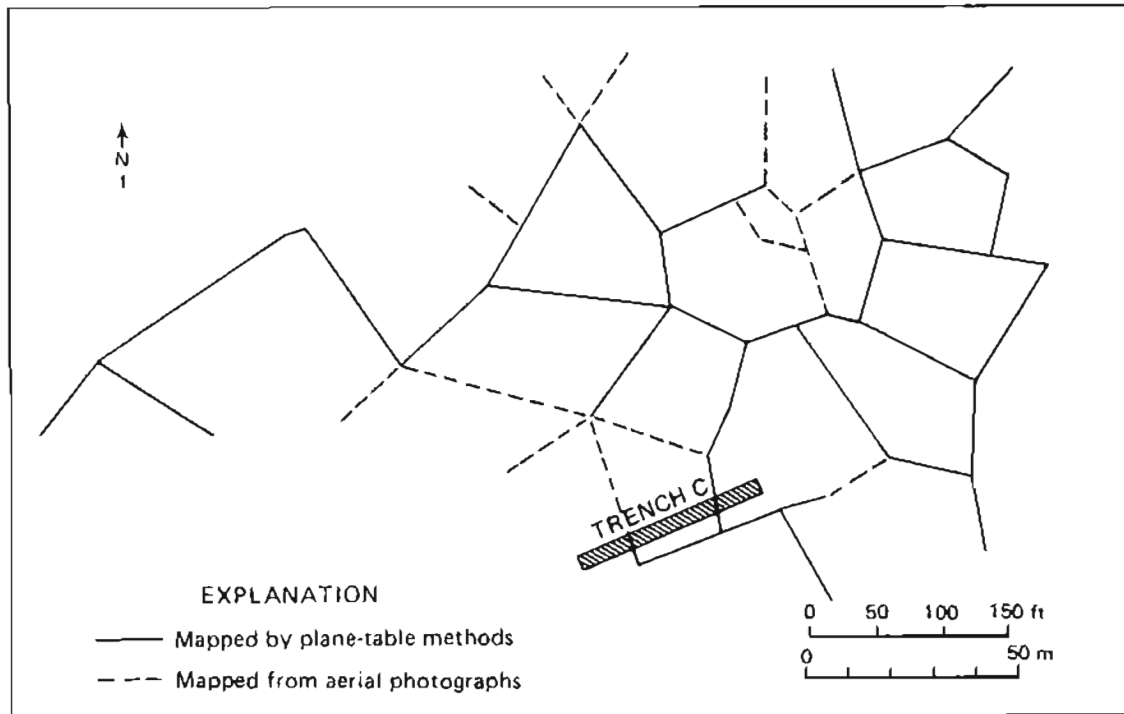


Figure 36. Plane-table map of large-scale polygons, Donnelly Dome area, Alaska (modified from Péwé and others, 1969, fig. 4).

m) below the ground surface and all bend and curve to varying degrees (fig. 37). Some wedges widen and narrow again; many terminate in a sharp hook, and some terminate in large footlike masses or bulges.

Wedge sediments consist of brownish silt in the upper part and greenish-gray silt in the middle and lower parts. Mixed with the silt are pebbles and cobbles, which are the same size as clasts in the outwash gravel. Outwash sediments adjacent to the wedges contain more fine material than the nearby undisturbed outwash material. Adjacent to the sediment wedges, generally on one side, is an iron-stained zone that is widest at the top and narrows downward (fig. 37). The light-gray to tan silt in the wedge adjacent to the brown or reddish gravel strikingly outlines wedges in the field.

Hypotheses about the origin of large-scale patterned ground in the Donnelly Dome area fall into two major groups: a) desiccation-crack hypothesis and b) thermal-contraction crack hypothesis. The first hypothesis is illogical because of the absence of clay-sized minerals. According to the thermal-contraction crack hypothesis, the polygonal pattern is produced by cooling and tensional cracking of the ground in the winter as a result of volume reduction caused by contraction of ice-cemented sediments. Two variants that must be considered in this hypothesis include seasonal-crack polygons and ice-wedge polygons.

Polygons do not crack in the seasonally frozen ground in the Donnelly Dome area today. Apparently, for seasonal contraction cracks to form under natural conditions, the former climate must have been colder. With greater cooling of the ground, permafrost was more widespread, and conventional ice

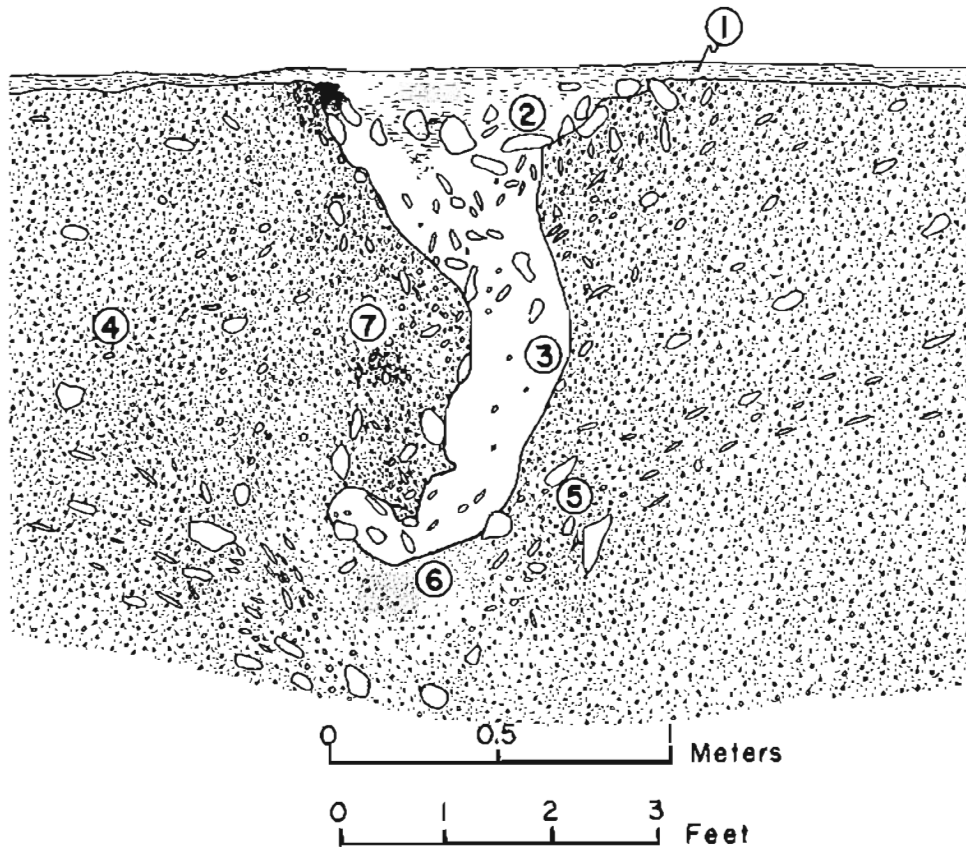


Figure 37. Diagrammatic sketch of ice-wedge cast, Donnelly Dome area, Alaska. Circled numbers indicate types of sediment: 1, silt mantle; 2, fill of upper part of wedge; 3, fill of middle and lower parts of wedge; 4, undisturbed outwash gravel; 5, disturbed outwash gravel; 6, sand; and 7, iron-stained sediments. No vertical exaggeration (from Péwé and others, 1965, fig. 17).

wedges formed by contraction cracking of former permafrost rather than as sediment wedges in the seasonally frozen ground. These wedges formed during the Donnelly Glaciation and subsequently melted. The resulting voids were filled with sediment from the adjacent gravel and overlying loess.

The climate in the Donnelly Dome area at the time the large-scale ice-wedge polygons formed was colder and more rigorous than today. Tree line was 1,500 to 1,800 ft (460 to 550 m) lower in the adjacent Yukon-Tanana Upland, and snowline was 1,500 ft (460 m) lower, based on a study of cirque floors. In Wisconsin time, the air temperature was at least 5.4°F (3°C) lower, about 21.6°F (-5.8°C), in contrast to the modern mean annual air temperature of 27°F (-2.8°C).

Study of large-scale patterned ground in the Donnelly Dome area demonstrates that extensive areas of ice-wedge-cast polygons can occur in coarse-grained sediments in regions where permafrost is actively growing, such as in central Alaska, and where large ice wedges are still present in fine-grained

sediments. Such an association supports the suggestion that permafrost and ice wedges thaw more rapidly in coarse-grained sediments than in ice-rich, fine-grained sediment.

247.8. Rise up the front of the terminal moraine of the Donnelly Glaciation.

247.4. Normal(?) fault, with movement in Holocene time (fig. 32). Road crosses a fault scarp approximately 10 ft (3 m) high. The Donnelly Dome fault extends east-west across the terminal moraine of Donnelly age, with the up-thrown side on the south. Donnelly Dome is bounded on the north by this fault.

246. Knob-and-kettle topography of the terminal moraine of the Donnelly Glaciation. This terrain is typical of terminal moraines of middle to late Wisconsinan age in Alaska.

Vegetation on the Donnelly moraine is typical of the Alaska Range near tree line. Both black and white spruce have very scattered distributions. Between the trees are shrubs of resin birch (Betula glandulosa), willows (Salix spp., especially S. pulchra), bog blueberry (Vaccinium uliginosum), and Labrador-tea (Ledum groenlandicum and L. decumbens). Between the shrubs and on exposed knobs are mats of crowberry (Empetrum nigrum), alpine bearberry (Arctostaphylos alpina), and lichens, especially Cladonia spp. Many spruce on the Donnelly moraine are less than 100 yr old, which indicates that under present climatic conditions an invasion by the trees is in progress.

245.2. STOP 13. DONNELLY TILL.

The light-yellowish-brown silty to sandy till is characteristic of the Donnelly Glaciation in the Delta River area on the north side of the Alaska Range. Schist fragments are also much more common in Donnelly-age till than in the more weathered till of the Delta Glaciation. Only about 5 percent of the granitic clasts are significantly weathered. Directly to the north of this stop, near Donnelly Dome, is a massive push moraine.

In the summer of 1964, the University of Alaska excavated and surveyed numerous archeological sites in the vicinity of Donnelly Dome. From the floors of numerous blowouts or from the thin loess blanket over Donnelly-age moraines, 533 artifacts showing different degrees of use were recovered. Although a few waste flakes of quartz and obsidian were found, most artifacts are gray chert, or less frequently basalt and siliceous siltstone, which are present as clasts with the same surface cortex in the local Donnelly till. Dominant elements include: a) bifacial, biconvex knives, b) end and side scrapers, c) large prismatic blades and bladelike flakes, d) wedge-shaped cores from which microblades were unidirectionally removed by indirect blows, e) core tablets, f) microblades, g) multiple burins on flakes, h) boulder-chip scrapers, and i) retouched blades. These forms are the key elements of the Denali Complex, which is defined from the artifact assemblage recovered from the Donnelly Dome sites. This complex is widespread in central Alaska and represents a core-blade-burin technology that is related to hunting activities such as butchering and skinning. Evidence from the Tangle Lakes area indicates that the Denali Complex is older than 8,000 yr and younger than 11,000 yr.

Game has been plentiful in the area, probably including, in late Wisconsinan or early Holocene time, herds of horses and bison. Game is no longer abundant, perhaps due in part to the area's ready accessibility to hunters.

244. Enter Mt. Hayes C-4 Quadrangle (fig. 38).

243.5. STOP 14. NORTH-CENTRAL ALASKA RANGE (fig. 39) AND CROSSING OF RICHARDSON HIGHWAY BY TRANS-ALASKA PIPELINE SYSTEM.

During good weather, this is a spectacular view of the Alaska Range, Delta River, and large alluvial fans. Black Rapids Glacier is in the distance. Looking south to the left, on the immediate skyline is a Donnelly-age lateral moraine, which is 650 ft (198 m) above the Delta River. The prominent lateral moraine on the other side of the valley is also of Donnelly age.

Trans-Alaska Pipeline System

The long-anticipated, vast petroleum potential of northern Alaska was in part realized with the discovery of oil at Prudhoe Bay in 1968. The 9.6 billion barrels of proven reserves suggest that one-third of the oil reserves of the United States may be in northern Alaska. To transport the warm crude oil from the North Slope to an ice-free port, a 48-in.-diameter (1.2 m) pipeline was built traversing Alaska from Prudhoe Bay to Valdez.

The Trans-Alaska Pipeline System (TAPS) was the largest privately funded construction effort in history. It was built in 1974-1977 by the Alyeska Pipeline Service Company, which is owned by eight oil companies. At the peak of construction in 1975, 21,600 persons were employed in the effort. The pipeline transports about 1.2 million barrels of crude oil daily to Valdez and is designed to transport as many as 2 million barrels per day.

TAPS is one of the most remarkable construction achievements in a permafrost environment. About 400 mi (643 km) of this 800-mi-long (1,285 km) pipeline extends south from Fairbanks (figs. 2 and 25) and traverses about 300 mi (480 km) of permafrost terrain described in this guidebook (fig. 40).

The cost of constructing TAPS was about \$8 billion. Probably about \$1 billion of that amount was necessary to learn about, combat, accommodate, and otherwise work with the perennially and seasonally frozen ground, which emphasizes the impact that frozen ground had on the cost of this major construction project.

Thawing problems

The pipeline was designed for burial in permafrost along most of the route, and the oil temperature (at full production) was estimated at 158-176°F (70-80°C). Such an installation could have thawed the surrounding permafrost.

Thawing of the widespread ice-rich permafrost by a buried warm-oil line could cause liquefaction, loss of bearing strength, and soil flow. Differential settlement of the line could occur, and mudflows of thawed soil could form on slopes. The greatest differential settlement could occur in areas of ice wedges, where troughs could form and deflect surface water into the trenches, causing erosion and more thawing. Engineers studied the poten-



Figure 38. Infrared photograph of surface of Donnelly moraine looking north from Mile 244 on the Richardson Highway; Donnelly Dome is on left and Granite Mountain is on the right. The Yukon-Tanana Upland is about 22 mi (35 km) to the north. Photograph 419A by T.L. Péwé, August 4, 1949.

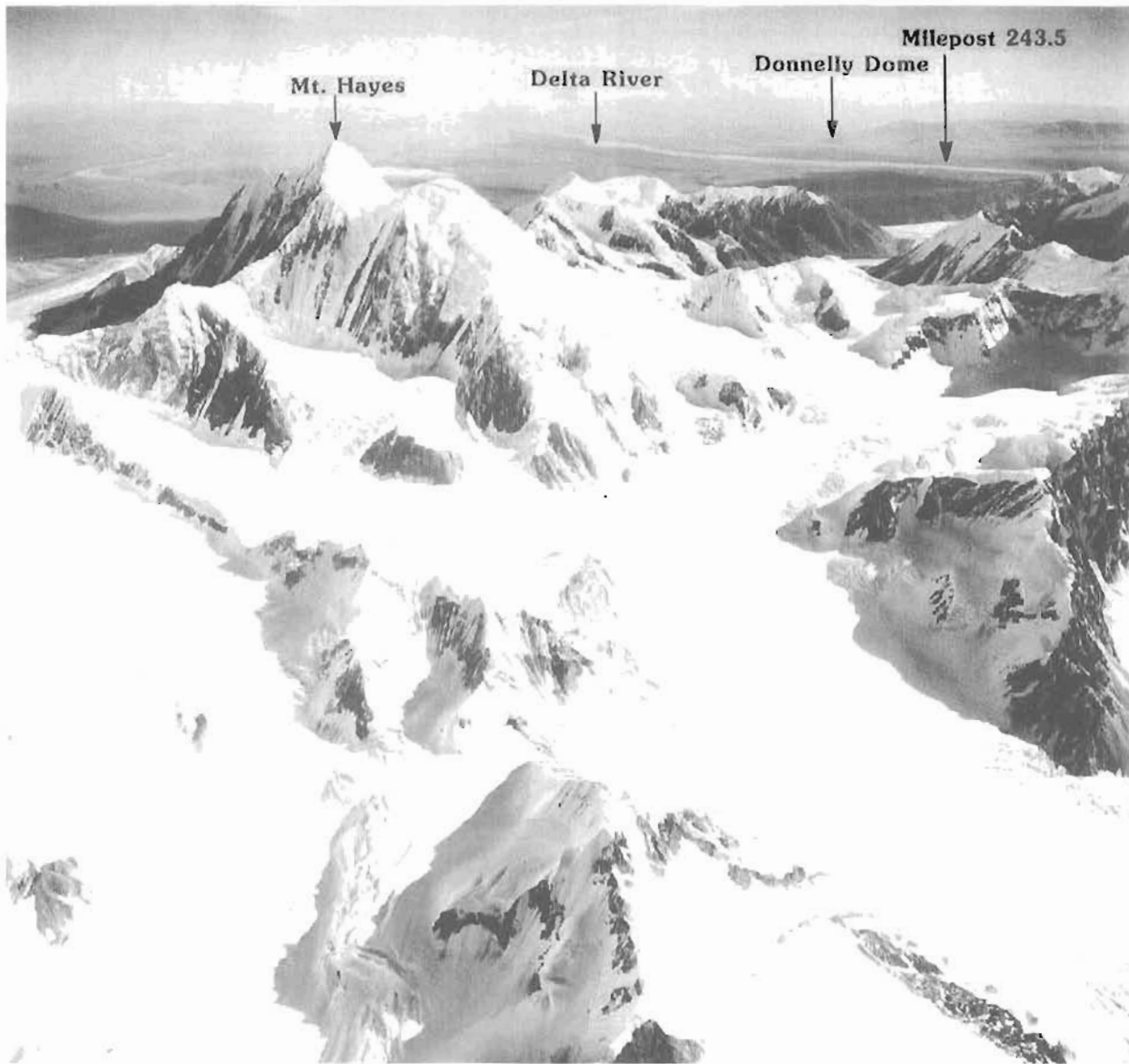


Figure 39. Oblique aerial view of Mt. Hayes in the Alaska Range, with the Delta River in distance. Photograph 58ORT-55RT-M864SRW-9M58 by U.S. Air Force, August 29, 1949.

tial permafrost problems and constructed many pipeline test sections in several permafrost areas. Several construction modes were designed and tested in and over varying permafrost and nonpermafrost terrains to ensure the integrity of the warm-oil pipeline.

Construction modes

The pipeline was built in three modes, depending on environment, terrain, and permafrost conditions (fig. 41). Oil is pumped through the pipe at temperatures up to 145°F (63°C), depending on production rates and how the oil

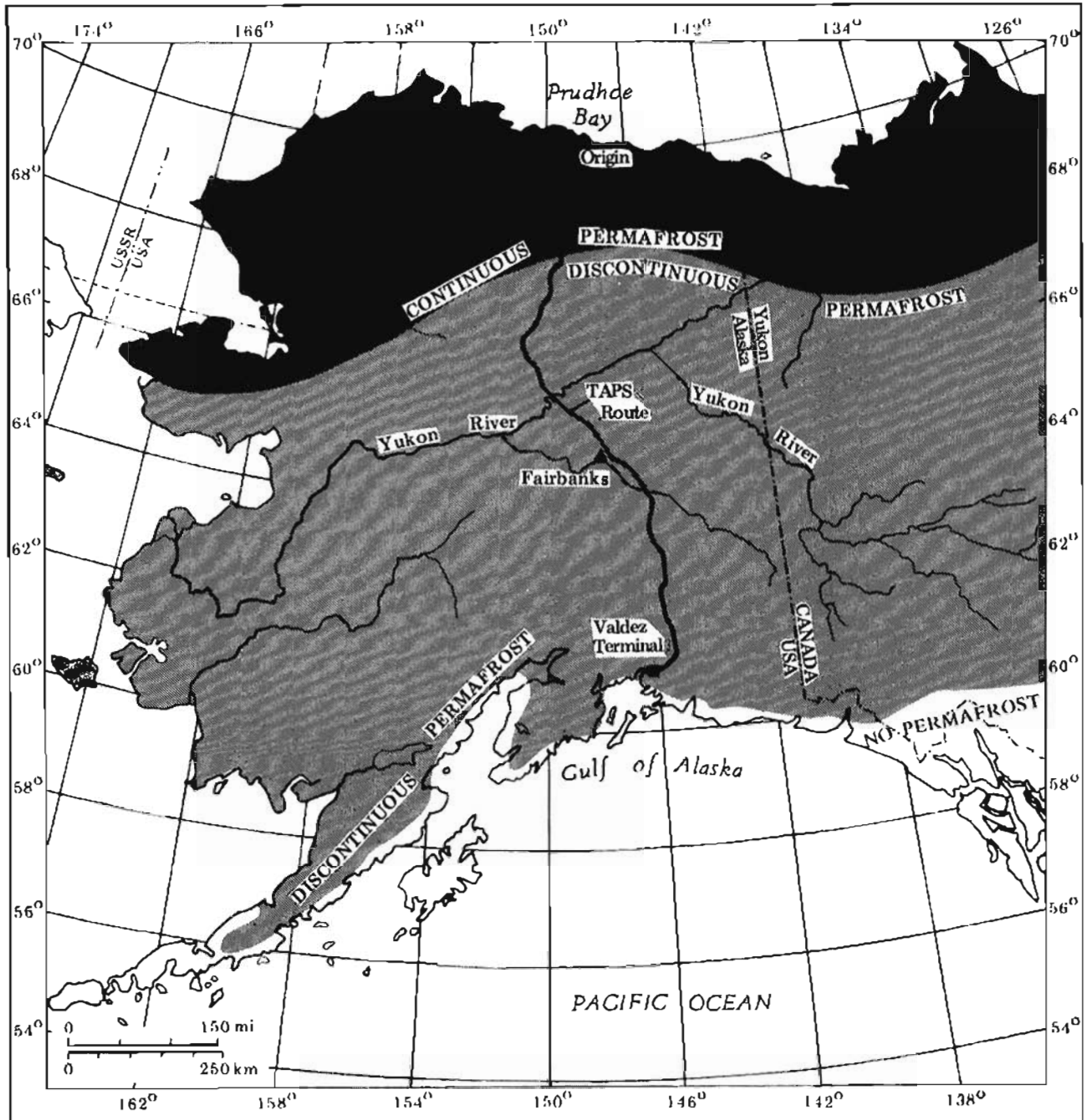


Figure 40. Index map of Alaska indicating route of the Trans-Alaska Pipeline System.

is handled before delivery to the pipeline from wells in the Prudhoe Bay field. Because of heat generated by pumping and friction with the pipe, oil moving through the system at the design rate of 2,000,000 barrels per day (320,000 m³ per day) ranges in temperature from 130 to 140°F (55 to 60°C). Potential effects of the heat on frozen ground along the route determined the mode of pipeline installation.

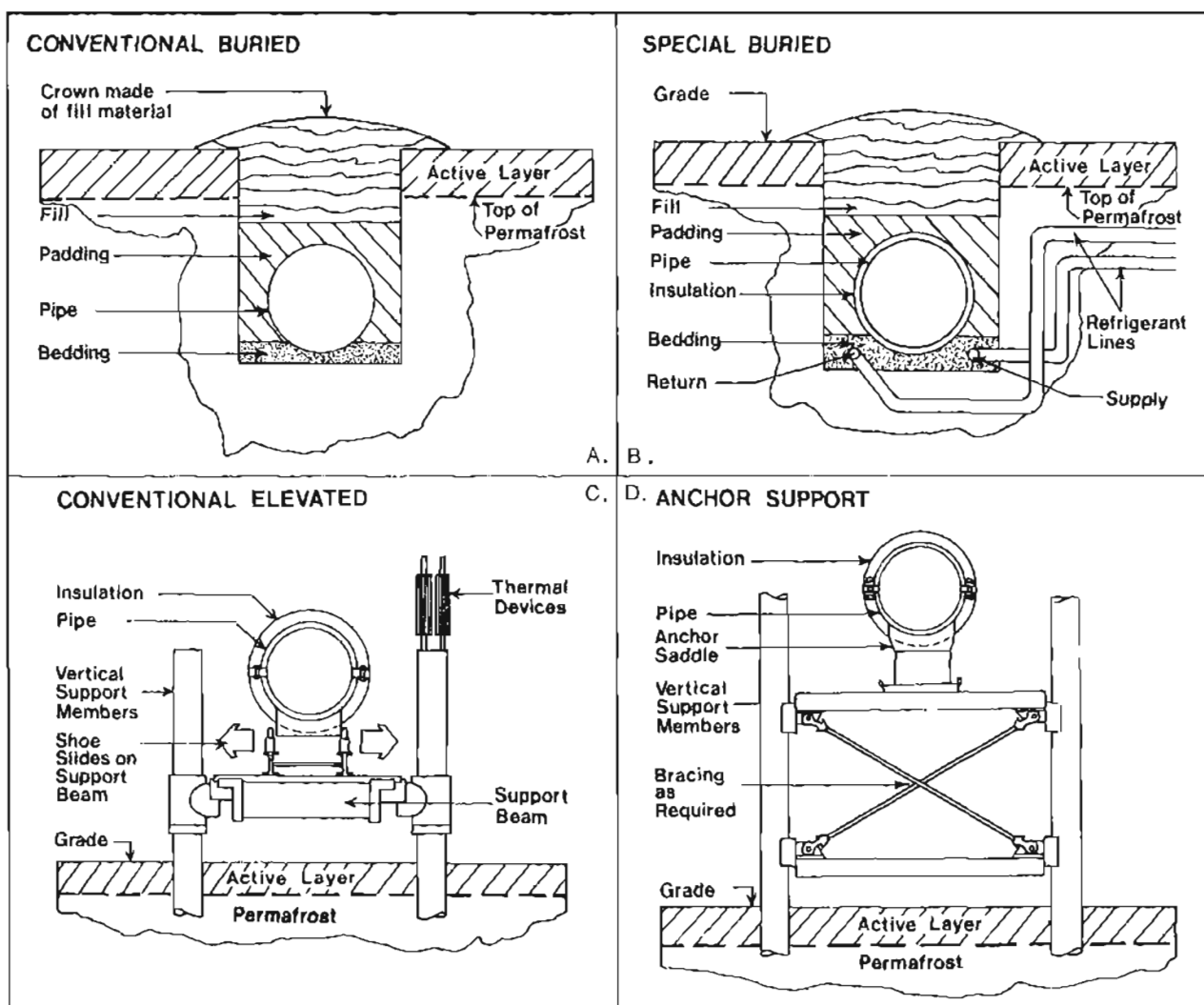


Figure 41. Different construction modes used in construction of the Trans-Alaska Pipeline System: A, conventional buried; B, special buried; C, conventional elevated; and D, anchor support. Diagram courtesy of Alyeska Pipeline Service Company.

Conventional burial

In areas where the ice content of permafrost is very low or absent or where no permafrost exists, the pipe is buried in the conventional manner, as it is in most areas of the world. About 409 mi (658 km) of the pipeline were installed conventionally (fig. 41A).

Special burial

In seven short sections of the line [totaling 7 mi (11.2 km)], the pipe was buried and then frozen into the ground (fig. 41B). Some sections are crossings for caribou and other animals and include both ice-poor and ice-rich permafrost environments. The pipe is insulated with 3 in. (7.6 cm) of polyurethane foam covered with a resin-reinforced fiberglass jacket. The tempera-

ture of the permafrost in which the pipe is buried is maintained by pumping refrigerated brine through pipes buried beneath the pipeline. Refrigeration units are powered by electric motors.

Conventional elevated and anchor support

About half the pipeline (382 mi or 615 km) is built above ground because of the presence of ice-rich permafrost (fig. 41C). Construction of a large pipeline above ground is a major effort, especially in permafrost terrain. Although the pipeline successfully discharges its heat into the air and does not directly affect the underlying permafrost, other problems with permafrost and associated phenomena must be considered. As indicated in figure 41C, the pipe is clamped in a saddle assembly placed on a crossbeam installed between steel vertical-support members (pilings) placed in the ground. The 120,000 vertical-support members (VSMs) used along the TAPS route are 18-in.-diameter (45 cm) steel pipes that are subject to frost heaving. To eliminate frost heaving, each VSM is frozen firmly into the permafrost using a thermal device that is installed in the steel pipe. The devices consist of metal tubes filled with ammonia, which becomes a gas in winter and rises to the top of the tubes. In the cold atmosphere it liquefies, running down the pipe and thereby chilling the ground whenever the ground temperature exceeds the air temperature. The devices are nonmechanical and self operating. Aluminum fins on top of the VSMs permit rapid dispersion of heat (fig. 41D).

To compensate for expansion of the above-ground pipe caused by the warm oil and contraction caused by extremely cold air temperatures in winter, the line is built in a flexible zigzag configuration, which converts expansion of the pipe into lateral movement. This design also safely accommodates pipe motions induced by earthquakes. The pipe is secured in a saddle assembly and mounted on a sliding shoe that slides on the crossbeam (fig. 41D). As the line expands, the pipe can slide across the beam; as it contracts, the pipe is free to slide back. On the crossbeams, the pipe is anchored in position on special platforms at the end of each zigzag configuration [every 800-1,800 ft (240-540 m)] (fig. 41D).

Above-ground pipe is insulated with a 4-in.-thick (10 cm) layer of resin-impregnated fiberglass that is jacketed with galvanized steel. This insulation keeps the oil warm and pumpable for a sufficient period of time to complete any unexpected maintenance, should oil movement stop for any reason. The crude oil is moved through the pipeline by a series of 12 pump stations.

The start-up process for TAPS began on June 20, 1977, when oil entered the line at Pump Station 1 at Prudhoe Bay. The first oil reached the Valdez Terminal on July 28, 1977.

The pipeline crossing of the Richardson Highway at this locality is refrigerated (fig. 42). The pipeline is buried at least 6 ft (1.8 m) beneath the road surface in a corrugated metal casing that is 115 ft (35 m) long. Permafrost is protected from pipeline heat at this location by 12 in. (30.5 cm) of polystyrene insulation throughout the length of burial. The perennially frozen ground consists of sandy gravel that contains up to 15 percent moisture and is frozen to depths of more than 43 ft (13 m). Thermal piles---as in the elevated section---keep the ground frozen. Here there is no mechanical freezing facility as at some other highway crossings. To date, there has been no difficulty with this crossing.



Figure 42. View (to the south) of the refrigerated crossing beneath the Richardson Highway by the Trans-Alaska Pipeline System at Mile 243.5, Richardson Highway, Mt. Hayes D-4 Quadrangle, Alaska. Vertical thermal piles equipped with heat-radiating fins keep the ground around the pipe on either side of the highway frozen. In the background, the elevated pipeline crosses ice-rich permafrost in till of the Donnelly Glaciation. Photograph 4652 by T.L. Péwé, June 29, 1981.

242.2. On the skyline to the left, the pipeline is arched to provide an elevated animal crossing.

241.3. Crest of prominent Donnelly lateral moraine, which is about 12,000 to 13,000 yr old.

240.2. The view to the south is of several glacially scoured rock knobs (roches moutonnées).

239.9. To the right are two loess-covered roches moutonnées of schist. Quartz veins still retain surface glacial polish.

238.15. To the left, roches moutonnées of schist occur across the small lake. To the right, 300 ft (91 m) off the Richardson Highway, is an important exposure of Quaternary sediments in the bluff along the Delta River. The following section is exposed:

Depth	Stratigraphy
0 to 3 ft (0 to 0.9 m)	Loess with numerous organic laminations and shells of pulmonate snails, including <u>Succinea avara</u> , <u>Discus chronk-hitei</u> , and <u>Euconulus fulvus alaskensis</u> .
3 to 7 ft (0.9 to 2.1 m)	Loess with some organic layers and no fossils. Organic material from a few mm above the base of the interval dated 1,950 ± 150 yr B.P. (L-163 K).
7 ft (2.1 m)	Jarvis Ash Bed, 0.3 in. (6 mm) thick. An organic layer 1.1 in. (27 cm) below the ash bed dated 5,650 ± 250 yr B.P. (L-137 Q).
7 to 12 ft (2.1 to 3.6 m)	Loess with little organic material.
12 to 28 ft (3.6 to 8.5 m)	Light-yellowish-brown, sandy to silty boulder till of Donnelly age.
28 to 41 ft (8.5 to 12.5 m)	Sandy outwash gravel (probably advance Donnelly outwash).
41 to 70 ft (12.5 to 21.4 m)	Colluvial cover.

237.5. Flood plain of the Delta River. Strong, persistent winds and a wide, vegetation-free flood plain make the Delta River an ideal area for observing wind as a geologic process (fig. 31). Winds from the south and east have blown great clouds of silt from the Delta River and Jarvis Creek flood plains since at least the Delta Glaciation and have blanketed the adjacent terrain with loess (Péwé and Holmes, 1964, pl. 1). Clouds of silt are blown as high as 4,000 ft (1,200 m) above the land surface today and cover hundreds of square miles. As might be expected, areas leeward of source areas, such as the Delta River flood plain, are most heavily blanketed with silt. Smaller areas east of the Delta River that break the regular wind flow are also heavily covered.

Deposits of windblown sediments are also thickest near the flood plains. Leaves and limbs of trees near the river are covered by fine silt during much of the summer. In many areas, tree trunks have small cones of fresh silt at their bases, the result of the silt washing down the tree from limbs and leaves. The floor of the forest is dusty, and a gradual accumulation of silt requires that new adventitious roots be extended laterally at higher and higher intervals by white-spruce trees. A constant regeneration of the surface vegetation is required. Deposits of loess are 1 to 40 ft (0.3 to 12 m) thick. Much more forest vegetation is present in upper loess layers than in lower layers, which suggests that vegetation near the ground surface has not decayed and disappeared like it has deeper in the section.

Almost all loess in the immediate area is Holocene in age. Radiocarbon dates indicate that the Jarvis Ash Bed (near the middle of most loess sections) is about 3,500 yr old.

235.9. From here to Ruby Creek (fig. 43), the scarp that is 60 to 100 ft (18 to 30 m) high on the left was cut by the Delta River into an alluvial fan of Ruby Creek. After the Wisconsin glacier withdrew from the Delta River valley, streams deposited large gravel alluvial fans that were truncated as the Delta River shifted from one side of the valley to the other. These fans are capped with a veneer of loess 1 to 40 ft (0.3 to 12 m) thick.

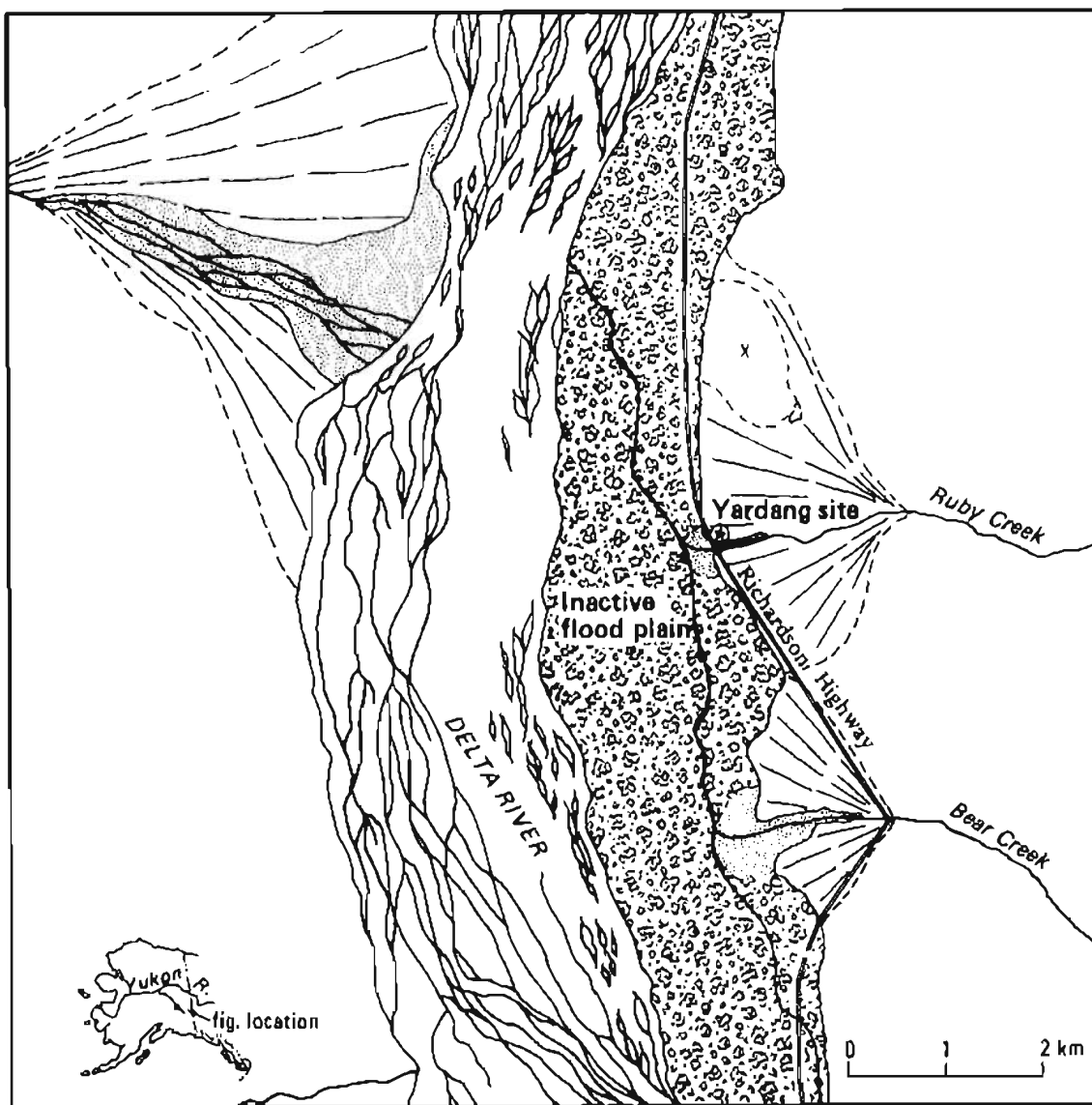


Figure 43. Landform map of part of the Delta River valley in the vicinity of the Yardang Site, central Alaska Range (from Reger and others, 1964, fig. 1).

235. Start up younger fan of Ruby Creek.

234.8. Yardang Site (fig. 43).

The alluvial fan is composed of pebbles and cobbles of schist, gneiss, and quartz, and a large percentage of pebbles and cobbles of coal and orange-brown siltstone of Tertiary age derived from the head of Ruby Creek in the Jarvis Creek coal field. Ruby Creek wandered over its gravel fan, removing or burying any surface loess until about 6,000 yr ago, when Ruby Creek began to entrench its fan. Retrenchment may have resulted from downcutting by the Delta River, but probably occurred because the Delta River shifted to the east side of the valley, nipping the fan and thereby shortening the course of Ruby Creek. For the past 6,000 yr, loess has accumulated on most of the gently sloping fan, burying successive generations of white-spruce forests.

The loess is unconsolidated and possesses crude vertical jointing. It is tan-gray and is mottled by iron oxides and organic material. The silt has rather distinct laminations that parallel the surface of the alluvial fan and are caused by the presence of forest layers or iron-oxide staining. White-spruce stumps up to 1 ft (0.3 m) in diameter are common in the loess. Organic-rich layers indicate that the loess has been deposited on forest floors, thereby burying successive generations of vegetative mats. A radio-carbon date of $5,900 \pm 250$ yr (I-646) for a spruce stump 2 in. (5.1 cm) above the base of the loess (fig. 44) indicates that as much as 16 ft (4.9 m) of loess has been deposited on the fan in the last six millenia.

About 3,500 yr B.P., the Jarvis Ash Bed was deposited on the fan and buried by subsequent loess. The ash bed has a relatively uniform thickness of 0.04 to 0.7 in. (1 to 5 mm) and consists mostly of glass. At the time of ash deposition, the Ruby Creek flood plain extended about 500 ft (150 m) north of

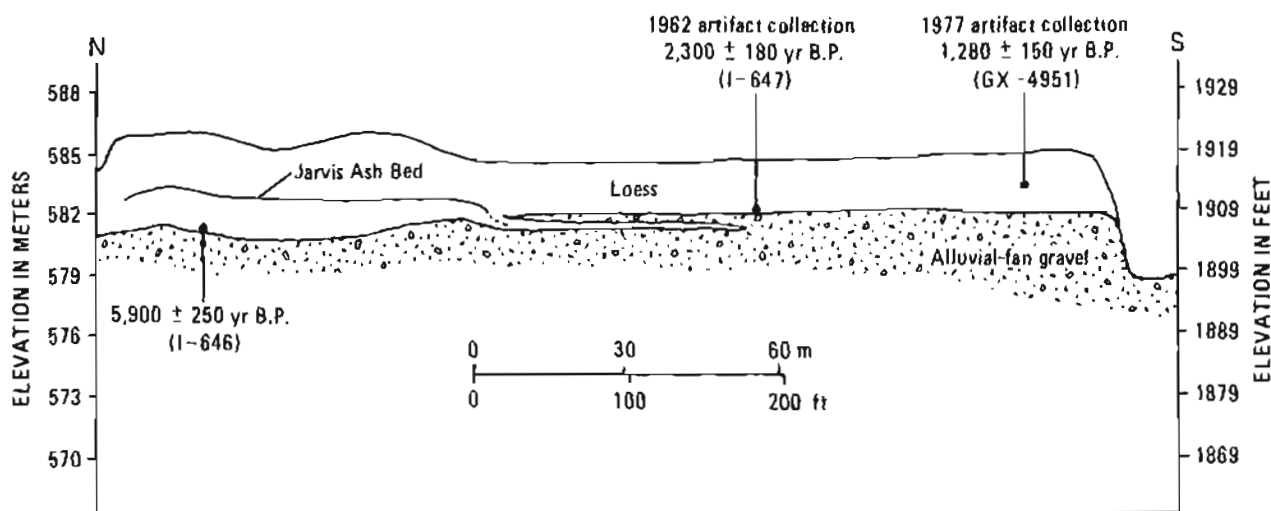


Figure 44. Stratigraphy of the Yardang Site (Mt. Hayes 252), Mile 243.8, Richardson Highway, central Alaska Range (modified from Reger and others, 1964, fig. 3).

its present location at the bridge, and the ash, therefore, was not preserved or buried there. Approximately 2,300 yr ago, Ruby Creek moved to the south side of its flood plain, and loess began to accumulate on gravel of the inactive flood plain. For the last 2,300 yr, Ruby Creek has not swung to the north, and 10 ft (3 m) of loess has accumulated over the gravel surface, burying forests as it accumulated.

Strong wind action in the Delta River valley attacked the unprotected loess deposit once the vegetation was broken during road construction. In the unconsolidated loess, yardangs 3 to 5 ft (0.9 to 1.5 m) high and 4 to 10 ft (1.2 to 3 m) long were carved. These features are similar to the yardangs cut in slightly more consolidated material elsewhere in the world. Because of their low resistance to erosion, most yardangs no longer exist.

Twenty-four undiagnostic artifacts, concentrated in an area 6 in. (15 cm) in diameter, were found during the summer of 1962 in an organic-rich layer 0.3 in. (6 mm) thick a few inches above the gravel-loess contact near the center of the section (fig. 44). Organic material in the artifact layer was dated at $2,300 \pm 180$ yr B.P. (I-647). The collection of end and side scrapers, utilized flakes, and fragments at the Yardang Site represents the first instance where an assemblage of artifacts this old was absolutely dated and placed in its geologic context in interior Alaska.

In 1977, C.E. Holmes discovered numerous pieces of bone, quartz fragments, and an antler harpoon head on a deflation surface cut in the loess about 175 ft (53 m) east of and stratigraphically higher than the collection of artifacts found in 1962 (fig. 44). The 1977 collection was associated with fire-cracked rocks and fragments of wood charcoal, which are dated at $1,280 \pm 150$ yr B.P. (GX-4951). Because these remains were recovered as surface finds, their temporal relationship is not unequivocally established. The remains probably represent only a brief reoccupation of the site. The open-socket harpoon head has a line hole perpendicular to the plane of the head and is unique among the inventory of artifacts from the Interior because it is typical of marine-mammal-hunting cultures along the coast. It may represent a trade item.

From the bridge at Ruby Creek, it is possible to see (on the left) the ridge between Ruby Creek and Bear Creek. At an elevation of 4,000 ft (1,212 m), cobbles derived from glacial drift of Delta age were found. The lateral moraine of Donnelly age in this area is near 3,000 ft (909 m) elevation, approximately at tree line.

234.7. For the next mile (1.6 km), where the Richardson Highway crosses ice-rich silt blanketing the Ruby Creek fan, the surface of the highway is irregular.

234 to 233.5. Alluvial fan of Bear Creek.

233.8. Bear Creek bridge. Upstream from the bridge, one can see a yellowish gravel that was deposited against the Donnelly-age lateral moraine.

231.8. Start of Darling Creek fan (fig. 45).



Figure 45. Richardson Highway under construction (1951) at Mile 231.8, looking southwest up Darling Creek alluvial fan. The trees were cut, but the low vegetation was not removed. Gravel was dumped over the vegetation, which remained as an insulating blanket. There is about 3 to 6 ft (0.9 to 1.8 m) of perennially frozen, ice-rich silt over the alluvial-fan gravel. Photograph 518 by T.L. Pêwé, June 17, 1951.

231. To the left [on the ridge between Darling Creek and an unnamed creek to the south at Benchmark Darling (4,927 ft or 1,502 m elevation)] is the type locality of the Darling Creek Glaciation. Deeply stained, washed gravel of pre-Illinoian age lies on schist bedrock. Other deposits of this age occur at the head of Ruby Creek.

230. To the left is an outcrop of loess and the Jarvis Ash Bed.

229.9. To the left is the scar of a 1950 forest fire.

227. Gunnysack Creek and section through alluvial fan. Brownish-purple fan gravel is also exposed across the Delta River beneath the Holocene moraine.

226.6. STOP 15. FALLS CREEK AND BLACK RAPIDS GLACIER (fig. 46).

Black Rapids Glacier gained worldwide attention in 1937 when it advanced spectacularly at rates of up to 200 ft (61 m) a day (fig. 47). It was feared



Figure 46. Aerial view (to the northeast) of the Delta River and terminus of the Black Rapids Glacier. Pre-1937 moraines can be seen near the river, and the location of Stop 15 is indicated. Photograph 627RT-55RT-M864-55SRW-9M58 by U.S. Air Force, August 29, 1949.

that the glacier would quickly reach the Richardson Highway, destroy it, and also destroy the historic Black Rapids Roadhouse, which was built along the highway near this locality. A radio announcer was stationed at the roadhouse to broadcast the details of the glacier crunching through the building. How-

ever, Black Rapids Glacier did not reach the Richardson Highway as predicted, although studies by Péwé in 1949 revealed that earlier Holocene advances had crossed the river.

Just east of the Richardson Highway near the mouth of Falls Creek is a large pod of greenish, fine-grained amphibolite that is cut by numerous quartz veins. This rock is more resistant to glacial scouring than the surrounding schist and protrudes as a knob; it displays excellent glacial polish and grooving that record glacier movement down the Delta River valley (from south to north), probably during the Donnelly Glaciation. From the top of the amphibolite outcrop is a good view (to the west) of Black Rapids Glacier and moraines of several Holocene advances.

During the earliest recognized Holocene advance of Black Rapids Glacier, ice pushed across the valley, riding a few hundred yards up onto the opposite bedrock wall. The ice dam temporarily blocked and diverted the Delta River, which cut a bedrock gorge that was later partially blocked by the fan of Falls Creek to form Hidden Lake (fig. 48). With thinning and recession of the ice dam, the Delta River returned to its present course and lower Falls Creek was diverted north through the former river channel to enter the Delta River at this location. Later shifting of the creek in response to rapid sedimentation removed debris from the amphibolite outcrop.

To the north across the river, one can see pinkish gravel of the Gunnysack Creek alluvial fan underlying the oldest Holocene moraine of Black Rapids Glacier. The earliest Holocene advance of Black Rapids Glacier pushed the Delta River eastward at that location and caused it to truncate the fan of Gunnysack Creek.

At Stop 15 near the mouth of Falls Creek, the Richardson Highway is cut through bouldery till of the oldest recognized Holocene advance of Black Rapids Glacier. In the upper part of this till are several discrete blocks and pods, which are up to 6 ft (1.9 m) in diameter and as thick as 2 ft (0.6 m) (fig. 49). These unique erratics are composed of pieces of the former turf- and loess-covered outwash fan of Black Rapids Glacier, which was overridden during this early advance. Some blocks near the north end of the road-cut are undeformed internally, although in a thin surface rind, silty block material is mixed with angular to subangular gravel from the enclosing till. These blocks were probably frozen when initially plowed up by the advancing glacier and were deposited before they thawed. Although we do not know how far the blocks were carried by the advance, the fact that they remained intact indicates they were undoubtedly transported only a short distance at or close to the surface, probably as part of the push moraine in front of the advancing glacier. Their thicknesses demonstrate that the blocks were plowed up in late winter when the outwash fan was frozen at least 2 ft (0.6 m) deep, perhaps by a surge that died out before the following summer. Two thin, discontinuous layers of turf [separated by 3 to 5 in. (7.6 to 12.7 cm) of sandy loess in one undeformed block] were dated at $3,120 \pm 120$ yr B.P. (I-12,109) and $4,350 \pm 140$ yr B.P. (I-12,108). This indicates that the earliest known Holocene advance of Black Rapids Glacier occurred sometime after 3,100 yr B.P. and that the glacier had not previously expanded to an equivalent position for at least 1,200 yr. Other nearby pods are made up of turf and loess that are thoroughly mixed with gravel from the enclosing till, demonstrating that they thawed and were remolded, but not destroyed, before being deposited by the ice.



A.



B.

Figure 47. Photographs of the terminus of Black Rapids Glacier in 1937 and 1951 illustrate the jagged surface of seracs at maximum surge compared to the relatively smooth, down-wasted surface of the lower glacier 14 yr later. A. View (to the north) of 1937 terminus of Black Rapids Glacier. Panorama by O.W. Geist and J.L. Giddings, April 1937. B. Same view of 1951 terminus of Black Rapids Glacier. Photographs 502-509 by T.L. Pêwê, June 1951.



Figure 48. View west of Hidden Lake on the east side of Delta River valley near Black Rapids Glacier, Mt. Hayes C-4 Quadrangle, Alaska. This lake occupies a bedrock gorge cut when the Delta River was deflected by the oldest Holocene advance of Black Rapids Glacier. The gorge subsequently was blocked by the alluvial fan of Falls Creek to impound the lake. Photograph 494 by T.L. Pewé, June 15, 1951.



Figure 49. Reddish-yellow pod of remolded outwash incorporated into till of the earliest known Holocene advance of Black Rapids Glacier, Mile 226.7, Richardson Highway. Sample bag is 12 in. (30.5 cm) long. Photograph 4657 by T.L. Péwé, June 23, 1981.

Two radiocarbon dates of thin, felted peat and a branch recovered from between thin distal gravel of the Falls Creek fan and the underlying oldest Holocene till are dated at less than 190 yr B.P. (I-12,110) and less than 230 yr B.P. (I-12,111), respectively. They provide a minimum age for the oldest Holocene advance, but the moraine could be considerably older.

Attempts to date this moraine and the other prehistoric Holocene moraines of Black Rapids Glacier have utilized dendrochronology and lichenometry, but the results are not conclusive. Péwé's preliminary dendrochronologic studies from 1951 through 1957 convinced him that the multiple Holocene moraines of Black Rapids, Castner, and Canwell Glaciers probably were built by concurrent advances during the past 400 yr. His observations of spruce colonization on the 1937 terminal moraine of Black Rapids Glacier demonstrate that near-tree-line conditions, including cool summer temperatures, severe winds, and shifting substrates due to melting ice cores, delay tree growth on moraines in this part of the central Alaska Range for at least 15 to 20 yr following construc-

tion of the moraines. This delay factor must be added to ring counts of trees (table 4) to estimate the ages of Holocene moraines.

The oldest Holocene terminal moraine of Black Rapids Glacier is compound (fig. 50) and adjoins a forest of spruce that is significantly older than the trees growing on the moraine. West of the Delta River, a dense forest with thick turf and many older fallen and decayed trees estimated to be 350 to 500 yr old is just beyond the limit of Holocene glaciation (fig. 50). The oldest solid-center tree sampled in this forest in 1951 was 228 yr old (table 4). A similar forest exists beyond the oldest Holocene moraine east of the Delta River and south of Gunnysack Creek. In contrast, trees estimated to be as old as 133 yr--and older trees with rotten centers--were growing on the oldest Holocene moraine of Black Rapids Glacier in 1951 (table 4). Thus, spruce and poplar trees were apparently present in this part of the Delta River valley before the earliest Holocene advance of Black Rapids Glacier. Based on tree-ring evidence and the development of an incipient soil on this moraine (which indicates it was built more than 200 yr ago), Pêwê estimates the age of the oldest Holocene moraine of Black Rapids Glacier at 330 yr B.P. and correlates it with similar moraines at nearby Castner and Canwell Glaciers.

An arcuate terminal moraine 1 mi (1.6 km) in front of the 1937 terminal moraine appears fresh, and has no turf cover, and locally contains a small ice core. In 1951, 80-yr-old trees in a first-generation forest on this moraine were cored. According to Pêwê, the moraine formed about 130 yr B.P. Mendenhall (1900) visited the terminus of Black Rapids Glacier in 1898 and stated that the glacier had evidently advanced a few years earlier, leaving a fresh-looking moraine.

The 1937 advance of Black Rapids Glacier was a rapid surge, and a 300-ft-high (90 m) cliff of ice formed the terminus (fig. 47A). After this surge, the ice thinned rapidly, and today little ice is visible from the Richardson Highway. The terminal moraine is still ice cored. The first spruce trees, which were 4 yr old, were found in 1957, 20 yr after the advance, growing on the moraine where the ice core was no longer present.

Although the age interpretations of the moraines of Black Rapids Glacier based on the tree-ring evidence seem logical, the tree-ring evidence is not complete. Especially critical is an assessment of the history of the Delta River valley in terms of processes that could kill trees growing on moraines, including repeated large wildfires, severe infestations by spruce-bark beetles, and severe wind storms. Another phenomenon that must be evaluated is the timing and magnitude of Holocene tree-line fluctuations in the area. The upper limit of spruce is about 800 ft (242 m) above the terminal moraine of Black Rapids Glacier, but the Holocene moraines of Castner and Canwell Glaciers are less than 200 ft (61 m) below this level. The development of a tree-ring-width chronology for the Delta River valley would greatly strengthen the application of dendrochronology in the central Alaska Range and would provide a firm basis for dendroclimatic extrapolations.

In an attempt to date Holocene moraines above tree line in the central Alaska Range, Reger initially utilized lichenometry at Black Rapids, Canwell, Gulkana, and College Glaciers (fig. 51). The most useful lichen for this purpose is crustaceous Rhizocarpon geographicum, which abounds in the central Alaska Range, is easily recognized, and is reliable for dating elsewhere. The

Table 4. Results of tree-ring counts on cores collected in 1951 from trees growing on Holocene moraines and outwash surfaces of Black Rapids Glacier. Locations of trees (relative to landforms) are shown on figure 50.

Field no.	Tree type	Trunk diameter 18 in. above base (in.)	Tree-ring count	Estimated loss of tree-rings due to dry rot	Estimated age of tree (yr)	Landform
1	spruce ^a	16	126	6	132	Moraine
2	"	12	131	2	133	Moraine
3	"		113	1 ^b	114 ^{bc}	Moraine
4	"	17	104	- ^b	104 ^{bc}	Moraine
5	"	16	124	1	125	Moraine
6	"	16	99	3	101	Moraine
7	"	17	165	5	170	Outside old-est moraines
8	"		110	0	110	Hidden Lake drainage
10	"	12	76	5	81	Moraine
11	"	4	32	0	32	Outwash
12	"	3	40	0	40	Outwash
13	"	5½	57	0 ^b	57 ^{bc}	Outwash
14	cottonwood	8	50	- ^b	50 ^{bc}	Moraine
15	spruce	6	55	1	56	Moraine
21	"	5	34	0	34	Moraine
22	"	9	60	0	60	Outwash
23	"	10	63	0	63	Outwash
24	"	14	65	0	65	Outwash
25	spruce ^d	13	151	2	153	Outwash outside of old-est moraine
26	"	15	226	2	228	Outwash outside of old-est moraine
27	spruce	18	110 ^b	Rotten core	110 ^{bc}	Moraine
28	"	13	67 ^b	0	67 ^{bc}	Moraine
30	spruce ^d	26	117 ^b	Only outer 3 in. of tree counted: core rotten ^b	300 ^{bc}	Outwash outside of old-est moraine
31	"	8	72 ^b	- ^b	72 ^b	Moraine
32	"	12	95	3	98	Moraine
33	"	6	69	11	80	Moraine

^aWhite spruce (*Picea glauca*) unless otherwise indicated.

^bSome rings not distinguishable.

^cMinimum age.

^dIn forest with 24-in.-diameter standing spruce with rotten cores; many large rotten logs on forest floor covered with moss.

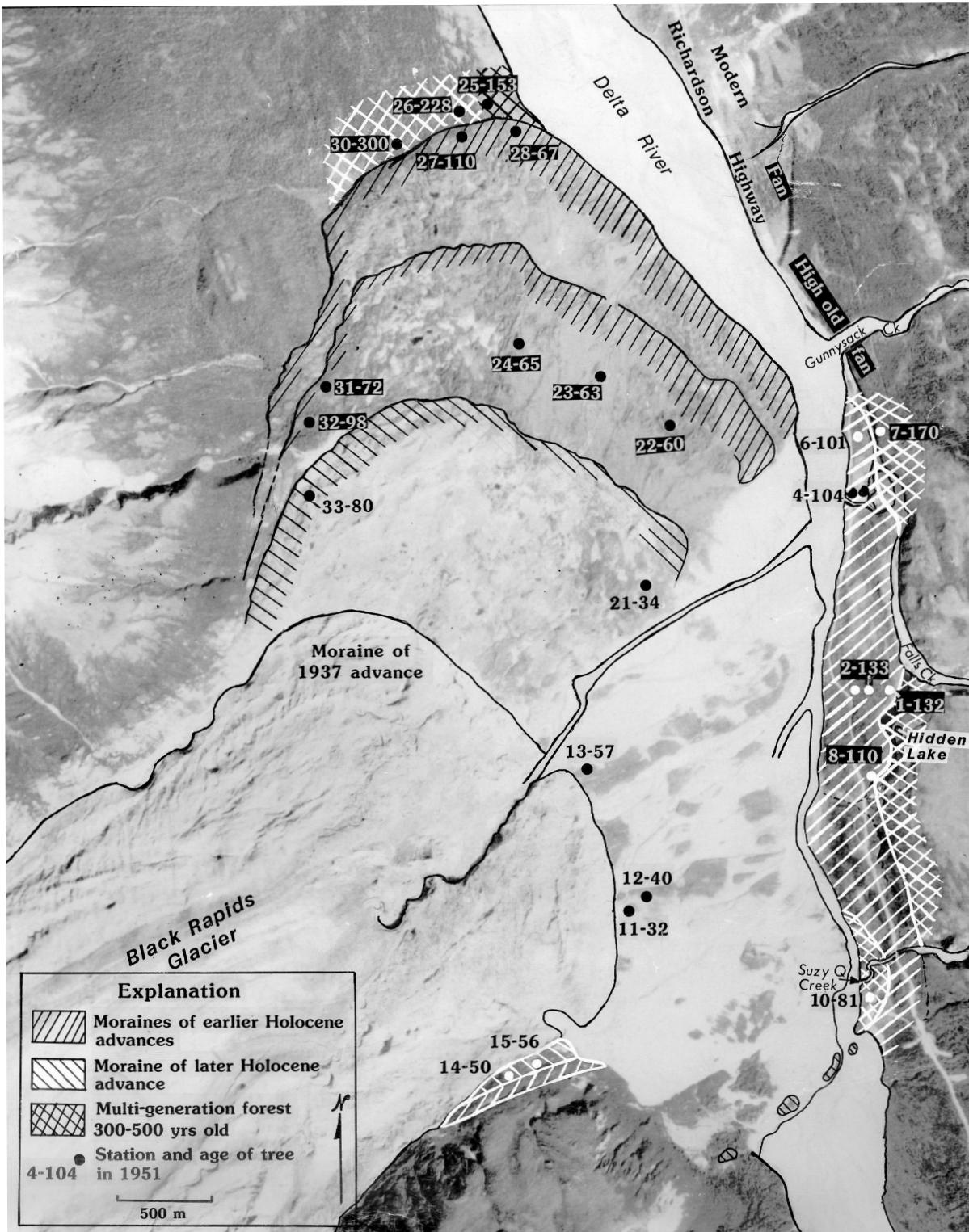


Figure 50. Landform map of Holocene glacial deposits at the terminus of Black Rapids Glacier, central Alaska Range, Alaska. Numbers indicate station and age of tree in 1951.

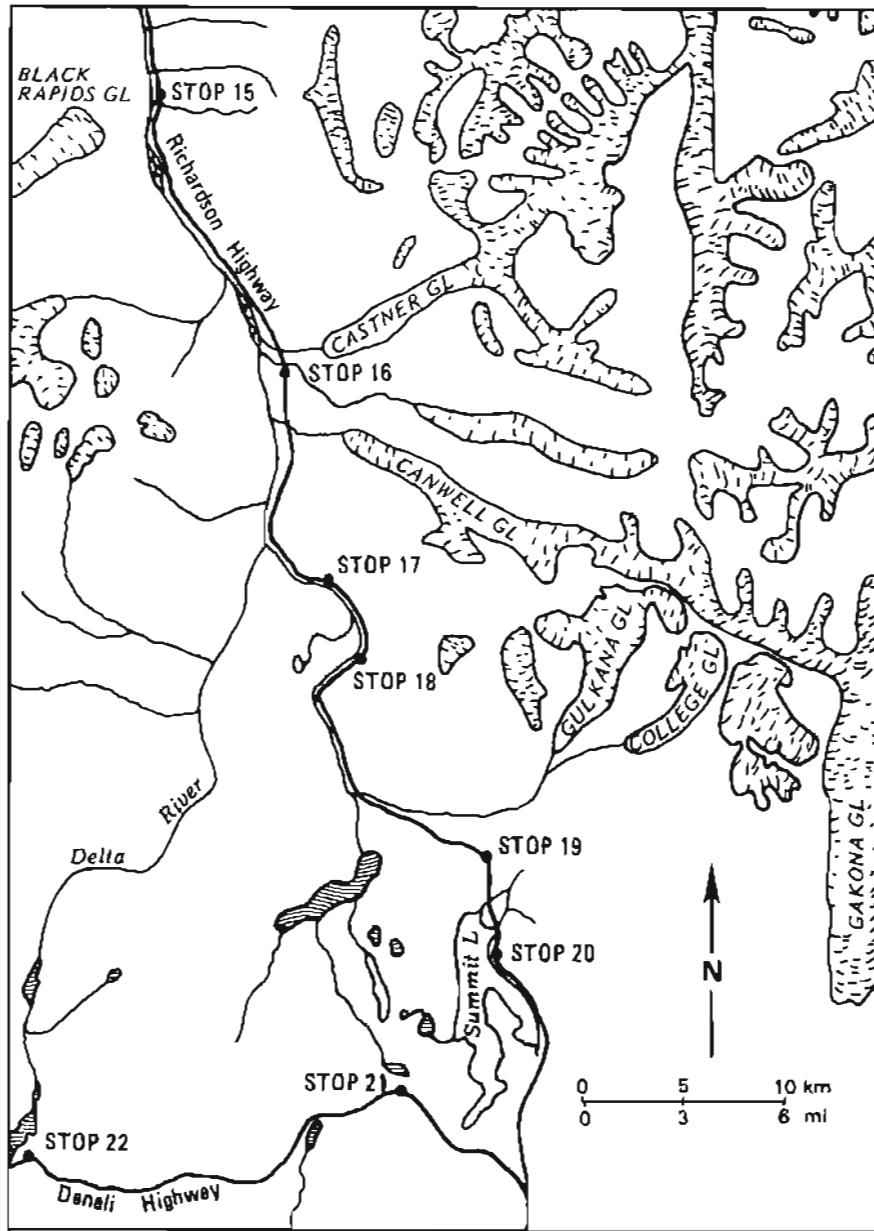


Figure 51. Index map of the central Alaska Range showing major glaciers in the vicinity of the Richardson Highway (modified from Reger, 1964, fig. 2).

initial lichen-growth curve for *R. geographicum* was calibrated with the ages of moraines that extend below tree line at Black Rapids and Canwell Glaciers (fig. 52); these moraines were dated by Péwé using dendrochronology (Reger and Péwé, 1969). However, the growth-rate curve for the same species in the St. Elias Mountains, which was calibrated using photographic, dendrochronologic, and radiocarbon evidence (Denton and Karlén, 1973, 1977), is very different than the curve initially developed for the central Alaska Range (fig. 52). Recent work by Ten Brink and his associates along the north flank of the central Alaska Range essentially duplicates the curve developed by Denton and

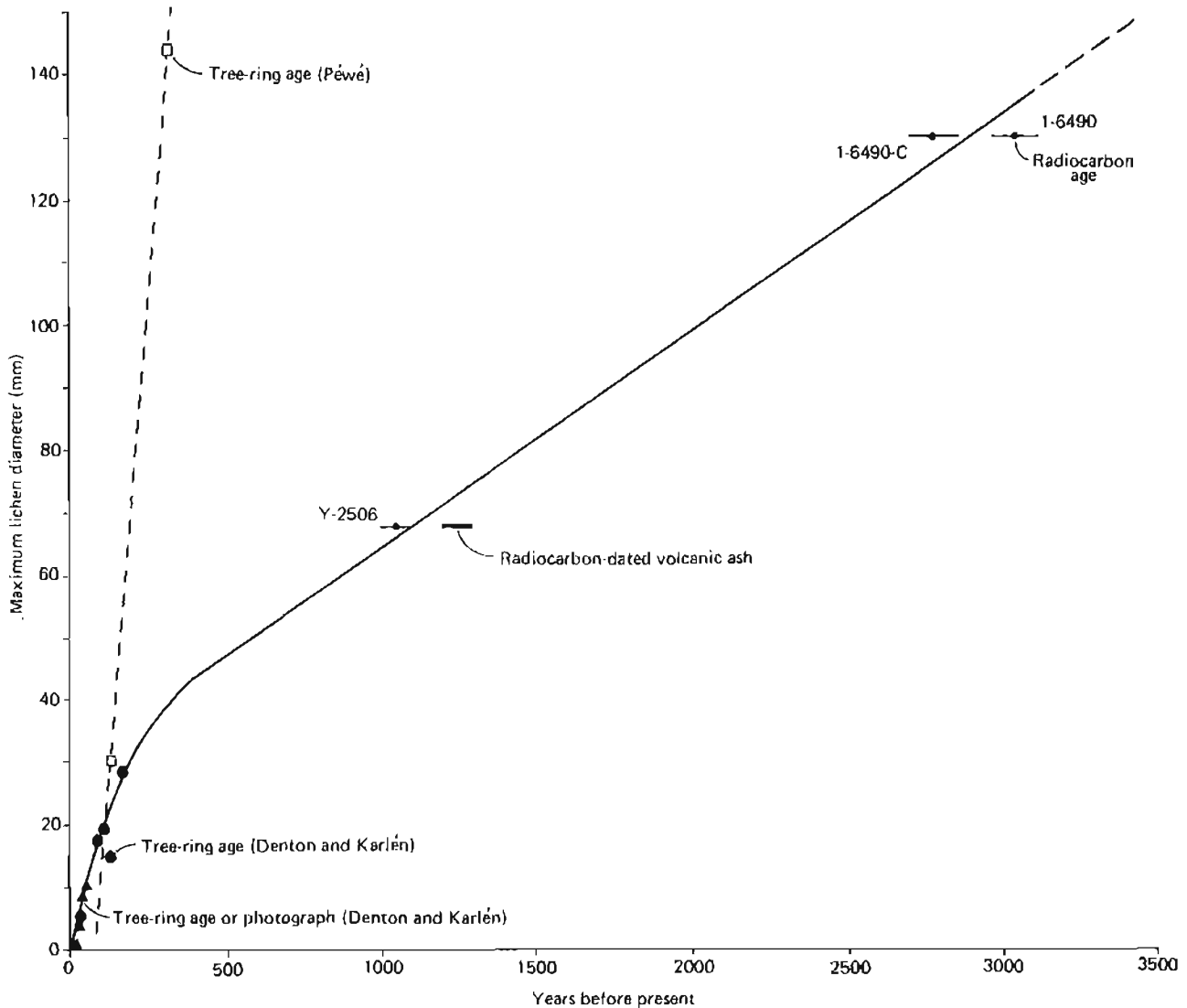


Figure 52. Comparison of *Rhizocarpon geographicum* growth curves initially developed for the central Alaska Range by Reger and Péwé (1969) (dotted line), based on dendrochronology by Péwé (unpublished), and for the St. Elias Mountains by Denton and Karlén (1973; 1977) (solid line). Recent work by Ten Brink and others (personal commun., December 2, 1982) produced a tree-ring and radiocarbon-substantiated growth curve for this species in the north-central Alaska Range that closely approximates the Denton-Karlén curve.

Karlén, which suggests that there is a problem with using tree-ring ages to date the Holocene moraines in the Delta River valley.

The earliest Holocene terminal moraines of Black Rapids Glacier are generally unsatisfactory for lichenometry because of the dense vegetation cover and the effects of eolian activity. Dead *R. geographicum* thalli up to

3.15 in. (80 mm) in diameter were observed on the oldest Holocene terminal moraine east of the Delta River, and widely scattered live thalli up to 1.18 in. (30 mm) in diameter were measured. On this moraine west of the Delta River, dead thalli up to 2.95 in. (75 mm) in diameter were observed, and live thalli up to 1.57 in. (40 mm) in diameter were measured. The moraine is partly blanketed with eolian sand, and dead lichen thalli show the effects of sandblasting. Assuming, as work by Ten Brink and others suggests, that the lichen-growth curve of Denton and Karlén (1973; 1977) is approximately correct for the central Alaska Range, the lichens indicate that the oldest recognized Holocene moraine of Black Rapids Glacier is at least 1,265 to 1,450 yr old, not less than 400 yr as the trees indicate. If the present crustaceous lichens in the densely forested area represent plants that secondarily colonized the old moraine after the development of the heavy tree cover, the lichens indicate that the dense forest developed about 194 yr ago; this possibility is not ruled out by the tree-ring data (table 4). The largest live thalli west of the Delta River indicate that lichens growing on the oldest Holocene terminal moraine were killed about 320 yr B.P. by windblown sand from the active outwash plain of the younger Holocene advance, which, according to the tree-ring evidence, is much younger. Live R. geographicum west of the Delta River probably represent a secondary colonization that occurred after eolian activity diminished.

The largest R. geographicum on the younger Holocene terminal moraine of Black Rapids Glacier is dated by trees at about 150 yr B.P. and ranges from 0.43 to 1.68 in. (11 to 43 mm) in diameter; average diameter is 0.95 in. (24 mm) (fig. 53). Wherever possible, lichens were measured on large boulders on parts of the moraine that were not ice cored. Lichen sizes suggest this moraine is at least 140 yr old and may be as old as 390 yr.

Scattered R. geographicum up to 0.16 in. (4 mm) in diameter were measured on the 1937 terminal moraine of Black Rapids Glacier on boulders that were no longer part of the ice-cored moraine (fig. 53).

225.4. To the right is an excellent overlook of the terminus of Black Rapids Glacier. Hidden Lake and the Holocene diversion channel of the Delta River are on the left (east). Scattered R. geographicum grow on boulders in this forest.

225.1. Enter Mt. Hayes B-4 Quadrangle. From 226.5 to 224.4, the Richardson Highway traverses the oldest Holocene moraine of Black Rapids Glacier.

224.8. Crossing of Suzy Q Creek. The later Holocene moraine forms the prominent, unvegetated gravel ridge just west (right) of the highway. Remnants of this moraine can also be seen across the Delta River. For the next 4 mi (6.4 km), the faint shoreline of a temporary lake, which formed by damming of the Delta River during this advance, is visible across the river at the base of the slope in the alders and willows.

222.5. To the right are several gravel groins that extend across the flood plain of the Delta River; these structures protect this buried segment of the Trans-Alaska Pipeline System in this reach of the Delta River, where widespread and thick seasonal stream icings promote local scouring. Across the Delta River to the west is a 2-mi-long (3.2 km), U-shaped, hanging tributary valley that was occupied by ice during the Donnelly Glaciation. Up the

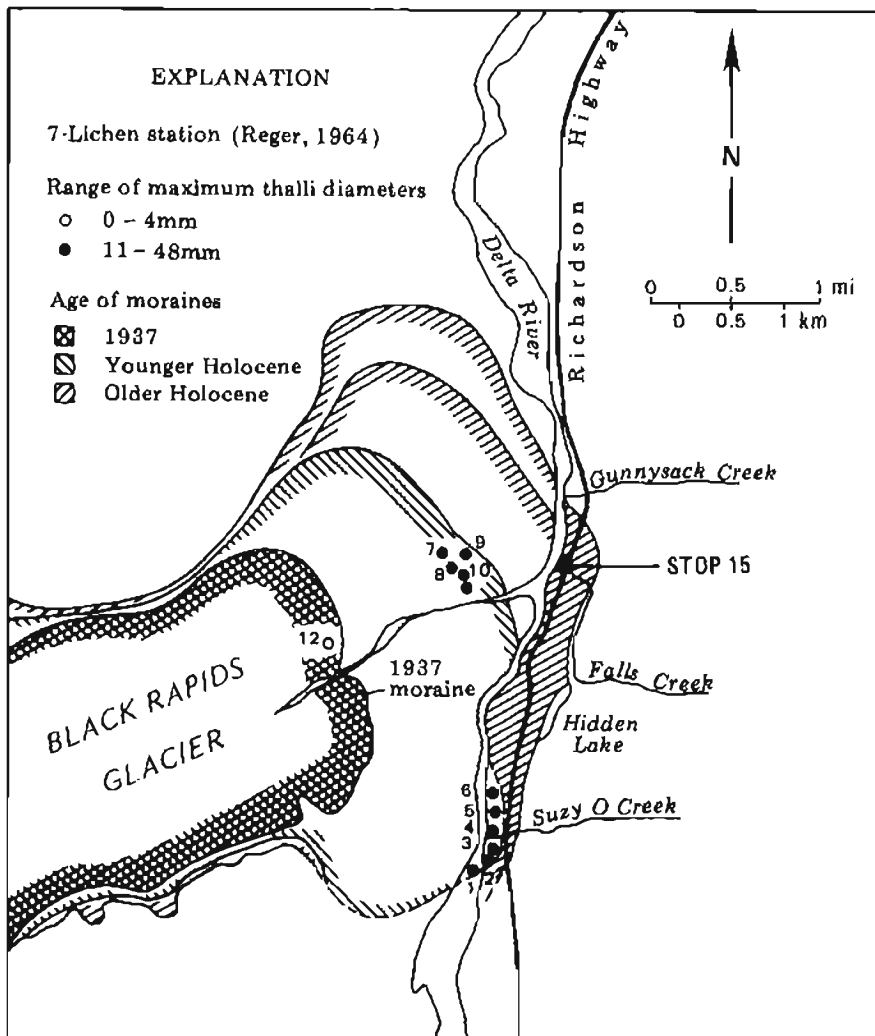


Figure 53. Relationship of maximum-diameter Rhizocarpon geographicum thalli to Holocene moraines of Black Rapids Glacier, central Alaska Range (modified from Reger and Pêwé, 1969, fig. 3).

Delta River to the southeast is our first view of the Holocene moraines of the Castner and Canwell Glaciers. Valley walls in this area are cut in schist of Precambrian and early Paleozoic age, but Rainbow Mountain 8 mi (13 km) to the south just beyond the Canwell Glacier and across the Denali fault is composed of late Paleozoic marine sedimentary and volcanoclastic rocks.

222. Here, dust frequently blows from the flood plain of the Delta River.

219.4 To the right (west) is Pump Station 10 of the Trans-Alaska Pipeline System.

217.2. On the left (east) is the terminus of Castner Glacier (fig. 54). Stagnant ice of the later Holocene advance is exposed 1,000 ft (300 m) to the east (left).

To the right, the elevated Trans-Alaska Pipeline System crosses the flood plain. The pipeline is not mounted on thermal piling because the ground is thawed and water flows through the flood-plain gravel.



Figure 54. Oblique aerial view (to the northeast) of the Richardson Highway, the TAPS route, and the termini of Canwell and Castner Glaciers in the central Alaska Range. Dashed line around glacial moraines indicates terminus of younger Holocene advances. Photograph 620RI-55RT-M864-55SRW-9M58 by U.S. Air Force, August 29, 1949.

217. The two Holocene advances of Castner Glacier, which Pêwê considers comparable to the earlier and later Holocene advances of Black Rapids Glacier, are recorded by moraines near the Richardson Highway. Part of the older terminal moraine is plastered on the bedrock hill at Mile 216.7 adjacent to the highway, just across Lower Miller Creek. The terminal moraine of the later Holocene advance is to the left (east of the highway at Mile 217) and is ice cored. In 1951, Pêwê measured trees up to 102 yr old growing on the ice-cored moraine.

Five small meltwater lakes dammed by Castner Glacier periodically break out from beneath the glacier and produce brief floods on the outwash fan.

Early stages in revegetation of both the moraine and outwash fan can be seen at this point. Dominant shrubs include buffaloberry (Shepherdia canadensis) and willow (Salix spp.). The legumes, Hedysarum spp., Astragalus spp., and Oxytropis spp., occur in abundance, as does dwarf fireweed (Epilobium latifolium). Scattered grasses are primarily Festuca rubra and Hierochloa alpina. A few mats of Dryas spp. are also present. Young white spruce have colonized the outwash fan and the oldest part of the moraine.

216.7. To the right (west) is a low knob of quartz diorite. Plastered against this bedrock hill is part of the moraine of the older Holocene advance of Castner Glacier, a moraine composed of a variety of schistose metamorphic rocks from up the valley.

216. STOP 16. CROSSING OF THE DENALI FAULT BY THE TRANS-ALASKA PIPELINE SYSTEM.

The Denali fault is one of the longest crustal breaks in Alaska. This right-lateral, strike-slip fault is topographically expressed as an arcuate trough that can be traced without interruption from the southwestern Alaska Range through the crest of the range into the Shakhwak Trench, Yukon Territory, Canada, and perhaps into Chatham Strait in southeastern Alaska (fig. 55). Some of the largest glaciers in the Alaska Range, many of which surge, occupy segments of the Denali fault-line valley, including the Chistochina, Gakona, Canwell, Black Rapids, Susitna, and Muldrow Glaciers. Recent work on the Denali fault has defined the McKinley and Hines Creek strands, which bifurcate just east of the Richardson Highway and rejoin west of Denali National Park-Preserve (fig. 55). Geologic evidence indicates that average rates of displacement along the Denali fault, measured over 10,000- to 65,000,000-yr periods, vary from 0.04 to 1.38 in. per yr (0.1 to 3.5 cm per yr). Offsets of glacial deposits of Donnelly age, Holocene alluvial fans, and at least 20 drainages along the McKinley strand west of here (fig. 56) demonstrate that 17 to 200 ft (5 to 60 m) of right-lateral movement and 20 to 33 ft (6 to 10 m) of vertical movement have occurred during the past 10,000 yr. Although numerous microseisms and a few small earthquakes have been detected along the eastern Denali fault system, historic offset is not well documented.

The TAPS route crosses the McKinley strand of the Denali fault near pipeline Milepost 589 [between upper and lower Miller Creeks approximately 3 mi (5 km) south of Pump Station 10]. The 48-in.-diameter (1.2 m) pipe is supported through this zone of potential fault movement on 47-ft-long (14 m) concrete 'sleepers' that are spaced approximately 60 ft (18.2 m) apart for a distance of 1,960 ft (594 m) (fig. 57). This design allows a maximum lateral

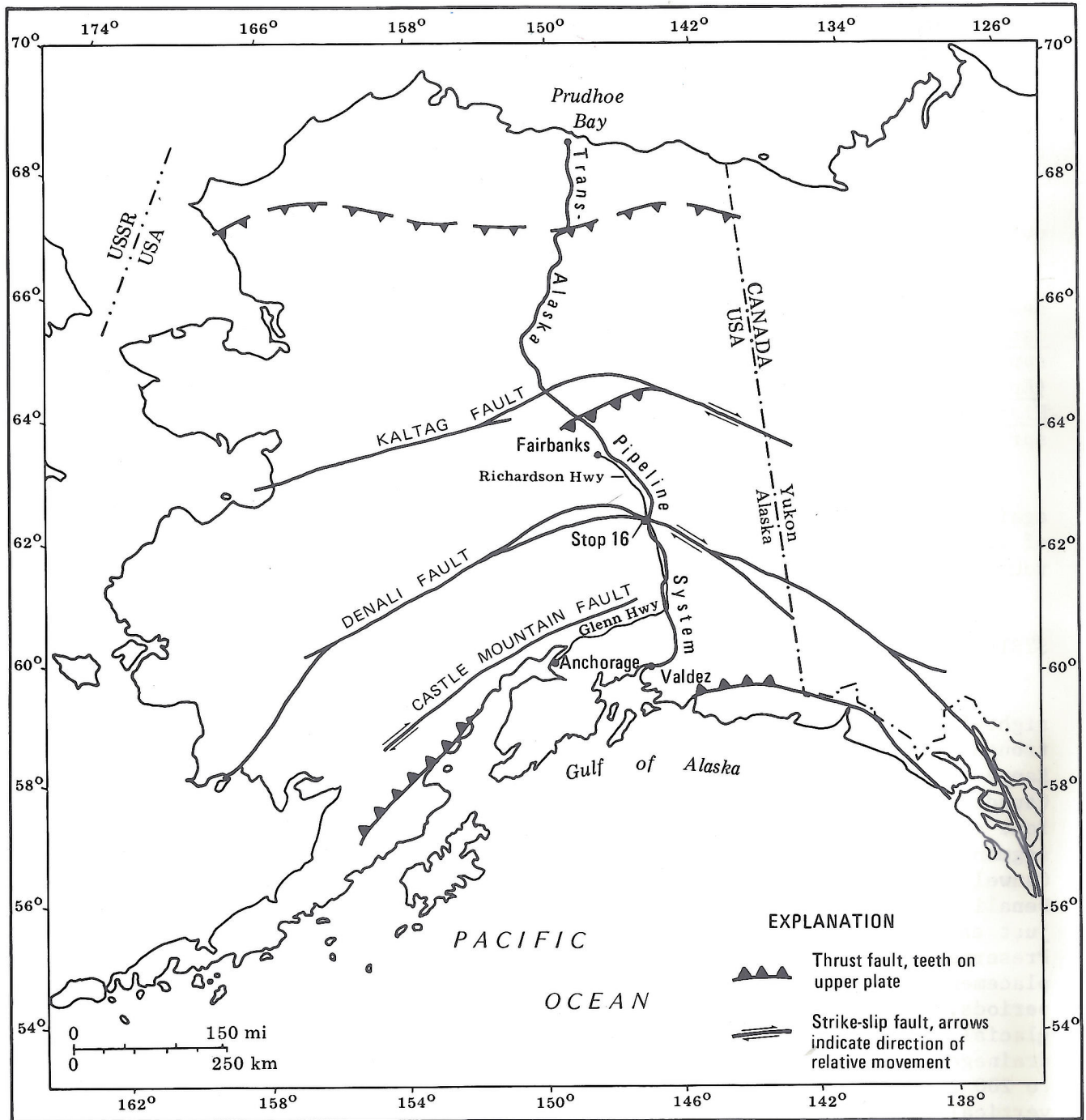


Figure 55. Relation of major faults in Alaska to the TAPS route, Richardson and Glenn Highways, and Stop 16 (modified from Stout and others, 1973, fig. 1).

displacement of 20 ft (6 m) and 6 ft (1.8 m) of vertical displacement due to fault movement. A project-wide, computer-based seismic-monitoring system provides instantaneous detection, evaluation, and automatic reporting of earthquake activity to the Valdez Operations Center. Seismic activity is



Figure 56. Oblique aerial view (to the west-northwest) along the trace of the McKinley strand of the Denali fault (arrows) in the drainage of Augustana Creek between the Delta River and Black Rapids Glacier, Mt. Hayes B-4 Quadrangle, Alaska. Photograph 94-3 by R.D. Reger, July 20, 1982.



Figure 57. View (to the south) of the special-design crossing of the Denali fault zone by the Trans-Alaska Pipeline System, Mt. Hayes B-4 Quadrangle, Alaska. Photograph courtesy of Alyeska Pipeline Service Company.

detected by accelographs located at Pump Stations 1, 4 through 12, and at the Valdez Terminal.

215. To the left (east) is Canwell Glacier, which displays clear evidence of older and younger Holocene advances. Lateral moraines of the older advance are well preserved upglacier, and a fragment of the terminal equivalent of this moraine exists at Mile 215 on the south side of Upper Miller Creek (fig. 54). A spruce log collected by Péwé in 1953 in till of this moraine is dated at less than 200 yr B.P. by the radiocarbon method (W-268); however, Meyer Rubin (written commun., 1964) stressed that the log could be older than 200 yr. A well-developed forest and turf are developed on this moraine fragment. Spruce stumps up to 159 yr old were present in 1951; these trees were probably cut down 10 to 15 yr earlier. Diameters of *R. geographicum* on the south lateral moraine of the older advance range from 5.2 to 6.34 in. (132 to 161 mm) and average 5.67 in. (155 mm) (fig. 58). These sizes indicate that the oldest Holocene moraine is at least 3,160 yr old and may be as old as 3,640 yr. The thick moss cover on the remnant of the older Holocene terminal moraine is unfavorable for lichen growth.

The terminal moraine of the later Holocene advance is well preserved near the highway (fig. 58). A prominent gravel ridge that is 10 to 15 ft (3 to 4.6

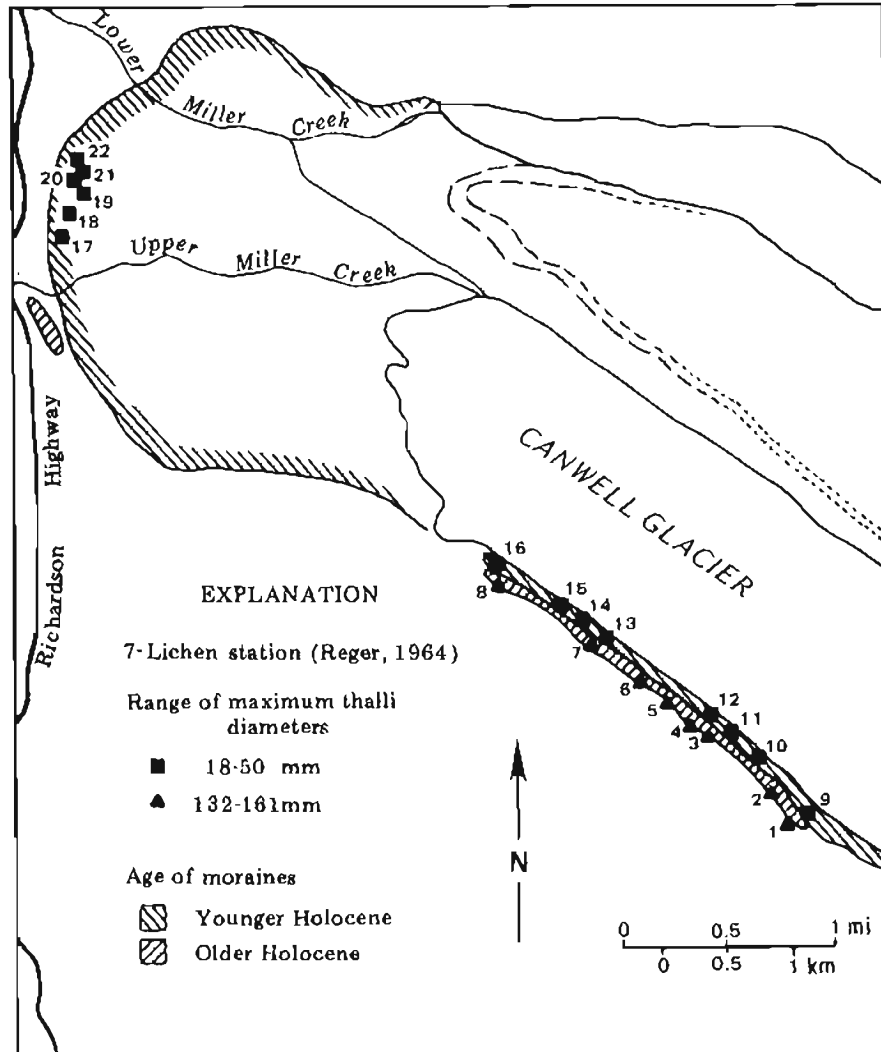


Figure 58. Relationship of maximum-diameter *Rhizocarpon geographicum* thalli to Holocene moraines of Canwell Glacier, central Alaska Range (modified from Reger and Péwé, 1969, fig. 5).

m) high is forested with a few white spruce, willows, and alders; it has no turf, and lichen-bearing boulders are scattered. In 1951, the oldest tree recorded on this moraine was 102 yr old. *R. geographicum* measure 1.1 to 1.97 in. (28 to 50 mm) in diameter on the south lateral moraine of Canwell Glacier, but on the terminal moraine they are only 0.71 to 1.3 in. (18 to 33 mm) in diameter, perhaps because of the tree cover (fig. 58). Assuming that the largest lichens on the lateral moraine (which is above tree line) most accurately represent the age of the younger Holocene moraine, the size of the lichens indicates that this moraine is about 550 yr old.

Three small meltwater lakes are impounded by Canwell Glacier. Occasionally these lakes burst out from beneath their ice dam and produce rapid rises in Miller Creek.

214. To the left, the large area of iron-oxide staining on Rainbow Mountain (in the distance) is caused by weathering of pyrite. To the right (west),

at the fork in the large creek directly across the Delta River, is the trace of one of four imbricate thrust faults. This particular thrust, the largest of the four, strikes east-west and dips 34° N. It extends at least 15 mi (2.4 km) to the west and is subparallel to the Denali fault (J.H. Stout, personal commun., 1965).

212.1. Volcanic flows and agglomerates of Pennsylvanian age are exposed in the rock quarry to the left.

211.95. To the left, fossils of late Paleozoic age are exposed in steeply dipping limestone. According to C.L. Rowett, former invertebrate paleontologist at the University of Alaska, the beds are early Pennsylvanian (pre-Desmoinesian) in age. Some fossils that occur here include:

Aulophyllid coral, genus undetermined
Cladochonus cf. C. texansensis Moore and Jeffords
Composita sp.
Linoproductus (sensu stricto) sp.
Echinoconchus sp.
Spirifer cf. S. rockymountainus Marcou
Spirifer spp.
Aviculopecten sp.
Pseudoparalegoceras n. sp.
 Phillipsid trilobite, genus undetermined

210.7. To the left is the 'Green Thumb,' an active solifluction fan on which no trees grow. The road is not satisfactorily maintained where it crosses the lower part of the fan.

210. STOP 17. RAINBOW MOUNTAIN (fig. 59).

To the left, the till (bedded?) fill indicates that this rock gorge existed prior to the Donnelly Glaciation. Rainbow Mountain is essentially a strike ridge trending northwest that rises abruptly more than 4,200 ft (1,280 m) above the valley floor. Much of the western slope of the ridge approximates a dip slope. The mountain is composed of folded and faulted detrital rocks, including 'graywacke,' limestone, andesitic and dacitic pyroclastic rocks, and minor andesite flows of Mississippian(?) and Pennsylvanian age that have been intruded by andesite, granodiorite, and quartz diorite of Mesozoic age.

The green and maroon colors are predominantly associated with the volcanic rocks and the yellow and green colors are associated with siltstone and sandstone. The sill-like porphyritic andesite intrusions are characteristically purplish green and the rhyolites are dark green.

209. To the left is a stabilized scree-slope deposit.

207. STOP 18. ACTIVE ROCK GLACIER (fig. 60).

This rock glacier is about 1 mi (1.6 km) long and originates in the empty cirque at the top of Rainbow Mountain. Tertiary continental sedimentary rocks are exposed in the lower valley wall across Phelan Creek.

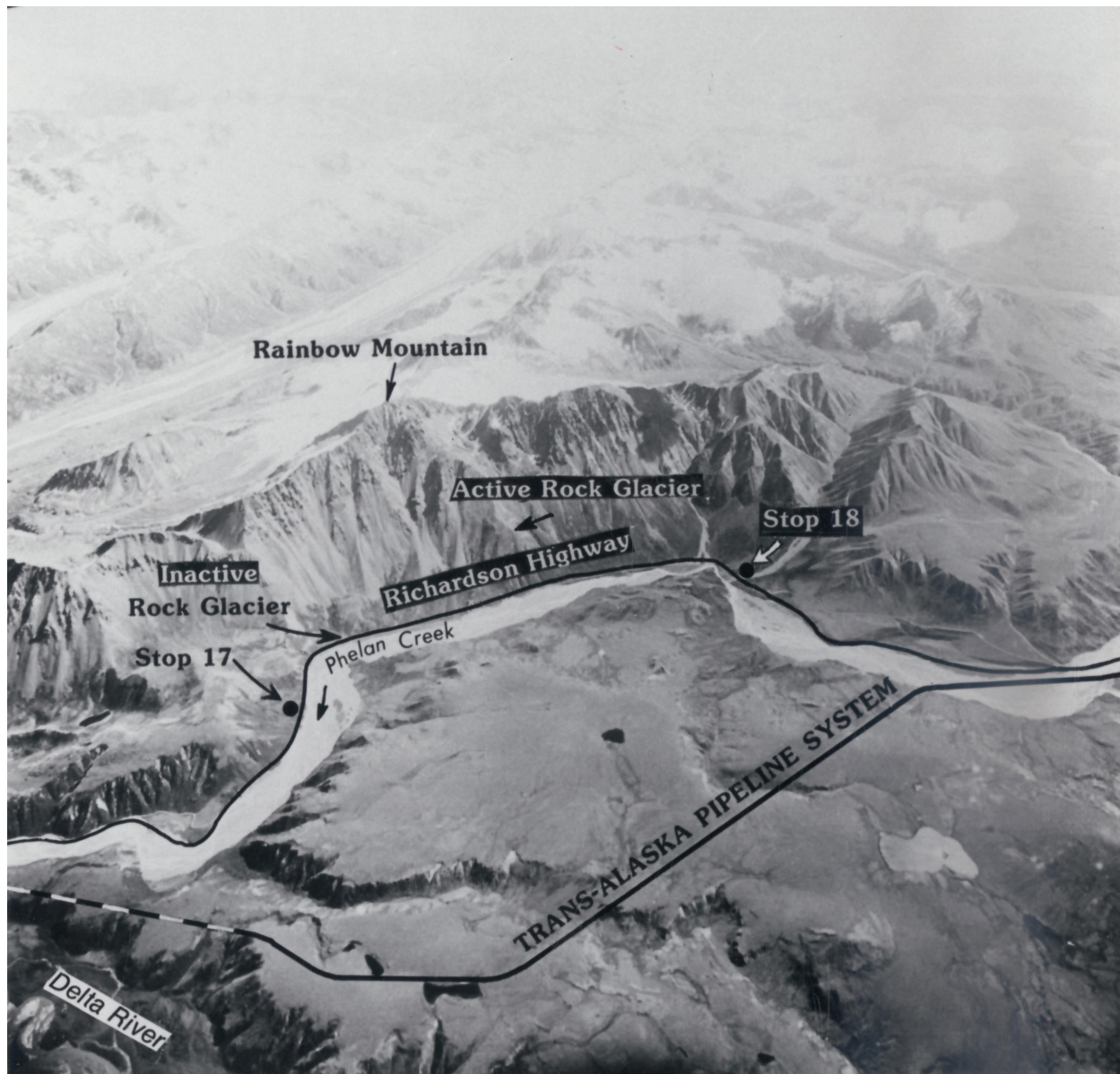


Figure 59. Oblique aerial view (to the east) of the Rainbow Mountain area near the crest of the Alaska Range, Mt. Hayes B-4 Quadrangle, Alaska. Photograph by U.S. Army Air Corps, 1943.

From Rainbow Mountain to Isabel Pass, the road travels upward through the altitudinal tree line. As the upper limit of trees is approached, spruce trees become scattered, but are generally upright and relatively fast growing. Open stands of white spruce can be seen along the terraces of Phelan Creek to 3,000 ft (900 m) elevation, and scattered spruce occur at elevations up to 3,500 ft (1,200 m) in this area. No old stumps are found above present tree line, and many trees at or near tree line are less than 100 yr old, indicating that tree line is now as high as it has been in recent times and that it may actually be rising in some localities.



Figure 60. View of an active rock glacier on the west flank of Rainbow Mountain from Mile 206.8 on the Richardson Highway in the upper Delta River area. The steep front of the rock glacier with no patination on the rocks indicates that the rock glacier is flowing and is cemented by interstitial ice. Photograph 678 by T.L. Péwé, July 12, 1952.

At tree line and above is a zone of shrubs that is narrow on steep slopes, as in the area around Rainbow Mountain, or very extensive, as in the Isabel Pass-Summit Lake area. This zone consists primarily of the same plants that are found in the open spruce stands at lower elevations, including shrubs, resin birch, willows, Labrador-tea, and blueberry. Scattered through the shrubs is a moss mat of *Hylocomium splendens*. Between the tall shrubs and on exposed ridges are mats of *Cladonia* lichens, crowberry (*Empetrum nigrum*), alpine bearberry (*Arctostaphylos alpina*, and lingenberry (*Vaccinium vitis-idaea*). Because of the abundant lichens, this vegetation zone was utilized heavily by caribou---small herds were frequently seen in the winter months in the Isabel Pass-Summit Lake area feeding on lichens before the caribou were decimated.

207. To the right, note the boulder bed across Phelan Creek. This boulder bed appears to be a 4-ft-thick (1.2 m) layer of outwash gravel deposited on a terrace surface cut into Tertiary bedrock. A 100-ft-thick (30 m) remnant of a landslide, talus deposit, or rock glacier from Rainbow Mountain overlies the outwash. The outwash gravel appears to be a continuation of the outwash gravel on the terrace surface directly ahead, on this side of Phelan

Creek. If this interpretation is correct, the 'landslide' is post-Donnelly in age.

To the left is the contact between Paleozoic and Tertiary rocks. Directly ahead, across Phelan Creek, at an altitude of 4,000 ft (1,212 m), till of Donnelly age occurs on top of the low hill. (The road from Mile 206.8 to Mile 204.7 is now on the flood plain of Phelan Creek, not on a terrace as shown on the U.S. Geological Survey Mt. Hayes B-4 (1958) topographic map).

206.2. To the left, an alluvial fan has buried the terrace surface in the distance. This terrace surface is probably of late Donnelly or early post-Donnelly age and bears large-scale polygonal ground similar to that exposed near Donnelly Dome.

205. To the left an alluvial fan has buried the surface of two terraces. These terrace remnants are matched by terrace remnants on the other side of Phelan Creek valley. Their gradient is less than the gradient of Phelan Creek.

204.7. Enter Mt. Hayes A-4 Quadrangle.

204. To the left are coal-bearing Tertiary rocks that underlie glacial drift and are subject to landsliding.

203. Lower terrace surface.

203.3. Higher terrace surface.

200.1. Edge of terrace composed of outwash gravel. The route climbs onto the terrace that is graded to a terminal moraine of the Summit Lake advance (late Donnelly Glaciation) (fig. 33).

199. Isabel Pass, elevation 3,285 ft (995 m).

197.7. STOP 19. GULKANA GLACIER VIEW AND RICHARDSON MONUMENT.

The pingolike knob standing above the outwash fan of Gulkana Glacier (to the southeast) is composed of rounded cobble gravel. Surface drainage from Gulkana Glacier wanders back and forth across the outwash fan, sometimes draining through the Delta, Tanana, and Yukon Rivers to the Bering Sea and sometimes into the Copper River to the Pacific Ocean. For the last few years, the drainage has been artificially diverted into the Delta River.

The Richardson Highway connects Valdez and Fairbanks and is the oldest major transportation route in Alaska. The highway was initiated as the Fairbanks-Valdez Trail in 1901, when Congress appropriated funds for its construction. In 1904, funds were appropriated to survey a wagon road along this route. In the early years, it was mainly a winter sled and wagon road, and the first complete truck and auto trip was reportedly made in 1913. In the 1920s, the road was named the Richardson Highway after W.P. Richardson, who was president of the Alaska Road Commission from 1905 to 1917.

Gulkana Glacier was intensively studied from 1960 to 1966 under a program of integrated investigations directed by the Department of Geology, University of Alaska, Fairbanks. Since 1966, the glacier has been continuously monitored

by the Water Resources Branch of the U.S. Geological Survey as part of their ice-and-water-balance studies of selected glacier basins for the International Hydrological Decade (1965-1974). Gulkana Glacier, located 4 mi (6.4 km) north-east of Isabel Pass, is one of several temperate valley glaciers on the south side of the Alaska Range (fig. 61).

A gravel road branching from near the Richardson Monument at Isabel Pass extends to within 2 mi (3.2 km) of the terminus of Gulkana Glacier, which is flanked by College Glacier on the east and West Gulkana Glacier on the west (fig. 61). Gulkana Glacier originates in three adjacent compound cirques with an average elevation of 6,500 ft (1,970 m) above sea level. Ice from these cirques converges to form a simple, south-flowing valley glacier that extends about 2.5 mi (4 km) to its terminus [elevation about 3,830 ft (1,160 m)]. A sequence of arcuate end and parallel lateral moraines of Holocene age encircle the terminal areas of Gulkana, West Gulkana, and College Glaciers.

The meteorology, mass budget, surface flow, subglacial topography, and ice structures of Gulkana Glacier have been studied in detail. The glacier is roughly 'T-shaped,' with the horizontal bar representing the complex accumulation zone and the vertical bar representing the south-flowing ablation zone. Accumulation in three cirques produces three major ice streams, which are delineated by medial moraines (fig. 62). Ice stream 3 is cleaved by a bedrock bastion into two unequal parts, 3a and 3b. The glacier is moderate in size, with a surface area of 8.5 mi² (21.8 km²). The accumulation zone comprises about 60 percent of the total area; in the 1966 and 1967 hydrologic years, which were apparently about average, the accumulation-area ratios were 0.59 ± 0.02 and 0.60 ± 0.03 , respectively. Two large icefalls that are present are Moore Icefall (in the eastern cirque) and Gabriel Icefall (just below firn line in the western ice stream) (fig. 62).

Mass-balance studies during the 1966 and 1967 hydrologic years indicate that Gulkana Glacier is in a near-continental climate. During those years, weather patterns were normal at low-altitude stations in the region and at Gulkana Glacier. During 1966, the winter snowfall in the Gulkana Glacier basin, measured in mid-May, was 5 to 10 times higher than the winter snowfall recorded at several low-altitude sites in the Copper River basin (to the south) and in the Tanana River valley (to the north). Equilibrium-line altitude (ELA), where the mass balance equals zero, is high at Gulkana Glacier, about 5,775 ft (1,750 m) on the average, compared to $5,840 \pm 100$ ft ($1,770 \pm 30$ m) in 1966 and $5,740 \pm 66$ ft ($1,740 \pm 20$ m) in 1967. The average ice balance ranges from -10.73 ft (3.25 m) at 4,175 ft (1,265 m) to +6.6 ft (2 m) at 7,950 ft (2,410 m) (fig. 63). The average activity index, or ice balance versus altitude, is low; in 1966 it was 0.07 in. per ft (6 mm per m).

In 1961, a study was undertaken to determine the relative importance of various means of energy transmittal that cause melting of glacial ice. Energy-exchange processes include radiation, condensation, evaporation, and conduction from precipitation and the atmosphere. Solar radiation is commonly accepted as the most important energy source for ablation. In a study of solar radiation on Gulkana Glacier at an elevation of 4,800 ft (1,465 m), a net-total radiometer continuously recorded radiation flux during the melt season. During the 53 periods (each 24 hr long) with reliable radiation data, a total of 8,300 g-cal per cm² of heat was received by the surface of the glacier. During the same interval, 51.4 in. (131 cm) water equivalent of ice and snow melted, a

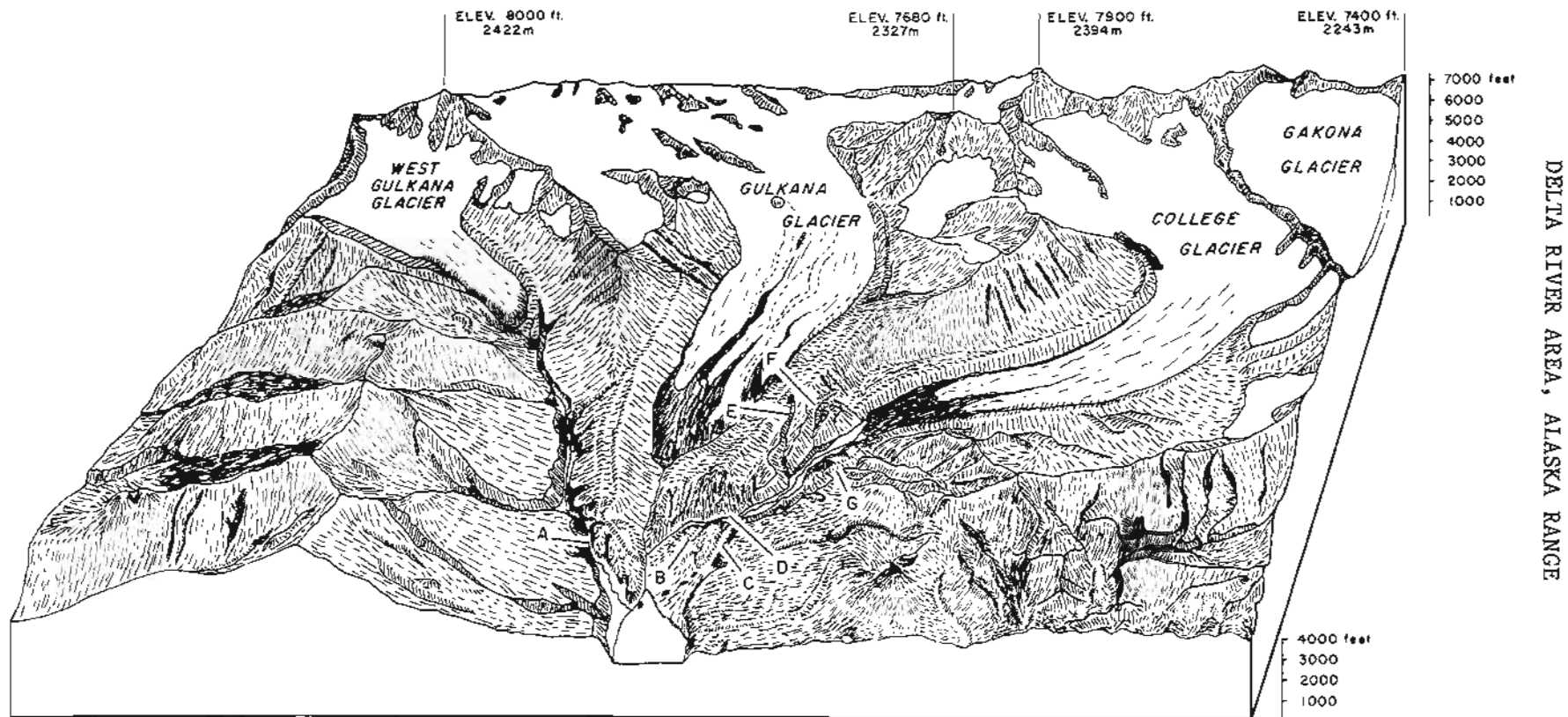


Figure 61. Block diagram of the Gulkana-College Glaciers area, south-central Alaska Range. A, West Gulkana Creek; B, 1875-1900 A.D. ice-marginal channel of Gulkana Glacier; C, 260- to 560-yr-old ice marginal channel of Gulkana Glacier; D, College Creek canyon; E and F, latest Wisconsinan ice-marginal channels of College Glacier (modified from Reger, 1964, frontispiece).

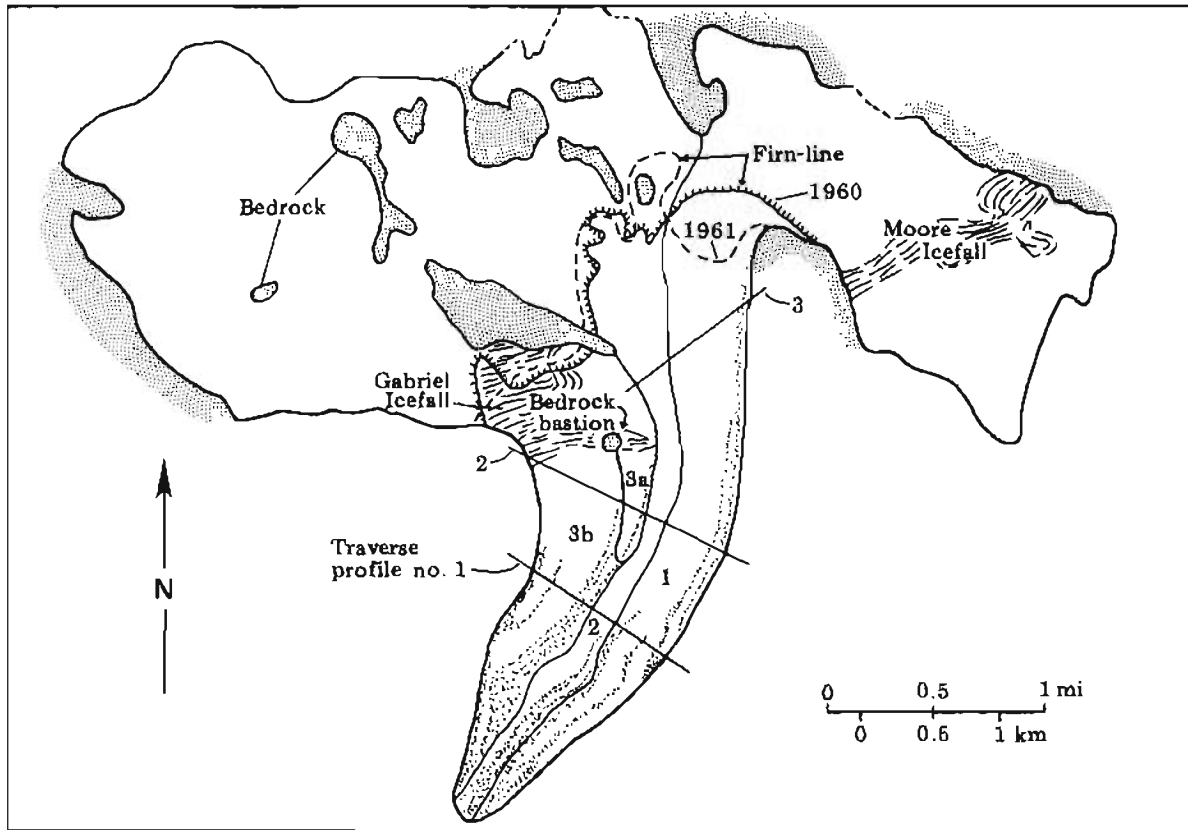


Figure 62. Map of Gulkana Glacier, central Alaska Range, showing accumulation and ablation areas, principal ice streams and icefalls, transverse profiles along which motion and ice-thickness surveys were made, and 1960 and 1961 firn lines (from Moores, 1962, fig. 2).

process requiring 10,400 g-cal per cm^2 of heat. Radiation received was equal to 75 percent of the energy required to melt the glacial ice and apparently 89 percent of the energy required to ablate the snow.

Surface motion in the ablation zone of Gulkana Glacier was studied in 1960 and 1961. On either side of the exposed bedrock bastion, the glacier flows as two ice streams. Below the bastion, these ice streams retain their identity as 'velocity ice streams,' each with its own axis of maximum velocity (fig. 64). These velocity ice streams merge near the terminus to form one stream. The velocity in the eastern ice stream is greater than 125 ft per yr (41 m per yr) near firn line. The velocity decreases downglacier to zero (stagnant ice) near the terminus.

The latest Wisconsinan and Holocene variations of Gulkana and College Glaciers are partially documented by photographs, geomorphic evidence, two radiocarbon dates, and several lichenometric dates (fig. 65). Because the Holocene moraines of these glaciers occur above tree line where organic material is rarely preserved, and because they predate the photographic record, they are best dated by lichenometry. However, the length of life of the lichen species imposes a limit on surface ages that can be determined by this method. The growth curve for *R. geographicum* that was derived by Denton and Karlén (1973; 1977) [which is generally supported by Ten Brink (unpublished data)]

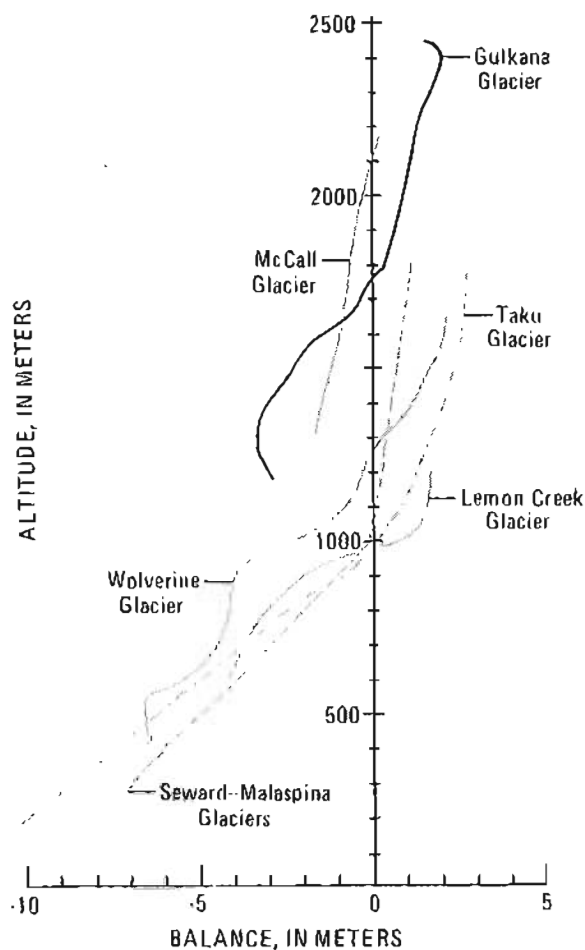


Figure 63. Comparison of ice balance-altitude curves for Gulkana Glacier and other representative Alaskan glaciers (modified from Meier and others, 1971, fig. 1).

for the central Alaska Range], extends to 3,200 yr B.P. (fig. 52), but it may be valid for several more centuries. Assuming their curve is correct for the central Alaska Range and considering the other evidence, minor advances of Gulkana Glacier occurred about 5,700 yr, 3,890(?) yr, 2,970 yr, 800 yr, and 260 to 180 yr B.P. and from 1875 to 1900 A.D. (fig. 65). Advances of College Glacier occurred about 5,700 yr and 260 yr B.P. and from 1900 to 1920 A.D. (fig. 65). Other undocumented minor Holocene advances also probably occurred.

Probable latest Wisconsin margins of Gulkana Glacier are documented by two small, subdued terminal moraines near the south margin of the outwash fan 1.9 and 2.1 mi (3 and 3.4 km) from the 1962 terminus. They probably represent recessional positions of Gulkana Glacier during the waning phase of the Summit Lake (Donnelly IV) advance and may be 9,500 to 10,000 yr old (fig. 65). Two limits of College Glacier, which are roughly equivalent in age to the terminal moraines of Gulkana Glacier, are documented by two curved, ice-marginal channels incised 300 to 365 ft (90 to 110 m) into bedrock beneath the Wisconsin glacial floor 1 and 1.4 mi (1.6 and 2.2 km) west of the 1962 terminus of College Glacier.

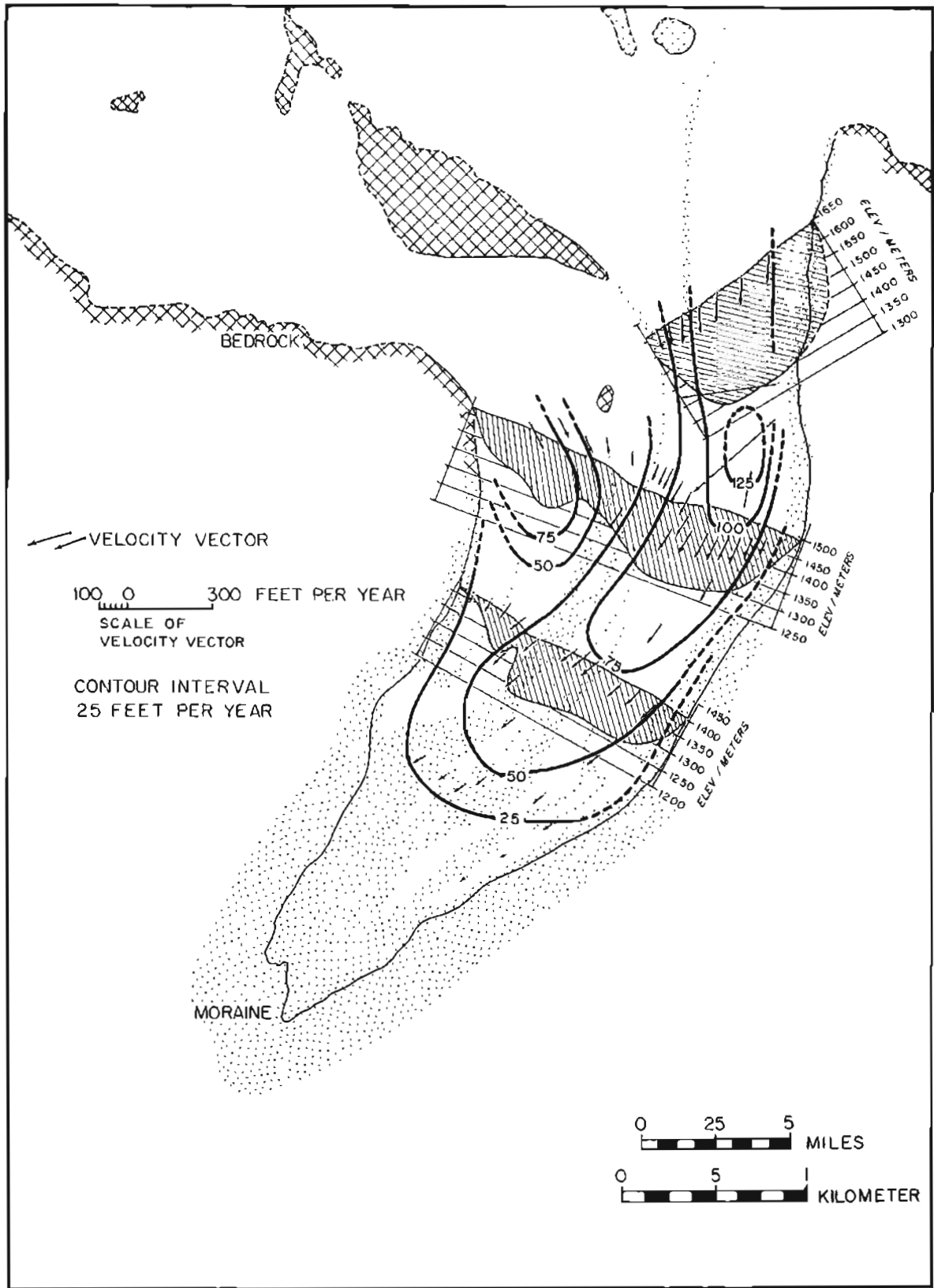


Figure 64. Yearly surface velocity (1960-61) and subsurface topography of Gulkana Glacier, central Alaska Range (from Moores, 1962, in Ostenso and others, 1965, fig. 3).

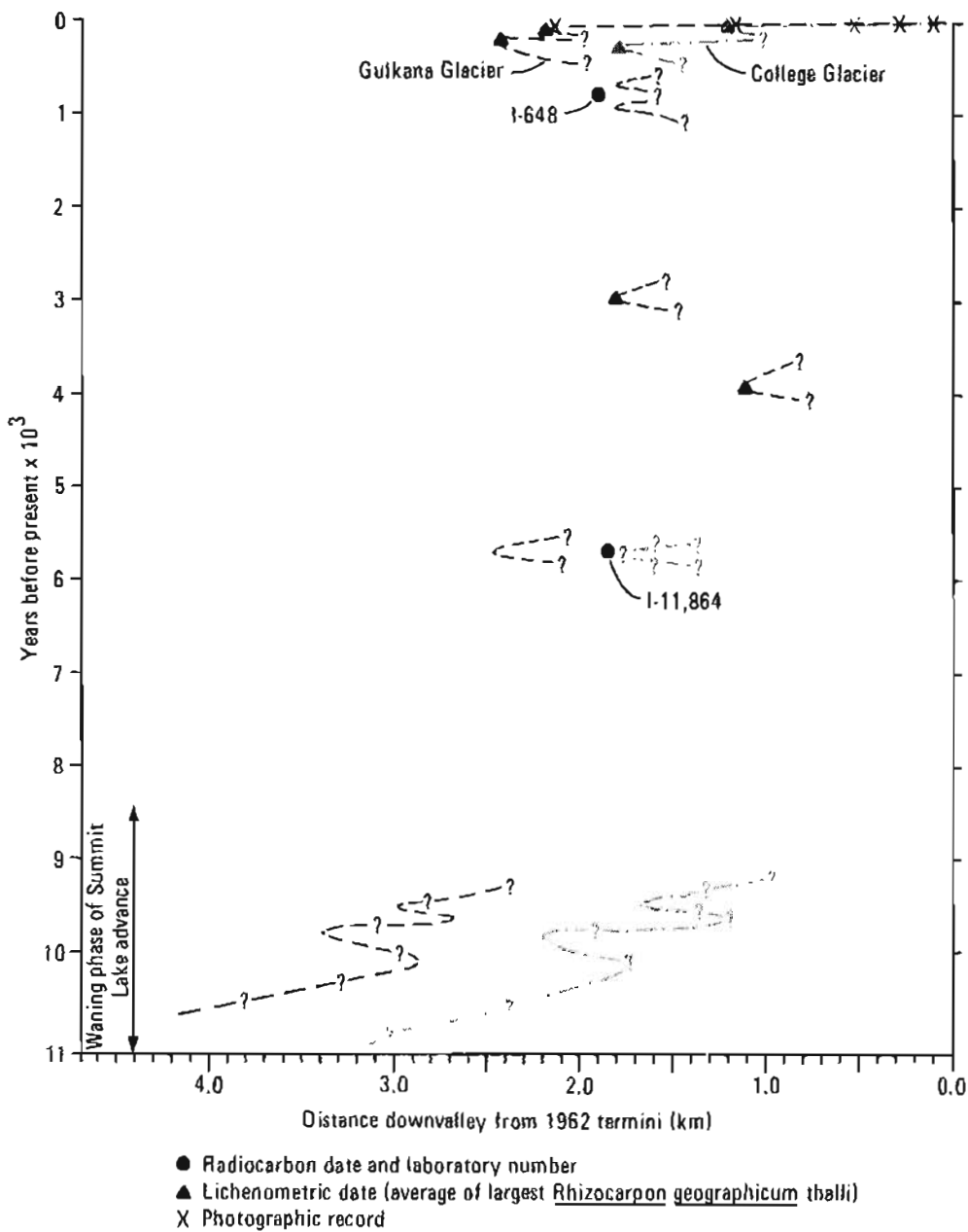


Figure 65. Approximate variations of Holocene terminal positions of Gulkana and College Glaciers relative to their 1962 termini. Advances and relative positions during waning phase of Summit Lake (Donnelly IV) advance are inferred from locations of buried lateral moraines, terminal moraines older than the range of lichen dating, and ice-marginal stream canyons.

After retreat of College Glacier from these positions, College Creek cut into bedrock at least as deep as 380 ft (115 m). The presence [only 19 ft (5.8 m) above the present flood plain of College Creek] of foreset fan-delta beds dated at $5,700 \pm 260$ yr B.P. (I-11,864) (fig. 66) demonstrates: a) that major Holocene downcutting by College Creek to a level below the modern flood

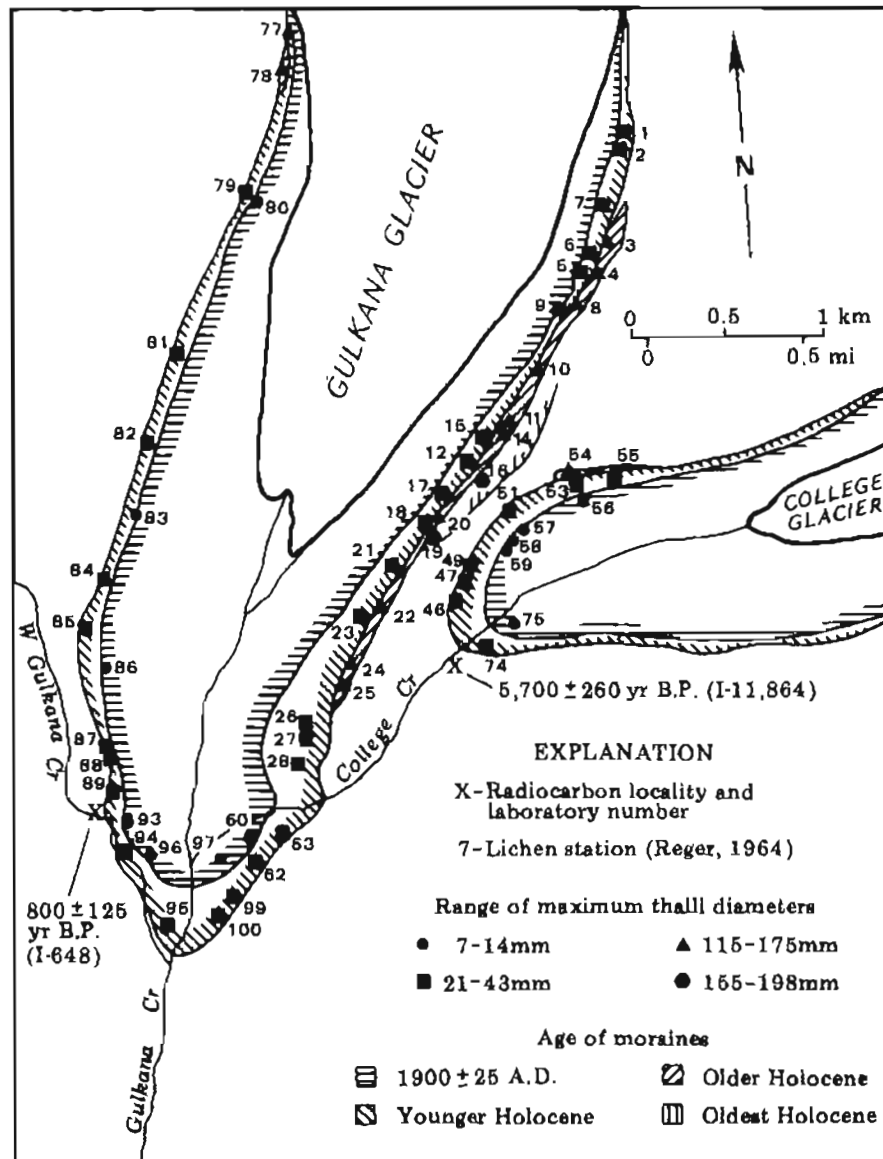


Figure 66. Relationship of maximum-diameter *Rhizocarpon geographicum* size ranges to Holocene moraines and 1962 ice limits of Gulkana and College Glaciers, central Alaska Range (modified from Reger, 1964, fig. 7).

plain ceased prior to 5,700 yr B.P.; b) that a brief episode of gravel and sand alluviation (valley filling) occurred in the College Creek drainage close to 5,700 yr B.P., probably in response to a minor readvance of College Glacier, but perhaps the result of a sudden influx of outwash from the east margin of Gulkana Glacier; and c) that Gulkana Glacier concurrently advanced to a position close to 1.6 mi (2.5 km) downvalley from its 1962 terminus, briefly blocking College Creek to form a temporary lake in which the fan delta was deposited (fig. 65).

An advance of Gulkana Glacier about 3,890 yr B.P. is recorded by a fragment of lateral moraine along the east side of the east lateral-moraine complex of Gulkana Glacier. This moraine is flat topped and bears incipient stone rings. It has no terminal equivalent. Boulders are densely covered with R. geographicum that range in size from 6.1 to 7.8 in. (155 to 198 mm) and have an average maximum diameter of 6.69 in. (170 mm). Assuming that the largest thallus most closely approximates the age of this advance, the moraine could be as old as 4,670 yr, based on a linear extrapolation of the Denton and Karlén growth curve for this species; however, extensions beyond 3,200 yr are very tentative. There is no positive evidence for an equivalent advance of College Glacier, although either of two buried lateral moraines outside the remnant of the 2,970-yr-old lateral moraine is a reasonable candidate.

Gulkana Glacier readvanced about 2,970 yr B.P. and overrode the 3,890(?) -yr-old terminal moraine (figs. 65 and 66). The most prominent 2,970-yr-old moraine is preserved in the east lateral-moraine complex of Gulkana Glacier as a narrow, continuous ridge and as a small patch of till outside the northwest 180-yr-old lateral moraine (fig. 66, stas. 77 and 78). This moraine is not ice cored. Diameters of largest R. geographicum thalli on this moraine range from 4.53 to 6.89 in. (115 to 175 mm) and average 5.39 in. (137 mm). Based on the size of the largest R. geographicum measured on this moraine and on the linear extrapolation of the growth curve for this lichen, this advance could have occurred as long ago as 4,030 yr B.P.

A single minor pulse, or perhaps two minor pulses, of Gulkana Glacier about 800 yr B.P. apparently stopped close to but less than 1.2 mi (1.9 km) downvalley from the 1962 terminus. This fluctuation is documented by an outwash terrace in the southwestern terminus, where a 0.28-in.-thick (7 mm) peat, dated at 800 ± 125 yr B.P. (I-648), is preserved in a thin sand layer overlying at least 4 ft (1.3 m) of gravel and underlying 10 ft (3 m) of gravel (fig. 66). This peat also provides a minimum date for the cutting of the lower west Gulkana Creek canyon. An alternate interpretation is that either the upper or lower terrace gravel, or perhaps both, are derived from a minor advance or minor advances of West Gulkana Glacier, but this hypothesis is not supported by field evidence. No equivalent advance of College Glacier has been identified.

About 260 yr B.P. and perhaps as early as 560 yr B.P., College Glacier advanced to a position 1.1 mi (1.8 km) downvalley from the 1962 terminus (fig. 66). This brief pulse is recorded by a series of nested terminal and lateral moraines on which the largest R. geographicum thalli range from 1.14 to 1.97 in. (29 to 50 mm) and average 1.42 in. (36 mm). A discontinuous outwash terrace 5.9 to 7.9 ft (1.8 to 2.4 m) above the present flood plain in the canyon of College Creek is graded from these moraines to the easternmost of two side-glacial drainage channels in the east terminal zone of Gulkana Glacier (fig. 61), indicating that Gulkana Glacier was also in a very extended state (1.5 mi or 2.4 km beyond the 1962 terminus) at this time (fig. 65). This ice-marginal channel at 3,740 ft (1,133 m) elevation was formerly interpreted as the drainage course for waters spilling out of an ice-dammed lake in College Creek canyon, but no lake deposits have been found to support this concept. Only sandy gravel and gravel are present in terrace deposits. Thus, gravel aggradation in College Creek probably kept pace with the rising base level induced by an advance of Gulkana Glacier, which gradually blocked the mouth of College Creek canyon. The largest lichens on the terminal and lateral moraines formed

by this advance of Gulkana Glacier range from 0.83 to 1.69 in. (21 to 43 mm) and average 1.14 in. (29 mm), indicating that the glacier remained in an extended position until about 180 yr B.P. Based on the size of the largest R. geographicum, this advance could have occurred as early as 390 yr B.P. A small ice core is still preserved in these lateral moraines, as demonstrated by fresh slumping and debris-flow activity above an elevation of 4,400 ft (1,333 m).

Between 1875 and 1900 A.D., Gulkana Glacier readvanced to a position 1.4 mi (2.3 km) downvalley from the 1962 terminus, again blocking College Creek and building a small, 8-ft-high (2.5 m) terminal moraine. This advance was apparently more rapid than the previous advance---or at least aggradation in College Creek did not keep pace with rising base level induced by gradual blocking of its canyon---because a small temporary lake formed at the mouth of the College Creek canyon; about 20 ft (6 m) of medium sand soon filled this impounded basin. Lake waters drained through an ice-marginal channel at 3,700 ft (1,121 m) elevation in the east terminal area (fig. 61). Lateral moraines of this late-19th-century advance are much less conspicuous than those of earlier advances, although the ice core is well preserved. Largest R. geographicum on moraines of this advance range from 0.28 to 0.55 in. (7 to 14 mm) and average 0.39 in. (10 mm) (fig. 66).

A historic advance of College Glacier between 1900 and 1920 A.D. is indicated by small moraines on which the largest R. geographicum range from 0.24 to 0.39 in. (6 to 10 mm) and average 0.31 in. (8 mm) (fig. 65). The terminal moraine of this minor expansion is 0.8 mi (1.2 km) downvalley from the 1962 terminus (fig. 65).

A 1910 photograph of lower Gulkana Glacier by Fred Moffit (fig. 67) shows that the terminus remained close to the 1875-1900 A.D. terminal moraine for several years; the smooth glacier surface and debris-covered terminus indicate that the glacier had a slightly negative budget for several years prior to 1910. Between 1910 and 1966, periodic aerial photographs (1941, 1954, and 1957) record a general thinning and shrinkage of Gulkana Glacier. The average rate of retreat was about 120 ft per yr (36 m per year); total retreat of the terminus was 1.25 mi (2 km). In 1966, the terminus receded an average of 145 ft (44 m) and in 1967 it melted back another 165 ft (50 m). In the Gulkana Glacier basin, the area of ice-cored moraine, most of which developed after 1910, is 0.6 mi² (1.5 km²). Between 1941 and 1962, College Glacier retreated 0.34 mi (0.54 km), averaging about 85 ft per yr (26 m per yr).

195. STOP 20. SUMMIT LAKE (fig. 68).

Summit Lake occupies a depression formed when glacial ice of late Donnelly age stagnated and melted in place. Ice-contact ('dead-ice') deposits are well developed at the southern end of the lake.

To the west and south of Summit Lake are the Amphitheater Mountains, which consist of small knobs---mostly of metabasalt---that protrude 2,000 to 3,000 ft (600 to 900 m) above the drift-covered lowland. The lowland is generally underlain by Tertiary sandstone and conglomerate and some coal beds. The Denali Highway traverses the southern Amphitheater Mountains area from Paxson to the Maclaren River. Glaciers originating on the south side of the Alaska Range pushed over and through these mountains.



Figure 67. Photographs of the terminal zone of Gulkana Glacier in 1910 and 1952 illustrate a dramatic change in the glacier (from Sellmann, 1962, fig. 8).

- A. View (to the northwest) toward West Gulkana Glacier showing Gulkana Glacier very close to the 1875-1900 A.D. lateral moraines. U.S. Geological Survey photographs 423-424 by F.H. Moffit, July 15, 1910.
- B. Same view from 4,650 ft (1,409 m) elevation showing ice-free valley previously occupied by Gulkana Glacier. Photographs 666-668 by T.L. Pêwé, July 12, 1952.



Figure 68. View (to the north) from Summit Lake of the snow-covered south-central Alaska Range and Gulkana Glacier. Isabel Pass is to the upper left. Photograph 797 by T.L. Pélwé, September 7, 1952.

Paxson Mountain is an elongate, 2,000-ft-high (600 m) prominence of metabasalt that can be seen clearly (to the south) from Summit Lake. The overflow gorges and the drift cover on the mountain record a complex glacial history typical of the Amphitheater Mountains. Isolated erratics atop Paxson Mountain are thought to be early to mid-Pleistocene in age (fig. 69) and a large, weathered overflow gorge that is easily visible on the skyline of the mountain was probably cut across the crest of the mountain at that time. During the next glacial advance (mid- to late Quaternary age), ice-marginal streams cut open-ended gorges at lower levels on Paxson Mountain. These notches are partially filled with frost-rived rubble. The Wisconsin advances surrounded Paxson Mountain. Fresh overflow notches were cut at elevations of 3,000 to 4,000 ft (1,150 to 1,212 m), and young drift surrounds the mountain below this elevation. Cirques on Paxson Mountain appear to be Wisconsinan and pre-Wisconsinan in age.

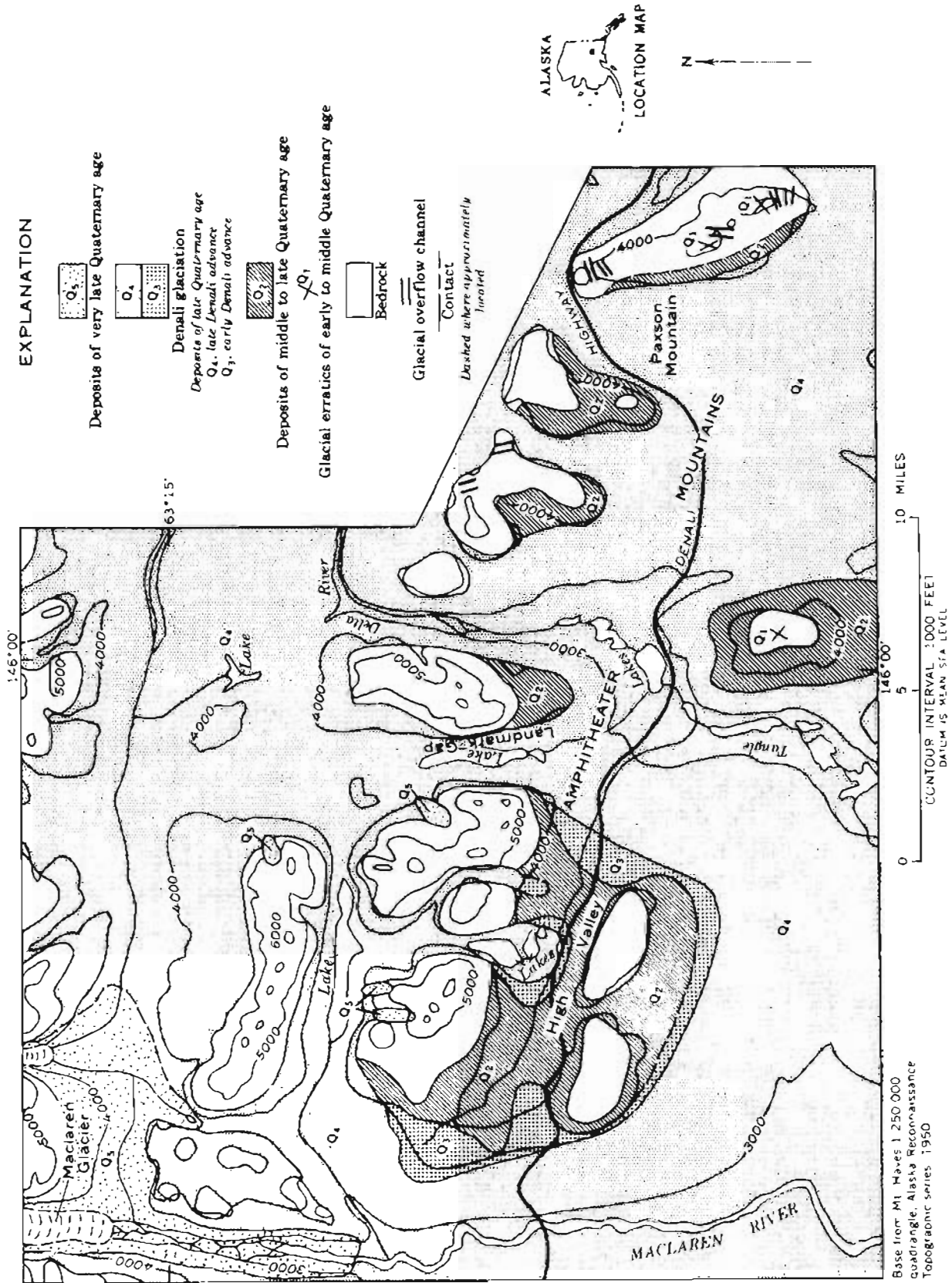


Figure 69. Glacial deposits in the headwaters area of the Delta River, Amphitheater Mountains, Alaska (from Péwé, 1961, fig. 357).

191. Fish Creek. In July or August, a run of red salmon migrates from the Pacific Ocean through the Copper River to spawn near this location.

190.5. To the right is an artificial meander cutoff. Tertiary claystone with unidentifiable plant fragments is exposed in the bottom of the cut.

190.5 to 185.6. Paxson Canyon is cut in stratified and unstratified drift. An esker traverses the top of the right canyon wall.

193. From Mile 193 to Paxson, the Richardson Highway is in the Mt. Hayes A-3 and A-4 Quadrangles.

185.4. Paxson, at the junction of the Richardson and Denali Highways. The climate of both the Gulkana Upland and the south flank of the east-central Alaska Range is transitional between the maritime climate of coastal Alaska and the continental climate of the Interior. Summers are short and cloudy. Long, cold winters are dominated by stable, dry continental air masses. From 1917 through 1943, a very discontinuous climatic record was maintained at Paxson at 2,750 ft (833 m) elevation. This incomplete record shows that the average annual temperature was about 23.9°F (-4.5°C); the average summer temperature was about 50°F (10°C). During this period, average annual precipitation was about 19.7 in. (50 cm), and average summer precipitation was about 8.3 in. (21 cm).

On south-facing slopes in this part of the northern Gulkana Upland, tree line generally occurs at 2,500 to 3,200 ft (758 to 970 m) elevation. Shrubs of resin birch (*Betula glandulosa*) and willow (*Salix* spp.) are the most common shrubs in the brush zone between 2,500 and 3,500 ft (758 and 1,060 m) elevation. Alpine tundra occurs on south-facing slopes above 3,000 to 3,500 ft (910 to 1,060 m). On north-facing slopes, tree line is generally about 2,500 to 3,100 ft (758 to 940 m) elevation, the brush zone occurs between 2,900 and 3,500 ft (878 and 1,060 m) elevation, and shrub tundra covers some slopes and ridges above 3,000 ft (910 m). Above 4,000 to 4,500 ft (1,212 to 1,357 m) on north-facing slopes, patches of herbaceous-lichen tundra, angular frost-rived rubble, and outcrops of bedrock occur, except in local, highly favorable, moist sites where lush grasses and sedges grow.

Turn right and proceed west on the Denali Highway.

0.25 (Denali Highway).¹² Enter Mt. Hayes A-4 Quadrangle.

0.3 (Denali Highway). To the right, Tertiary rocks crop out at the base of the cliff. To the left is Paxson Mountain.

2.5 (Denali Highway). Ice-contact deposits of the late Wisconsin Summit Lake advance dam Summit Lake.

4.1 (Denali Highway). To the right are ice-contact deposits. Directly ahead is an excellent view of small, open-ended bedrock notches that were cut by former ice-marginal streams.

¹² Miles west of Paxson on the Denali Highway.

Winter snow distribution is important in determining the pattern of vegetation in these irregular ice-contact deposits. Pockets of grasses (mostly Festuca altaica) and sedges (Carex spp.) are found where the snow collects on the leeward side of ridges and in depressions. Associated with these areas are loose mats of lichens, primarily Peltigara spp., Cladonia spp., and Stereocaulon spp. Alpine tundra of Dryas octopetala, low sedges, and other low, matted plants can be seen above the shrub zone on the slopes of Paxson Mountain.

6 (Denali Highway). To the left on Paxson Mountain is an overflow gorge of Wisconsinan age.

7.2 (Denali Highway). STOP 21. ALASKA RANGE PANORAMA.

To the north is the Delta River pass, through which glacier ice from the south side of the Alaska Range pushed north to the Tanana River valley. Bedrock at this location is greenstone and metabasalt, probably Triassic in age. This location is above timberline in alpine-tundra vegetation.

10 (Denali Highway). Valley filled with ice-contact deposits of Donnelly (Denali II) age. Here the tundra is less shrubby, and extensive stands of sedges, cottongrass (Eriophorum spp.), and grasses are interspersed with low willows. Low, matted shrubs of crowberry (Empetrum nigrum), alpine bearberry (Arctostaphylos alpina), lingenberry (Vaccinium vitis-idaea), narrow-leaf Labrador-tea (Ledum decumbens), and lichens grow on exposed ridges.

To the west, the Denali Highway passes alternately through shrub tundra, low sedge and grass tundra, lichen-covered ridges of low, matted tundra, and occasionally, very open stands of black and white spruce.

11 (Denali Highway). Beginning of the Eleven Mile Hill grade, where the road traverses perennially frozen, ice-rich silty till of the Donnelly Glaciation. Road construction and maintenance have been difficult in this segment of the highway because thawing permafrost and intense seasonal frost action provide an unstable roadbed.

13 (Denali Highway). Top of Eleven Mile Hill. The Denali Highway crosses silty till of Wisconsinan age. Lower slopes in the immediate foreground are blanketed with silty till, but the valley bottoms 5 mi (8 km) ahead contain ice-stagnation deposits. Tops of hills on the right (north) stood above Donnelly-age ice (both early and late Denali age). Directly ahead, 15 mi (24 km) in the distance, is High Valley (fig. 69).

16.4 (Denali Highway). Road on silty till. A good view of large area of ice-contact deposits is directly ahead. The gravel pit ahead is in these deposits.

17 (Denali Highway). To the left are ice-contact deposits.

20 (Denali Highway). Round Tangle Lake in the heart of the late Wisconsin esker-and-kame topography (fig. 70). Such topography is well illustrated on the Mt. Hayes A-4 and A-5 and Gulkana D-4 and D-5 Quadrangle topographic maps.



Figure 70. Oblique aerial view (to the north) of Round and Long Tangle Lakes and Sugarloaf Mountain with ice-stagnation deposits in the foreground, Mt. Hayes A-5 Quadrangle, Alaska. Photograph 93-18 by R.D. Reger, July 20, 1982.

20.4 (Denali Highway). STOP 22. ICE-STAGNATION DEPOSITS AND TANGLE LAKES.

Drainage here is north through the Alaska Range into the Tanana River and eventually the Yukon River. In the far distance [about 8 mi (13 km) directly north on the west side of the river] is a well-developed rock glacier that formed in Holocene time.

20.7 (Denali Highway). Tangle Lake campground.

20.8 (Denali Highway). Enter Mt. Hayes A-5 Quadrangle.

21.2 (Denali Highway). Tangle River, source of the Delta River.

22.2 (Denali Highway). STOP 23. ROADCUT IN SMALL ESKER.

From the top of the esker to the left (south) and east are extensive, unmodified ice-stagnation deposits. To the right (north) is Landmark Gap (figs. 69 and 71), through which a glacier poured southward from the Alaska Range. In Wisconsinan time, the elevation of the ice surface as it emerged from the gap was 4,000 ft (1,212 m). In the past, some ice from the Alaska Range was confined to wide, deep major river valleys such as the Maclaren River valley, but most ice filtered through gaps and passes in the Amphitheater Mountains, where it was joined by local glaciers (fig. 69).

Several glaciations are recorded, each less extensive than the former. The earliest glacial advance is probably early to mid-Quaternary in age and covered the 6,000-ft-high (1,818 m) peaks of the Amphitheater Mountains, leaving isolated erratics atop some peaks. This advance probably correlates with the Darling Creek Glaciation of the lower Delta River valley (fig. 33). The second glacial advance (probably mid- to late Quaternary in age) pushed south into the Copper River basin but did not cover peaks of the Amphitheater Mountains. Many overflow channels were cut as drainage flowed through swales in bedrock ridges of the Gulkana Upland. During this advance, an olive-colored silty till was deposited in the lowlands and on the lower flanks of the Amphitheater Mountains. This till is now covered by later Quaternary drift sheets, except above an elevation of 4,000 ft (1,212 m) and on the floor of High Valley (fig. 71). No morainal forms of this glaciation are preserved in the area. This glacial advance is tentatively correlated with the Delta Glaciation in the lower Delta River valley (fig. 33).

The next two major glacial advances, which are closely related in extent and age, are grouped together and named the Denali Glaciation after the Denali Highway. The Denali Glaciation is probably Wisconsinan in age (fig. 33) and undoubtedly correlates, at least in part, with late Wisconsin glaciations and high lake levels in the Copper River basin (fig. 33). Glaciers did not cover the Amphitheater Mountains, but moved through gaps and were joined by local cirque ice. On the south side of the Alaska Range, ice was thick in deep major valleys such as the Maclaren River valley, but it was relatively thin in higher valleys and across interfluves. For example, glacial ice was relatively thin in the Tangle Lakes lowland and in nearby lowlands at altitudes of 3,000 to 4,000 ft (909 to 1,212 m). During thinning and retreat, most ice that covered the interfluves and higher lowlands stagnated, and many ice-contact features formed, including eskers, kames, crevasse fillings, and pit-

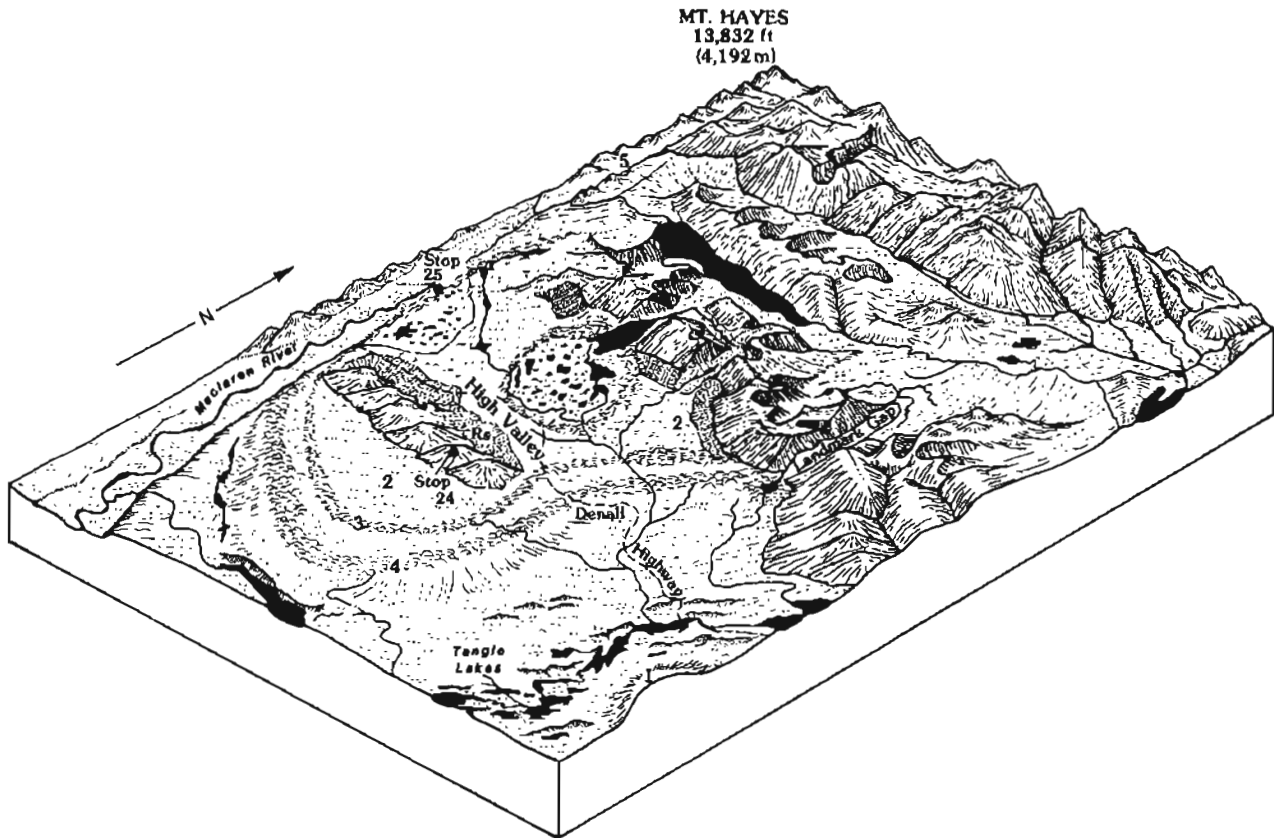


Figure 71. Physiographic diagram of the Mt. Hayes A-5 Quadrangle, Alaska. 1, glacial erratics of early to mid-Quaternary age; 2, deposits of Illinoian age; 3, moraine of early Wisconsinan age (Denali I Glaciation); 4, moraine of late Wisconsinan age (Denali II Glaciation); 5, deposits of Holocene glaciation; RS, rubble sheet of Wisconsinan age. Compare diagram with geologic map of glacial deposits (fig. 73) (modified from Kachadoorian and Pèwè, 1955).

ted surfaces. The Tangle Lakes complex at the head of the Delta River occupies an area of strikingly fresh ice-stagnation features that cover an area of several hundred square miles.

In early Holocene time, glaciers in the Alaska Range and small glaciers in the Amphitheater Mountains advanced a short distance and then retreated, leaving arcuate moraines at the mouths of short valleys (fig. 33).

Around the large lake south of this location is a prominent proglacial-postglacial shoreline at 2,900 ft (879 m) elevation, about 52 ft (16 m) above the present lake. A radiocarbon date for wood fragments from the lowest lake sediments exposed along lower Rock Creek demonstrates that general deglaciation of the Tangle Lakes area was complete and the high-level lake existed prior to $11,800 \pm 750$ yr B.P. (UCLA-1859). Three additional radiocarbon dates document the existence of this high-level lake until at least 9,100 yr B.P.: a) $10,150 \pm 280$ yr B.P. (UGa-572) for charcoal from the upper sediments of a sandy spit at the 2,900-ft (879 m) level at archeological site Mt. Hayes 111 near here; b) $9,720 \pm 320$ yr B.P. (W-975) for wood from an ancient beaver dam

in lacustrine deposits on lower Rock Creek; and c) $9,100 \pm 80$ yr B.P. (UCLA-1858) for a Populus log from the top of the lacustrine section on Rock Creek. Apparently the lake partially drained abruptly, perhaps about 8,200 yr B.P. but possibly as late as 5,000 to 7,000 yr B.P., when an esker ridge at the north end of the present lake was breached. The lack of wave-cut benches or beaches between the 2,900-ft (879 m) level and the present lake level indicates that the present lake level [2,848 ft (863 m)] has apparently been maintained since that time. The large gravel fan near the Tangle Lake campground may have been built as part of the breaching process or as a result of it.

Pollen studies suggest that the earliest postglacial flora in the Tangle Lakes area was a treeless shrub-herb tundra, which included sage (Artemisia spp.) and other composites, fireweed (Epilobium spp.), carices, other herbs, several genera of low shrubs such as willow (Salix spp.), birch (probably Betula glandulosa), and probably ericaceous shrubs. Poplar (Populus) invaded the area about 9,500 yr B.P. By 9,100 yr B.P., when white spruce (Picea glauca) arrived, probably from the north, a near-modern vegetation existed in the Tangle Lakes area, except that spruce and alder (Alnus spp.) were less abundant and shrub birch was probably more common. Sometime later, perhaps about 6,500 to 8,400 yr B.P., spruce became rare or disappeared from the Tangle Lakes area. Spruce did not return until about 3,500 yr B.P., when it probably reappeared as scattered small stands or isolated trees. This re-invasion apparently coincided with the onset of regional climatic deterioration, although this correlation remains to be verified elsewhere.

The Tangle Lakes area is exceptionally rich in lithic archeological remains compared to other parts of interior Alaska. More than 200 surface and near-surface sites have been found along the crests of eskers and other ridges in the vicinity of the lakes where a thin, discontinuous Holocene loess blankets the ice-contact deposits. Most lithics are fashioned from clasts in the local gravel or perhaps from material brought in from a bedrock quarry in Landmark Gap. Lithic sites invariably offer excellent vantage points for observing large herbivores in the surrounding lowlands.

The main elements of the artifact assemblage in the Tangle Lakes area are typical of the Denali Complex as defined from sites in the Donnelly Dome area, where a hunting-oriented culture left a tool kit dominated by microblades, wedge-shaped cores formed by the systematic removal of microblades and larger blades, burins for graving wood and bone, side scrapers or unifacial knives, boulder-chip scrapers, and biconvex-bifacial knives. In this part of the Tangle Lakes area, this inventory or elements of it are only found in sites at or above the 2,900-ft (879 m) shoreline; lower sites contain totally different assemblages, some of which are characterized by notched projectile points of the Northern Archaic Tradition that are about 4,000 to 5,000 yr old. Therefore, in this immediate area, the Denali Complex predates the abrupt lowering of the 2,900-ft (879 m) lake. At the Mt. Hayes 111 archeological site, the Denali Complex has been dated younger than $10,150 \pm 280$ yr B.P. (UGa-572) and older than $8,155 \pm 265$ yr B.P. (UGa-927). Elsewhere in the Tangle Lakes area (archeological site Mt. Hayes 149), Denali artifacts have been recovered from sediments dated at $9,060 \pm 425$ yr B.P. (UGa-941).

The Tangle Lakes and Donnelly Dome areas evidently were especially favorable environments for herding animals. The relatively abundant archeo-

logical remains provide good evidence that large herbivores were abundant, at least seasonally. Until their recent decimation by modern hunters, large herds of caribou passed through the Tangle Lakes area during their seasonal migrations.

26.5 (Denali Highway). Start up right (west) lateral moraine of a former glacier that flowed south through Landmark Gap in Wisconsinan time.

28.1 (Denali Highway). Top of prominent lateral moraine of early Denali age (figs. 68 and 71).

29 (Denali Highway). High Valley (fig. 68), which extends from Mile 28 to Mile 36.5. Ahead on the right across High Valley at an elevation of 4,855 ft (1,481 m) are large steps cut in bedrock. These steps are cryoplanation terraces that stand above the upper limit of Wisconsin ice in this area.

29.5 (Denali Highway). STOP 24. WHISTLER RIDGE CRYOPLANATION TERRACE SITE.

Whistler Ridge is one of two localities just south of the Denali Highway where cryoplanation terraces and related periglacial landforms have been studied in detail (fig. 72); the Phalarope Lake site is 3.7 mi (6 km) west of here near Mile 35 on the Denali Highway. These sites are typical of bedrock ridges in the Gulkana Upland, where many ridge crests exhibit inactive but well-preserved cryoplanation terraces. The vegetation at this alpine locality is typical shrub and herbaceous-lichen tundra of the northern Gulkana Upland.

Bedrock is a complex succession of slightly epidotized dacite tuffs, agglomerates, and flows of Triassic(?) age. Cherts are locally present. These rocks are intruded by rhyolite, dacite, and andesite dikes and by small diorite-gabbro stocks of Jurassic(?) age (fig. 73). Small, inactive rock glaciers occupy hollows in the north-northeast flank of the ridge at an average elevation of 4,100 ft (1,242 m), and extensive but stabilized rubble sheets cover lower ridge flanks between about 3,780 and 4,150 ft (1,145 and 1,258 m). Whistler Ridge is surrounded by an olive-gray, silty till of the Delta Glaciation. Moraines of the Denali I and II advances were deposited nearby by ice masses flowing south through the valley now occupied by Glacier Lake and by ice masses in the Tangle Lakes lowland to the east and south.

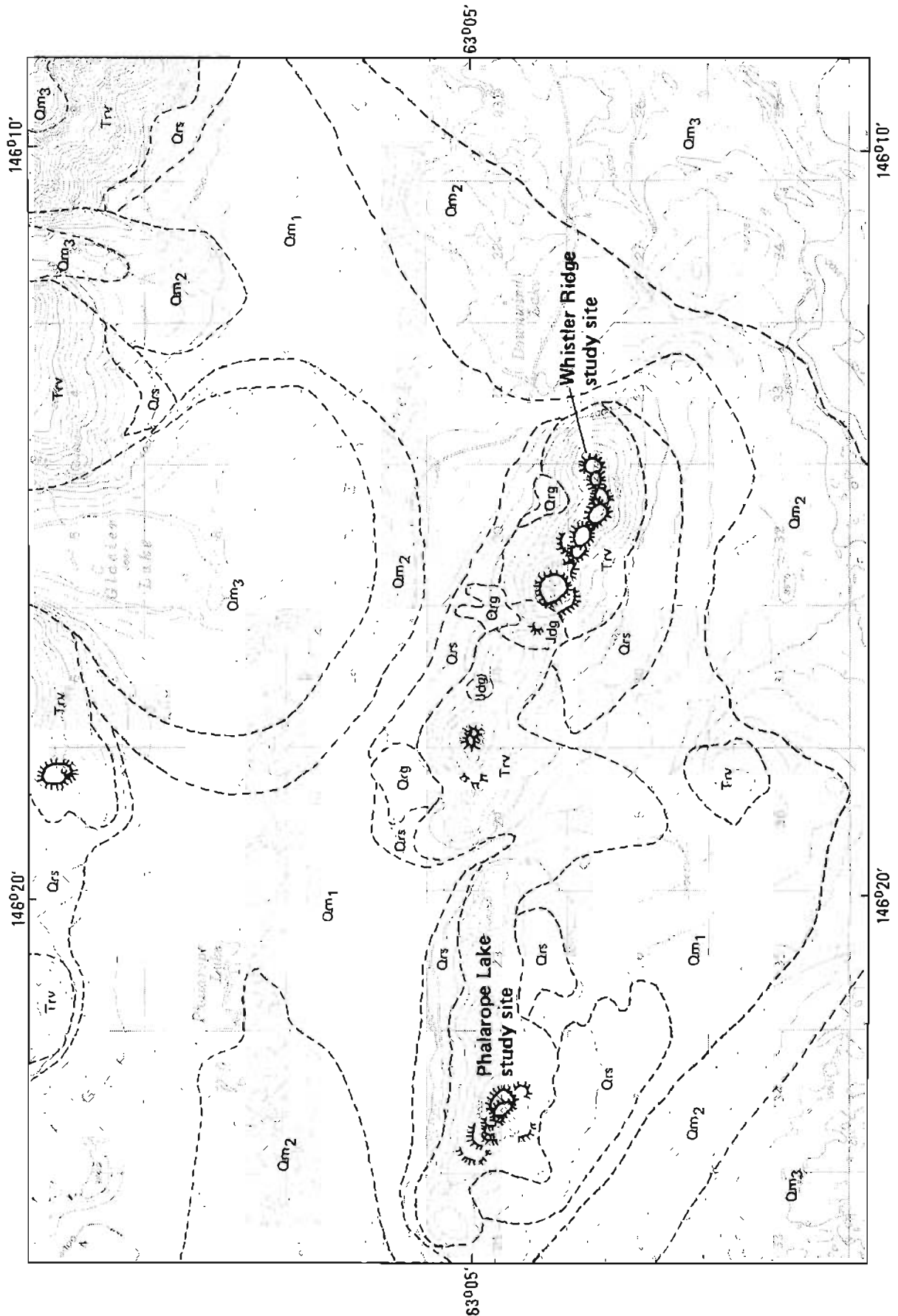
The Whistler Ridge site features an outstanding series of cryoplanation terraces that were notched in the bedrock ridge 700 to 1,100 ft (212 to 334 m) above the Denali Highway (fig. 74). Both ridge-crest and hilltop forms are present between 4,390 and 4,790 ft (1,330 and 1,451 m) elevation. Scarp heights vary from less than 10 ft (3 m) to about 45 ft (13.6 m). The mean direction that scarps face is 296.8 degrees, but the scarp orientation varies considerably (mean angular deviation of perpendiculars to scarps of 10 ridge-crest terraces at this locality is 67.2 degrees). Scarps are generally covered by coarse bedrock rubble. Although terrace treads appear to be nearly level planes, especially when viewed from the side (fig. 72), these surfaces are rarely level or planar. Most treads are actually broad, convex slopes that contrast markedly with steeper surrounding surfaces. They generally slope 1 to 5 degrees and may decline as steeply as 10 degrees. Tread areas on Whistler Ridge range from about 21,520 to 408,880 ft² (2,000 to 38,000 m²).

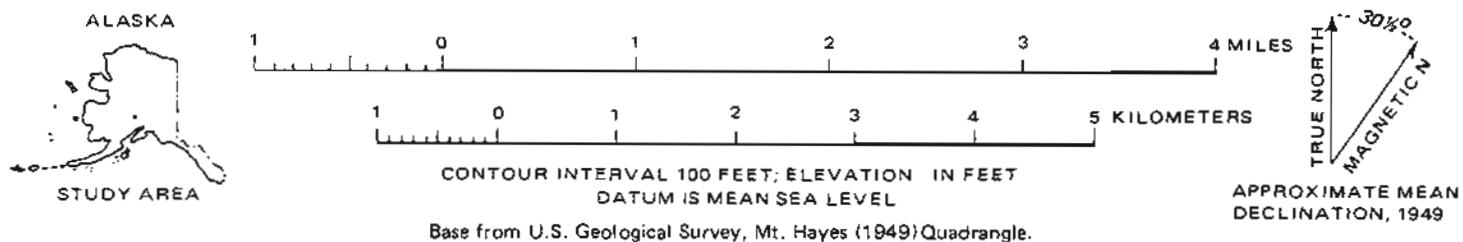


Figure 72. Oblique aerial view (to the south) of Whistler Ridge cryoplanation-terrace site and the Denali Highway, Mt. Hayes A-5 Quadrangle, Alaska. Gulkana Upland and Tangle Lakes are in the background. Photograph 93-12 by R.D. Reger, July 20, 1982.

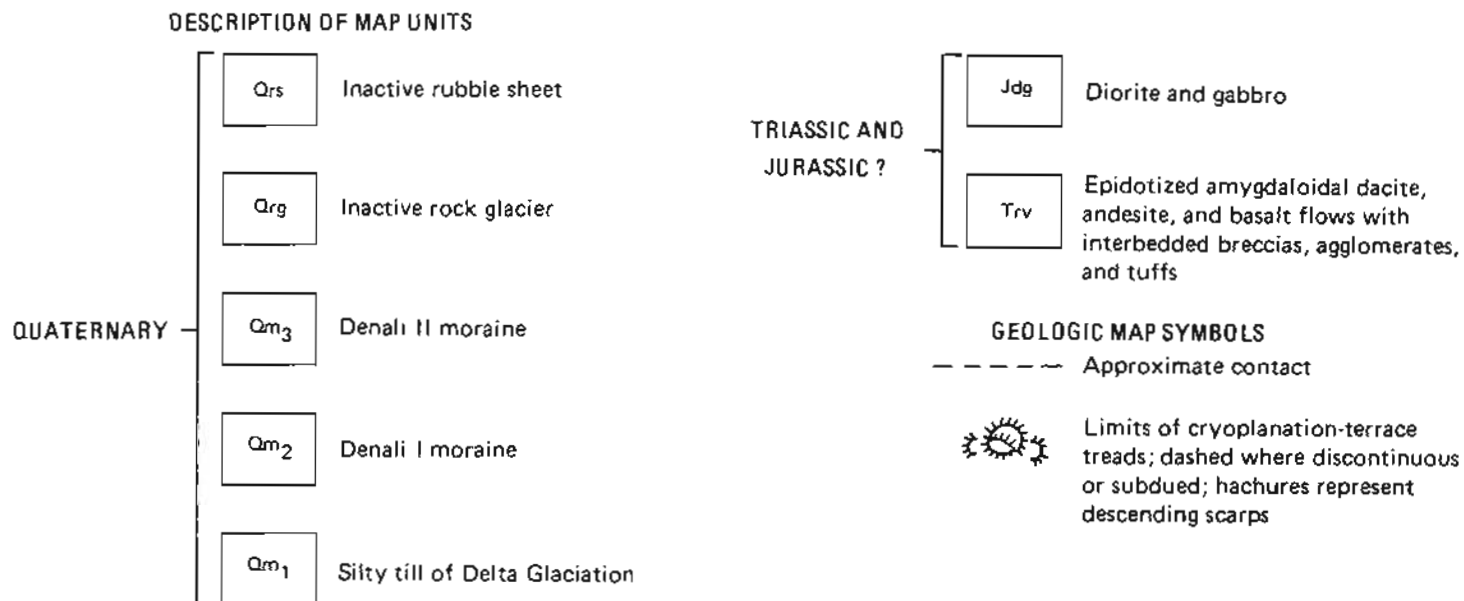
Treads are actually bedrock surfaces mantled by silty, angular bedrock rubble. On Whistler Ridge, less than 1 percent of the clasts in the tread debris is exotic to the local bedrock. Although no holes have been dug to bedrock at this site, cryoplanation terraces on Indian Mountain in west-central Alaska have similar morphologies, and excavations to bedrock demonstrate that the rubble veneer generally ranges from less than 3.3 ft (1 m) to as much as 10 ft (3 m) thick. Drill holes, pits, and trenches on the summit terrace of Indian Mountain encountered permafrost at depths of 1.7 to 6.5 ft (0.5 to 2 m) below the ground surface. Ground ice was present in silty fillings of bedrock joints as clear lenses, seams, and layers as thick as 0.6 in. (1.5 cm) and as unfoliated wedges up to 12 in. (30.5 cm) wide. On Whistler Ridge, tread material is sorted by frost action and mass movement into a variety of microrelief features. Near the bases of some ascending scarps, tread rubble is overlain by fans of organic silt.

Classic transverse nivation hollows indent the upper side slopes of Whistler Ridge (fig. 72). Bedrock slopes surrounding the terraces are littered with the products of terrace cutting and weathering of side slopes. This debris is moving or has moved downslope under the influence of gravity,





EXPLANATION



DELTA RIVER AREA, ALASKA RANGE

Figure 73. Bedrock and surficial geology in the vicinity of the Phalarope Lake and Whistler Ridge cryoplanation study sites (modified from Kachadoorian and Pêwé, 1955, pl. 1).

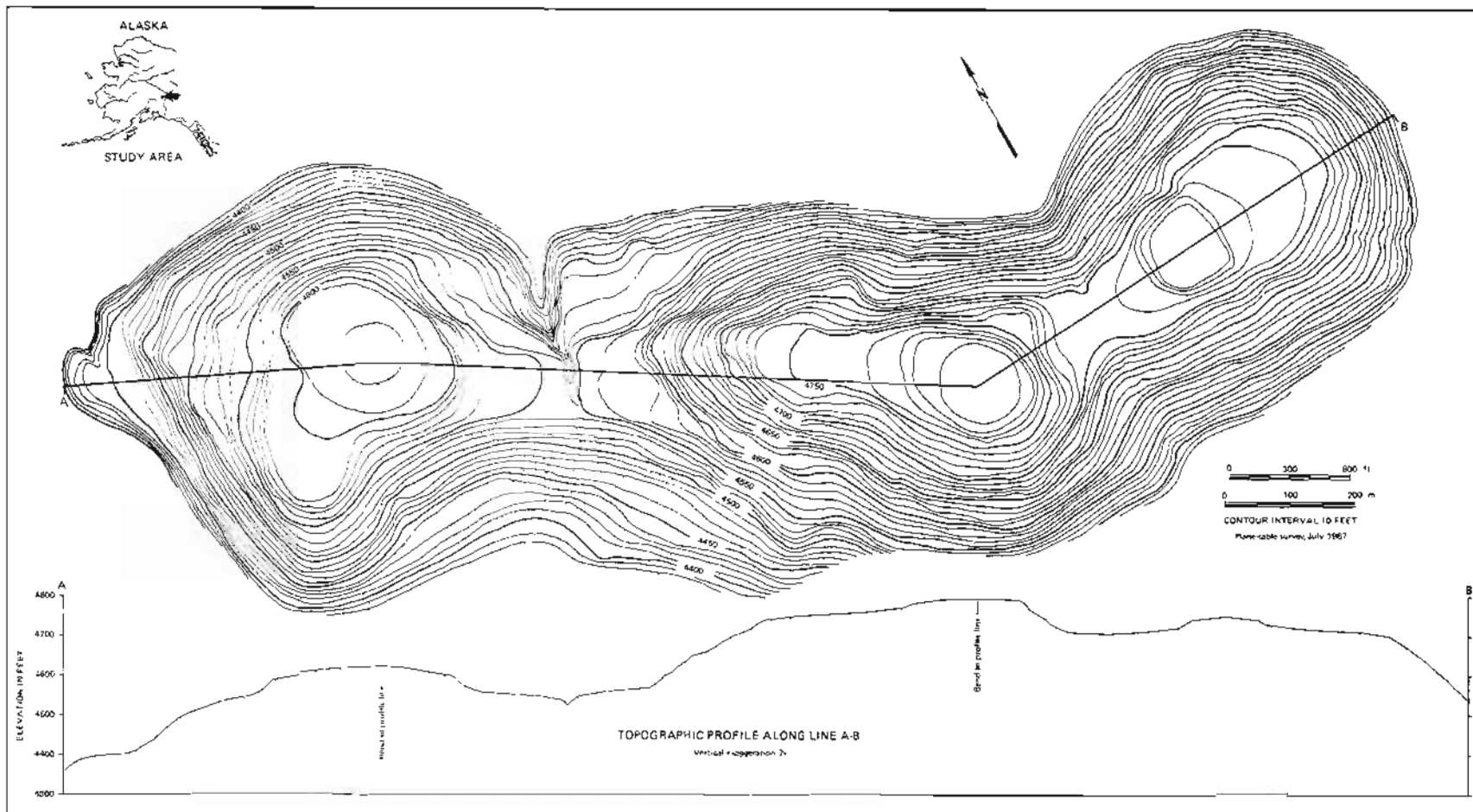


Figure 74. Plane-table map and topographic profile of the Whistler Ridge cryoplanation-terrace site, Mile 29.5, Denali Highway, Mt. Hayes A-5 Quadrangle, Alaska. Site was surveyed in July 1967 (modified from Reger, 1975, pl. 3).

primarily by solifluction and frost creep. Displacement has produced many typical periglacial microrelief forms, including rock-debris benches and turf-banked lobes. Rubble sheets at the base of the side slopes are extensions of this debris blanket that flowed as solifluction sheets out over the silty till surrounding the ridge. They are composed of open-work, angular debris as large as 3 ft (0.9 m) and averaging about 4 in. (10.2 cm) in diameter. Rubble sheets are 2 to 10 ft (0.6 to 3 m) thick and generally slope 8 to 10 degrees with lobate outer margins. Most of the silty matrix in the rubble sheets was removed by rill wash and piping and redeposited downslope as silt fans and aprons.

Cryoplanation terraces form on the crests and flanks of ridges and hills when nivation attacks bedrock in transverse nivation hollows and causes gradual entrenchment of the hollows. Mechanisms that work in concert with nivation to remove the products of this weathering process include mass movement, frost action, piping, and wind deflation. Nivation does not significantly excavate the floors of transverse hollows in permafrost areas because the local permafrost table acts as a 'base level of nivation,' which controls the essentially horizontal expansion of the hollow floor during scarp recession. Bedrock structures are indiscriminately truncated during scarp retreat, although nivation can cut preferentially along nearly horizontal zones of structural weakness.

The products of nivation are removed from nivation hollows onto terrace treads by meltwater washing and mass movement. A shallow permafrost table in tread debris serves as an impenetrable barrier to moisture from snow melt, slope runoff, and melting ground ice and promotes saturation of tread debris. Because of this high moisture content, gelifluction and frost creep transport the products of scarp destruction across the gently sloping terrace tread and down steeper side slopes.

The angularity (preservation) of terrace form is a function of the dynamic interaction of processes that both cut and destroy (by slope rounding) the terrace. The characteristic stepped slopes and ridges and planar hill tops that typify cryoplanation terraces develop only where scarp retreat is more active than rounding of the terrace, so that treads form faster than they are destroyed. The balance between the forces of terrace formation and the forces of terrace destruction is controlled mainly by climate, topographic location, and bedrock type. Terrace formation is favored by a cold, dry periglacial climate with shallow permafrost; terrace destruction is favored by climatic amelioration.

The cryoplanation terraces on Whistler Ridge are inactive. Fresh bedrock surfaces are not exposed in ascending scarps over a large enough area to indicate significant scarp retreat. Sorted microrelief features that demonstrate across-tread transport of debris are generally stabilized. The ages of these terraces can be indirectly determined by evaluating the spatial relationships of the terraces and nearby glacial deposits.

A major inundation of Whistler Ridge by ice of the Delta Glaciation is demonstrated by the blanket of silty till that surrounds the ridge and covers the adjacent lowlands (fig. 73), and by the presence in tread debris of rare (<1 percent), subrounded to well-rounded pebble and cobble erratics of quartz, purplish-brown amygdaloidal dacite, and granitic rocks from the

Amphitheater Mountains north of the Denali Highway and from the Alaska Range. These erratics also occur in the silty Illinoian(?) till that surrounds the ridge. Erratics on Whistler Ridge are remnants of that part of the Illinoian(?) till sheet that was deposited on the ridge where the terraces now exist. The intensive scouring during the Delta Glaciation destroyed any cryoplanation terraces that previously existed on the ridge.

Two major advances of the Wisconsin Denali Glaciation are recorded by distinctive moraines in the nearby lowlands (fig. 73). Ice of these glaciations was much thinner and less extensive than earlier inundations, and there were many ice-free nunataks and refugia in the Gulkana Upland (including Whistler Ridge). These enclaves were exposed to rigorous periglacial conditions of intense frost weathering and nivation, widespread shallow permafrost, and accelerated mass movement of the debris mantle. As a result of these conditions, bedrock ridges and hills in the Gulkana Upland were notched to form cryoplanation terraces and small rock glaciers developed on north-facing slopes; rubble sheets also spread across lower ridge flanks during the Denali Glaciation. Thus, the inactive, well-preserved cryoplanation terraces on Whistler Ridge are probably younger than 75,000 yr (fig. 33).

30.4 (Denali Highway). The Denali Highway follows the crest of a terminal moraine built by the lobe of ice that flowed south through Glacier Gap in Denali I time. High Valley is about 4,000 ft (1,212 m) above sea level and is unique because it was ice free---but surrounded by glaciers---in Wisconsin time. In Denali time, glaciers that pushed south from the Alaska Range and filled major valleys and lowlands pushed only short distances into High Valley. Ice that plowed through Glacier Gap was derived primarily from local sources. About 98 percent of the till stones represent lithologies from the Amphitheater Mountains.

Like Whistler Ridge, lower slopes in High Valley, especially those facing north, are blanketed by a 2- to 10-ft-thick (0.6 to 3 m) sheet of inactive rubble derived from upslope by frost riving during the rigorous climate of the Denali Glaciation. Some rubble sheets extend out over silty till of Delta age.

During the rigorous climate of Wisconsin time, small rock glaciers originated on the north side of the bedrock ridge south of the highway and pushed a short distance into High Valley.

31.2 (Denali Highway). Dissected rock glacier of Wisconsin age on left. This feature originated on a ridge of metabasalt.

32.2 (Denali Highway). On the north side of the road are temporary ponds in kettles of the Denali I moraine. Floors of these depressions exhibit outstanding examples of frost-sorted patterned ground (fig. 75), including stone circles, stone polygons, stone pits, and stone stripes. Circles and polygons that occur on level to very gently sloping (less than 2 degrees) surfaces are most common and vary in diameter from about 1.3 to 6.6 ft (0.4 to 2 m). Stone pits are less common and occur in similar situations, but stone stripes are perpendicular to pond shorelines on slopes of 3 to 10 degrees. Patterns are not present on slopes steeper than 10 degrees or in surface water deeper than 5 ft (1.5 m). All patterned microrelief features occur in situations of fluctuating water levels and are best developed in kettle depressions because of the presence of diamictic material and sufficient moisture.



Figure 75. Frost-sorted stone rings in till of late Wisconsinan age, Mile 32.2, Denali Highway, central Alaska. Photograph PK3095 by T.L. Pêwê, July 1954.

32.5 (Denali Highway). Roadcut through rock-glacier rubble.

34.5 (Denali Highway). To the right, an inactive rubble sheet that is 3 to 7 ft (0.9 to 2.1 m) thick and that overlies silty till of Delta age extends from a ridge of metabasalt. This rubble was wedged from bedrock by frost action during the rigorous climate of Denali time. Unlike the higher ridges to the north in the Amphitheater Mountains, this ridge was not high enough to support glaciers.

35 (Denali Highway). On the crest of the ridge about 0.5 mi (0.8 km) south of Denali Highway, well-preserved cryoplanation terraces form large steps between 4,470 and 4,710 ft (1,355 and 1,427 m) elevation (fig. 76). This ridge is composed of slightly epidotized dacite tuff, agglomerate, and flows of Triassic(?) age that are intruded by rhyolite, andesite, and dacite dikes of Jurassic(?) age. The cryoplanation terraces formed by scarp retreat and overtread transport of weathering products during Denali time, when permafrost was more shallow and widespread and nivation was more effective than today.

35.4 (Denali Highway). The 4,081-ft (1,237 m) summit of the Denali Highway.

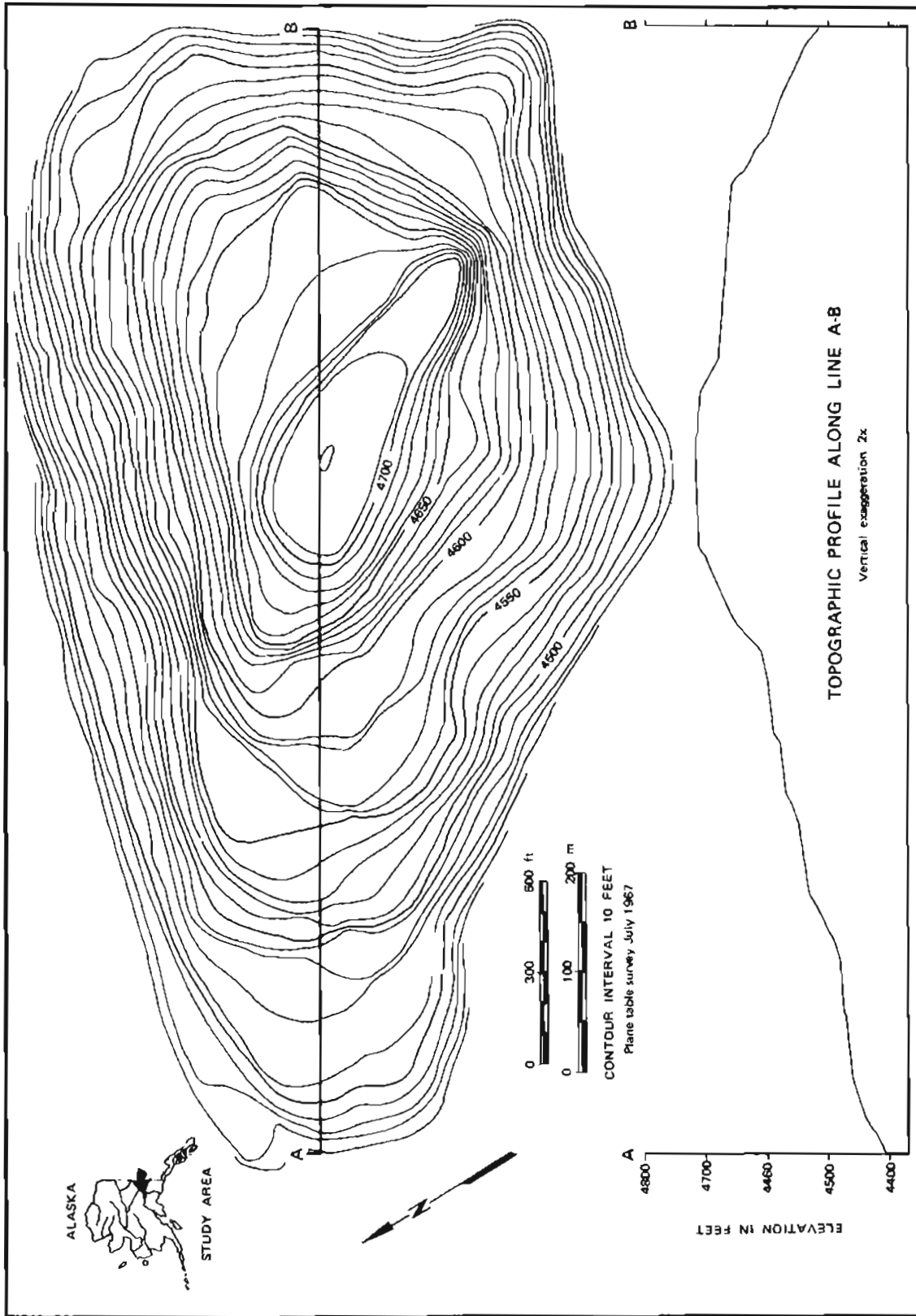


Figure 76. Plane-table map and topographic profile of the Phalarope Lake cryoplanation-terrace site, Mile 35, Denali Highway, Mt. Hayes A-5 Quadrangle, Alaska. Site was surveyed in July 1967 (from Reger, 1975, pl. 2).

35.6 (Denali Highway). To the right is a lobe of early Wisconsin (Denali I) moraine that was deposited when Maclaren Glacier pushed over the east wall of the Maclaren River valley and protruded a short distance into High Valley.

36.6 (Denali Highway). View of the Maclaren River valley and Maclaren Glacier. The Denali Highway traverses the valley. Ice-stagnation deposits cover the valley floor in the vicinity of the Susitna River bridge.

36.9 (Denali Highway). The Denali II moraine, especially east of the road, has numerous kettle depressions, many with outstanding examples of active (frost-sorted) patterned ground. Many kettles are partially filled with water during rainy periods, a condition that promotes frost action because periodic inundation inhibits the growth of vegetation on depression floors.

40.8 (Denali Highway). STOP 25. PALSAS.

The presence of permafrost in this part of the northern Gulkana Upland is confirmed by ice-rich palsas on both sides of the Denali Highway. The mound to the south (left) has been sectioned by construction activity (fig. 77). A radiocarbon age of $10,565 \pm 225$ yr B.P. (GX-2049) for the lowest exposed peat



Figure 77. View of palsa sectioned during construction of the Denali Highway in the Maclaren River valley, Mt. Hayes A-5 Quadrangle, Alaska. Photographer unknown, August 25, 1965.

in contact with ice indicates that this palsa formed in Holocene time and provides a minimum date for deglaciation of this part of Maclaren River valley.

41 (Denali Highway). Enter Mt. Hayes A-6 Quadrangle.

41.1 (Denali Highway). Ascend into ice-stagnation deposits. This large mass of stream-washed gravel was probably deposited in a very large hole in stagnant glacial ice. There are several large kettle holes in this area; the kettle on the right (north) is steep walled and is approximately 50 ft (15 m) deep. These features are essentially unmodified by postglacial processes.

42 (Denali Highway). Maclaren River and view of Maclaren Glacier. The Susitna River cuts through ice-contact deposits here.

45 (Denali Highway). East entrance to Crazy Notch. This steep-walled, open-ended valley, with its floor at about 3,270 ft (991 m) elevation, was cut through this bedrock ridge by a subaerial stream that was probably subglacial both east and west of the ridge, as demonstrated by the presence of eskers that trend into the notch.

46 (Denali Highway). West exit from Crazy Notch. The two esker trains that join here extend northwest and southwest. Structures within the eskers indicate that paleodrainage was eastward about 12,000 to 13,000 yr B.P., when stagnant ice masses about 350 to 800 ft (106 to 242 m) thick filled the low areas on either side of this ridge. The Denali Highway is built along the crest of the southwest-trending esker train for the next 6 mi (9.7 km).

47 (Denali Highway). To the right (northwest) is an excellent example of a rock glacier extending west from the bedrock ridge bisected by Crazy Notch.

49 (Denali Highway). Palsas 6 ft (1.8 m) high and 15 ft (4.6 m) in diameter occur in the fens to the right (northwest).

50 (Denali Highway). STOP 26. ROADCUT THROUGH ESKER.

Selected References

- Ager, T.A., 1982, Quaternary history of vegetation in the north Alaska Range, in Coonrad, W.L., ed., The United States Geological Survey in Alaska: Accomplishments during 1980: U.S. Geological Survey Circular 844, p. 109-111.
- Ager, T.A., and Sims, J.D., 1981, Holocene pollen and sediment record from the Tangle Lakes area, central Alaska: *Palynology*, v. 5, p. 85-98.
- Blasing, T.J., and Fritts, H.C., 1975, Past climate of Alaska and northwestern Canada as reconstructed from tree rings, in Weller, Gunter, and Bowling, S.A., eds., *Climate of the Arctic*: Fairbanks, University of Alaska Geophysical Institute, p. 48-58.
- Bond, G.C., 1976, Geology of the Rainbow Mountain-Gulkana Glacier area, eastern Alaska Range, with emphasis on upper Paleozoic strata: Alaska Division of Geological and Geophysical Surveys Geologic Report 45, 47 p.
- Brogan, G.E., Cluff, L.S., Korringa, M.K., and Slemmons, D.B., 1975, Active faults of Alaska, in Pavoni, N., and Green, R., eds., *Recent crustal movements: Tectonophysics*, v. 29, no. 1-4, p. 73-85.

- Church, R.E., Pêwé, T.L., and Andresen, M.J., 1965, Origin and environmental significance of large-scale polygonal ground near Big Delta, Alaska: U.S. Army Cold Regions Research and Engineering Laboratory Research Report 159, 75 p.
- Cropper, J.P., 1982, Climate reconstructions (1801 to 1938) inferred from tree-ring width chronologies of the North American Arctic: *Arctic and Alpine Research*, v. 14, no. 3, p. 223-241.
- Davidson, D.T., Roy, C.J., and others, 1959, The geology and engineering characteristics of some Alaskan soils: Ames, Iowa State University Bulletin 186, 149 p.
- Denton, G.H., and Karlén, Wibjorn, 1973, Lichenometry: Its application to Holocene moraine studies in southern Alaska and Swedish Lapland: *Arctic and Alpine Research*, v. 5, no. 4, p. 347-372.
- _____, 1977, Holocene glacial and tree-line variations in the White River valley and Skolai Pass, Alaska and Yukon Territory: *Quaternary Research*, v. 7, no. 1, p. 63-111.
- Fernald, A.T., 1965a, Glaciation in the Nabesna River area, upper Tanana River valley, Alaska, *in* Geological Survey research 1965: U.S. Geological Survey Professional Paper 525-C, p. C120-C123.
- _____, 1965b, Recent history of the upper Tanana River lowland, Alaska, *in* Geological Survey research 1965: U.S. Geological Survey Professional Paper 525-C, p. C124-C127.
- Forbes, R.B., Smith, T.E., and Turner, D.L., 1974, A solution to the Denali fault offset problem: Alaska Division of Geological and Geophysical Surveys Annual Report, 1973, p. 25-27.
- Gedney, Larry, and Estes, Steven, 1982, A recent earthquake on the Denali fault in the southeast Alaska Range, *in* Short notes on Alaskan geology: Alaska Division of Geological and Geophysical Surveys Geologic Report 73, p. 51-54.
- Geist, O.W., and Pêwé, T.L., 1957, Quantitative measurements of the 1937 advance of the Black Rapids Glacier, Alaska [abs.]: Alaska Science Conference, 5th, Anchorage, 1954, Proceedings, p. 51-52.
- Hamilton, T.D., 1982, A late Pleistocene glacial chronology for the southern Brooks Range: Stratigraphic record and regional significance: *Geological Society of America Bulletin*, v. 93, no. 8, p. 700-716.
- Hance, J.H., 1937, The recent advance of Black Rapids Glacier, Alaska: *Journal of Geology*, v. 45, p. 775-783.
- Hanson, L.G., 1963, Bedrock geology of the Rainbow Mountain area, Alaska Range, Alaska: Alaska Division of Mines and Minerals Geologic Report 2, 82 p.
- Haugen, R.K., and Brown, Jerry, 1978, Climatic and dendroclimatic indices in the discontinuous permafrost zone of the central Alaskan highlands, *in* International Permafrost Conference, 3rd, Edmonton, Alberta, 1978, Proceedings: National Research Council of Canada, v. 1, p. 392-398.
- Holmes, G.W., 1965, Geologic reconnaissance along the Alaska Highway, Delta River to Tok Junction, Alaska: U.S. Geological Survey Bulletin 1181-H, 19 p.
- Holmes, G.W., and Benninghoff, W.S., 1957, Terrain study of the Army Test Area, Fort Greely, Alaska: U.S. Geological Survey, Military Evaluation of Geographic Areas, v. 1, 287 p.
- Holmes, G.W., and Foster, H.L., 1968, Geology of the Johnson River area, Alaska: U.S. Geological Survey Bulletin 1249, 49 p.

- Holmes, G.W., and P  w  , T.L., 1965, Geologic map of the Mt. Hayes (D-3) Quadrangle, Alaska: U.S. Geological Survey Geologic Quadrangle Map GQ-366, scale 1:63,360, 1 sheet.
- Hudson, Travis, and Weber, F.R., 1977, The Donnelly Dome and Granite Mountain faults, south-central Alaska, *in* Blean, K.M., ed., The United States Geological Survey in Alaska: Accomplishments during 1976: U.S. Geological Survey Circular 751-B, p. B64-B66.
- Jacoby, G.C., and Cook, E.R., 1981, Past temperature variations inferred from a 400-yr tree-ring chronology from Yukon Territory, Canada: *Arctic and Alpine Research*, v. 13, no. 4, p. 409-418.
- Kachadoorian, Reuben, Hopkins, D.M., and Nichols, D.R., 1954, A preliminary report of geological factors affecting highway construction in the area between the Susitna and Maclaren Rivers, Alaska: U.S. Geological Survey Open-file Report 54-137, 74 p.
- Kachadoorian, Reuben, and P  w  , T.L., 1955, Engineering geology of the southern half of the Mt. Hayes (A-5) Quadrangle, Alaska: U.S. Geological Survey Open-file Report 55-78, 27 p.
- Kreig, R.A., and Reger, R.D., 1982, Air-photo analysis and summary of landform soil properties along the route of the Trans-Alaska Pipeline System: Alaska Division of Geological and Geophysical Surveys Geologic Report 66, 149 p.
- Mayo, L.R., and P  w  , T.L., 1963, Ablation and net total radiation, Gulkana Glacier, Alaska, *in* Kingery, W.D., ed., *Ice and snow: Properties, processes, and applications*: Cambridge, Massachusetts Institute of Technology Press, p. 633-643.
- Meier, M.F., Tangborn, W.V., Mayo, L.R., and Post, Austin, 1971, Combined ice and water balances of Gulkana and Wolverine Glaciers, Alaska, and South Cascade Glacier, Washington, 1965 and 1966 hydrologic years: U.S. Geological Survey Professional Paper 715-A, 23 p.
- Mendenhall, W.C., 1900, A reconnaissance from Resurrection Bay to the Tanana River, Alaska, in 1898: U.S. Geological Survey 20th Annual Report, pt. 7, p. 265-340.
- Mitchell, J.M., Jr., 1956, Strong surface winds at Big Delta, Alaska: An example of orographic influence on local weather: *Monthly Weather Review*, v. 84, no. 1, p. 15-24.
- Moffit, F.H., 1912, Headwater regions of Gulkana and Susitna Rivers, Alaska: U.S. Geological Survey Bulletin 498, 82 p.
- _____, 1942, Geology of the Gerstle River district, Alaska, with a report on the Black Rapids Glacier: U.S. Geological Survey Bulletin 926-B, p. 107-160.
- _____, 1954, Geology of the eastern part of the Alaska Range and adjacent areas: U.S. Geological Survey Bulletin 989-D, p. 65-218.
- Moore, E.A., 1962, Configuration of the surface velocity profile of Gulkana Glacier, central Alaska Range, Alaska: Fairbanks, University of Alaska, M.S. thesis, 47 p.
- Nelson, G.L., 1978, Geohydrology of the Delta-Clearwater area, *in* Johnson, K.M., ed., The United States Geological Survey in Alaska: Accomplishments during 1977: U.S. Geological Survey Circular 772-B, p. B38.
- Ostenso, N.A., Sellmann, P.V., and P  w  , T.L., 1965, The bottom topography of Gulkana Glacier, Alaska Range: *Journal of Glaciology*, v. 5, p. 651-660.
- Ostrem, G., Haakensen, N., and Eriksson, T., 1981, The glaciation level in southern Alaska: *Geografiska Annaler*, v. 63A, no. 3-4, p. 251-260.

- Packer, D.R., Brogan, G.E., and Stone, D.B., 1975, New data on plate tectonics of Alaska, *in* Pavoni, N., and Green, R., eds., *Recent crustal movements: Tectonophysics*, v. 29, no. 1-4, p. 87-102.
- Page, R.A., 1972, Crustal deformation on the Denali fault in Alaska, 1942-1970: *Journal of Geophysical Research*, v. 77, p. 1528-1533.
- Page, R.A., and Lahr, John, 1971, Measurements of fault slip on the Denali, Fairweather, and Castle Mountain faults, Alaska: *Journal of Geophysical Research*, v. 76, p. 8534-8543.
- Péwé, T.L., 1951a, An observation on wind-blown silt: *Journal of Geology*, v. 59, no. 4, p. 399-401.
- _____, 1951b, Recent history of Black Rapids Glacier, Alaska [abs.]: *Geological Society of America Bulletin*, v. 62, no. 12, p. 1558.
- _____, 1952, Preliminary report of multiple glaciation in the Big Delta area, Alaska [abs.]: *Geological Society of America Bulletin*, v. 63, no. 12, p. 1289.
- _____, 1953, Big Delta area, Alaska, *in* Péwé, T.L., and others, Multiple glaciation in Alaska: *U.S. Geological Survey Circular* 289, p. 8-10.
- _____, 1955, Middle Tanana River valley, *in* Hopkins, D.M., Karlstrom, T.N.V., and others, Permafrost and ground water in Alaska: *U.S. Geological Survey Professional Paper* 264-F, p. 126-130.
- _____, 1957, Recent history of Canwell and Castner Glaciers, Alaska [abs.]: *Geological Society of America Bulletin*, v. 68, no. 12, pt. 2, p. 1779.
- _____, 1961, Multiple glaciation in the headwaters area of the Delta River, central Alaska, *in* Short papers in the geologic and hydrologic sciences 1961: *U.S. Geological Survey Professional Paper* 424-D, p. D200-D201.
- _____, 1965a, Middle Tanana River valley, *in* Péwé, T.L., Ferrians, O.J., Jr., Nichols, D.R., and Karlstrom, T.N.V., Guidebook for field conference F, central and south-central Alaska, International Association for Quaternary Research, 7th Congress, Fairbanks, 1965: Lincoln, Nebraska Academy of Sciences, p. 36-54 (reprinted 1977, College, Alaska Division of Geological and Geophysical Surveys).
- _____, 1965b, Fairbanks area, *in* Péwé, T.L., Ferrians, O.J., Jr., Nichols, D.R., and Karlstrom, T.N.V., Guidebook for field conference F, central and south-central Alaska, International Association for Quaternary Research, 7th Congress, Fairbanks, 1965: Lincoln, Nebraska Academy of Sciences, p. 6-36 (reprinted 1977, College, Alaska Division of Geological and Geophysical Surveys).
- _____, 1965c, Delta River area, Alaska Range, *in* Péwé, T.L., Ferrians, O.J., Jr., Nichols, D.R., and Karlstrom, T.N.V., Guidebook for field conference F, central and south-central Alaska, International Association for Quaternary Research, 7th Congress, Fairbanks, 1965: Lincoln, Nebraska Academy of Sciences, p. 55-93 (reprinted 1977, College, Alaska Division of Geological and Geophysical Surveys).
- _____, 1966, Ice wedges in Alaska---classification, distribution, and climatic significance, *in* International Conference on Permafrost, 1st, Lafayette, Ind., 1963, Proceedings: National Academy of Science, National Research Council Publication 1287, p. 76-81.
- _____, 1968, Loess deposits of Alaska: International Geological Congress, 23rd Session, Prague, 1968, Proceedings, v. 8, p. 297-309.
- _____, 1973, Ice-wedge casts and past permafrost distribution in North America: *Geoforum*, v. 15, p. 15-26.

- Péwé, T.L., 1975, Quaternary geology of Alaska: U.S. Geological Survey Professional Paper 835, 145 p.
- Péwé, T.L., Church, R.E., Andresen, M.J., 1969, Origin and paleoclimatic significance of large-scale polygons in the Donnelly Dome area, Alaska: Geological Society of America Special Paper 103, 87 p.
- Péwé, T.L., and Holmes, G.W., 1964, Geology of the Mt. Hayes (D-4) Quadrangle, Alaska: U.S. Geological Survey Miscellaneous Geologic Investigations Map I-394, scale 1:63,360, 2 sheets.
- Péwé, T.L., and others, 1953, Tentative correlation of glaciations in Alaska, in Péwé, T.L., and others, Multiple glaciation in Alaska: U.S. Geological Survey Circular 289, p. 12-13.
- Post, Austin, and Mayo, L.R., 1971, Glacier-dammed lakes and outburst floods in Alaska: U.S. Geological Survey Hydrologic Investigations Atlas HA-455, 10 p., scale 1:1,000,000, 3 sheets.
- Ragan, D.M., 1964, Structures at the base of an ice fall on the Gulkana Glacier, eastern Alaska Range [abs.]: Geological Society of America Special Paper 76, p. 220-221.
- Reed, B.L., and Lanphere, M.A., 1974, Offset plutons and history of movement along the McKinley segment of the Denali fault system, Alaska: Geological Society of America Bulletin, v. 85, no. 12, p. 1883-1892.
- Reed, J.C., Jr., 1961, Geology of the Mount McKinley Quadrangle, Alaska: U.S. Geological Survey Bulletin 1108-A, 36 p.
- Reger, R.D., 1964, Recent glacial history of Gulkana and College Glaciers, central Alaska Range, Alaska: Fairbanks, University of Alaska, M.S. thesis, 75 p.
- _____, 1968, Recent history of Gulkana and College Glaciers, central Alaska Range, Alaska: Journal of Geology, v. 76, no. 1, p. 2-16.
- _____, 1975, Cryoplanation terraces of interior and western Alaska: Tempe, Arizona State University, Ph.D. thesis, 326 p.
- Reger, R.D., and Péwé, T.L., 1969, Lichenometric dating in the central Alaska Range, in Péwé, T.L., ed., The periglacial environment, past and present: Montreal, McGill-Queens University Press, p. 223-247.
- _____, 1976, Cryoplanation terraces: Indicators of a permafrost environment: Quaternary Research, v. 6, no. 1, p. 99-109.
- Reger, R.D., Péwé, T.L., Hadleigh-West, Frederick, and Skarland, Ivar, 1964, Geology and archeology of the Yardang Flint Station: Fairbanks, University of Alaska, Department of Anthropology and Geography Anthropological Papers, no. 2, v. 12, p. 92-100.
- Rice, E.F., 1980, The shake-down years: Alyeska Reports, September 1980, p. 1-6.
- Richter, D.R., and Matson, N.A., 1971, Quaternary faulting in the eastern Alaska Range: Geological Society of America Bulletin, v. 82, no. 6, p. 1529-1540.
- Ritter, D.F., and Ten Brink, N.W., 1980, Alluvial fan development in the Nenana Valley, Alaska, and implications for site discovery [abs.]: Geological Society of America Abstracts with Programs, v. 12, no. 7, p. 510.
- _____, 1982, Paraglacial fan formation and glacial history, Nenana Valley, Alaska: Journal of Geology [in press].
- Rutter, N.W., 1965, Foliation pattern of Gulkana Glacier, Alaska Range, Alaska: Journal of Glaciology, v. 5, p. 711-718.
- Schweger, C.E., 1981, Chronology of late glacial events from the Tangle Lakes, Alaska Range, Alaska: Arctic Anthropology, v. 18, no. 1, p. 97-101.

- Sellman, P.V., 1962, Flow and ablation of Gulkana Glacier, Alaska: Fairbanks, University of Alaska, M.S. thesis, 36 p.
- Skarland, Ivar, and Keim, C.J., 1958, Archeological discoveries on the Denali Highway, Alaska: Fairbanks, University of Alaska, Department of Anthropology and Geography Anthropological Papers, v. 6, p. 79-88.
- Sloan, C.E., Zenone, Chester, and Mayo, L.R., 1976, Icings along the trans-Alaska pipeline route: U.S. Geological Survey Professional Paper 979, 31 p.
- Stout, J.H., 1976, Geology of the Eureka Creek area, east-central Alaska Range: Alaska Division of Geological and Geophysical Surveys Geologic Report 46, 32 p.
- Stout, J.H., Brady, J.B., Weber, F.R., and Page, R.A., 1973, Evidence for Quaternary movement on the McKinley strand of the Denali fault in the Delta River area, Alaska: Geological Society of America Bulletin, v. 84, no. 3, p. 939-948.
- Tangborn, W.V., Mayo, L.R., Scully, D.R., and Krimmel, R.M., 1977, Combined ice and water balances of Maclure Glacier, California, South Cascade Glacier, Washington, and Wolverine and Gulkana Glaciers, Alaska, 1967 hydrologic year: U.S. Geological Survey Professional Paper 715-B, 20 p.
- Ten Brink, N.W., and Ritter, D.R., 1980, Glacial chronology of the north-central Alaska Range and implications for discovery of early-man sites [abs.]: Geological Society of America Abstracts with Programs, v. 12, no. 7, p. 534.
- Ten Brink, N.W., and Waythomas, C.F., 1982, Late Wisconsin glacial chronology of the north-central Alaska Range---A regional synthesis and its implications for early human settlements: Unpublished report, 27 p.
- Thorson, R.M., Dixon, E.J., Jr., Smith, G.S., and Batten, A.R., 1981, Interstadial proboscidean from south-central Alaska: Implications for biogeography, geology, and archeology: Quaternary Research, v. 16, no. 3, p. 404-417.
- Wahrhaftig, Clyde, 1958, Quaternary and engineering geology in the central part of the Alaska Range: U.S. Geological Survey Professional Paper 293, 118 p.
- _____, 1965, Physiographic divisions of Alaska: U.S. Geological Survey Professional Paper 482, 52 p.
- Wahrhaftig, Clyde, and Cox, Allan, 1959, Rock glaciers in the Alaska Range: Geological Society of America Bulletin, v. 70, no. 4, p. 383-436.
- Watson, C.E., 1959, Climate of Alaska, in Climate of the states: Washington, D.C., U.S. Weather Bureau, Climatography of the United States 60-49, 24 p.
- Welsch, Dennis, Goodwin, Robert, and Ten Brink, Norman, 1982, Late Quaternary glaciations of the Talkeetna Mountains, Alaska [abs.]: Geological Society of America Abstracts with Programs, v. 14, no. 6, p. 353-354.
- Wendler, G., Kodama, Y., and Eaton, F., 1980, On the frequency of strong winds in the Big Delta area: Fairbanks, University of Alaska, Geophysical Institute Scientific Report UAF R-277, 23 p.
- West, F.H., 1967, The Donnelly Ridge Site and the definition of an early core and blade complex in central Alaska: American Antiquity, v. 32, no. 3, p. 360-382.
- _____, 1975, Dating the Denali Complex: Arctic Anthropology, v. 12, no. 1, p. 76-81.
- _____, 1981, The archaeology of Beringia: New York, Columbia University Press, 268 p.

COPPER RIVER BASIN

O.J. Ferrians, Jr.,¹³ By D.R. Nichols,¹⁴ and J.R. Williams¹³

Résumé of Quaternary Geology

The Copper River basin is an intermontane basin that ranges from 500 to 4,000 ft (150 to 1,200 m) above sea level and is rimmed by 4,500- to 16,500-ft-high (1,370 to 5,000 m) peaks of the Alaska Range and the Talkeetna, Chugach, and Wrangell Mountains. Rocks bordering the basin range in age from middle(?) Paleozoic to Tertiary. They consist largely of schist, greenstone, graywacke, slate, shale, and sandstone locally associated with minor altered limestone, tuffaceous beds, and basalt flows and are intruded by a wide variety of igneous rocks. Large parts of the Wrangell and Talkeetna Mountains and local areas in the Chugach Mountains are underlain by considerable thicknesses of basaltic and andesitic lava flows. Thin andesite and volcanoclastic debris flows are interbedded with Pleistocene deposits in the eastern and southeastern Copper River basin.

During one or more early Pleistocene glaciations, glaciers advancing from the surrounding mountains covered the entire basin floor. During subsequent glaciations, ice may have covered all but small areas of the basin floor, but during the last major glaciation large areas were ice free.

In the early stages of each major Pleistocene glaciation, ice advances in the surrounding mountains dammed the drainage of the Copper River basin to form an extensive proglacial lake. Because the glaciers fronted in deep lake water, end moraines and associated features in the lower part of the basin (Copper River trough) are generally absent (fig. 78). However, glacial landforms, although modified, are still preserved below former lake levels in the higher parts of the basin (Copper-Susitna Lowland). As the glaciers retreated, their deposits were reworked by lake currents or buried by lacustrine sediments. The complicated interfingering of lacustrine and glacial deposits and numerous shoreline features at elevations below 2,650 ft (810 m) indicate that the lakeshore fluctuated widely as the water level lowered during retreat of glaciers at the end of the last major glaciation (Wisconsin).

Following retreat of the glaciers and drainage of the lake (before 9,000 yr B.P.), permafrost began to form in lacustrine and glacial deposits, rivers began downcutting into Pleistocene sediments, and cliff-head dunes and loess deposits began to accumulate locally. Muskegs and marshes that occupy depressions on the old lake floor are perched on poorly drained, perennially frozen lake sediments. Numerous active thaw lakes are also present (fig. 79).

Most damage and ground breakage that occurred in the Copper River basin during the major earthquake of March 27, 1964, was restricted to the southern half of the basin. Several buildings were shaken from their foundations, and the foundations of several other structures were damaged. Dishes were broken

¹³U.S. Geological Survey; 4200 University Drive; Anchorage, Alaska 99508-4667.

¹⁴U.S. Geological Survey; Mail Stop 903; Box 25046; Denver, Colorado 80225.

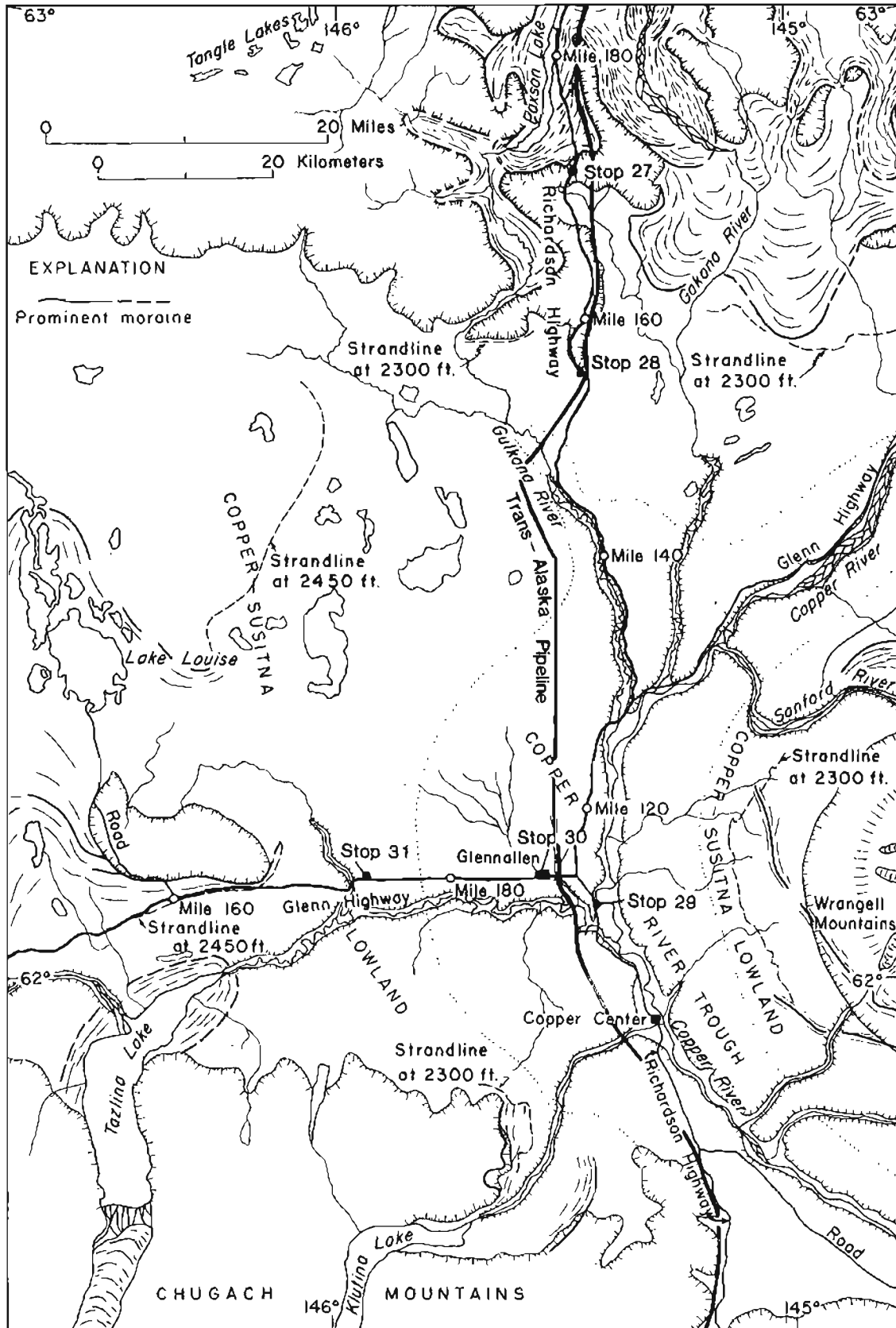


Figure 78. Index map of the Copper River basin, Alaska, showing field-trip stops.



Figure 79. Shore of a typical thaw (thermokarst) lake about 40 mi. (64 km) northwest of Glennallen, Alaska. Bank is undercut because of thawing of permafrost, and vegetation mat of peat is draped over 8- to 12-ft-high (2.4 to 3.9 m), steep bank that is caving into lake. Trees in the foreground are leaning toward the lake and will cave into the lake as the undercutting progresses. Photograph by O.J. Ferrians, Jr., June 23, 1960.

in many dwellings, and locally, sewer lines and other underground pipes were damaged. Ground cracks commonly occurred on flood plains of major rivers; locally, in low terraces adjacent to flood plains; in deltas; along margins of lakes; along the toes of alluvial fans; in highway fill; along the face of steep slopes of river bluffs and hillsides; and in areas cleared of vegetation. These ground cracks in unconsolidated deposits generally were restricted to areas where one or more of the following conditions existed: a) permafrost was absent or deep, b) the ground-water table was near the surface, c) bedrock was relatively deep, and d) slopes were steep.

Road Log and Locality Descriptions

183.3.¹⁵ Enter Gulkana D-3 Quadrangle. Road generally follows base of slope on eastern side of valley of the Gulkana River. Roadcuts expose col-

¹⁵Miles from Valdez on the Richardson Highway.

luvium (a mixture of glacial drift and greenstone) that underlies the drift at a shallow depth.

182.5. Enter Gulkana D-4 Quadrangle. Straight ahead is Paxson Lake, which is approximately 10 mi (16 km) long and 0.8 mi (1.2 km) wide.

182.2. To the right is the Gulkana River delta, which forms the forested neck of land extending into the lake.

181.5. Roadcut in highly fractured greenstone. Highway parallels eastern shore of Paxson Lake and lies at the base of the north-trending hill to the east. The lower steep slope along the western flank of this hill generally is covered by colluvium from greenstone bedrock (which underlies the hill at shallow depth) and from glacial drift, which generally mantles the bedrock.

179.2. To the left is an access road to the Trans-Alaska Pipeline about 1 mi (1.6 km) to the east. Numerous pipeline access roads are present along the highway. Sections of elevated pipeline can be seen intermittently along the hillside to the left.

179. For the next 6 mi (10 km), the highway is underlain by thick glacial drift that forms a complex morainal system of the last major glaciation (Wisconsin). During this glaciation, ice from the Alaska Range flowed south down the trough now occupied by Paxson Lake (figs. 78 and 80).

178.5 Cryoplanation terraces are common on low bedrock ridges of the Gulkana Upland (Gulkana D-4 Quadrangle) above glacial deposits of Wisconsinan age. They can be seen on the summit of flat-topped mountains across Paxson Lake to the right.

177.8. Enter Gulkana D-3 Quadrangle.

176.7. Roadcut through deposit of till; exposed best on left.

To the left is a short section of pipeline that is buried to allow easy crossing for caribou and moose. Several heat pipes have been installed along both sides of the buried pipeline to prevent excessive thaw of ice-rich permafrost and possible damage to the pipeline.

172. The rounded hills to the south were not overridden by ice during the last major glaciation; however, they were overridden during one or more earlier glaciations.

171.5. To the right, two prominent terraces can be seen at the base of the hill across the drainageway of a former outwash stream emanating from the glacier that occupied Paxson Lake trough during the last major glaciation (fig. 81). The terraces were formed by this outwash stream (fig. 82). The meltwater stream flowed to the south through the depression now occupied by Meier Lake and formed a large delta where it emptied into a proglacial lake at an elevation of about 2,650 ft (808 m). Delta deposits dammed the drainageway and formed Meier Lake. The highway crosses the delta about 2 mi (3 km) to the south.



Figure 80. View (to the northwest) from Mile 179.7, Richardson Highway, with Paxson Mountain in the background. Paxson Lake occupies the glaciated trough in foreground. Photograph by O.J. Ferrians, Jr., August 30, 1955.

171.1. Highly fractured greenstone is exposed in the roadcut. For the next mile (1.6 km), the highway parallels the eastern shore of Meier Lake and for a short distance is underlain by outwash gravel and sand deposited by the outwash stream previously mentioned.

170.2. STOP 27. FROST-RIVED GRANITE BLOCKS NEAR SITE OF MEIER ROADHOUSE (fig. 83).

170. To the left is the site of Meier Roadhouse, one of the oldest roadhouses along the Richardson Highway. The main structure was destroyed by fire in September 1960.

Numerous large blocks of weathered granite are exposed conspicuously on the hillside to the left. The well-jointed character of the granite makes it especially susceptible to frost heaving. The presence of these large blocks of frost-rived granite indicates that the hill was not only just outside and above the glacier border during the last major glaciation, but also was above the level of a large lake that existed in the Copper River basin. Therefore, the hill was exposed to a periglacial climate more rigorous than that of today.



Figure 81. View (to the west) from Mile 171.5, Richardson Highway, of former drainageway of proglacial stream from a glacier occupying Paxson Lake trough during Wisconsinan time. Photograph by O.J. Ferrians, Jr., August 30, 1955.

169.8. To the right is a roadcut in outwash gravel.

169.3. To the right is a gravel pit in the large delta mentioned at Mile 171.5. Well-preserved foreset beds are present locally in this deposit. A local resident reported that a mammoth tusk was unearthed by construction workers during excavation of this pit. For the next 3 mi (5 km), the highway is underlain by silty lacustrine sand.

166. For the next 5 mi (8 km), the highway crosses a north-trending hill composed of diorite bedrock with a veneer of glacial drift.

165. Enter Gulkana C-3 Quadrangle.

161. Highway crosses low terrace of Haggard Creek. To the south, a rock quarry is at the north end of the hill. The diorite rock from this quarry was hauled to Gakona, 30 mi (48 km) to the south, and used to protect a high river bluff from undercutting by the Copper River.

160.8. For the next 2.5 mi (4 km), the highway ascends and then follows



Figure 82. Well-developed gravel terraces of Wisconsinan age at north end of Meier Lake. View (to the northwest) from Mile 170.9, Richardson Highway. Photograph by O.J. Ferrians, Jr., August 30, 1955.

the western flank of this hill, which is underlain by diorite bedrock covered by a veneer of glacial drift.

158.2. To the left is a section of elevated oil pipeline.

For the next 3 mi (5 km), the highway ascends and follows the western flank of Hogan Hill. A veneer of glacial drift overlies greenstone, which crops out along the highway at Mile 158.1 and Mile 155.5. Diorite bedrock crops out intermittently below the road level along this section of highway. A rock quarry is present on the left side of the highway at Mile 158.

155.4. STOP 28. VIEW OF WRANGELL MOUNTAINS. Straight ahead on a clear day is an excellent view (from left to right) of Mt. Sanford, Mt. Wrangell, Mt. Drum (fig. 84), and the floor of the Copper River basin. The peaks are



Figure 83. Oblique aerial view (to the northwest) showing Meier Lake, the Richardson Highway, and frost-riven blocks of granite on hill in foreground. Photograph by R.D. Reger, May 21, 1982.

late Tertiary and Quaternary volcanoes. Dome-shaped Mt. Wrangell is still active and occasionally emits steam and ash. The Copper River trough and a large portion of the Copper River-Susitna Lowland (physiographic divisions of the Copper River basin) were covered by an extensive proglacial lake during the last major glaciation (Wisconsin).

155.2. Trans-Alaska Pipeline crosses under the highway and remains buried for approximately 2 mi (3.2 km), where it is underlain by ice-rich permafrost. Normally the pipeline would have been elevated here; however, it has been buried because, according to biologists, this area is an important migration route for caribou. Because of the required burial, the line was heavily insulated and refrigerated to keep the underlying ice-rich permafrost



Figure 84. View (to the south) from Mile 155.4, Richardson Highway, of the snow-covered Wrangell Mountains and the floor of the Copper River basin; from left to right, Mt. Sanford, 16,237 ft (4,949 m), Mt. Wrangell, 14,163 ft (4,317 m), and Mt. Drum, 12,010 ft (3,661 m). Photograph by O.J. Ferrians, Jr., August 31, 1955.

frozen. Refrigerated brine is circulating through pipes buried beneath the pipeline. The building containing the refrigeration plant can be seen from the highway. This is the longest refrigerated section of the Trans-Alaska Pipeline System.

For the next 5.4 mi (8.2 km), the highway crosses a lacustrine plain that is underlain by stony silt (gravelly, clayey silt). These fine-grained deposits and other similar fine-grained deposits in the Copper River basin generally are poor foundation materials and construction on them commonly results in serious maintenance problems, especially where surface drainage is poor. Construction disrupts the thermal regime of the ground, causing a lowering of the permafrost table and consequently, melting of any ground ice, which in turn causes settlement. When saturated with water, the thawed silt loses volume and bearing strength, causing settlement of the roadbed. Once thawed, these deposits are highly susceptible to frost heaving.

149.8. For the next 1.8 mi (2.9 km), at an elevation between 1,950 and 2,000 ft (595 and 610 m), the highway crosses nearshore lacustrine sand and fine-gravel deposits; these sediments are underlain by fine-grained lacustrine deposits at relatively shallow depth, generally less than 10 ft (3 m).

149.5. Enter Gulkana C-4 Quadrangle.

148. Highway descends about 50 ft (15 m) over colluvial deposits to the narrow sand- and silt-mantled terrace of Sourdough Creek. To the right is Sourdough Lodge, which was established in 1904.

147.7. Crossing of Sourdough Creek. Along the south side of the creek is a colluvium-covered slope similar to that along the north side.

147.5. To the right is an access road to a park area along the Gulkana River near the mouth of Sourdough Creek. Shortly after this road was constructed for access to a gravel pit in the summer of 1955, severe differential settlement occurred because of disturbance to the ground surface and the resultant thawing of the underlying ice-rich permafrost (fig. 85). Consequently, the road has required considerable maintenance over the years.

147. For the next 17 mi (27 km), the highway continues across the lacustrine plain, which is underlain generally by massive pebbly silt.

146. Enter Gulkana C-3 Quadrangle.

145.4. Enter Gulkana B-3 Quadrangle.

138. Drainageway of small stream that is a tributary to the Gulkana River. For several miles, the highway is parallel to the valley of the deeply entrenched Gulkana River, which can be seen through the trees to the right.

137. Highway is underlain by a sandy facies of the lacustrine deposits, and consequently the area is fairly well drained and supports a relatively tall stand of poplar and white-spruce trees.

130. Abandoned permafrost thermal-recording station.



Figure 85. Access road at Mile 147.5, Richardson Highway, showing severe differential settlement caused by disturbing the ground surface and the resultant thawing of the underlying ice-rich permafrost. Photograph by O.J. Ferrians, Jr., August 30, 1955.

The Copper River basin is in the zone of discontinuous permafrost. Permafrost probably is present everywhere in the basin except beneath large lakes and major streams. The permafrost table is 1 to 2 ft (0.3 to 0.6 m) below the surface in some muskegs with thick *Sphagnum* moss, 2 to 5 ft (0.6 to 1.5 m) below the surface in lacustrine and fine-grained glacial deposits, and 6 to more than 10 ft below the surface (1.8 to more than 3 m) in granular alluvial and glacial deposits. Permafrost generally ranges from 100 to 200 ft (30 to 60 m) thick, is marginal in temperature [31.1° to 29.3° F (-0.5° to -1.5° C)], and includes ice as pervasive, segregated, interstitial, thin to thick lenses and layers (and in a few isolated places, as vertical wedges). Consequently, the permafrost is in a delicate state of equilibrium and, if thawed by minor changes in the regimen of ground-surface temperatures such as that brought on by most construction projects, considerable surface subsidence may occur. However, because of its thickness, attempts to thaw the permafrost

and stabilize the ground prior to construction generally are impractical.

Because of problems encountered in constructing highways and buildings on permafrost in the Copper River basin, a cooperative study of the engineering aspects of perennially frozen ground was undertaken in 1954 by the U.S. Geological Survey and predecessor organizations to the Alaska Department of Highways (Alaska Road Commission and Bureau of Public Roads). Six roadway sections and one apartment house were selected for study. All roadway sections were instrumented by continuously recording thermographs to obtain ground-surface temperatures and by four vertical, 20-ft-long (6.1 m) thermistor cables. The cables were installed in the centerline, shoulder, and ditch of the road and one in undisturbed ground beside the road.

A control station was set up at Mile 130 on the Richardson Highway. At the control stations, in addition to the three vertical thermistor cables in the road, a cable was placed horizontally across the road at a depth of 3 ft (0.8 m), and 20-ft-long (6.1 m) cables were placed vertically in undisturbed ground on both sides of the road; another 20-ft-long (6.1 m) cable was placed vertically in the centerline of an adjacent section of an old, abandoned roadway (fig. 86). The highway at the control section was built on undisturbed ground in 1951. The roadway was hand cleared, and trees were laid normal to the centerline on the undisturbed vegetation mat. In 1952, approximately 3 ft (0.9 m) of relatively clean, coarse gravel and sand was spread over the section with a minimum of disturbance. However, by 1954, differential subsidence necessitated placing another 0.5 ft (0.2 m) of gravel over the area to maintain a smooth surface. This section was paved originally in 1956 and has been patched and repaved several times since. A good riding surface seldom lasts more than a year.

The adjacent old road was constructed in the pre-World War II era and widened. Additional gravel was placed on the surface during wartime construction. When originally constructed, the roadway was cleared and stripped to the frozen portion of the organic mat. In 1959-60, permafrost was at a depth of a little more than 16 ft (4.9 m), and seasonal freezing of the ground with considerable ice growth extended to a depth of almost 10 ft (3 m). Under the newer road, permafrost had degraded from 5 ft (1.5 m) in 1954 to about 11 ft (3.4 m) in 1959-60, largely as a result of an abnormally warm summer in 1957, when thawing intercepted a relatively permeable sand bed.

129.6. Roadcut showing character of the massive lacustrine pebbly silt. Although the silt is exposed best on the right, slopewash partially obscures the view. The highway descends into an abandoned drainageway connecting valleys occupied by the Gulkana and Copper Rivers and then ascends back up onto the lacustrine plain.

128.8. Northern junction of the Richardson and Glenn Highways (Tok Cutoff). Glenn-Rich International Motel is on the right. Turn left on Glenn Highway.

0.6 (Glenn Highway).¹⁶ For the next 0.4 mi (0.6 km), the highway follows the abandoned drainageway mentioned above to the edge of a high bluff

¹⁶Miles east from northern junction of the Glenn and Richardson Highways.

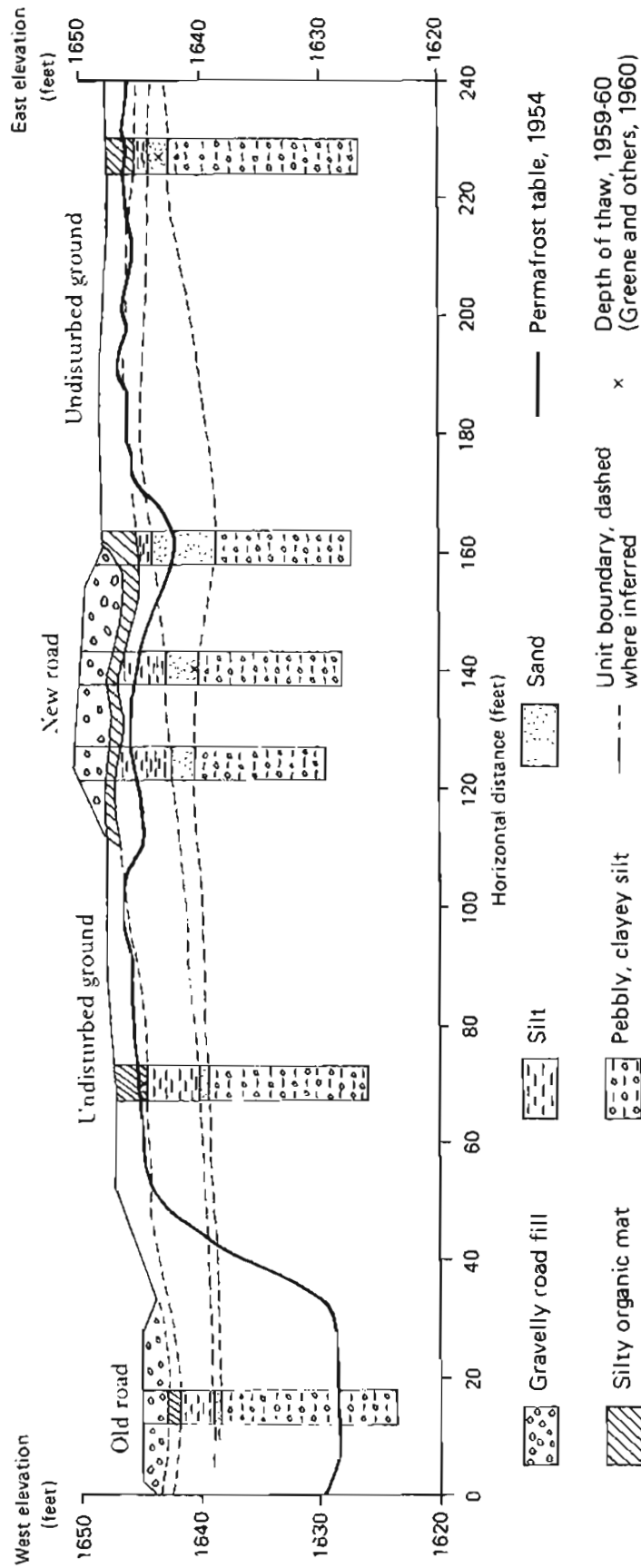


Figure 86. Cross section of permafrost table and geology at Mile 130, Richardson Highway, as determined from drill holes made during installation of thermistor cables.

of the Copper River. The edge of this bluff is underlain by windblown sand and silt (cliff-head dunes) interbedded with peat and other organic material. Cliff-head dunes began to form soon after the extensive proglacial lake drained and river downcutting formed bluffs. Organic material from the base of a nearby dune was radiocarbon dated at $9,400 \pm 300$ yr B.P. (W-714), and windblown material is still being deposited along the edge of bluffs that are unvegetated.

1 (Glenn Highway). Highway descends the steep, 300-ft-high (90 m) bluff. Along the left side of the highway, deposits laid down in the extensive proglacial lake that occupied a large part of the Copper River basin during the last major glaciation are exposed. These deposits include not only typical laminated lake sediments, but also nonsorted and poorly sorted lake sediments that have been described as glaciolacustrine diamicton deposits (Ferrians, 1963b). The nonsorted deposits commonly are till-like in character. Along this section of the highway, considerable slumping has occurred both upslope and downslope from the road where the Copper River has undercut the bluff. Recently, a long dike was constructed to protect the bluff from undercutting.

1.4 (Glenn Highway). Sand- and silt-mantled gravel terraces of the Gakona River.

1.7 (Glenn Highway). Gakona River.

1.8 (Glenn Highway). Gakona Roadhouse---one of the oldest roadhouses in the Copper River basin---was established in 1910.

Gakona Section

During each major glaciation, glaciers advancing in the mountains surrounding the Copper River basin dammed the drainage of the basin, thus impounding an extensive proglacial lake. The lake that existed during the last major glaciation covered more than $2,000 \text{ mi}^2$ ($5,200 \text{ km}^2$) of the basin floor, and numerous glaciers and sediment-laden glacial streams debouched into it. The 300-ft-high (90 m) bluff along the west side of the Gakona River offers a good view of the type of sediments that were deposited in this lake.

The uppermost 15 to 30 ft (4.5 to 9.1 m) of the section consists of windblown sand and silt interbedded with peat and other organic material. Approximately 200 ft (60 m) of sediments underlying the windblown material was deposited in the extensive proglacial lake during the last major glaciation. Radiocarbon dating (in the 1960s) of organic material bracketed these lacustrine sediments between a maximum age of greater than 38,000 yr B.P. (W-531) and a minimum age of $9,400 \pm 300$ yr B.P. (W-714). Because of the possibility of dating the initiation of the last major glaciation in the Copper River basin, a large sample of the older organic material was submitted to the Groningen Laboratory in the Netherlands, where the carbon-enrichment method is used to extend the range of radiocarbon dating. The results of their measurements were inconclusive. One measurement gave an absolute age of $43,440 \pm 250$ yr B.P. (GrN-4086), but because this age was younger than two dates on unenriched portions of the same sample---greater than 46,000 yr B.P. (GrN-4165) and greater than 49,000 yr B.P. (GrN-4448)---the laboratory concluded that the sample was contaminated during the enrichment process. Consequently, the analysis was repeated and the sample yielded an absolute age of $58,600 \pm 1,100$ yr B.P. (GrN-4798). Because of the possibility of contamination during the

enrichment process, it is difficult to accept the accuracy of this date without further evidence; however, we can conclude that the organic material is at least older than 55,000 yr B.P.

Radiocarbon-age determinations of $28,300 \pm 1,000$ yr B.P. (W-1343) and $31,300 \pm 1,000$ yr B.P. (W-843) were obtained from organic material collected from a bluff along the Sanford River about 10 mi (16 km) east of here. These two age determinations date a time interval when the lake level was below an elevation of approximately 2,150 ft (655 m). These radiocarbon dates indicate that the last major glaciation in the Copper River basin is comparable in age to the last major Wisconsin glaciation in central North America. Other exposures less than 1 mi (1.6 km) downstream from here provide stratigraphic evidence for two major glaciations older than the last major glaciation (fig. 87).

Return to Richardson Highway.

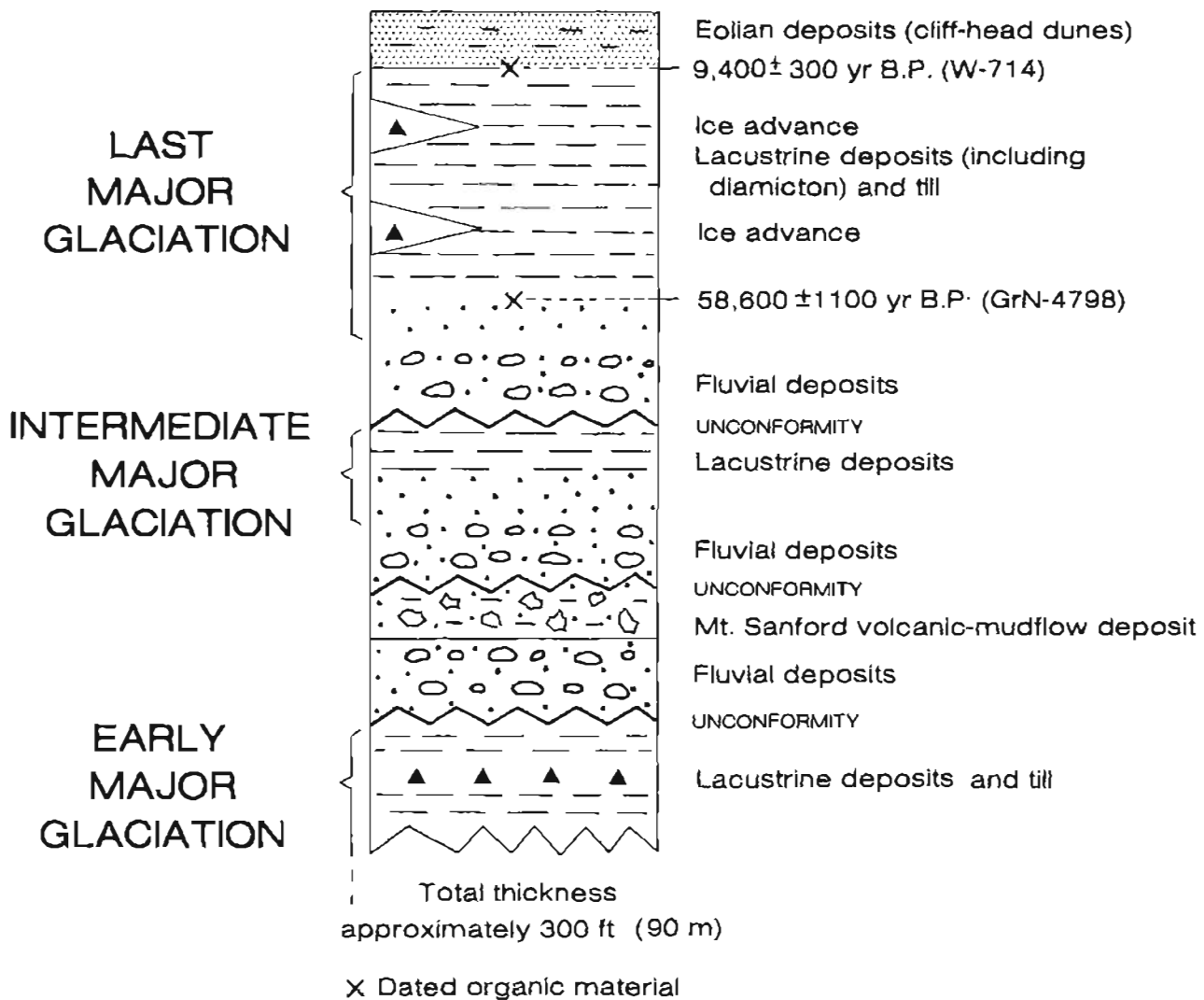


Figure 87. Generalized stratigraphic section of Pleistocene deposits in the east-central part of the Copper River basin, Alaska.

Richardson Highway

128.8.¹⁷ Highway on lacustrine plain. Stabilized cliff-head sand dunes are present along the bluff of the Copper River (to the left).

127.8. Highway descends a colluvium-covered bluff of the Gulkana River.

127.5. Low gravel terrace of the Gulkana River. To the left is the Indian village of Gulkana.

127.1. The Gulkana River is one of the few clear-water streams in the Copper River basin. Most major rivers in the basin are fed by glaciers and consequently carry a large load of suspended sediment.

127. Highway ascends a colluvium-covered bluff to the tread of a high gravel terrace.

125.6. Highway on lacustrine plain.

124.8. Enter Gulkana A-3 Quadrangle. This area is underlain generally by pebbly, clayey silt.

121.1. Well at end of access road to the right was drilled to a depth of 354 ft (107.9 m) and encountered highly saline water. The minimum temperature recorded over a period of several years in this hole, from below the zone of mean annual temperature fluctuation, was 31°F (-0.7°C). Permafrost occurs to a depth of 120 ft (36.6 m) in Wisconsinan and possibly older deposits and hence probably formed during Holocene time.

118.2. Poor drainage and ice-rich permafrost at the west end of the State of Alaska Department of Transportation airstrip have caused serious problems. Differential subsidence of the blacktop-runway surface resulted from degradation of permafrost. Wells at the airstrip were drilled to a depth of 293 ft (89.4 m) before encountering water, which is generally high in chlorides, especially at the 433-ft (132 m) level; water from the 293-ft (89.4 m) level is not potable without treatment to reduce the chloride content.

117.6. Incised flood plain of Dry Creek.

115.4. Saline water was reported from a 321-ft-deep (97.8 m) well drilled at Gateway Lodge.

112.5. STOP 29. SIMPSON HILL ROADCUT AND COPPER RIVER BLUFF.

Roadside turnout on east side of highway provides easy access to the abandoned Simpson Hill roadcut (a short distance to the southeast) and to spectacular exposures along the Copper River (a short distance to the east). It also provides an overview of the Copper River and from left to right, Mt. Sanford [16,237 ft (4,949 m)], Mt. Drum [12,010 ft (3,661 m)], Mt. Wrangell [14,163 ft (4,317 m)], and Mt. Blackburn [16,523 ft (5,036 m)]. Cones of the Drum group of mud volcanoes are also visible. Shrub Mud Volcano is 14 mi (23

¹⁷ Miles from Valdez on the Richardson Highway.

km) to the east-northeast, Upper Klawasi Mud Volcano is 14 mi (23 km) to the east, and Lower Klawasi Mud Volcano is 7 mi (11 km) to the east-southeast (fig. 88). Lower Klawasi Mud Volcano is the largest diameter cone of the Drum mud-volcano group (fig. 89); the base measures approximately 6,000 ft (1,830 m) east-west and 8,200 ft (2,500 m) north-south. Lower Klawasi Mud Volcano is about 150 ft (46 m) high. The pool in the crater is 15 ft (4.6 m) lower than the crest, is 175 ft (53.4 m) in diameter (fig. 90), and discharges carbon-dioxide gas through Na-HCO₃-Cl water with as much as 28,000 ppm dissolved solids. The cone lies on the lower slopes of the Wrangell Mountains and is composed of clayey silt with small, angular rock fragments.

Simpson Hill roadcut

In the spring of 1954, during construction of a new telephone line up-slope and parallel to the road, a wide swath of spruce forest was removed. This stripping produced rapid degradation of the permafrost table during the summer and the release of free moisture in lacustrine deposits beneath the roadbed. The increased moisture caused saturation of the fill and development of small slumps in the outer part of the road prism (Nichols and Yehle, 1961a). Early in September of that same year, a maintenance crew made cuts in the bluff immediately uphill and downhill from the fill and dumped the cut material on the outer part of the road to bring it back to grade. Overnight, a 15-ft-wide (4.6 m) section of the paved road and shoulder slumped through a vertical distance of 10 ft (3 m), apparently along a concave glide plane. To

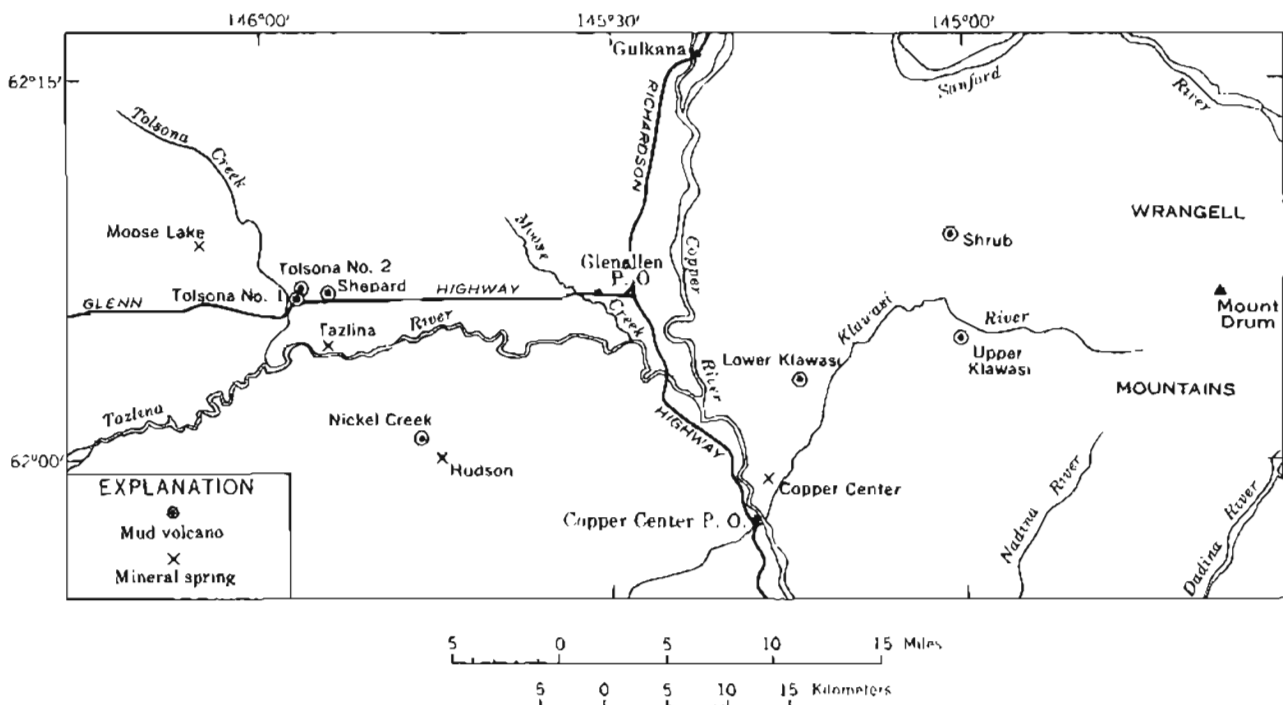


Figure 88. Location of mud volcanoes and mineral springs in the southeastern Copper River basin (from Ferrians and Nichols, 1965, fig. 8-42).

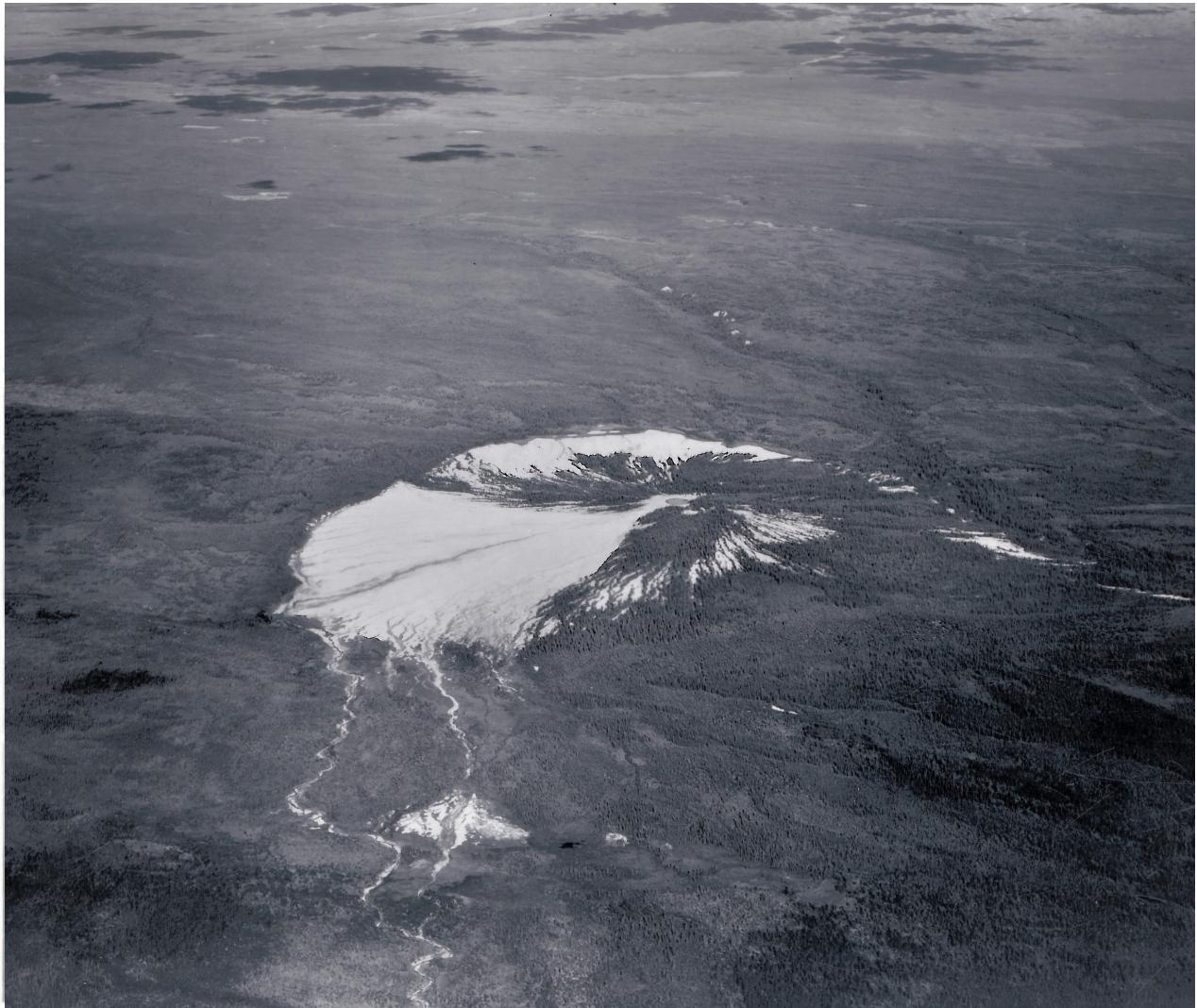


Figure 89. Aerial view of Lower Klawasi Mud Volcano. Photograph by Bradford Washburn, August 7, 1938.

repair this major damage, large amounts of silt were excavated along the cut and dumped into the slump area. Almost a year later, the same part of the road again subsided 10 ft (3 m), following attempts to level minor slumps by the addition of a small amount of fill (fig. 91). Subsequently, deeper cuts have been made into the hill to obtain the required road width rather than again replacing the slumped material with fill. Nevertheless, sliding continued and constituted a never-ending maintenance problem (fig. 92). As a result of this problem and the likelihood of further retreat of the Copper River bluff by river undercutting upslope from Simpson Hill, the road was relocated a short distance to the west (fig. 93).

The old roadcut exposes several layers of volcanic ash in lacustrine pebbly silt and varved silt and clay.

Mud Volcano	Diagrammatic cross-section N S	Approximate dimension * of cone		Alt. ^o of crest	Approx. * diam. of "crater"	Surf. water temp., ^o F.	Est. water disch., gpm.	
		Base	Hgt.					
Druva Group	Shrub		3600 4200	310	2950	120	54	< 1/4
	Upper Klawasi		4200 6700	300	3017	150	86.5	2-5
	Lower Klawasi		6000 8200	150	1875	175	82	5-10
Tolsona Group	Nickel Creek		800 1000	60	2025	150	cold	< 1/4
	Shepard		1300 1600	25	2172	15	—	—
	Tolsona No. 1		600 900	25	2045	30	38-55	< 1/4
	Tolsona No. 2		2000 2300	40	2085	150	40-60	< 1/4

* =in feet, ■ = active spring, ● =inactive spring.

Figure 90. Comparison of certain physical characteristics of mud volcanoes, Copper River basin, Alaska (from Nichols and Yehle, 1961b, table 1).

Copper River Bluff Section (fig. 94)

Most material in this section was deposited during the last major glaciation.

COPPER RIVER BLUFF SECTION

Unit	Thickness in ft (m)	Ft (m) above river to top of unit
Vegetation mat and soil profile developed on eolian silt and sand.	2.7 (0.9)	260.0 (78.8)
Lacustrine deposits: Massive, dark-gray, clayey silt with lenses of silt and volcanic ash.	6.5 (2.0)	257.3 (78.0)
Gradational contact		
Glacial deposits: Dark-gray till with a silty sand matrix and subrounded pebbles, cobbles, and boulders. Thin sandy lenses in upper 2 ft.	15-25 (4.6-7.6)	250.8 (76.0)

Unit	Thickness in ft (m)	Ft (m) above river to top of unit
Lacustrine deposits		
a. Amorphous masses of blue-gray, phyllitic-appearing clay with a few pebbles. Extreme deformation by shearing locally.	5 (1.5)	230.8 (69.9)
b. Well-laminated, blue-gray, clayey silt with several 1- to 4-in.-thick (2.5 to 10 cm) volcanic-ash beds.	5 (1.5)	225.8 (68.4)
c. Massive, blue-gray, blocky silty clay.	10-15 (3-4.5)	220.8 (66.9)
Glacial deposits		
a. Massive, dark-gray, clayey silt with columnar joints and conchoidal fracture and numerous scattered pebbles and cobbles. Apparent bedding locally.	10-20 (3-6)	208.3 (63.1)
b. Gradational zone between (a) and (c).	10 (3)	193.3 (58.6)
c. Typical blocky, fractured till with numerous pebbles, cobbles, and boulders in a clayey, sandy silt matrix. Contorted and faulted varved silt and clay incorporated as large and small masses in till and in shear zones near base.	30-40 (10-12)	183.3 (55.6)
Lacustrine deposits		
a. Horizontally laminated and varved light-gray and dark-blue-gray silty clay with several thin, highly contorted zones. Includes scattered pebbles and cobbles.	22 (6.7)	148.3 (44.9)

Unit	Thickness in ft (m)	Ft (m) above river to top of unit
b. Medium to coarse dark-gray sand with steep, south-dipping foreset beds. Granules, pebbles, and cobbles scattered throughout.	3 (0.9)	126.3 (38.3)
Fluvial deposits with rapid lateral variation		
a. Fine pebble and pea gravel in coarse-sand matrix.	0.3 (0.1)	123.3 (37.4)
b. Horizontally bedded, medium to coarse sand with thin pumiceous pebbly zones and scattered clastic 'boulders' of till and varved silt and clay. One-ft-thick bed near middle dips steeply northwest.	26 (7.9)	123.0 (37.3)
Disconformity		
c. Horizontally bedded, gray to brown silt and fine sand highly contorted in upper 3 ft.	5 (1.5)	97.0 (29.4)
d. Dark-gray, coarse to medium sand with gravelly beds.	4 (1.2)	92.0 (27.9)
e. Well-rounded gravel with a few thin, sandy beds. Iron- and manganese-oxide staining locally, particularly near base.	25 (7.6)	88.0 (26.7)
f. Well-bedded, fine to coarse, dark-gray to greenish-gray sand.	0-3 (0-0.9)	63.0 (19.1)
Mt. Sanford volcanic mud-flow deposits: Silty sand matrix with subrounded to angular pebbles and cobbles, largely of andesite. Sharp	0-3 (0-0.9)	61.5 (18.6 m)

Unit	Thickness in ft (m)	Ft (m) above river to top of unit
color variations laterally and vertically from pink, green, and brick-red to gray. Generally massive but with local lenses of well-sorted sand or gravel.		
Prevolcanic-mudflow fluvial deposits: Alternating sand and well-rounded coarse gravel with rounded detrital 'blocks' of till and lacustrine sediments locally iron-oxide stained; cross-bedding dips steeply to the south.	60 (18.3)	60 (18.3)
Copper River level	- - -	0

The following reconstruction of events, from the oldest to the youngest, is inferred from the character and relations of the glacial, lacustrine, and fluvial deposits exposed in this Copper River bluff section.

1. Fluvial deposition with incorporation of blocks of older sediments, probably from nearby riverbanks; 0-60 ft (0-18.3 m) above river level.
2. Downstream terminus of coherent deposits from the Mt. Sanford mudflow. Deposits diluted here; 60-61.5 ft (18.3-18.6 m).
3. Reworking of Sanford volcanic-mudflow deposits and continued fluvial deposition. Disconformity probably represents erosion during one or more glaciations or periods of river downcutting or both; 61.5-123.3 ft (18.6-37.4 m).
4. Rapid change from fluvial to lacustrine deposition---onset of deteriorating climatic and glacial conditions; 123.3-126.3 ft (37.4-38.3 m).
5. Rising lake level with probable ice rafting of coarse fragments and periodic slumping or iceberg drag of sediments to cause contortions; 126.3-148.3 ft (38.3-44.9 m).
6. Overriding of lacustrine deposits by first ice advance of last major glaciation and incorporation of varves in till; 148.3-183.3 ft (44.9-55.6 m).
7. Gradual thinning of ice to increase buoyancy and eventual floating of ice near terminus with rapid deposition from melting at base of ice; 183.3-208.3 ft (55.6-63.1 m).
8. Retreat of ice front south of this point with continued rapid lacustrine deposition and at least minor volcanic activity, as suggested by thin ash beds; 208.3-230.8 ft (63.1-69.9 m).



Figure 91. View (to the south) of slump block of fine-grained highway fill material at Simpson Hill, near Mile 112 on the Richardson Highway. Centerline of road was formerly over exposed part of sheared culvert. Bulldozer tracks on slump-block surface are a continuation of those at road level on right side of photograph. Compare with figure 92 and note same culvert in both pictures. Photograph by D.R. Nichols, September 1955.

9. Readvance of ice of last major glaciation, strongly deforming lake sediments, and deposition of sandy till; 230.8-250.8 ft (69.9-76.0 m).
10. Retreat of ice of last major glaciation (final retreat in this area) and resumption of lacustrine deposition; 250.8-257.3 (76.0-78.0 m).
11. Drainage of lake at close of Wisconsinan time, downcutting of the Copper River, and inauguration of eolian activity to form the present surface; 257.3-260 ft (78.0-78.8 m).

The continuous and widespread lacustrine sedimentation between episodes of till deposition, as postulated in events (6) and (9), indicates that the ice thinned and retreated at least 5 mi (8 km), but did not retreat suffi-



Figure 92. View (to the north) of abandoned roadcut on Simpson Hill showing successive slumps that destroyed old road surface. Compare with figure 91 and note same culvert in both pictures. Photograph by O.J. Ferrians, Jr., September 1977.

ciently to permit complete lake drainage. Ice retreat in this area may have coincided with the lowering of lake level 28,000 to 31,000 yr B.P. Consequently, event (8) probably represents interstadial rather than interglacial conditions. Only with complete removal of ice as a barrier to drainage of the Copper River, as indicated by cessation of lacustrine deposition and initiation of subaerial or fluvial conditions, can we assume that an interglacial climate existed.

Glenn Highway

189.¹⁸ Southern junction of the Richardson and Glenn Highways near

¹⁸Miles from Anchorage on the Glenn Highway.



Figure 93. View (to the north) of Simpson Hill near Mile 112, Richardson Highway, showing new roadcut and site of old roadcut where serious slumping problems occurred (figs. 91 and 92). Photograph by O.J. Ferrians, Jr., July 1967.

Glennallen. Much land around the junction of the Glenn and Richardson Highways was withdrawn from homesteading to evaluate the area as a townsite. Because of saline ground water and permafrost problems, plans for the townsite were abandoned. A well drilled to a depth of 323 ft (98 m) at the road junction (Rosent's Roadhouse) in the fall of 1959 encountered water with 2,270 ppm dissolved solids and some gas. This roadhouse has changed ownership several times over the years and burned down a few years ago. The Ahtna Lodge, which also is located at the junction across the highway from the former Rosent's Roadhouse, does not have a well, and water is hauled to the facility by tanker truck.

188.3. The Trans-Alaska Pipeline crosses the highway in a special buried mode. The pipeline is heavily insulated, and refrigerated brine circulating



Figure 94. View (to the north) of high bluff on west side of the Copper River near Mile 112.5, Richardson Highway, exposing thick section of Pleistocene deposits. Photograph by O.J. Ferrians, Jr., September 8, 1956.

in pipes under the pipeline keeps the underlying ice-rich permafrost frozen. This pipeline was constructed in an above-ground mode on vertical support members (VSMs) across most of the Copper River basin to avoid thawing the permafrost (fig. 95).

188.1. Enter Gulkana A-4 Quadrangle.

187.6. A 100-ft-deep (30 m) well produces slightly hard but potable water from glacial deposits below permafrost.

186.2. STOP 30. GLENNALLEN PERMAFROST PROBLEMS.

Numerous buildings in the Glennallen area have had severe structural problems because of differential settlement caused by thawing of permafrost. Most buildings in Glennallen are constructed on colluvial-mantled terrace deposits of Moose Creek. Colluvial deposits [1 to 15 ft (0.3 to 4.6 m) thick] consist largely of gravelly silty clay; terrace deposits [10 to 30 ft (3 to 9 m) thick] are largely silty sandy gravel or gravelly sand and overlie a thick sequence of fine-grained, ice-rich, glaciolacustrine deposits. Permafrost generally lies 5 to 10 ft (1.5 to 3 m) below the surface and is deeper in



Figure 95. The Trans-Alaska Pipeline elevated above the ground on steel vertical-support members (VSMs) to prevent thawing of the underlying ice-rich permafrost. Expansion of the pipe is handled by the trapezoidal zig-zag configuration---the 'shoes' under the pipe are teflon coated and allow the pipe to slide laterally on the steel cross-members connecting the VSMs. View to the north overlooking the valley of the Klutina River in the Copper River basin. Photograph by O.J. Ferriars, Jr., September 1977.

areas of ground scarring. Moisture content is low in unfrozen granular terrace deposits, but is sufficient to act as a cementing agent and to form local ice lenses and stringers. Small amounts of ground water perched on the permafrost provide limited seasonal supplies of potable water. Maintenance of the permafrost level in this area is difficult because of its marginal temperature; total artificial destruction of the permafrost before construction is virtually precluded by its considerable depth. A number of methods have been adopted in design and construction of new buildings and in rehabilitating existing structures with varying degrees of success (figs. 96 and 97).

The Glennallen ACS microwave tower, constructed in 1960 utilizing the 'Long thermopile' in the foundation, has---almost alone among the structures at Glennallen---remained stable, even through the Alaskan Good Friday Earthquake of March 27, 1964.

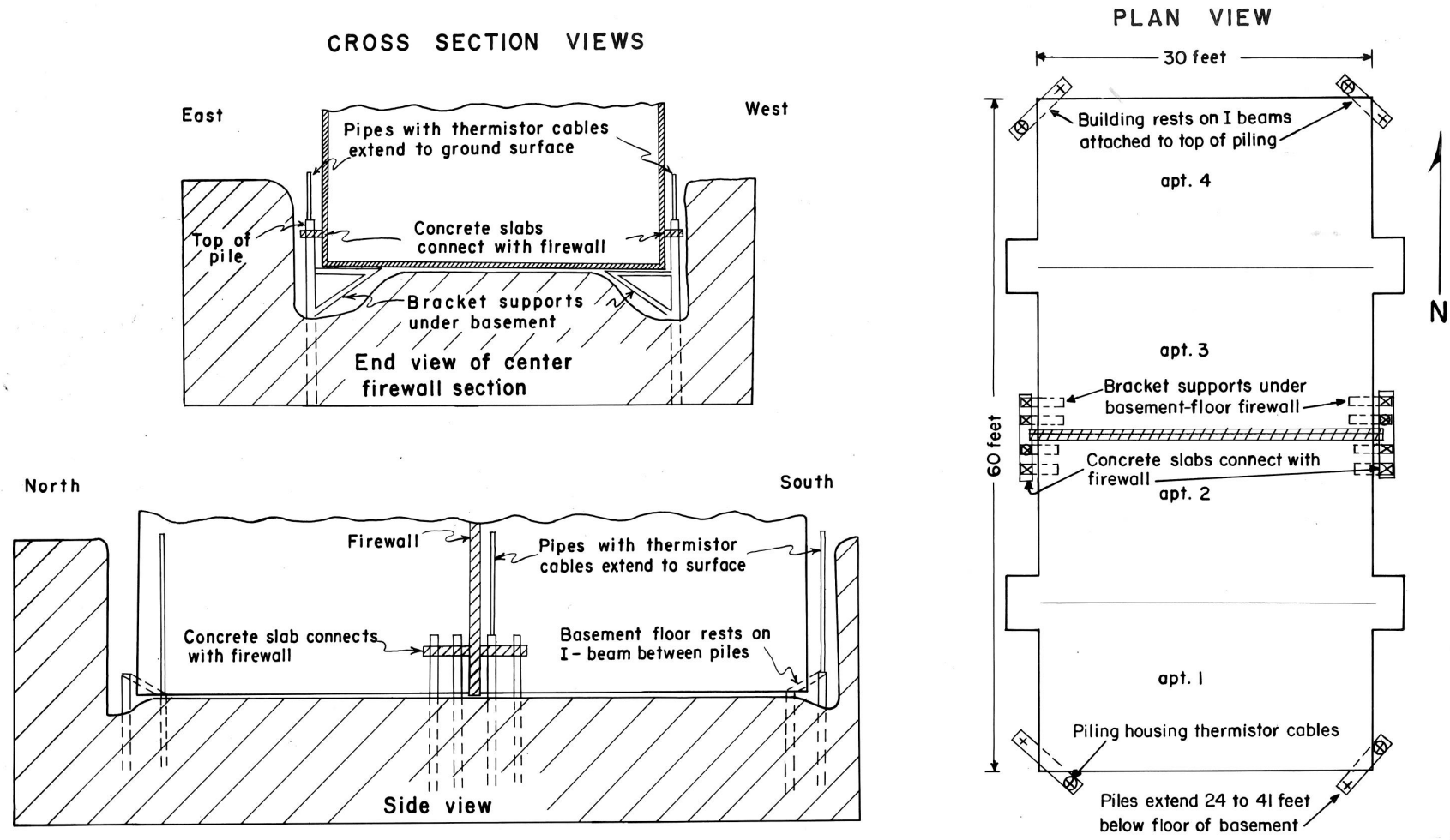


Figure 96. Piling- and cable-installation plan for Alaska Department of Highways apartment house at Glennallen, Alaska.



Figure 97. Schoolhouse at Glennallen built in 1952-53 on ice-rich permafrost. Air vents, which are open, allow cold air to enter the crawlway in winter to counteract heat from building. The vents are closed during the summer. Jacks are used to counteract differential settlement. The system was only partially successful, and the school was demolished in the 1960s. Photograph 915 by T.L. Péwé, May 4, 1954.

Although well water at Glennallen is hard, it is not the salty water typical of deep wells in the area. Most wells at Glennallen are less than 100 ft (30 m) deep and do not intersect saline aquifers 300 to 500 ft (40 to 150 m) below the ground surface.

185.9. Swale, crossed by road for next 0.2 mi (0.3 km), that is probably an early drainageway of Moose Creek.

185.7. Telephone poles on the right are tilted by frost jacking.

185., 184.6, 184.3. Three minor strandlines occur at about 1,510 ft (460 m), 1,545 ft (471 m), and 1,560 ft (475 m). Other higher strandlines, which are recognized elsewhere in the southeastern part of the Copper River basin, lie at 1,600 ft (490 m), 1,700 ft (520 m), 1,800 ft (550 m), and 1,900 ft (580 m), but are not apparent along the road, probably because of modification by drainage swales that developed after drainage of the lake at the close of Wisconsinan time.

183.3. Road crosses 1.2 mi (1.9 km) of sand and gravel that occur in a broad swath north from the Tazlina River. The swath apparently represents a course of the Tazlina River that formed at least 9,000 yr B.P., soon after drainage of the lake. Poorly sorted sandy gravel and gravelly sand are exposed in the gravel pit north of the highway at Mile 182.7 and south of Mile 182.4.

182.7. A well drilled at Glennallen Lodge to a depth of 502 ft (153 m) encountered water (Na-Ca-Cl type) with 3,240 ppm total dissolved solids.

182. Construction of the highway for the next 3.3 mi (5.3 km) has impeded the normal flow of drainage in a series of poorly drained swales and muskegs on the lacustrine plain. In these areas, water has collected along the shoulders of the highway. The resulting thawing of permafrost in the poorly drained swales and muskegs and under culverts causes differential subsidence of the road and slumping of the shoulders. Seasonal freezing of the wet ground produced considerable annual frost heaving in wet areas under the road prism.

177.1 to 176.3. Several small, almost imperceptible strandlines lie at altitudes of 2,000 ft (610 m), 2,050 ft (625 m), and 2,090 ft (637 m) in the next 0.8 mi (1.3 km). On the strandlines are discontinuous deposits of poorly sorted sand and sandy gravel, generally less than 10 ft (3 m) thick; some of these deposits were used as limited borrow sources for road construction.

173.2. STOP 31. TOLSONA NO. 1 MUD VOLCANO (fig. 90).

Tolsona No. 1 cone of the Tolsona group of mud volcanoes is 0.12 mi (0.2 km) north of the highway. This mud volcano is one of four mud-volcano cones and two mineral springs that compose the Tolsona group of mud volcanoes, which is largely west of the Copper River and contains much smaller cones than those of the Drum group east of the river (fig. 90). Springs from the Tolsona group emit methane gas and cool sodium-chloride and calcium-chloride waters.

The Tolsona No. 1 Mud Volcano, at an elevation of 2,045 ft, is about 25 ft (7.5 m) high, 600 ft (180 m) wide, and 900 ft (270 m) long. The crater is

about 30 ft (9 m) in diameter. The temperature of the water discharged from the vents ranges between 38° and 55°F (3.3° and 12.8°C). The cone has gently sloping sides that rise to a slightly domed crest on which the activity of several gas and water vents has varied from year to year.

Nichols and Yehle (1961b) suggested the water could be derived from meteoric or other water (or both) circulated with saline ground water formed by evaporation from glacial lakes and later reconcentrated by permafrost from highly diluted volcanic water or from a connate source. They proposed that the gas is probably derived from coal beds similar to the Tertiary or older coal beds exposed near Atlasta House 7.5 mi (12.5 km) to the west, or from marsh gas from buried Pleistocene deposits, or, alternatively, from slightly organic, nonpetroliferous connate water associated with Cretaceous bedrock.

Grantz and others (1962) proposed that the gas and water are connate in origin and are derived from Cretaceous or older marine rocks that are inferred to underlie the area. In support of this thesis, they report the presence of foraminifera, Inoceramus shell fragments, echinoid spines and plates, and ophiuran ossicles on the surface of the cone. A few Inoceramus prisms have been collected from nearby till and proglacial lake deposits, but they are strongly abraded. Grantz and others (1962) pointed out that although the gas resembles marsh gases and contains little of the higher hydrocarbons, similar gases occur in oil fields elsewhere in the United States. The presence of gas and salt water under pressure in nearby wildcat wells further supports this thesis.

The age of the cone is assumed to be late Pleistocene. The small size of the cones and the lack of included angular rock fragments suggest that the cone formed largely by quiet, gradual accretion of mud rather than by explosive action.

Tolsona No. 2 Mud Volcano lies 0.4 mi (0.6 km) north-northeast of Tolsona No. 1, but cannot be seen from the highway.

173.1. Road descends bluff composed of frozen, ice-rich glaciolacustrine silt and clay and mantled by colluvium.

172.9. Gravelly terrace deposits of Tolsona Creek.

172.6. Massive, lacustrine pebbly silt and varved silt and clay overlying till are exposed in bluffs.

171.9. Lacustrine plain composed largely of pebbly, clayey silt.

171.2. Enter Gulkana A-5 Quadrangle.

170. To the right is a side road to Tolsona Lake Resort. This road follows the site of a former esker now removed for road material. At the resort on the lakeshore, the esker consists of gravel deposits about 80 ft (24 m) thick that rest on glaciolacustrine deposits. Most surficial deposits in this area are lacustrine silt, clay, stony silt, and stony clay. Small seepages of gas and saline water occur both at Tolsona Lake and at Moose Lake, located northwest of Tolsona Lake. For the next 4 mi (6.4 km), the highway crosses a series of north-trending, till-cored ridges that are draped with lake sediments.

166.2. To the right is Atlasta House. The hill behind this lodge is formed of poorly consolidated sandstone, coal, clay, and gravel of Tertiary age. Coal beds are as thick as 2 ft (0.6 m).

164. To the right, for the next 6 mi (9.6 km), a moraine of late Wisconsinan age occurs as hummocky terrain on the southern slope of Tazlina Hill. This moraine probably is about 11,000 or 12,000 yr old. To the left (south), Tazlina Lake and Tazlina Glacier may be seen in the distance. Because the lake is fed by glacial meltwater, it has a considerable amount of gray rock flour in suspension, and its bottom is covered by the same material. The lake is at least 370 ft (110 m) deep. At the outlet of the lake at its northern end, the Tazlina River crosses conglomerate of the Matanuska Formation (Cretaceous) and enters a canyon cut in Pleistocene glacial and glaciolacustrine deposits.

156. To the left is Tazlina Glacier Lodge. The Glenn Highway is underlain by stony silt or clay, and the lake behind the lodge is perched on this same impermeable material. A well dug beside the lake encountered dry gravel, and water pumped into the well disappeared into the gravel. Many lakes in this part of the Copper River basin are perched on impermeable sediments and do not reflect the water table in the underlying materials.

154.8. To the right, a large pit is at the base of a hill around which a shoreline related to the 2,450-ft (750 m) lake level was formed. The former shoreline is marked by a wave-cut notch with basal boulders that have been winnowed from the underlying till. For approximately the next 9 mi (14.5 km), the highway crosses a broad valley that was occupied by a northward-moving glacial lobe during late Wisconsinan time. Within this valley, the highway crosses several north-trending till ridges that are draped with lacustrine sediments. The intervening lowlands generally are underlain by fine-grained lacustrine deposits.

154.1. Enter Gulkana A-6 Quadrangle.

146. For the next 4 mi (6.5 km), the highway winds through kames and eskers composed of sand and fine gravel.

144.5. Enter Valdez D-8 Quadrangle.

142. To the right is Slide Mountain and for the next 4 mi (6.5 km), the highway follows the southern flank of Slide Mountain (fig. 98). Large landslides in shale of the Matanuska Formation have moved down this unstable slope in the last 10,000 yr or more. Some slides are stabilized and spruce forests are growing on them. Others have moved recently---movement in 1946 formed the large scar that can be seen from near Mile 141. Minor movement occurred in several places within the slide zone during the earthquake of March 27, 1964. The brown rock at the summit of the mountain is poorly consolidated gravel and sand of Tertiary age.

138. Highway begins steep descent into canyon of the Little Nelchina River. In a cut through shale of the Matanuska Formation, the road has slumped in several places. Cuts in frozen shale also have slumped.

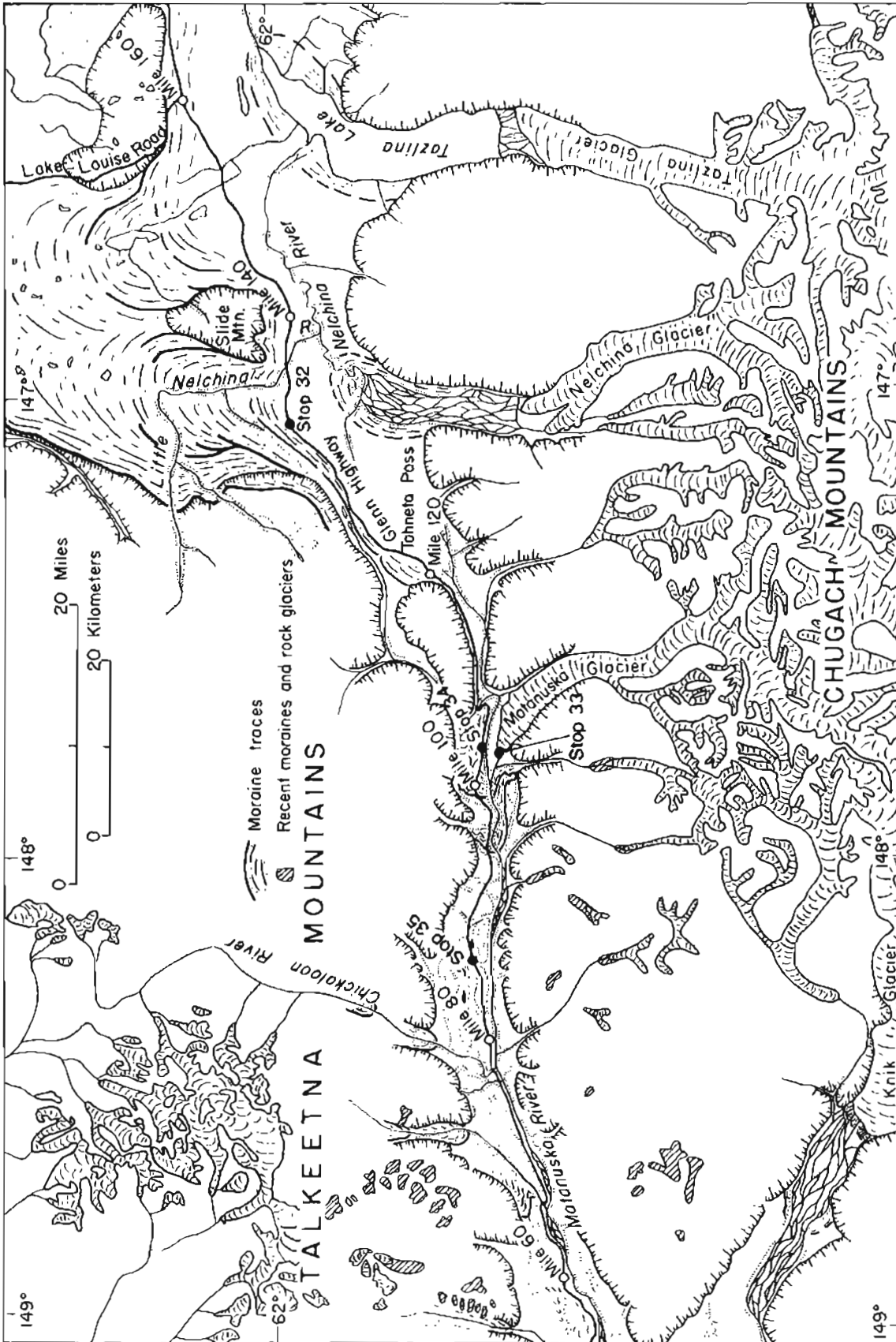


Figure 98. Index map of the upper Matanuska Valley and Nelchina River area, Alaska, showing field-trip stops.

137.4. Little Nelchina River. Shale of the Matanuska Formation, capped by terrace gravel, occurs along the east side of the river upstream from the bridge. The terrace gravel and canyon are slightly older than $10,250 \pm 250$ yr B.P. (W-767); therefore, the glacier must have retreated from this point before that date. Highway begins ascent to till-covered surface bordering the canyon of the Little Nelchina River.

135.5. Enter Anchorage D-1 Quadrangle.

133. From here to Eureka Lodge (at Mile 128), the highway follows a series of low till ridges that form a summit more than 3,300 ft (1,000 m) above sea level.

130. To the right, an unsuccessful oil well 8,546 ft (2,600 m) deep (Eureka No. 2) was drilled. Shale of the Matanuska Formation is overlain by glacial deposits.

129.4. STOP 32. NELCHINA GLACIER VIEW. Eureka Summit, elev. 3,322 ft (1,010 m).

To the south is a good view of the Nelchina Glacier, the broad outwash plain in front of the glacier, and the Nelchina River canyon, which is cut into glaciolacustrine deposits and other glacial drift. The western part of the end moraine of a major glacial advance during late Wisconsinan time can be seen to the northwest.

During Wisconsinan time, the Talkeetna Mountains, which are remote from moist maritime air, were not heavily glaciated. Glaciers from the Chugach Mountains, because of their proximity to these air masses, advanced more than 50 mi (80 km) north of their present location and coalesced to form a great piedmont glacier that fronted in a glacial lake. Evidence of pre-Wisconsinan glaciation is obscure, and is either at high elevations or in areas north of the highway.

In late Wisconsinan time, the expanded glaciers from the Nelchina and Tazlina valleys in the Chugach Mountains were separated into three lobes by low bedrock hills; a lobe moved northward through the Little Nelchina valley; a lobe moved northward through the valley now occupied by Old Man Lake east of Slide Mountain and west of Lake Louise Road; and a lobe moved eastward down the Tazlina valley below Tazlina Lake. Outwash from the Little Nelchina lobe was graded to deltas that are about 2,650 ft (808 m) above sea level. Successively younger deltas, which can be traced back along outwash channels to recessional moraines, formed as the lake level dropped. One outwash deposit, which is graded to a delta at elevation 2,500 ft (760 m), is dated radiometrically as slightly older than $13,280 \pm 400$ yr B.P. (W-583). The lake level had dropped to about 2,450 ft (750 m) elevation by the time the ice strongly readvanced, the last major readvance of Wisconsinan age. As the ice retreated from this moraine, the lake level remained at elevation 2,450 ft (750 m), forming weakly developed beaches. Apparently this lake level was maintained by a threshold on the Tyone River north of Tyone Lake between about 11,000 and 12,000 yr B.P.

As the glacier retreated, it split into two individual valley glaciers, one from the Nelchina valley and one from the Tazlina valley. About this

time, probably about 10,250 yr B.P., the lake level dropped from 2,450 ft (750 m) to a level of about 2,300 or 2,350 ft (700 or 715 m), where it remained until the glaciers retreated to within 8 or 10 mi (13 to 16 km) of their present positions. This drop in lake level marks the beginning of the disintegration of the ice dam blocking drainage through the Chugach Mountains. Although there were some fluctuations in lake level, the lowering of the lake was rapid and, according to evidence in the east-central part of the basin, the lake level was below 1,700 ft (520 m) before $9,400 \pm 300$ yr B.P. (W-714).

Since withdrawal of the glaciers, minor advances have occurred, and major rivers have cut deep canyons through glacial and glaciolacustrine deposits. Also, a minor amount of loess and some cliff-head dunes were deposited along the northern edge of the river canyons.

128. Eureka Lodge. For the next 7 mi (11.2 km), the highway crosses Tahnetta Pass over a gently irregular surface that was scoured by overriding glaciers. Shale of the Matanuska Formation is very close to the surface, and the road fill is largely shale from pits along the southern flank of Sheep Mountain and from side borrow. The shale is a poor aquifer, and attempts to obtain fresh water from it have failed.

125. To the right is the site of Alaska Oil and Gas Development Company well, Eureka No. 1. This well was drilled in 1953-54 and reached a depth of 4,818 ft (1,460 m) without producing oil or gas.

120. For the next 3 mi (4.8 km), the highway winds along the southern shoulder of Sheep Mountain. Roadcuts are alternately in till, in gravel, or in sandstone of the Matanuska Formation. Fossil mollusks and some leaves can be found locally in exposures of sandstone.

116. To the left is a good view of the northern Chugach Mountains and the divide separating the Matanuska Valley drainage basin from the Copper River drainage basin. Glacial ice probably moved westward from the Copper River basin to the Matanuska Valley during Wisconsinan time, but during the later part of Wisconsinan time, the pass probably was free of ice and was the site of outwash streams emanating from glaciers in the Copper River basin.

115. For the next 3 mi (4.8 km), the Glenn Highway crosses large alluvial fans along the southern side of Sheep Mountain. The rusty color of the gravel apparently is caused by oxidation of iron by sulfuric-acid water. The high sulfate content in the water comes from deposits of gypsum in hydrothermally altered rocks of the Talkeetna Formation, which is Early Jurassic in age. In some mountain gullies, talus and alluvial deposits of Pleistocene age are cemented into conglomerate by iron oxides. During Pleistocene time, Sheep Mountain probably was completely covered by glacier ice from sources in the Chugach Mountains; erratic boulders from that source are found at elevations as high as 6,240 ft (1,900 m).

112. For the next 2 mi (3.2 km) on the right, the angular accumulations of rock in talus cones and in small, inactive landslides are derived from the Talkeetna Formation, which consists chiefly of volcanic rocks altered to greenstone.

110. Jackass Canyon, a sharp curve with roadcuts in coarse alluvial-fan gravel overlying shale of the Matanuska Formation, and for the next 0.5 mi (0.8 km), the road crosses a small alluvial fan.

109.5. The highway route for the next 3.5 mi (5.6 km) (fig. 99) continues between the southern foot of Sheep Mountain and the Matanuska River.

109.1. To the right is a major roadcut in the toe of an inactive rock glacier that consists of boulders of the Talkeetna Formation in a matrix of silty material.

108.8. To the right in the roadcut, a radiometric date for organic material collected at the contact between outwash and the overlying talus indicates that the outwash deposit is older than $3,620 \pm 250$ yr B.P. (W-573) and that the talus accumulated during the last 3,620 yr. The highway is passing through a marginal glacial spillway.

108. Begin steep descent into the canyon of Caribou Creek, past many roadcuts in ice-contact and deltaic sand and gravel and talus from the slopes of Sheep Mountain.

107.1. Caribou Creek rises in the high part of the southeastern Talkeetna Mountains and, during the retreat of the glaciers in late Wisconsinan time, was temporarily blocked by the Matanuska Glacier, which formed a moraine at an elevation of 2,500 ft (758 m) about 1 mi (1.6 km) upstream from the bridge. The creek was diverted west through the valleys of Dan and Pinochle Creeks north of the highway and formed the spectacular glacial spillway occupied by Pinochle Creek between Miles 98 and 97. After crossing the bridge, the Glenn Highway ascends a steep slope cut into the Talkeetna Formation.

106.1. To the right are ice-contact sand and gravel. These deposits and others at similar elevations across the valley of Caribou Creek are associated with an advance position of Matanuska Glacier sometime prior to 4,000 yr B.P.

105.9. To the south is Lion Head (fig. 99), a steep, glacier-scoured hill of felsic, porphyritic intrusive rock of Tertiary age. The south face overlooking Matanuska Glacier is nearly vertical and rises 1,400 ft (424 m) above the Matanuska River, which is tightly confined between the glacier and Lion Head at this point.

Selected References

- Andreason, G., Grantz, A., Zietz, I., and Barnes, D., 1964, Geologic interpretation of magnetic and gravity data in the Copper River basin, Alaska: U.S. Geological Survey Professional Paper 316-H, p. 135-153.
- Capps, S.R., 1940, Geology of the Alaska Railroad region: U.S. Geological Survey Bulletin 907, 201 p.
- Connor, C.L., 1982, Pollen evidence for a mid-Wisconsin interstadial event in south-central Alaskan glaciolacustrine sediments [abs.]: Program and abstracts, American Quaternary Association Biennial Conference, 7th, Seattle, University of Washington, June 1982, p. 84.
- Eckhart, Richard, 1951, Gypsiferous deposits on Sheep Mountain, Alaska: U.S. Geological Survey Bulletin 989-C, p. 39-61.
- Ferrians, O.J., Jr., 1963a, Till-like glaciolacustrine deposits in the Copper River basin, Alaska [abs.]: Geological Society of America Special Paper 73, p. 151.



Figure 99. Oblique aerial photograph on the Glenn Highway west from Mile 109.5 to 105 showing the Matanuska River flowing west past the mouth of Caribou Creek to Lion Head, beyond which it flows along the terminus of the Matanuska Glacier. Lion Head, the prominent knob near the glacier (middle left), is felsic rock of Tertiary age. Photograph by R.D. Reger, May 21, 1982.

- Ferrians, O.J., Jr., 1963b, Glaciolacustrine diamicton deposits in the Copper River basin, Alaska, in Short papers in geology and hydrology 1963: U.S. Geological Survey Professional Paper 475-C, p. C121-C125.
- _____, 1966, Effects of the earthquake of March 27, 1964, in the Copper River basin area, Alaska: U.S. Geological Survey Professional Paper 543-E, 28 p.
- _____, 1971, Effects of the earthquake of March 27, 1964, in the Copper River basin area, Alaska [abs.], in The great Alaska earthquake of 1964 (geology): National Academy of Science Publication 1601, p. 282-283.
- _____, 1971, Preliminary engineering geologic maps of the proposed trans-Alaska pipeline route, Gulkana Quadrangle: U.S. Geological Survey Open-file Report 71-102, scale 1:125,000, 1 sheet.
- Ferrians, O.J., Jr., Kachadoorian, Reuben, and Greene, G.W., 1969, Permafrost and related engineering problems in Alaska: U.S. Geological Survey Professional Paper 678, 37 p.
- Ferrians, O.J., Jr., and Nichols, D.R., 1965, Copper River basin, in Pêwè, T.L., Ferrians, O.J., Jr., Nichols, D.R., and Karlstrom, T.N.V., Guidebook for field conference F, central and south-central Alaska, International Association for Quaternary Research, 7th Congress, Fairbanks, 1965: Lincoln, Nebraska Academy of Science, p. 93-114 (reprinted 1977, College, Alaska Division of Geological and Geophysical Surveys).
- Ferrians, O.J., Jr., Nichols, D.R., and Schmoll, H.R., 1958, Pleistocene volcanic mudflow in the Copper River basin, Alaska [abs.]: Geological Society of America Bulletin, v. 69, no. 12, pt. 2, p. 1563.
- Ferrians, O.J., Jr., and Schmoll, H.R., 1957, Extensive proglacial lake of Wisconsin age in the Copper River basin, Alaska [abs.]: Geological Society of America Bulletin, v. 68, no. 12, pt. 2, p. 1726.
- Grantz, Arthur, 1953, Preliminary report on the geology of the Nelchina area, Alaska: U.S. Geological Survey Open-file Report 53-79, 2 p.
- _____, 1961a, Geologic map and cross sections of the Anchorage (D-2) Quadrangle and northeasternmost part of the Anchorage (D-3) Quadrangle, Alaska: U.S. Geological Survey Miscellaneous Geologic Investigations Map I-342, scale 1:48,000, 1 sheet.
- _____, 1961b, Geologic map of the north two-thirds of Anchorage (D-1) Quadrangle, Alaska: U.S. Geological Survey Miscellaneous Geologic Investigations Map I-343, scale 1:48,000, 1 sheet.
- _____, 1964, Stratigraphic reconnaissance of the Matanuska Formation in the Matanuska Valley, Alaska: U.S. Geological Survey Bulletin 1181-I, 33 p.
- Grantz, Arthur, and Jones, D.L., 1960, Stratigraphy and age of the Matanuska Formation, south-central Alaska, in Short papers to the geologic sciences 1960: U.S. Geological Survey Professional Paper 400-B, p. B347-B350.
- Grantz, Arthur, White, D.C., Whitehead, H.C., and Tagg, A.R., 1962, Saline springs, Copper River Lowland, Alaska: American Association of Petroleum Geologists Bulletin, v. 46, no. 11, p. 1890-2002.
- Greene, G.W., Lachenbruch, A.H., and Brewer, M.C., 1960, Some thermal effects of a roadway on permafrost, in Short papers in the geologic sciences 1960: U.S. Geological Survey Professional Paper 400-B, p. B141-B144.
- Hamilton, T.D., and Thorson, R.M., 1983, The Cordilleran ice sheet in Alaska, in Porter, S.C., ed., Late Quaternary of the United States: Minneapolis, University of Minnesota Press [in press].
- Mendenhall, W.C., 1905, Geology of the central Copper River region, Alaska: U.S. Geological Survey Professional Paper 41, 133 p.

- Nichols, D.R., 1956, Permafrost and ground-water conditions in the Glennallen area, Alaska: U.S. Geological Survey Open-file Report 56-91, 18 p.
- _____, 1960, Slump structures in Pleistocene lake sediments, Copper River basin, Alaska, *in* Short papers in the geologic sciences 1960: U.S. Geological Survey Professional Paper 400-B, p. B353-B354.
- _____, 1961, Analyses of gas and water from two mineral springs in the Copper River basin, Alaska, *in* Short papers in the geologic and hydrologic sciences 1961: U.S. Geological Survey Professional Paper 424-D, p. D191-D194.
- _____, 1965, Glacial history of the Copper River basin [abs.]: International Association for Quaternary Research Congress, 7th, Boulder, 1965, Abstract volume, p. 360.
- _____, 1966, Permafrost in the Recent Epoch, *in* International Conference on Permafrost, Lafayette, Ind., 1963, Proceedings: National Academy of Sciences, National Research Council Publication 1287, p. 172-175.
- Nichols, D.R., and Watson, J.R., Jr., 1955, Preliminary report on engineering-permafrost studies in the Glennallen area, Alaska [abs.]: Geological Society of America Bulletin, v. 66, no. 12, pt. 2, p. 1706.
- Nichols, D.R., and Yehle, L.A., 1961a, Highway construction and maintenance problems in permafrost regions: Annual Symposium on Geology as Applied to Highway Engineering, 12th, Knoxville, 1961, Proceedings: University of Tennessee Engineering Experiment Station Bulletin 24, p. 19-29.
- _____, 1961b, Mud volcanoes in the Copper River basin, Alaska, *in* Raasch, G.D., ed., Geology of the Arctic: Toronto, University of Toronto Press, v. 2, p. 1063-1087.
- _____, 1969, Engineering geologic map of the southeastern Copper River basin, Alaska: U.S. Geological Survey Miscellaneous Geologic Investigations Map I-524, scale 1:125,000, 1 sheet.
- Olson, E.A., and Broecker, W.S., 1959, Lamont natural radiocarbon measurements V: American Journal of Science, v. 257, no. 1, p. 1-28.
- Péwé, T.L., 1975, Quaternary geology of Alaska: U.S. Geological Survey Professional Paper 835, 145 p.
- Rubin, Meyer, and Alexander, Corrinne, 1960, U.S. Geological Survey radiocarbon dates V: American Journal of Science Radiocarbon Supplement, v. 2, p. 129-185.
- Schmoll, H.R., 1961, Orientation of phenoclasts in laminated glaciolacustrine deposits, Copper River basin, Alaska, *in* Short papers in the geologic and hydrologic sciences 1961: U.S. Geological Survey Professional Paper 424-C, p. C192-C195.
- Thorson, R.M., Dixon, E.J., Jr., Smith, G.S., and Batten, A.R., 1981, Interstadial proboscidean from south-central Alaska: Implications for biogeography, geology, and archaeology: Quaternary Research, v. 16, no. 3, p. 404-417.
- Vogel, J.C., and Waterbolk, H.T., 1972, Groningen radiocarbon dates X: Radiocarbon, v. 14, no. 1, p. 6-110.
- Williams, J.R., 1970, Ground water in the permafrost regions of Alaska: U.S. Geological Survey Professional Paper 696, 83 p.
- Williams, J.R., and Johnson, K.M., 1980, Map and description of late Tertiary and Quaternary deposits, Valdez Quadrangle, Alaska: U.S. Geological Survey Open-file Report 80-892C, scale 1:250,000, 2 sheets.

OVERVIEW OF
THE MATANUSKA GLACIERBy
Daniel E. Lawson¹⁹

STOP 33. MATANUSKA GLACIER.

The Matanuska Glacier is one of the largest valley glaciers in south-central Alaska (fig. 100). It flows generally north about 28 mi (45 km) from the ice fields of the central Chugach Mountains and drains approximately 250 mi² (647 km²) of the highest part of the range. Relief in the accumulation area is about 5,000 ft (1,500 m) and includes Mt. Marcus Baker at 13,370 ft (4,011 m).

The glacier is composed of several ice streams, with the two major tributaries joining about 22 mi (35 km) upstream from the present terminus (fig. 101). The width of the glacier increases from 1.5 mi (2.2 km) at this ice-stream confluence to about 2 mi (3 km) where it leaves the Chugach Mountains and enters the Matanuska Valley to spread laterally and develop a more lobate shape that averages about 3 mi (5 km) in width. The thickness of the ice is unknown; a 1,000-ft (300 m) thickness was calculated for the glacier near the firn line by assuming a basal shear stress of 1 bar and determining an average slope for the ice surface.

Near the terminus margin, downwasting and apparent stagnation of parts of the glacier have resulted in a coalesced cover of supraglacial debris over about two-thirds of the lobe (fig. 100). A portion of the northernmost stagnant ice is covered by a forest; some of the stagnant ice is actively degrading to form a 'glacial' karst topography. Only along the western margin is the ice surface generally free of debris. The ice stream that terminates there appears to be more active than the remainder of the glacier, as noted by Mendenhall in 1898. The glacier surface near the terminus margin is heavily crevassed as the result of lateral ice spread and flow over a ridge and a depression in the glacier bed. The clean, white to blue ice provides the focal point for the beautiful view of the glacier from the Glenn Highway.

Flow rates measured by surveying stakes set in the ice surface about 6 mi (10 km) upglacier from the terminus in June 1980 and 1981 ranged from 1.8 to 2.1 ft (0.55 to 0.64 m) per day. In the terminal lobe [within 1 mi (0.6 km) of the ice margin] rates are generally slower and more variable. Rates in the summer of 1979 were 1 to 1.2 ft (0.3 to 0.36 m) per day, and in the summers of 1980 and 1981, they averaged 0.7 ft (0.21 m) per day. During February 1980, marginal flow rates decreased to 0.25 ft (0.08 m) per day.

Although the position of the glacier margin has remained reasonably stable during the last 400 yr (Williams and Ferrans, 1961), the glacier has been characterized by thinning and by locally confined, possibly oscillating advances and retreats of at least several hundred yards. This marginal motion has developed an ice-cored area 330 to 1,650 ft (100 to 500 m) wide that

¹⁹U.S. Army Cold Regions Research and Engineering Laboratory; Box 282; Hanover, New Hampshire 03755.



Figure 100. Oblique aerial photograph (to the east) of the terminus of the Matanuska Glacier (1964). The Glenn Highway follows the left border of photograph.

parallels the lobe margin (fig. 102). Parts of this area are underlain by 100 ft (30 m) or more of basal ice interbedded with overridden sediments.

Observations and photographs by local residents and visiting scientists indicate advances of the western margin in 1966-1970, possibly in 1955-1957, and in the mid-1940s. The most recent advance began in late summer 1978 in the central part of the western ice stream. Movement totalled about 155 ft (50 m) by June 1980. Later the zone of movement spread from the center toward the outer margins of the ice stream. The outermost ice did not show a significant marginal advance until 1981. This style of movement suggests that only the western ice stream of the glacier is advancing, while adjacent ice moves at a slower rate and retards motion of the advancing ice stream.

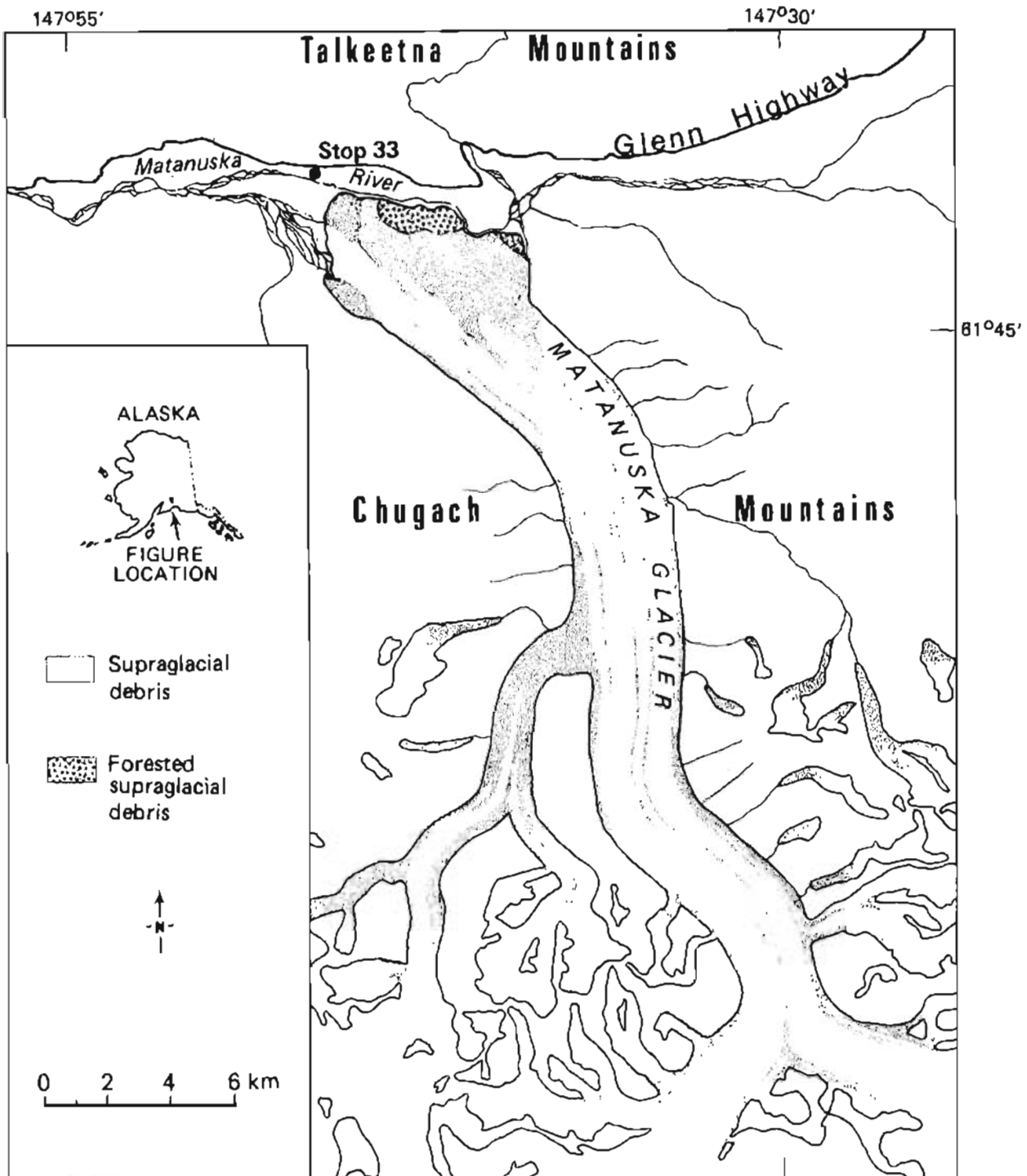


Figure 101. Map of the Matanuska Glacier and vicinity.

The advancing ice margin is characterized by a steep-walled face that in some places has exceeded 65 ft (20 m) in height. Ice movement up and over sediments and stagnant ice along this margin caused extensive oversteepening and calving. Sediments along the margin were either shoved ahead into ridges paralleling the ice front or were overridden and sometimes deformed.

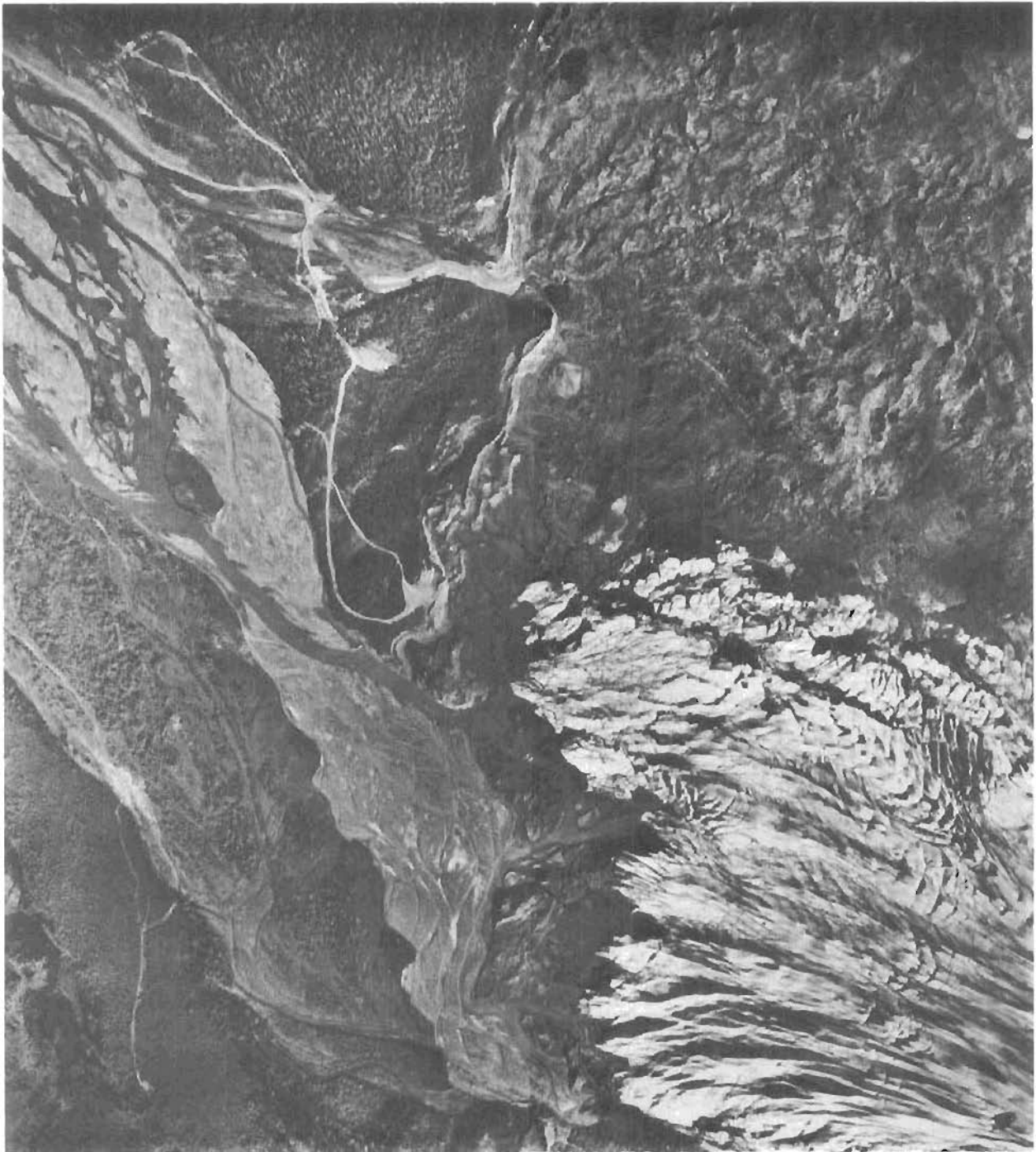


Figure 102. Vertical aerial photograph of part of the western terminus of the Matanuska Glacier. A zone of ice-cored marginal sediments parallels the active ice margin. The excursion onto the glacier departs from the parking lot at the end of the gravel road near the center of the photograph. North is at the top of the photograph.

Sediments are distributed unevenly within the glacier, with debris concentrated mainly in a thin basal zone that varies spatially in thickness from about 10 to 80 ft (3 to 25 m). Within this basal ice, two additional layers

or facies are distinguished by the distribution and content of debris. In the lowest stratified facies, debris is concentrated in thin, discontinuous and irregular strata that are separated by relatively clean, clear ice. Individual strata may contain up to 90 percent sediment (10 percent ice), although the zone as a whole contains an average 25 percent debris by volume. In the upper facies [10.7 to 26 ft (0.2 to 8 m thick)], debris is dispersed in a uniformly random pattern and only composes about 4 percent of the facies by volume. The overlying englacial-zone ice, excluding the randomly scattered debris bands within it, contains a negligible 0.002 percent debris by volume.

Analyses of the properties of the debris and ice indicate that, excluding the supraglacial debris derived from erosion of valley walls and nunataks, most debris appears to be subglacially derived. Sediment in the stratified facies is entrained during freeze-on of ice that apparently originates from ground water composed of both meltwater and meteoric water at and beneath the glacier sole. The dispersed facies, however, is composed of ice formed by recrystallization of snow in the glacier's accumulation area---ice that has undergone further recrystallization and deformation as it moved over a stationary bed probably composed of bedrock. Particulate matter was abraded or plucked from the bed during regelation or by some similar, highly localized mechanism.

Debris transported on top of or within the glacier is deposited along the margin or beneath the glacier by a variety of processes. The primary processes that directly release and deposit the glacial debris include subsurface and subglacial melting due to either temperature and pressure effects during regelation or to temperature effects alone, and ablation of ice exposed along the margin. Secondary or re-sedimentation processes are generally more important and rework, transport, and redeposit sediment that has already been released from the glacier by primary processes. Re-sedimentation processes, which can operate subaerially, englacially, or subglacially, include: a) sediment flow (the downslope transport of sediment-water mixtures under the force of gravity), b) slumping, c) spalling (the outward failure and collapse of sediments on sloping and differentially melting glacier ice), d) meltwater sheet and rill flow, e) gravitational settling in air or water, and f) fluvial and lacustrine processes.

The distinction between these groups of processes provides a meaningful system for separating material deposited by the Matanuska Glacier into two general groups. The resulting genetic classification distinguishes glacial deposits with primary sedimentological properties from glacial deposits with properties derived from secondary transport or deposition. Till is restricted by definition to material deposited directly from glacier ice by a primary process. This definition results in classifying some glacial diamictons as nontills, most notably sediment-flow deposits. The origin of sediments deposited by the Matanuska Glacier can be determined by detailed sedimentological analyses of characteristics that include grain-size distribution, pebble fabric, sedimentary structures, bedforms, contact features, and deposit geometry and dimensions.

The spatial distribution of depositional processes (and hence of deposits in the terminus environment) reflects variability in sediment and meltwater availability, local and regional slope and elevation, location of the active ice margin, and extent and thickness of sediments covering stagnant or inactive glacial ice (figs. 103 and 104). The general interrelationship of pro-

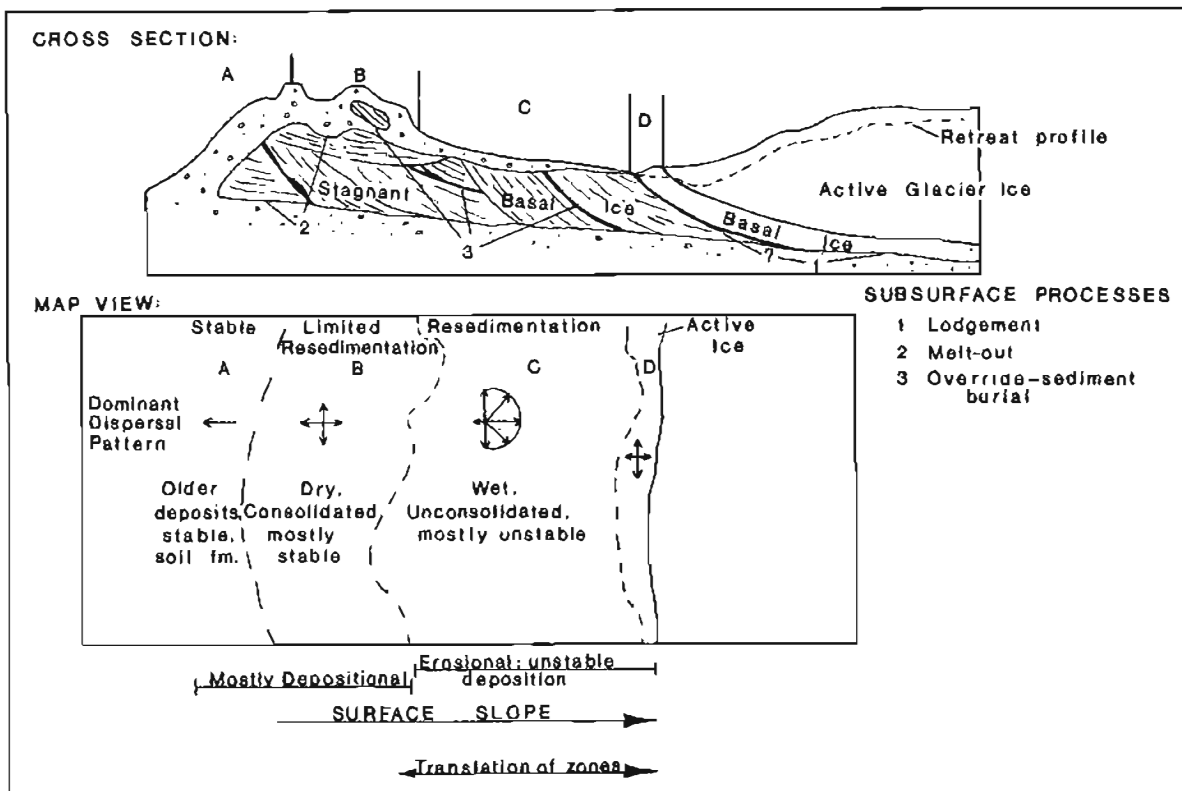


Figure 103. Spatial distribution of depositional processes in relation to the ice-margin position and topographic slope, where the ice-cored moraine slopes toward the active ice (from Lawson, 1977, fig. 72).

cesses develops a composite stratigraphic sequence defined in terms of three facies associations: a) an upper, subaerial resedimented facies association, b) a middle till facies association, and c) a lower, subglacial resedimented facies association. Within these associations, the deposits produced by the individual primary or secondary processes often do not show a repetitive sequence. In general, ice-marginal sequences that develop adjacent to the glacier are more complex than the idealized composite sequence because of repeated periods of erosion and deposition by secondary processes and vertical repetition of the upper two facies associations caused by glacial advances that override older deposits.

Selected References

- Lawson, D.E., 1977, Sedimentation in the terminus region of the Matanuska Glacier, Alaska: Urbana, University of Illinois, Ph.D. thesis, 294 p.
- _____, 1979a, A comparison of the pebble orientations in ice and deposits of the Matanuska Glacier, Alaska: *Journal of Geology*, v. 87, p. 629-645.
- _____, 1979b, A sedimentological analysis of the western terminus region of the Matanuska Glacier, Alaska: U.S. Army Cold Regions Research and Engineering Laboratory Report 79-9, 122 p.
- _____, 1979c, Characteristics and origins of the debris and ice, Matanuska Glacier, Alaska: *Journal of Glaciology*, v. 23, p. 437-438.

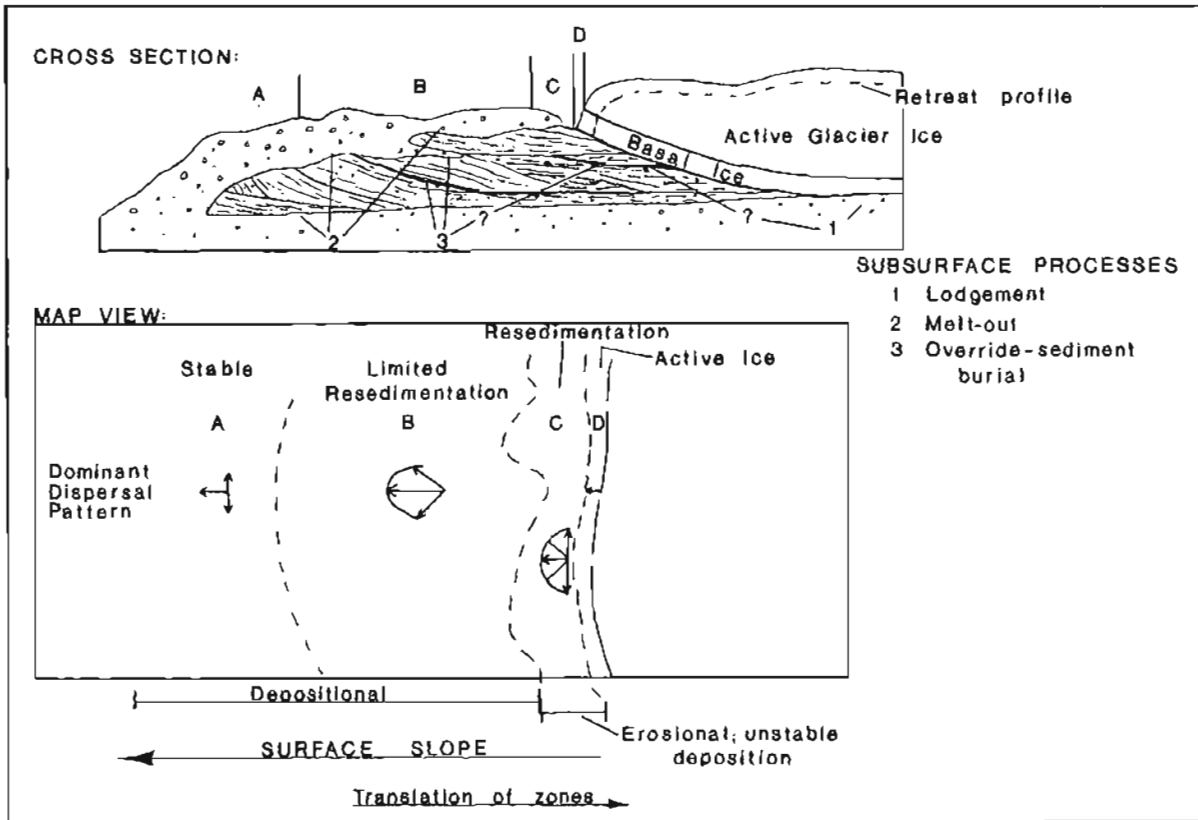


Figure 104. Spatial distribution of depositional processes in relation to the ice-margin position and topographic slope, where the ice-cored moraine slopes away from the active ice (from Lawson, 1977, fig. 73).

Lawson, D.E., 1981a, Distinguishing characteristics of diamictons formed at the margin of the Matanuska Glacier, Alaska: Symposium on Processes of Glacier Erosion and Sedimentation, Geilo, Norway, August 1980, Proceedings, *Annals of Glaciology*, v. 2, p. 78-84.

_____, 1981b, Sedimentological characteristics and the classification of depositional processes and deposits in the glacial environment: U.S. Army Cold Regions Research and Engineering Laboratory Report 81-27, 16 p.

Lawson, D.E., and Kulla, J., 1978, An oxygen isotope investigation of the origin of the basal ice of the Matanuska Glacier, Alaska: *Journal of Geology*, v. 86, no. 6, p. 673-685.

Mendenhall, W.C., 1900, A reconnaissance from Resurrection Bay to the Tanana River, Alaska, in 1898: U.S. Geological Survey 20th Annual Report, pt. 7, p. 265-340.

Williams, J.R., and Ferrians, O.J., Jr., 1961, Late Wisconsin and Recent history of the Matanuska Glacier, Alaska: *Arctic*, v. 14, no. 2, p. 82-90.

UPPER COOK INLET REGION AND THE MATANUSKA VALLEY

Richard D. Reger²⁰ By
and Randall G. Updike²¹

INTRODUCTION

Physiography and Geology

Upper Cook Inlet region

The upper Cook Inlet region encompasses Cook Inlet in the vicinity of Anchorage and includes Knik Arm, Turnagain Arm, and the southern Susitna lowland. The area occupies a large structural trough that extends from the Gulf of Alaska northward between the rugged, intensely glaciated Alaska Range, Kenai-Chugach Mountains, and Talkeetna Mountains (fig. 105). Most of the lowland is below 500 ft (152 m) elevation, although isolated uplands such as Mt. Susitna reach 4,396 ft (1,332 m). Local relief generally ranges from 50 to 250 ft (15 to 76 m). Towering peaks of the nearby Alaska Range, Talkeetna Mountains, Chugach Mountains, and Kenai Mountains are 6,000 to 12,000 ft (1,818 to 3,636 m) high.

Crystalline igneous and metamorphic rocks, primarily of Mesozoic age, form a basement complex exposed at and around Mt. Susitna and as roches moutonnées near mountain fronts. Overlying these rocks are weakly consolidated, petroleum- and coal-bearing, clastic sedimentary rocks of Tertiary age that are exposed in marginal uplands and are as thick as 13,000 ft (3,939 m) in the deeper parts of the structural trough. The surface of the upper Cook Inlet lowland is mantled by late Quaternary deposits that comprise extensive moraines and other ice-contact complexes, alluvium of associated proglacial fluvial systems, and extensive plains underlain by glaciomarine deposits. The total thickness of Quaternary deposits varies from less than 1 ft (0.3 m) on marginal highlands and lower mountain slopes to more than 4,250 ft (1,288 m) south of the Castle Mountain fault along the lower Susitna River.

Several large, silt-laden, braided streams, like the Susitna River, flow into upper Cook Inlet from glaciers in the mountains. Hundreds of small, irregular lakes occupy kettles in moraines and ice-stagnation complexes. Extensive swamps occupy plains underlain by impervious glaciomarine and glaciolacustrine deposits.

Most of the upper Cook Inlet region has no permafrost. However, in especially favorable situations in lowland fens (like beneath black-spruce 'islands'), where surface insulation is high and incident solar radiation is low, isolated pods of ice-rich permafrost are as thick as 30 ft (9 m) and range in area up to 500 to 600 ft² (46.5 to 55.7 m²).

Matanuska Valley

The Matanuska Valley is one of two long extensions of the Cook Inlet-

²⁰DGGS; 794 University Avenue, Suite 200; Fairbanks, Alaska 99709-3645.

²¹U.S. Geological Survey, Mail Stop 905; 507 National Center, Reston, Virginia 22092.



Figure 105. Major physiographic subdivisions of south-central Alaska relative to the field-trip route (modified from Wahrhaftig, 1965, pl. 1).

Susitna Lowland into bordering mountainous highlands (fig. 105). It extends east from west of the agriculturally important Palmer area about 80 mi (128 km) to the southwestern corner of the Copper River basin and generally ranges in width from 2 to 5 mi (3.2 to 8.1 km). Since prehistoric time, this narrow corridor has served as a major trading route between upper Cook Inlet and the Copper River basin. The valley floor slopes west from about 2,000 ft (606 m) elevation to about 200 ft (61 m) elevation. Differential glacial erosion has carved the main valley floor into a series of subparallel, discontinuous bedrock ridges that stand 500 to 1,000 ft (152 to 303 m) high and trend downvalley. Narrow bedrock troughs and basins between these ridges are occupied by small, deep, clear lakes, ponds, or peat-filled fens. In the western half of the Matanuska Valley, these bedrock ridges and troughs are obscured by kame-esker complexes and outwash-terrace deposits. Ice-sculpted bedrock walls are steep and rise several thousand feet above the valley floor. Evidence of intense glaciation is obvious in tributary valleys headed by rugged cirques that are still occupied by small glaciers and active rock glaciers in the highlands enclosing the Matanuska Valley.

Bedrock structure is complex in this narrow belt of intensely faulted Jurassic sedimentary and volcanic rocks, Cretaceous marine rocks, and Tertiary continental sedimentary rocks. Major structural discontinuities marking the boundaries between the Matanuska Valley, the Talkeetna Mountains to the north, and the Chugach Mountains to the south are the Castle Mountain and Border Ranges faults, respectively. Eocene gabbro sills, dikes, and stocks intrude older sedimentary rocks and support high-standing, resistant ridges and hills. For many years, the Paleocene Chickaloon Formation provided south-central Alaska with good-quality bituminous coal for heating, lights, and transportation.

The Matanuska River and its tributaries drain the Matanuska Valley. This turbulent, silty river flows west from ice fields and snowfields high in the Chugach Mountains east of the Matanuska Glacier across braided flood plains and races through narrow, rock-walled canyons and gorges cut since the glacier that filled the Matanuska Valley receded about 10,000 yr B.P.

Most of the Matanuska Valley is permafrost free, except perhaps in particularly favorable peat-filled fens in the upper valley, where heat transfer into the peat during summer is less than heat flow out of the peat in winter. Perennially frozen ground is probably discontinuous in the Talkeetna Mountains and sporadic in the Chugach Mountains, where its presence is manifested by active rock glaciers. These permafrost-cored landforms are most prevalent in north-facing cirques and glaciated valleys sheltered from solar warmth.

Climate

The upper Cook Inlet-Matanuska Valley region has a climate that is transitional between the maritime climate of southern coastal Alaska and the more rigorous continental climate of the interior. Although regional variations are generally known for scattered, lowland stations along the coast and major rivers, these values are not representative of other lowland sites or of alpine locations. Alpine sites generally have cooler temperatures and higher precipitation values.

Mean annual temperature varies regionally from 30 to 36°F (-1 to 2.2°C); at Anchorage, where the long-term record is the most complete in the region, average annual temperature is 36°F (2.2°C). Average minimum winter temperatures generally range from 4 to 8°F (-15.6 to -13.3°C), although the coldest temperature measured at Anchorage is -38°F (-38.9°C). Throughout the region, average warmest summer temperatures range from 64 to 68°F (17.8 to 20°C); at Anchorage, the highest temperature measured is 86°F (30°C). Diurnal temperature variation ranges between 18 and 20°F (10 and 11°C). For the region, the thawing index²² varies from +2,800 to +3,000°F days, and the freezing index²³ varies from -2,500 to -3,000°F days.

Mean annual precipitation in the lowlands of the region generally ranges from 11 to 16 in. (27.9 to 40.6 cm). At Anchorage, mean annual precipitation is 14.5 in. (36.8 cm), the normal precipitation for the wettest months is 2.71 in. (6.9 cm), maximum annual precipitation is 18.9 in. (48 cm), and the mean annual snowfall is 59 in. (149.9 cm).

Most precipitation in south-central Alaska is from the north Pacific Ocean. Moisture-rich winter storms are spawned in the low-pressure center persisting in the Aleutian Islands and move northeast along the southern coast of Alaska, where they encounter the orographic barrier of the Kenai and Chugach Mountains. Very heavy snowfall occurs on the seaward flanks of these mountains as warm, moist air masses are forced up and over the mountain barrier. The loss of moisture on seaward flanks leaves north- and northeast-moving air masses relatively dry. This phenomenon and the blocking action of persistent, inland high-pressure centers cause winter precipitation values to rapidly decrease inland behind coastal mountains. Consequently, the altitude of the glacier equilibrium-line (ELA) increases from about 3,300 ft (1,000 m) on the ocean side of the Kenai and Chugach Mountains to about 4,950 ft (1,500 m) on the inland side of these mountains, and glaciers cover broad areas in the Kenai (1,638 mi² or 4,200 km²) and Chugach Mountains (6,800 mi² or 17,439 km²). Ice-flow rates, especially by tidewater glaciers, are high. In contrast, in the Talkeetna Mountains, which are situated leeward of the Chugach Mountains, ELA is about 5,940 ft (1,800 m), the area of glacier ice is only about 117 mi² (300 km²), and glaciers are much less active.

Crude estimates of modern snowline, based on approximate elevations of snowline in north-facing cirques on topographic maps, indicate that large topographic corridors, like the Cook Inlet-Susitna Lowland, are effective conduits for moving moisture-laden air masses to inland mountain highlands.

Wind velocity, direction, and duration are highly variable in the upper Cook Inlet-Matanuska Valley region, especially in hilly and mountainous terrain. Average wind velocity at Anchorage is about 5 mi per hr (8 km per hr). Prevailing winds blow from the northeast in winter, northwest in summer, and north in spring and fall. Infrequent wind damage, especially along mountain fronts and in mountain valleys, results from violent gusts that exceed 100 mi per hr (161 km per hr). In alpine areas, winter wind drifting of snow

²² Average number of degree-days above freezing, based on the Fahrenheit system.

²³ Average number of degree-days below freezing, based on the Fahrenheit system.

drastically alters snowfall patterns and promotes severe avalanche conditions.

Vegetation

Several distinctive forest types and plant associations are present in the upper Cook Inlet region as a result of the variable terrain, steep climatic gradients, complex fire history, and highly variable edaphic conditions.

The northernmost extension of the coastal spruce-hemlock forest densely covers lower, moderate to steep mountain slopes around Turnagain Arm. Closely growing Sitka spruce (Picea sitchensis) and western hemlock (Tsuga heterophylla) dominate the coastal forest, except along streams and on low terraces where tall black cottonwood (Populus trichocarpa) overtop these conifers. Because of high rainfall and humidity along the coast, mosses profusely cover the ground and lower limbs and trunks of trees. On moderately to well-drained sites elsewhere in the lowlands, the forests are closed and are composed of a mosaic of white spruce (Picea glauca), paper birch (Betula papyrifera humilis), Kenai birch (B. p. kenaica), aspen (Populus tremuloides), and balsam poplar (Populus balsamifera) in stands of different ages as a result of a complex fire history. Alders (Alnus spp.) and willows (Salix spp.) are dense along small stream courses, and large black-cottonwood groves are important on the flood plains and low terraces of large streams. Poorly drained lowland sites have treeless fens interspersed with an open forest dominated by black spruce (Picea mariana) and paper birch. These fens, many of which are quite wet, are especially prevalent in poorly drained areas on the sandy fan-delta plain east of the Susitna River (pl. 1). A wet tundra of sedges and grasses is widespread in coastal swamps bordering upper Cook Inlet.

Tree line ranges from about 1,700 ft (515 m) around Turnagain Arm up to about 2,800 ft (848 m) in the upper Matanuska Valley. Above tree line is a zone through 400 to 800 ft (121 to 242 m) of elevation in which mountain slopes and floors of alpine valleys are covered by dense to scattered alders with interspersed willow and resin birch (Betula glandulosa). Winter snow loads press the alders into growth positions subparallel to the sloping ground, which makes passage through them very difficult. Above the alder zone, beginning at about 2,500 to 3,200 ft (758 to 970 m) elevation, is the alpine shrub-herb tundra, an association of low-growing, wind-trimmed willow, birch, spruce, and juniper (Juniperus communis and J. horizontalis) shrubs interspersed with widespread mats of prostrate alpine plants and scattered cushion plants that grow in exposed situations among the rock rubble, patches of barren soil, and snow beds.

Soils

On most moderately to well-drained sites beneath the closed canopy of white spruce and paper birch in the upper Cook Inlet region, the dominant soils are podzols²⁴ that typically have moderately developed, gray-colored A2 horizons. These soils are formed by progressive leaching of soluble salts and organic matter from the parent material. An exception to this condition is in the lower Matanuska Valley, where the rate of modern loess accumulation

²⁴Spodosol soil order of the revised soil terminology, including Typic Cryorthods.

exceeds the rate of podzolization. In the Palmer area, for example, the Bodenburg series of soils, which is developed on well-drained, deep loess near the flood plains of the Knik and Matanuska Rivers, is classed as a regosol.²⁵ These soils have only incipient horizon differentiation, and there has been no translocation of clays. Profiles are typically mottled and streaked. Farther from modern sources of loess, where rates of silt accumulation are relatively low, soil profiles exhibit greater degrees of podzolization, that is, base saturation is lower, A horizons are better developed and more acidic, and carbon-nitrogen ratios are more variable.

Poorly drained sites typically have very acidic humic gleys and organic soils made up mainly of partially decomposed fragments of sedges, grasses, mosses, and shrubs with minor to moderate amounts of organic silt.²⁶

RÉSUMÉ OF QUATERNARY GEOLOGY

General Statement

The upper Cook Inlet-Matanuska Valley region was glaciated repeatedly in Quaternary time, and although the intensity of glaciation has considerably decreased since the last major ice expansion, the region is being glaciated today.

Early interpretations of the Quaternary history of the region by Karlstrom (1953; 1955; 1957; 1964; 1965), Miller and Dobrovolny (1959), Trainer (1960), and Trainer and Waller (1965) are based on: a) geomorphic evidence gathered from early aerial photography, maps, and field investigations; b) stratigraphic evidence gleaned from natural exposures in sea bluffs around Cook Inlet and in river bluffs or from artificial exposures available at the time; c) several radiometric dates for organic material collected from these sections; and d) subsurface data (well logs) from the Anchorage and Palmer areas. With the availability of better photography and maps, improved radiometric-dating methods, new stratigraphic sections, and literally hundreds of borehole logs (especially in the Anchorage area), these early chronologies were tested, and the following summary incorporates the resulting refinements and reinterpretations.

Late Pliocene-Early Pleistocene Glaciations and Interglaciations

Late Cenozoic events in the upper Cook Inlet-Matanuska Valley region prior to about 200,000 yr B.P. are only vaguely understood. Postglacial destruction of most initial evidence complicates the separation of the remains of old glaciations so that results of several ice advances tend to be attributed to a single event. Burial and erosion of deposits and ice-marginal features promote inaccurate estimates of ice limits, and major drainage changes (modified by later glaciation) cause confusion about directions of ice flow and locations of ancient source areas. Nonetheless, there is considerable evidence for late Pliocene-early Pleistocene glaciation.

²⁵Entisol soil order of the revised soil terminology, including Typic Cryorthents.

²⁶Histosol soil order of the revised soil terminology, including Sphagnic Borofibrists.

Mt. Susitna Glaciation

The earliest recognized glaciation (Mt. Susitna) was named by Karlstrom (1953) for the ice-rounded summit and upper slopes of Mt. Susitna, which are higher than the upper limit of the next younger (Caribou Hills) glaciation. The glaciated surface was cut across the quartz diorite bedrock and bears scattered erratics or small accumulations of graywacke-argillite, basalt, sandstone, quartzite, and greenstone erratics up to within 100 ft (30 m) of the 4,396-ft (1,332 m) crest of Mt. Susitna (pl. 1). No morainal form remains. Very old, ice-scoured surfaces thought to result from the Mt. Susitna Glaciation occur above 3,960 ft (1,200 m) elevation in the southwestern Talkeetna Mountains (pl. 1), near Chickaloon River, and above the level of the Caribou Hills Glaciation in the western Kenai Mountains. In the southwestern Talkeetna Mountains, granitic and ultrabasic erratics thought to be deposited during the Mt. Susitna Glaciation are only partially weathered, with surface pits as deep as 0.8 in. (2 cm); many ancient erratics that appear quite fresh were probably only recently exhumed by surface processes and exposed to weathering. The distribution of erratics and ice-modified surfaces indicates patterns of ice flow across modern stream divides during the Mt. Susitna Glaciation. Based on relative-age criteria, this glaciation has been correlated with the late Pliocene-early Pleistocene Browne Glaciation in the north-central Alaska Range and therefore is thought to be older than 2.7 million yr (Péwé, 1975, table 2).

Karlstrom (1964; 1965) postulated that during the Mt. Susitna Glaciation, extensive ice caps broken only by scattered nunataks were present in the Talkeetna, Chugach, and Kenai Mountains and in the Alaska Range. Ice drained through tributary valleys, like the Matanuska Valley, to coalesce in the lowlands and eventually fill the Cook Inlet-Susitna Lowland to present elevations of over 4,000 ft (1,212 m). Ice of this glaciation probably joined---through low passes and cols---ice sheets accumulating in the Copper River basin and in the Nushagak-Bristol Bay Lowland, and ice probably flowed south out of the Cook Inlet trough into the north Pacific Ocean to form an extensive ice shelf.

Mt. Susitna-Caribou Hills Interglaciation

Following the Mt. Susitna Glaciation, glaciers receded into their mountain source areas, and the results of the Mt. Susitna advance were modified by surface processes (Karlstrom, 1964). This interglaciation is not documented by stratigraphic evidence like buried soil profiles or forest beds, but its considerable length is indicated by the contrast in degree of preservation between landforms that evolved during the Mt. Susitna Glaciation and equivalent landforms that developed during the subsequent (Caribou Hills) glaciation. Only scattered erratics or accumulations of erratics remain of continuous sheets of Mt. Susitna drift. Ice-scoured bedrock surfaces of Mt. Susitna age are considerably modified by stream erosion and mass wasting so that topographic details like ice-marginal channels no longer exist.

Caribou Hills Glaciation

The Caribou Hills Glaciation was named by Karlstrom (1953) for considerably modified lateral moraines and associated drift blanketing the highest [2,850 ft (864 m)] surfaces of the Caribou Hills (fig. 105). In the type area, plunge pools and related stream channels carved by subglacial

streams in the weakly consolidated Tertiary bedrock are modified but preserved and document a former ice sheet that erratics of graywacke and granite prove was derived from the higher Kenai Mountains to the east. On the flanks of the Caribou Hills, well-preserved lateral moraines of the younger Eklutna Glaciation are plastered over drift of the Caribou Hills advance up to about 2,000 ft (606 m) elevation. Above this level, a series of ice-marginal stream channels, lateral moraines, and kame terraces record progressive thinning of glacial ice during the waning phase of the Caribou Hills Glaciation.

In the upper Cook Inlet region, ice-scoured benches and truncated spurs of Caribou Hills age occur below surfaces of Mt. Susitna age and above well-preserved features of the younger Eklutna Glaciation. These landforms are between 3,100 and 3,500 ft (939 and 1,061 m) elevation along the western front of the Chugach Mountains, between 2,700 and 3,200 ft (818 and 970 m) on the upper slopes of Mt. Susitna, and up to 3,750 ft (1,136 m) on the southwestern flank of the Talkeetna Mountains (pl. 1). Highly modified and dissected lateral moraines, with filled kettle depressions and rounded knobs, occur from 3,500 ft (1,061 m) to as high as 4,000 ft (1,212 m) on piedmont surfaces sloping west from the Kenai Mountains.

During the Caribou Hills Glaciation, ice accumulated in the highlands of south-central Alaska to form broad ice caps and advanced down major valleys to again cover the floor of the Cook Inlet-Susitna Lowland. Karlstrom (1964; 1965) postulated that the ice level reached altitudes of about 3,000 ft (909 m), but recent field work indicates that slopes that today are as high as 3,500 to 3,750 ft (1,061 to 1,136 m) in the upper Cook Inlet region were glaciated in Caribou Hills time. For at least the second time, ice from the Cook Inlet trough probably joined ice masses in the Copper River basin and the Nushagak-Bristol Bay Lowland. Morainal relations indicate that glacial ice from the coastal sides of the Aleutian and Alaska Ranges was more active than ice from the western Kenai Mountains and pushed much farther into the Cook Inlet lowland. Ice gradients sloped to low levels centered in the upper inlet area. Eventually, more vigorous ice accumulation in lower Cook Inlet apparently produced flow south into the north Pacific Ocean and formed another extensive ice shelf (Karlstrom, 1964).

Despite the better preservation of evidence for the Caribou Hills Glaciation compared to the older Mt. Susitna Glaciation, the age of neither event is firmly established. Geomorphic evidence for a considerable hiatus between the glaciations seems clear, but local rates of erosion are commonly very high in areas of moderate to high relief, and the possibility remains that moraines attributed to the Caribou Hills Glaciation were actually built during major stillstands or minor readvances in the waning phases of the Mt. Susitna Glaciation. Until stratigraphic evidence is found that demonstrates a significant interglaciation between the Mt. Susitna and Caribou Hills Glaciations, this problem will not be resolved.

Counts of surface boulders on moraines of the Caribou Hills Glaciation and three younger glaciations established ratios of granite erratics (resistant to frost splitting) to graywacke-argillite erratics (not resistant to frost splitting) (Karlstrom, 1964, p. 17-18). Karlstrom (1964) used these ratios as scales to roughly estimate that moraines of Caribou Hills age are 7.7 times older than the 20,000- to 25,000-yr-old moraines of the youngest (late Wisconsin) glaciation, or approximately 155,000 to 190,000 yr old (fig. 106). This rough estimate is based on the assumption that frost-

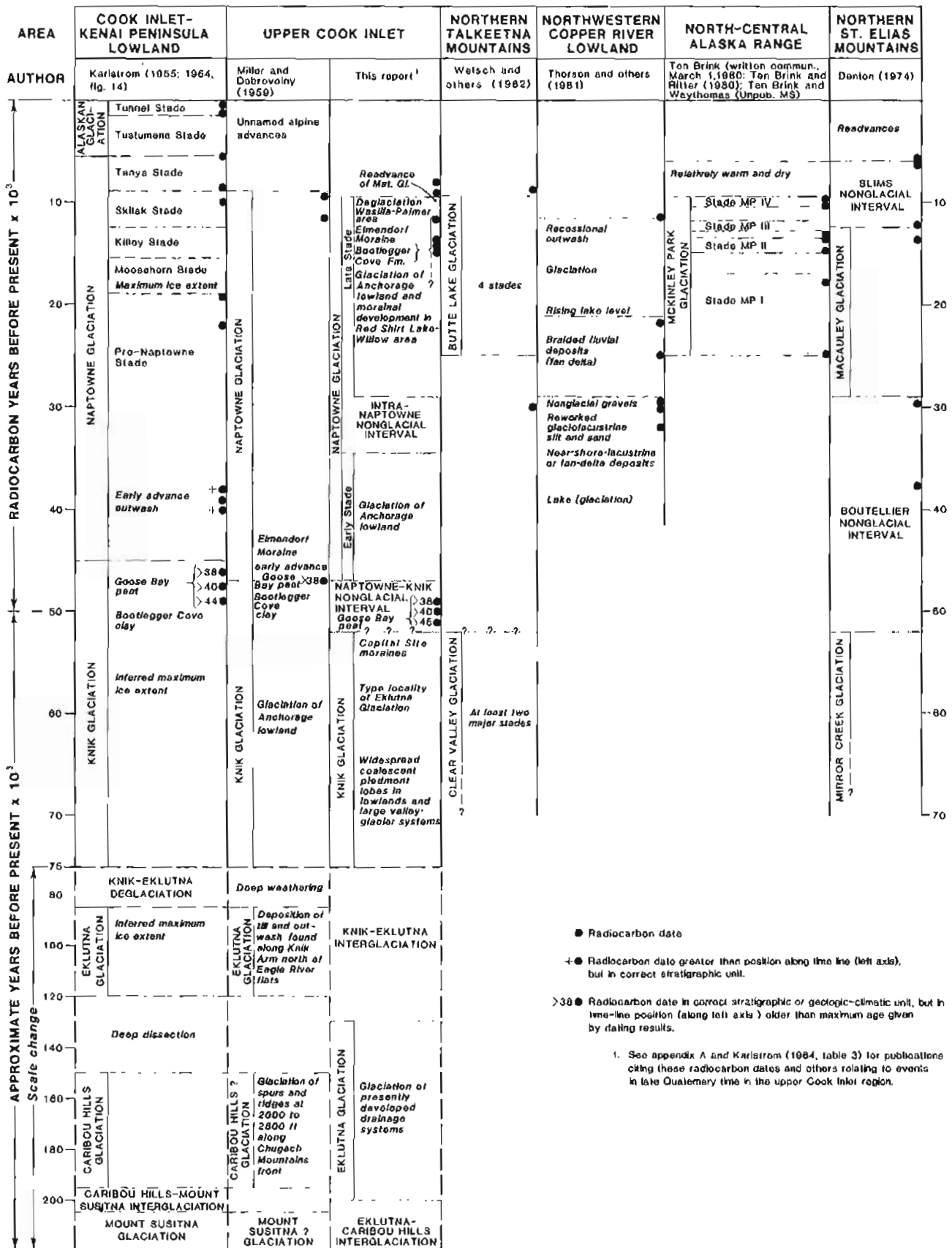


Figure 106. Tentative comparison of late Quaternary glacial chronologies in the upper Cook Inlet region with other areas in southern Alaska.

weathering rates were uniform during the past 150,000 to 190,000 yr, but evidence throughout Alaska clearly demonstrates that there has been considerable climatic variation during the past 150 to 200 millenia. Thus, frost-weathering, mass-wasting, and soil-forming processes have clearly functioned at varying intensities during this time, and the rate at which surface boulders have weathered has probably not been constant. Moraines of Caribou Hills age are probably much older than 150,000 to 190,000 yr.

Late Pleistocene Glaciations and Interglaciations

Based on evidence accumulated during the past decade, concepts of the timing and extent of late Pleistocene glacier expansions in the upper Cook Inlet-Matanuska Valley region have changed considerably (fig. 106). Pivotal to a reinterpretation of late Pleistocene events is a reassessment of the age and stratigraphy of the Bootlegger Cove Formation, previously called the Bootlegger Cove Clay. Marine mollusk shells from the upper third of the Bootlegger Cove Formation were initially dated by the uranium-ionium method at 33,000 to 48,000 yr (Sackett, 1958, in Karlstrom, 1964, p. 35). Later, Th²³⁰ dates for these shells yielded ages of 25,000 to 41,000 yr (Karlstrom, 1968). In 1972, Schmoll and others published four concordant radiocarbon dates between 13,690 ± 400 yr B.P. (W-2151) and 14,900 ± 350 yr B.P. (W-2369) for the shells. Their dates are generally accepted as valid and demonstrate that at least the upper part of the Bootlegger Cove Formation was deposited during a late phase of the Naptowne (late Wisconsin) Glaciation rather than during a late phase of the Knik (early Wisconsin) Glaciation, as previously concluded by Karlstrom (1964) and Miller and Dobrovolsky (1959) (fig. 106, cols. 1 and 2). Stratigraphic correlations in the Anchorage area and indirectly throughout the region are tied to this widespread, complex glaciomarine-estuarine unit. Thus, a significant change in the age of the Bootlegger Cove Formation in turn affected the ages of other units and disrupted the entire late Pleistocene regional chronology.

Caribou Hills-Eklutna Interglaciation

During the interglaciation between the Caribou Hills Glaciation and the subsequent Eklutna Glaciation, the entire Cook Inlet-Susitna Lowland was probably ice free. Evidence proposed for this nonglacial interval is the deep, broad canyons cut by stream erosion into surfaces mantled by drift of the Caribou Hills Glaciation on the western flank of the Kenai Mountains; these canyons were later partially filled by drift of the Eklutna advance (Karlstrom, 1964).

Eklutna Glaciation

Evidence for the Eklutna Glaciation is controversial for two main reasons. First, 40 to 60 ft (12 to 18 m) of weathered recessional outwash originally designated by Karlstrom (1964) as the type deposit for the Eklutna Glaciation in the canyon of Eklutna River has been reinterpreted as prograded fan-delta deposits laid down in an ice-marginal lake of late Knik (or possibly early Naptowne) age. Second, the uniform, deep (up to 175 ft or 53 m), buff-colored staining previously attributed to deep weathering in post-Eklutna time (Karlstrom, 1964; 1965) has been reinterpreted as staining by iron-bearing ground water percolating through the sediments after their deposition.

Nonetheless, a major glaciation clearly occurred between the Caribou Hills and Knik Glaciations in the upper Cook Inlet region, as indicated by obvious (but modified) moraines and distinctive, ice-scoured surfaces below the level of the Caribou Hills Glaciation and above and beyond the obvious limit of the Knik Glaciation. Glacial features of Eklutna age are generally related to present drainage systems. For example, notched bedrock ridges and distinctive lateral moraines of Eklutna age occur between 2,350 and 2,700 ft (712 and 818 m) elevation along the western flank of the Chugach Mountains between the Eklutna River valley and Turnagain Arm (pl. 1). Ice-marginal features indicate that during the Eklutna Glaciation, the Eklutna River, Eagle River, and Ship Creek valleys, and Turnagain Arm were major producers of ice flowing west into the lowland. In the southwestern Talkeetna Mountains, Eklutna-age moraines are plastered on ice-rounded surfaces blanketed by till of Caribou Hills age up to about 3,100 ft (939 m) elevation. On the flanks of Mt. Susitna, lateral moraines and ice-marginal features mapped as Eklutna in age form a gradient from nearly 2,900 ft (879 m) elevation on the north end of Mt. Susitna to about 2,700 ft (818 m) on the south end.

During the Eklutna Glaciation, ice spread from alpine ice caps for at least the third time to coalesce and completely cover the floor of the Cook Inlet-Susitna Lowland. Large trunk glaciers filled major tributary valleys, including the Matanuska Valley. Only scattered nunataks poked through the ice along the walls of upper valleys, but along ridges separating lower valleys, nunataks were larger than during earlier glaciations because ice levels were lower. In the Cook Inlet trough, Eklutna-age ice reached surfaces that today are 2,350 to 3,100 ft (712 to 939 m) in elevation.

A comparison of our partially dated, revised, late Quaternary chronology for the upper Cook Inlet region (fig. 106) with the oxygen-isotope stages of the world ocean-temperature sequence (Shackleton and Opdyke, 1973) indicates that the Eklutna Glaciation probably corresponds to oxygen-isotope stage 6 and is roughly Illinoian in age (130,000 to 200,000 yr old).

Eklutna-Knik Interglaciation

Evidence for the interglaciation between the Eklutna and Knik Glaciations is the distinct difference in preservation of subdued Eklutna moraines and more obvious Knik moraines. This geomorphic break is the most apparent in the entire morainal sequence; Karlstrom (1964) traced it around the margins of the Cook Inlet-Susitna Lowland and cited it as the limit of the Eklutna Glaciation. Karlstrom (1964) believed that the Eklutna-Knik Interglaciation persisted for about 10,000 yr and ended about 75,000 yr B.P. (fig. 106, col. 1). In our opinion, the distinctive geomorphic contrast between moraines we designate as Knik in age (pl. 1) (many previously mapped as Eklutna in age) and older moraines is good evidence that the interglaciation was longer than 10 millenia. A comparison with the oxygen-isotope chronology for world ocean temperatures (Shackleton and Opdyke, 1973) indicates that the Eklutna-Knik Interglaciation corresponds roughly with stage 5 of the sequence. Thus, it is probably generally equivalent to the Sangamon Interglaciation, which occurred from about 75,000 to 130,000 yr B.P. (fig. 106, col. 3).

Knik Glaciation

The type section of the Knik Glaciation is actually a composite assembled

by Karlstrom (1964), who correlated discontinuous exposures in the bluffs along the northwestern shore of Knik Arm. In his opinion, the type deposit for the Knik advance is the lower of two till sheets that are separated by outwash gravels, a thin glaciomarine diamicton, and two organic zones. Although we have not seen all units he described, we did measure the important bluff section along the northern shore of Goose Bay (pl. 1, loc. R). In that section, a highly compressed interglacial peat, the Goose Bay peat, lies below advance outwash and till of Naptowne age and above a recessional outwash that we consider late Knik in age. Farther up Knik Arm, a lower till is exposed; we consider it Knik in age and tentatively correlate it with the lowest till (designated as Eklutna in age by Miller and Dobrovolsky, 1959) exposed in the bluffs northeast of the mouth of Eagle River across Knik Arm. No type moraine of Knik age has been designated.

At Point Campbell and east of Point Woronzof south of Anchorage, an indurated, yellowish-tan to buff diamicton of Knik age that is documented in logs of deep boreholes crops out below ice-contact deposits and till of early Naptowne age. This unit varies from massive, pebbly sandy silt to finely laminated clayey silt and is interpreted as interbedded flowtill and fan-delta deposits that accumulated in a glaciomarine or glaciolacustrine environment. The deposit exhibits numerous deformational features, including folds with amplitudes up to 10 ft (3 m), low-angle intraformational faults, load-cast structures, and high-angle microfaults, which indicate a compressive stress environment under subaqueous, ice-marginal conditions where both low-angle slope failures and ice-shove processes were active. Subsurface stratigraphic relationships in this area support a Knik age for this diamicton, which is the oldest diamicton recognized in the subsurface in the Anchorage lowland and extends continuously beneath the city.

Knik moraines form at least three broad arcs extending from reentrants at 700 to 900 ft (212 to 273 m) elevation along the western front of the Kenai Mountains to Point Possession on the northern tip of the Kenai Peninsula (pl. 1). From the outer limits of these moraines, proglacial stream channels extend southwest through a complex of moraines and ice-contact deposits (of about the same age) that were derived from the western side of Cook Inlet. At Point Possession, cliff head sand dunes capping the sea bluff are underlain by 1 to 3 ft (0.3 to 0.9 m) of loess that in turn overlies Knik till. Tillstones are composed of lithologies from the Kenai Mountains and clastic coal fragments probably derived from subcrops of weakly consolidated Tertiary bedrock between Point Possession and the Kenai Mountain front. Granitic surface clasts have weathering pits up to 0.4 in. (1 cm) deep, and the till is weathered to depths of 5 to 7 ft (1.5 to 2.1 m).

Ice-stagnation deposits and associated moraines that we tentatively attribute to the Knik Glaciation occur on the western flank of the Talkeetna Mountains in the vicinity of Willow Creek up to an elevation of 2,400 ft (727 m) (pl. 1). Distinctive morainal arcs south of Willow Creek extend up to 1,550 ft (470 m) elevation; we have tentatively mapped these moraines as late Knik in age (pl. 1) because they exhibit well-developed podzol soils to depths of 4 ft (1.2 m), but we may revise this age assignment to late early Naptowne. These deposits were mapped as Eklutna in age by Karlstrom (1965).

On the western flank of the Chugach Mountains, slightly modified lateral moraines attributed to the Knik Glaciation form discrete bands above the

obvious level of the Naptowne Glaciation and below subdued moraines and side-glacial features probably formed during the Eklutna Glaciation. Older, higher Knik moraines form a gradient from 2,100 ft (636 m) elevation north of Eagle River to about 1,500 ft (455 m) along the mountain front at Turnagain Arm. Younger Knik moraines form broader ridges on the lower mountain slopes south-east of Anchorage to as low as 700 ft (212 m) elevation. These moraines were separated into Eklutna and Knik ages by Karlstrom (1965). Slightly modified, north-facing cirques in the western Chugach Mountains were cut during Knik time to levels as low as 3,200 to 3,500 ft (970 to 1,061 m).

A distinctive morainal limit surrounds Mt. Susitna and grades from about 1,800 ft (545 m) on the north end of the mountain to about 1,600 ft (485 m) on the south end. We tentatively date this morainal limit as Knik in age, but it could be early Naptowne. Moraines comprising the band are continuous with moraines from cirques of the same age cut into the eastern and western flanks of Mt. Susitna. Floors of these cirques range in elevation from 2,400 to 3,100 ft (727 to 939 m).

Most of the floor of the Susitna lowland is covered by drumlinized, silty ground moraine. These low, streamlined ridges that are oriented generally north-northwest (pl. 1) and ice-scoured, granitic bedrock ridges north of Mt. Susitna and west of the Susitna River are tentatively mapped as Knik features, but they probably are early Naptowne in age.

Stratigraphic and radiometric evidence indicates that the Knik Glaciation is early Wisconsinan in age. The Goose Bay peat, which overlies Knik recessional outwash, has been dated several times beyond the range of radiocarbon dating (app. A, loc. R). Peats thought to correlate with the Goose Bay peat because of similar stratigraphic position have been dated older than 38,000 to 45,000 yr (pl. 1 and app. A, locs. Q and T). An infinite date of greater than 44,000 yr B.P. was also obtained from an abraded log (probably reworked from Knik-age gravel) in the East Foreland area of the western Kenai Peninsula lowland (fig. 105 and app. A, L-117L). Minimum ages of 9,200 to 10,370 yr B.P. near Point Possession (pl. 1 and app. A, locs. D, F, and H) are not considered close limiting dates because the Knik till there was deeply weathered prior to deposition of the dated organic material. A published date of $11,930 \pm 250$ yr B.P. (W-360) for the basal organic silt overlying 'Knik'-age moraine south of Willow Creek is also probably not a close limiting age (pl. 1 and app. A, loc. L). We tentatively correlate this glaciation with ice advances that ended about 50,000 yr B.P. in the northern St. Elias Mountains (fig. 106, col. 7) and in the Brooks Range (Hamilton and others, 1980). Comparison with oxygen-isotope stages indicates the Knik Glaciation probably began about 75,000 yr B.P. (fig. 106, col. 3).

Moraines document at least one and perhaps two advances or stillstands of Knik age in the Chugach and Talkeetna Mountains. In the western Kenai Mountains and northern Kenai Peninsula lowland, there is evidence of at least three or more advances or stillstands during the Knik Glaciation. During Knik time, ice apparently covered the floor of the Cook Inlet-Susitna Lowland for the last time as broad lobes from tributary valleys coalesced. In the lowland, ice reached levels that today range from 700 to 2,400 ft (212 to 727 m) elevation. Local ice levels were controlled by nearness to source valley, slope of valley and lowland floor, elevation of source areas and productivity of sources. In general, ice gradients in the upper Cook Inlet

region sloped south to a central area where today Knik and Turnagain Arms split from upper Cook Inlet. Highland ice caps undoubtedly expanded during Knik time, but were probably smaller than earlier generations. Small cirque glaciers developed in extensive nunatak areas between major valley glaciers. Local moraine- and glacier-dammed lakes apparently formed on the floor of the Cook Inlet trough at least during the late stages of the glaciation.

Knik-Naptowne nonglacial interval

The Goose Bay peat is the type deposit for the nonglacial (interstadial?) episode between the Knik and Naptowne Glaciations. This peat crops out at several localities along the northwest shore of Knik Arm northeast of Goose Bay, but is best documented at the type locality at Goose Bay (pl. 1, loc. R). In the type section, the Goose Bay peat occurs beneath 13.2 to 26.4 ft (4 to 8 m) of advance outwash gravel that is overlain by 19.8 to 26.4 ft (6 to 8 m) of till, all of Naptowne age, and is underlain by over 10 ft (3 m) of recessional outwash gravel of late Knik age. The peat is discontinuous and up to 6.5 ft (2 m) thick. Most of the organic material is very dense, fibrous, woody sedge-moss peat, but the upper 12 to 14 in. (30.5 to 35.6 cm) and the basal 4 to 8 in. (10.2 to 20.3 cm) are organic silt. The high density of the peat is a result of glacier overpressures developed during the passage of Naptowne ice over the site. An unconformity of unknown, but probably short, duration occurs between the Goose Bay peat and the underlying recessional outwash gravel.

Study of pollen grains in the Goose Bay peat indicates that they comprise an assemblage similar to the modern spruce-birch forests in the area (T.A. Ager, personal commun., February 16, 1983). Palynological studies of a similar and possibly correlative peat exposed in the bluff along lower Eagle River (pl. 1, loc. Q) document an interstadial flora typical of modern muskegs in the area (Miller and Dobrovolsky, 1959, p. 19). Abundant spruce pollen and grains of poplar, sedge, and club moss were identified in that peat.

Several samples of Goose Bay peat and its possible equivalents on the southeast side of Knik Arm were dated greater than the detection limit of the radiocarbon method (older than 38,000 to 45,000 yr) (pl. 1 and app. A, locs. P, Q, R, and T). A radiocarbon-enrichment date on the Goose Bay peat is pending. We tentatively propose that the nonglacial (interstadial?) interval between the Knik and Naptowne Glaciations began about 52,000 yr B.P. and ended about 47,000 yr B.P. (fig. 106, col. 3).

Naptowne Glaciation

Most of the floor of the Matanuska Valley and the lowlands of the upper Cook Inlet region is covered by a complex of deposits laid down during the last major ice expansion. Most river and sea bluffs expose sediments of this age. The stratigraphy is incredibly complex in this region, where very active glaciers, many fronting in lakes or estuarine-marine water bodies, dynamically shifted their termini in response to various stimuli until about 10,000 to 11,000 yr B.P., when ice stagnation and deglaciation occurred.

The type area for the Naptowne Glaciation is a series of conspicuous, nested, spatulate end moraines that is crossed by the Sterling Highway just east of the small settlement of Sterling (formerly called Naptowne) in the

east-central Kenai Peninsula lowland. In the type area, moraines record four substadial positions, each successively less extensive than the previous. Correlations of these substadial moraines from one part of the region to another, without suitable stratigraphic verification or control, have been inaccurate (Karlstrom, 1964; 1965). No type section has been designated for the Naptowne Glaciation.

Moraines of Naptowne age are the most conspicuous, most continuous, and best preserved of the entire Pleistocene series. They are typically very fresh in appearance; knob-and-kettle topography is essentially unchanged since the moraines were built, and the frequency of kettle lakes is typically high. Ice-stagnation features such as kames, eskers, and crevasse-fill-ridge complexes have steep sides and unmodified summits or ridge crests. Drumlins appear remarkably fresh and ice-marginal features are sharp and well preserved. Proglacial and ice-marginal drainage systems are clearly related to specific moraines and many are graded to high-level shorelines or deltas built into local lakes or larger bodies of fresh, brackish, or marine waters. In lowland areas, stream systems are poorly integrated. The cover of postglacial loess is generally about 1 ft (0.3 m) thick, although close to flood-plain sources of windblown silt, maximum thickness of loess approaches 12 ft (3.6 m). Soil profiles vary in depth from 1 to 3 ft (0.3 to 0.9 m), and generally average about 1.5 ft (0.5 m).

We have not satisfactorily identified moraines of early Naptowne age in the upper Cook Inlet region. As previously indicated, we suspect that drumlinized ground moraine west of the Susitna River and north of Mt. Susitna and sandy ice-contact deposits in the vicinity of Willow Creek (pl. 1) are of early Naptowne age, but for now we tentatively assign them to the Knik Glaciation. Also, we suspect that the nested moraines south of Willow Creek in the area of the proposed new capital site (pl. 1) are late early Naptowne in age. No terminal moraine of early Naptowne age has been identified in south Anchorage, which suggests that glaciers of this age terminated in deep water; however, a series of drumlins aligned in at least four northeast-trending arcs in east and southeast Anchorage (pl. 1) could be remnants of early Naptowne end moraines that were overridden and molded into drumlins in late Naptowne time. Moraines of early Naptowne age have not been identified just south of Turnagain Arm on the Kenai Peninsula. We suspect that ice flowing south through the Anchorage lowland in early Naptowne time at least contacted and perhaps joined ice flowing west out of Turnagain Arm.

The most complete and conspicuous suite of late Naptowne ice-contact and related glaciofluvial landforms in the upper Cook Inlet region is exhibited in the bilobate complex at the mouth of the Matanuska Valley (pl. 1). Pitted outwash and nested end moraines record ice limits during most of the late phase of the complicated Naptowne Glaciation (from close to 10,000 to perhaps 29,000 yr B.P.). Glacier-flow indicators (drumlins and Rogen moraines) document the resurgence of the Knik lobe to build the Elmendorf Moraine while the Matanuska lobe was relatively weakly active. Abundant kame-esker complexes, esker-ridge systems, a crevasse-fill-ridge complex, and pitted-outwash trains and terraces are ample evidence that ice stagnation with considerable melt-water activity and downcutting by streams occurred in both lobes following the abrupt readvance of the Knik lobe to the Elmendorf Moraine.

Moraines and outwash older than the marine invasion during which the

Bootlegger Cove Formation was deposited are notched by wave-cut scarps as far north as the mouth of Willow Creek. Sand of fan deltas graded to the level of that marine transgression is exposed in roadcuts for several miles north of there.

Floors of the lowest, well-preserved, empty, north-facing cirques of Naptowne age occur at 3,600 to 4,000 ft (1,091 to 1,212 m) elevation in the precipitation shadow of the northwestern Chugach Mountains and at 3,500 to 3,850 ft (1,061 to 1,167 m) elevation in the moister southwestern Talkeetna Mountains.

Stratigraphic studies in the Anchorage area provide considerable insight about late Wisconsinan events in the upper Cook Inlet region. Interpretation of sea-bluff exposures and logs of over 950 boreholes in southwest Anchorage indicate the presence of early and late Naptowne deposits. At Point Campbell, the older (Knik-age), indurated diamicton previously described is overlain by a two-fold early Naptowne unit that consists of firmly indurated ice-stagnation material in a lower zone and till in an upper zone. This early Naptowne unit is most readily recognized in the Point Campbell area and includes a thin sand layer and 6 in. (15 cm) of discontinuous peat at the top. Directly overlying the early Naptowne unit (or the Knik-age diamicton, depending on location) is a complex late Naptowne unit composed of the Bootlegger Cove Formation in the east and, in the west, a thick succession of fan-delta silt, sand, and gravel derived from the north-northwest; the latter deposits exhibit conspicuous surface pitting indicative of the presence of considerable stagnant ice during their formation. The two late Naptowne units interfinger.

Seven facies recently identified in the Bootlegger Cove Formation developed in response to subtle changes in the glaciomarine depositional environment (Updike, 1982; Updike and others, 1982). Facies V contains numerous, scattered dropstones, some as large as 14 ft (4.2 m), that probably document the proximity of a calving glacier early in the development of the formation. Limited studies of microfossils, especially foraminifera and ostracada, in the Bootlegger Cove Formation indicate that the lower part was deposited in marine conditions of near-normal salinity and the upper part was deposited in a fan-delta environment with relatively low salinity. Sea-bluff exposures and logs of boreholes in the Anchorage area document the Bootlegger Cove Formation as high as a present elevation of 119 ft (36 m). On the west side of Fire Island, this formation crops out as high as 101 ft (30.6 m) elevation. It is also exposed in high bluffs along the Yentna River north of Mt. Susitna for 27 mi (43 km) upstream from its confluence with the Susitna River (pl. 1).

In addition to the thin and discontinuous peat overlying the twofold early Naptowne unit in the subsurface beneath southwest Anchorage, a middle Naptowne nonglacial interval is indicated in southeast Anchorage by a thin organic zone exposed in a large cut for the Alaska Railroad at Potter Hill (pl. 1, loc. 0). This organic horizon is overlain by silt, gravel, sand, and till left by the last (late Naptowne) advance of ice beyond the mountain front in Turnagain Arm.

The latest Naptowne event in the Anchorage area is best documented north of the city, where conspicuous outwash fans and terraces grade up to the

Elmendorf Moraine. These deposits overlie the Bootlegger Cove Formation.

The timing of the early Naptowne stade is tenuously established because most of the stade predates the limit of radiocarbon detection. A date of $39,000 \pm 2,000$ yr B.P. (app. A, L-163A) for deposits just predating the initial pulse of advance outwash into the western Kenai Peninsula lowland closely limits the first major intrusion of Naptowne ice from the southern Alaska Range east into the Cook Inlet trough. This is the oldest finite date for a Naptowne event in the Cook Inlet region, but the high standard deviation makes it suspect. This date and a limiting date in excess of 45,000 yr B.P. for a possible equivalent of the Goose Bay peat underlying Naptowne gravel near Chugiak (pl. 1 and app. A, loc. T) form the basis for our tentative estimate that the maximum age of the early Naptowne stade is about 47,000 yr (fig. 106, col. 3). A similar date of greater than 38,000 yr B.P. was obtained for wood fragments beneath Naptowne outwash in the Eagle River area (pl. 1 and app. A, loc. P). A pending radiocarbon-enrichment date for Goose Bay peat at the type locality should more closely date the beginning of the early Naptowne stade in the Anchorage area.

The $34,000 \pm 2,000$ yr B.P. date for wood from the Potter Hill cut (app. A, loc. O) provides a minimum date for the early Naptowne stade in the Anchorage area and defines the intra-Naptowne nonglacial interval there. However, a high counting error makes this date questionable.²⁷ A correlative(?) nonglacial interval in the northwestern Copper River basin is documented by fluvial gravel and reworked glaciolacustrine silt and sand that have been dated between $29,450 \pm 610$ yr B.P. (DIC-1819) and $32,000 \pm 2,735$ yr B.P. (BETA-1820) (fig. 106, col. 5). In addition, the intra-Naptowne nonglacial interval probably correlates with the last stage of the Boutellier nonglacial interval, which is well documented in the St. Elias Mountains and is dated as young as $29,000 \pm 460$ yr B.P. (GSC-769) (fig. 106, col. 7).

Events in late Naptowne time are firmly established by a succession of 11 radiocarbon dates and by correlation with other areas in southern Alaska, where numerous radiocarbon dates have been obtained (fig. 106). Many published radiocarbon dates for the upper Cook Inlet region relate to the duration of the Bootlegger Cove Formation. A date of greater than 40,000 yr B.P. provides a maximum age for this formation in the Point MacKenzie area (pl. 1 and app. A, loc. 5). A range of 13,690 to 14,900 yr B.P. for the upper third of the Bootlegger Cove Formation is indicated by four radiocarbon dates on marine mollusk shells (pl. 1 and app. A, locs. K, M, and N). Because the fossiliferous zones are high in the section, we estimate that the base of the Bootlegger Cove Formation is at least 18,000 yr old (fig. 106); it could be much older. Minimum ages for retreat of marine waters in which the Bootlegger

²⁷ Subsequent to completion of plate 1 and appendix A, another radiocarbon date (I-12,029) for the wood from the Potter Hill cut provided an infinite date (greater than 40,000 yr B.P.) (Schmoll and Yehle, 1983, p. 3). This reassessment and the local geomorphology suggest that the dated horizon probably predates rather than postdates the early Naptowne ice advance from Turnagain Arm. Thus, the organic layer is probably another equivalent of the Goose Bay peat. Regardless, subsurface stratigraphy in southwest Anchorage supports the concept of early and late stades during the Naptowne Glaciation.

marine waters in which the Bootlegger Cove Formation was deposited were determined by dating basal freshwater peat overlying the Bootlegger Cove Formation; these dates range from 8,290 to 9,300 yr B.P. on Fire Island²⁸ (pl. 1 and app. A, locs. B and E), from 11,600 to 11,690 yr B.P. in the Anchorage area²⁹ (pl. 1 and app. A, locs. J and K), and include 10,720 yr B.P. along the base of the scarp cut during the late Naptowne marine transgression about 10 mi (16 km) south of the confluence of Willow Creek and the Susitna River (pl. 1 and app. A, loc. I).

Other dates establish minimum ages for glacial advances and recessions. The age of the Elmendorf Moraine is closely bracketed between 11,690 and 13,690 yr B.P. (pl. 1 and app. A, locs. K and M). The Wasilla area about 12 mi (19.3 km) west of Palmer was deglaciated by 9,155 yr B.P., according to a basal-peat date in an ice-marginal stream channel at the mouth of the canyon of the upper Little Susitna River (pl. 1 and app. A, loc. C). An extensive Naptowne advance in the valley of Willow Creek prior to 9,870 yr B.P. (pl. 1 and app. A, loc. G) was probably late Naptowne in age. A minimum age of 7,890 yr B.P. for the recession of late Naptowne ice draining Turnagain Arm was obtained for peat in sand overlying till in the Potter Hill cut (pl. 1 and app. A, loc. A). However, this date is only a distant limit for the recession, as demonstrated by 12,000-yr-old till overlying Bootlegger Cove Formation in sea bluffs along the southern shore of Turnagain Arm as far west as a point about 10.7 mi (17.1 km) southeast of the Potter Hill cut (pl. 1). Farther south, late Naptowne ice of the Trading Bay lobe from the southern Alaska Range invaded the Boulder Point-East Foreland area of the western Kenai Peninsula lowland after 12,900 yr B.P. (app. A, W-416) and before 8,650 yr B.P. (app. A, L-163B). A readvance of Matanuska Glacier prior to 8,000 yr B.P. (app. A, W-431) probably documents the final pulse of the late Naptowne stade.

Perhaps 47,000 yr B.P., in response to general climatic deterioration, glaciers in the Kenai, Chugach, and Talkeetna Mountains and in the Alaska Range thickened and spread through preexisting valley networks into the upper Cook Inlet-Susitna Lowland. Early Naptowne ice from the Matanuska Valley and Knik River valley joined near Palmer. Ice flowing south from the upper Susitna lowland probably coalesced with the Matanuska-Knik Glaciers system and with ice from other west-trending valleys along the fronts of the Talkeetna and Chugach Mountains. The resulting trunk glacier probably flowed south through Anchorage to near Turnagain Arm. The lack of an obvious terminal moraine of early Naptowne age in that area indicates that the terminal zone of this trunk glacier may have floated in moderately deep lacustrine or marine water. Subsurface stratigraphy indicates that early Naptowne ice initially stagnated in both Anchorage and then readvanced slightly before retreating to the north. Proglacial streams deposited coarse-grained fan-delta complexes during ice recession perhaps about 34,000 yr B.P. (fig. 106, col. 3).

²⁸ Subsequent to completion of plate 1, we obtained a date of 11,450 ± 150 yr B.P. (BETA-5581) for basal peat overlying the Bootlegger Cove Formation on the west side of Fire Island.

²⁹ Subsequent to completion of plate 1, we obtained a date of 12,250 ± 140 yr B.P. (BETA-5580) for basal peat deposited on 8 to 12 ft (2.4 to 3.6 m) of fan-delta sand overlying the Bootlegger Cove Formation 0.6 mi (1 km) west-northwest of locality S, (Point MacKenzie).

The magnitude of glacier recession after the early Naptowne stade is unknown, but the presence of early Naptowne fluvial deposits and organic material in southeast Anchorage demonstrates that at least some of the lowland was ice free and stood above lake or marine waters. The lack of an obvious break in the Naptowne section above the Goose Bay peat at Goose Bay may indicate that ice persisted west and north of Anchorage during the intra-Naptowne nonglacial interval.

Approximately 29,000 yr B.P., the second major phase of the Naptowne Glaciation began with another influx of glacier ice that eventually reached deep marine waters in upper Cook Inlet. During late Naptowne time, this marine invasion flooded the Anchorage lowland, probably in response to interaction between a slight worldwide eustatic rise in sea level and isostatic depression of the floor of the Cook Inlet trough due to ice loading. Marine waters inundated the southern Susitna lowland at least 42 mi (68 km) inland from the present north shore of Cook Inlet. A calving ice front, probably positioned just north of south Anchorage, produced numerous icebergs that dumped stones and blocks to form dropstone-rich facies V of the Bootlegger Cove Formation. As late as 14,000 to 15,000 yr B.P., shallow marine waters with normal salinity still inundated at least part of the lowland in the Anchorage area, and active ice persisted in south Anchorage. Slightly before about 12,000 yr B.P., when the resurgence of the Knik lobe built the Elmendorf Moraine, fan-deltas had prograded from an ice mass in the southern Susitna lowland south and southeast into south Anchorage and buried stagnant glacier ice. The location of this ice mass is indicated by pitted outwash fronting the Elmendorf Moraine northwest of Anchorage (pl. 1). Relative-age relationships between wave-cut scarps, radiocarbon-dated basal peat, and the pitted gravel outwash fan previously mentioned indicate that marine-estuarine waters of the transgression occupied low areas west of the terminal-moraine complex west of Knik Arm until just before 12,000 yr B.P.

Not long after the culmination of the late Naptowne resurgence to the Elmendorf Moraine, the expanded Matanuska-Knik Glaciers system developed a dominantly negative budget. The final phase of the Naptowne Glaciation is characterized by ice stagnation, widespread subglacial meltwater activity, and rapid stream incision. Perhaps 10,000 yr B.P., the Matanuska Glacier began a sustained retreat of about 35 mi (56 km), which ended with a significant glacier readvance to a position 2.5 to 5 mi (4 to 8 km) beyond the modern terminus before 8,000 yr B.P.

Miller and Dobrovolsky (1959) place the end of the Naptowne Glaciation in the upper Cook Inlet-Matanuska Valley region at about 9,000 yr B.P. (fig. 106, col. 2). We place the end of the Naptowne Glaciation at about 9,500 yr B.P. (fig. 106, col. 3) and correlate this event with the end of the Butte Lake and McKinley Park Glaciations in the northern Talkeetna and north-central Alaska Range, respectively (fig. 106, cols. 4 and 6).

Four major problems related to the Naptowne Glaciation in the upper Cook Inlet-Matanuska Valley region remain to be resolved. First, the type locality of the Naptowne Glaciation represents only part of the late stade. In the type area, no type section has been identified and there are no radiometric dates to support correlations with other areas. A more complete record is preserved in the Anchorage-Palmer-Wasilla area; perhaps this glaciation should be renamed and a more appropriate type locality should be designated. Second,

there is considerable disagreement about 'Glacial Lake Cook,' which, according to Karlstrom (1964; 1965), had an important effect on the late Quaternary history of the Cook Inlet trough. He correlated shorelines of this former ice-dammed lake throughout the Cook Inlet trough at several elevations: a) about 750 ft (230 m), b) 500 to 600 ft (150 to 180 m), c) about 250 to 300 ft (75 to 90 m), d) about 110 to 150 ft (30 to 45 m), and e) about 50 ft (15 m). Although wave-cut scarps and lacustrine (marine?) deposits exist locally, for example on the Kenai Peninsula lowland, our observations and the work of others (Scott, 1982) do not support Karlstrom's correlations of these shorelines throughout this region of active tectonism, eustatic changes in sea level, proven marine transgression, and isostatic subsidence and rebound. Third, analyses of the timing and magnitude of isostatic land-level changes in the Cook Inlet trough are not complete. A comparison of the highest level of the Bootlegger Cove Formation in the Anchorage area (+119 ft or +38 m) with a conservative estimate of -132 ft (-40 m) for worldwide sea level about 14,000 yr B.P. (Dan Mann, personal commun., March 18, 1983) demonstrates at least 251 ft (76 m) of isostatic depression in the Anchorage lowland during the late stage of the Naptowne Glaciation. Fourth, many questions remain about moraines and ice-stagnation deposits that are now mapped as Knik in age, but that are suspected to be early Naptowne in age, and more diagnostic relative-age criteria must be developed for differentiating the ages of landforms that are related to various glaciations.

Early Holocene Glaciation

Karlstrom (1964) included in the last (Tanya) stage of his Naptowne Glaciation the interval from about 9,000 to 5,500 yr B.P., a time that is considered early Holocene by most workers (for example, Hopkins, 1975; Pêwé, 1975)(fig. 106, col. 1). However, Karlstrom's dating of this event is tenuous; of 10 radiocarbon dates he related to the Tanya stade, only two (both minimum ages) are tied to glacial deposits (Karlstrom, 1964, table 3). The basal peat overlying pond silt on the innermost end moraine of the series built 2.5 to 5 mi (4 to 8 km) downvalley from the Matanuska Glacier was dated at $8,000 \pm 300$ yr B.P. (app. A, W-431). These moraines could be either late Wisconsinan (pre-10,000 yr B.P.) or very early Holocene (post-10,000 yr B.P.) in age. A wood sample from a 5-ft-deep (1.5 m) roadcut section through postglacial peat and organic silt overlying glacial lake silts in the Kenai Mountains dated $6,800 \pm 550$ yr B.P. (L-137E in Karlstrom, 1964, table 3). All other dates for the Tanya stade are for basal wood, peat, or organic silt in fen sections unrelated to contemporary glacial deposits (Karlstrom, 1964, table 3). Therefore, their correlation with glacial events during this time is questionable. Work in the Chugach and Talkeetna Mountains indicates the probable presence of early Holocene glacial and periglacial features, but additional dates are necessary to establish a chronology.

Middle to Late Holocene Events

Alaskan Glaciation

As defined by Karlstrom (1964), the Alaskan Glaciation includes minor perturbations of existing glaciers or the development and decay of small alpine ice masses during the past 5,500 yr (fig. 106, col. 1). He grouped these ice expansions into two ages, Tustumena advances of middle Holocene age and Tunnel advances of late Holocene age. Fresh-looking moraines that docu-

ment these minor fluctuations occur in mountainous areas between ice fronts and late Naptowne moraines (pl. 1).

Tustumena advances

The type locality for middle Holocene advances is at the east end of Tustumena Lake along the central western flank of the Kenai Mountains (fig. 105), where remnants of small moraines of three advances occur within 1 mi (1.6 km) of and downvalley from moraines of Tunnel-age advances close to the present terminus of Tustumena Glacier. Vegetation is more continuous, mature, and variable on moraines of Tustumena advances than on younger moraines. In many valleys, moraines of Tustumena age are partially or completely buried by outwash, talus, or alluvial-colluvial fans and cones or have been partially eroded. Soil profiles typically are 4 to 12 in. (10.2 to 30.5 cm) deep and loess cover varies in thickness up to a maximum of 2 ft (0.6 m). Many valleys contain three moraines of Tustumena age. Till of the Tustumena III moraine of Bartlett Glacier is exposed in a railroad cut near Tunnel Section House in the north-central Kenai Mountains (fig. 105), where it buries ice-abraded and ice-transported wood. A radiocarbon age of $2,370 \pm 200$ yr B.P. (W-78 in Karlstrom, 1964, table 3) for this wood dates the ice advance, the youngest of the Tustumena series.

Tunnel advances

Within 0.5 to 1 mi (0.8 to 1.6 km) of Bartlett Glacier near the Tunnel Section House along the Alaska Railroad (fig. 105), two small moraines between the Tustumena III moraine just discussed and the modern ice terminus are the type examples of the Tunnel advances. This series of frontal fluctuations typically consists of two major and several minor advances. Moraines of this age are commonly not dissected and bear only incipient soils. Ice cores remain in many of the larger and younger moraines at higher elevations. A forest overridden by the Tunnel I advance of Bartlett Glacier was dated at $1,385 \pm 200$ yr B.P. (W-318 in Karlstrom, 1964, table 3). Wood buried by the Tunnel II moraine at nearby Spencer Glacier is younger than 400 yr B.P. (L-163G in Karlstrom, 1964, table 3). A date for wood buried by the Tunnel II advance of Tustumena Glacier is 400 ± 150 yr B.P. (L-117K in Karlstrom, 1964, table 3).

Historical records and botanical dating demonstrate that during the middle to late 1800s many glaciers in the Kenai and Chugach Mountains stood at their maximum extent for the preceding several centuries. Exceptions among ice streams that drain into Prince William Sound are Meeres, Harvard, and Harriman Glaciers, which were advancing into old forest in 1957. Columbia Glacier is the only tidewater glacier in North America that did not rapidly retreat by calving during Holocene time; it still maintains a tenuous, quasi-stable, extended position.

Other events

Middle to late Holocene nonglacial events include development of at least two, and perhaps three, generations of rock glaciers. These ice-cored and ice-cemented features occur between 3,700 and 4,200 ft (1,121 and 1,273 m) in the southern Talkeetna Mountains and between 3,500 and 5,000 ft (1,061 and 1,515 m) in the western Chugach Mountains. Protalus ramparts of middle to

late Holocene age were built around the lower margins of perennial snow beds along the bases of fresh cirque walls. Numerous large rock slides occurred in mountainous areas during or after deglaciation; lowland landslides were triggered during strong earthquakes by failure of dynamically unstable sediments (pl. 1). Talus cones and aprons and alluvial fans developed on lower valley walls and a series of cut-and-fill terraces in mountain valleys record changes in base level that are attributed mainly to short-duration ice advances, but they are also probably partially due to tectonism. The prominent Castle Mountain fault offsets late Naptowne deposits and modern stream alluvium west of Palmer (pl. 1). Ring counts of undisturbed trees that straddle the fault and radiocarbon dating of soil displaced by the fault indicate that movement occurred as recently as 225 to $1,860 \pm 250$ yr B.P. (W-2930 in Detterman and others, 1974).

Road Log and Locality Descriptions

102.1.³⁰ Turn off to Glacier View Resort.

101.9. STOP 34. OVERLOOK OF MATANUSKA GLACIER. Panorama to the south of Matanuska Glacier terminal area and maturely glaciated terrain of the northern Chugach Mountains. A large rock glacier is visible southwest of Matanuska Glacier at an elevation of 4,000 ft (1,212 m).

The late Wisconsin and Holocene history of Matanuska Glacier has been studied during the past 25 yr or more and is now fairly well understood for the lower (western) and upper (eastern) parts of the Matanuska Valley, although some uncertainties remain. Detailed mapping of surficial deposits must be completed before detailed interpretations are possible for the middle part of the valley, but some general observations and conclusions are possible.

About 29,000 yr B.P., a compound glacier formed by ice from the Matanuska Valley and Knik River valley spread as an extensive bulb beyond the mouth of the Matanuska Valley to a maximum position south of Anchorage and as far west as the Susitna River in the Willow Creek area (pl. 1). Ice apparently remained in a fairly extended state until about 10,000 yr B.P., when the Matanuska-Knik Glaciers system stagnated and the western half of the Matanuska Valley was filled with dead ice. During this stagnation phase, meltwater activity deposited discontinuous accumulations of ice-contact sand and gravel from the vicinity of Chickaloon west to near Wasilla, a distance of about 38 mi (61.2 km). Ice retreat in the upper Matanuska Valley left no prominent end moraines and was apparently complicated by the very irregular ice-scoured bedrock floor and by the nonsynchronous activities of several tributary valley glaciers. Complex high-level spillways and terraces cut in valley fill demonstrate progressive ice thinning and complex drainage changes. Many meltwater features are graded close to but above the present flood plain of the Matanuska River. The magnitude of the ice retreat is not known, but Matanuska Glacier probably receded upvalley at least to its present terminus.

During late Wisconsinan or early Holocene time, Matanuska Glacier re-advanced, as did several other glaciers in southern Alaska. The expanded Matanuska Glacier reached a maximum position 2.5 to 5 mi (4 to 8 km) beyond

³⁰Miles from Anchorage on the Glenn Highway as of 1982.

the modern glacier and resulted in blockages of both the upper Matanuska River and Caribou Creek on the north side of Matanuska Glacier and of Glacier Creek on the southwest side (fig. 107). Major spillways, termed the Pinochle Creek spillway and the Lake Creek spillway, formed north and west of Matanuska Glacier, respectively, when ponded meltwaters overflowed low divides and established new, temporary courses downvalley. A glacial-ice dam temporarily blocked Caribou Creek and formed a lake that flooded the Dan Creek drainage before draining west into upper Pinochle Creek (fig. 107). Rapid erosion by a suddenly larger Pinochle Creek cut a 400-ft-deep (121 m) canyon in soft shale of the Matanuska Formation. Later, ice thinning and recession allowed Caribou Creek to resume its former course and left the underfit course of Pinochle Creek that exists today (fig. 108). A large landslide subsequently blocked the former spillway between Dan and Pinochle Creeks.

An outer series of low moraines was deposited during glacier recession following formation of the terminal moraine 2.5 to 5 mi (4 to 8 km) downvalley from Matanuska Glacier. A basal peat date of $8,000 \pm 300$ yr B.P. (fig. 107; app. A, W-431) in an abandoned and dammed stream channel that formed beside the innermost moraine of the outer series provides a minimum age for this latest Wisconsinan or very early Holocene readvance.

After 8,000 yr B.P., Matanuska Glacier retreated upvalley an unknown dis-

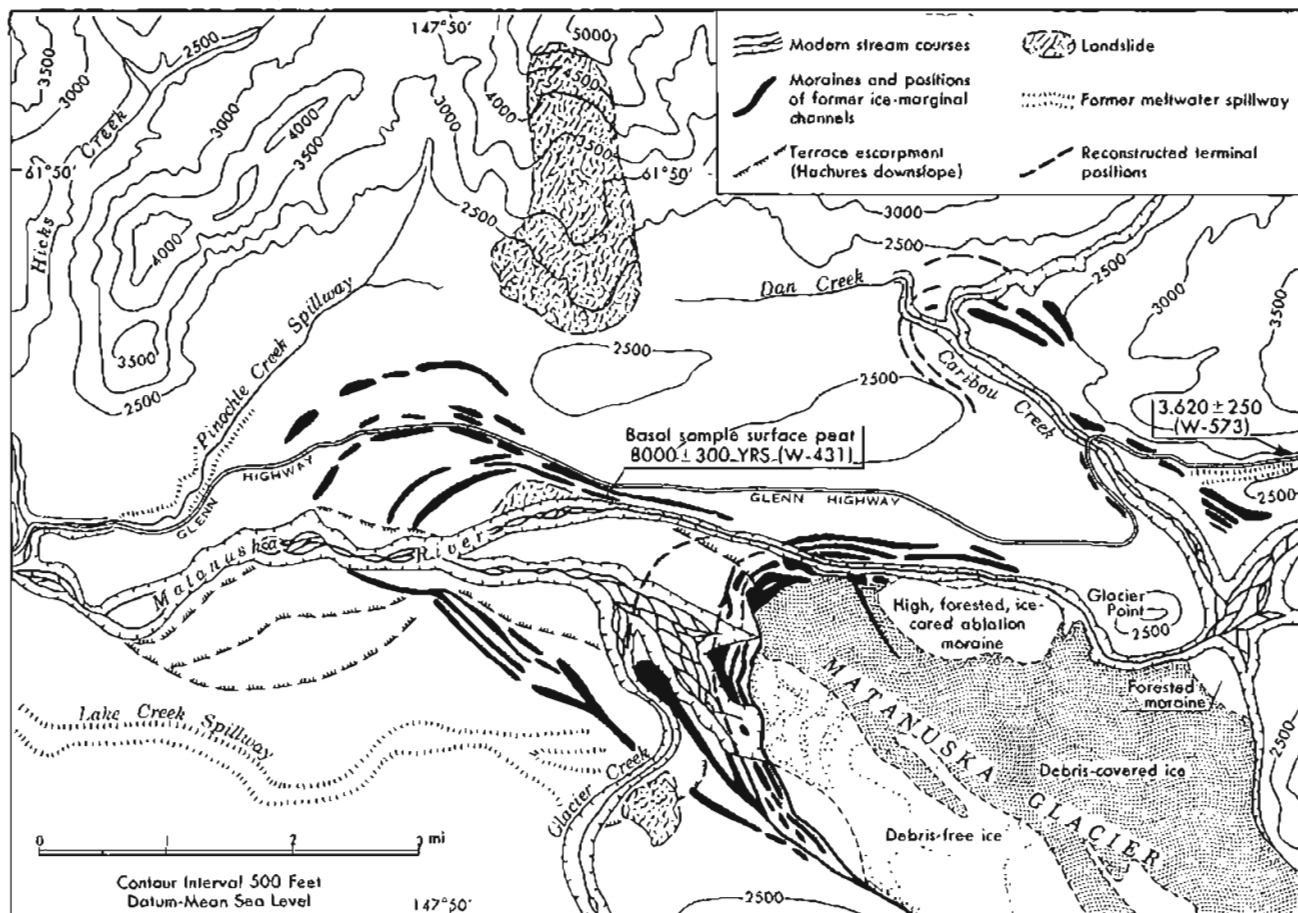


Figure 107. Sketch map of the present terminus of Matanuska Glacier and vicinity showing former terminal positions (modified slightly from Williams and Ferrians, 1961, fig. 1).



Figure 108. Oblique aerial view (to the southwest) of Pinochle Creek and Pinochle Creek spillway, Anchorage D-3 Quadrangle, Alaska. Photograph 88-13 by R.D. Reger, May 21, 1982).

tance, perhaps until after a soil formed in the area about $3,620 \pm 250$ yr B.P. (fig. 107, W-573) (Williams and Ferrians, 1961, p. 87). Subsequently, the glacier expanded to build an inner series of moraines 0.1 to 1 mi (0.2 to 1.6 km) from the present terminus, probably once again temporarily blocking lower Caribou Creek and diverting Glacier Creek (fig. 107). Geomorphological relationships, deposition of up to 12 in. (30.5 cm) of loess on the outermost moraine of the inner series, development of a 4- to 5-in.-thick (10.2 to 12.7 cm) weathering profile on this loess, and the antiquity of the surface vegetation indicate that this Holocene moraine is probably several thousand years old, but less than 4,000 yr old. A terminal-moraine remnant that is 0.25 mi (0.4 km) beyond the modern terminus and covered by a mature spruce forest, including trees as old as 145 yr (in 1982), appears to be much older than 145

yr, perhaps by several hundred years. Trees growing on inner moraines of the youngest group just beyond the active western terminus are 125 to 145 yr old. Since 1898, when the first photographs were taken of Matanuska Glacier, the terminus has remained fairly stable, although considerable thinning has occurred.

101. For the next 1.7 mi (2.7 km), the route traverses a series of low moraines that document minor latest Wisconsinan or perhaps very early Holocene fluctuations of Matanuska Glacier prior to 8,000 yr B.P.

99.1. The terminal moraine of the pre-8,000-yr readvance of Matanuska Glacier is plastered against a ridge of dark-gray shale of the Matanuska Formation of Cretaceous age.

98.6. Begin descent into Pinochle Creek spillway cut deep into the late Naptowne glacial floor through shale of the Matanuska Formation.

97.4. A notch to the northwest (right front) at about 2,050 ft (621 m) elevation allowed passage of overflow waters of late-Naptowne age; this overflow system closely predates the Pinochle Creek spillway. The complex melt-water course extended from the notch west through the Index Lake area, across a divide at about 1,840 ft (558 m) elevation, past the toe of a large, double-pronged, active landslide derived from the Chickaloon Formation on the southeast slope of 5,400-ft-high (1,636 m) Strelshla Mountain, and down the drainage of Packsaddle Creek to the present course of the Matanuska River. The Packsaddle Gulch spillway system was about 3.7 mi (5.9 km) long and part of a series of complex, temporary drainages that developed on the irregular bedrock floor of the Matanuska Valley as the ice-age glacier receded between 8,000 and about 10,000 yr B.P. The Packsaddle Gulch spillway, like the Pinochle Creek spillway, is graded to a level close to but slightly above the modern flood plain of the Matanuska River.

96.8. Crossing of Pinochle Creek. The roadcut ahead exposes coal-bearing Chickaloon Formation of Paleocene age.

96.6. Crossing of Hicks Creek on a low terrace of the Matanuska River. Begin ascent of canyon wall cut into the Matanuska Formation. To the left (south-southwest) is a good view of the inner gorge of the Matanuska River and glaciated surfaces on the north flank of the Chugach Mountains.

96.4 to 95.6. Roadcuts expose complexly faulted Matanuska Formation that is widespread in the Matanuska Valley and consists of a sequence of medium-gray, shallow- to deep-water marine shales and sandstones with local channel conglomerates. This Early to Late Cretaceous sequence reaches thicknesses of over 4,000 ft (1,212 m).

95.6. To the west (left) in the wall of the inner gorge is an excellent exposure of folded, coal-bearing Chickaloon Formation. Also visible are at least five distinct glacial benches above the inner gorge.

94.6. Crossing of Packsaddle Gulch and the former drainage course described at Mile 97.4.

94.2 to 89.1. The Glenn Highway traverses a glacial bench above the

inner gorge of the Matanuska River. The till cover is thin and discontinuous, and there are numerous exposures of the Paleocene Chickaloon Formation in the roadcuts. This unit unconformably overlies the Matanuska Formation and is at least 5,000 ft (1,515 m) thick in the Matanuska Valley. It is divided into a lower, coarse-grained sequence of conglomerates and sandstones, and an upper, finer-grained sequence of feldspathic siltstones and coals.

From Mile 93.2 to the south (left), one can see typical rugged Chugach Mountains topography, including numerous small cirque glaciers, hummocky end moraines of late Naptowne and early Holocene age that were deposited by ice from tributary valleys, several rock glaciers, and numerous late Naptowne ice-marginal features that slope gently westward.

At Mile 89.8 directly ahead (west-northwest) is an excellent view of Castle Mountain. The steep sides of this mountain are composed of about 3,000 ft (909 m) of Wishbone Formation, a sequence of Eocene conglomerates, sandstones, and siltstones. The top 200 ft (61 m) of the mountain consists of Eocene volcanic rocks.

The active Castle Mountain fault passes just north of Castle Mountain. In combination with the Caribou fault, it comprises a lengthy surface-rupture system that extends at least 124 mi (200 km) from the western Copper River basin west to the Susitna River and beyond (pl. 1); its western limit is not known. Detailed mapping along 22.4 mi (36 km) of the Castle Mountain-Caribou fault system about 10 mi (16.1 km) northwest of here indicates that at least 8.7 mi (14 km) of post-Paleocene and 3.1 mi (5 km) of post-Eocene right-lateral strike-slip displacement has occurred along this major crustal break. The dominantly dip-slip reverse displacement in post-Oligocene time ranges from about 1,650 ft (500 m) beneath the Susitna lowland to at least 1.9 mi (3 km) in the upper Matanuska Valley. The Castle Mountain fault offsets late Naptowne to modern surfaces west of Palmer (pl. 1). Tree-ring assessments indicate fault scarps are at least 225 yr old and radiocarbon dating of displaced soils demonstrates that fault scarps are younger than $1,860 \pm 250$ yr B.P. (W-2930 in Detterman and others, 1974). Preliminary analyses of seismicity of the Castle Mountain-Caribou fault system suggest a maximum credible earthquake with a magnitude of 7.4 within 25 mi (42 km) of the Glenn Highway (R and M Consultants, 1981). The calculated recurrence interval for this statistical event is about 400 yr, and estimates of associated ground motion give peak accelerations up to 1.0+ g and durations near 30 s.

The low ridge in the foreground is a large Tertiary (Eocene?) diabase intrusion of the Chickaloon Formation. This intrusive, which generally trends east-west and is offset by numerous faults, was relatively resistant to glacial scouring and thus remained standing above the less resistant Matanuska and Chickaloon Formations after retreat of late Naptowne ice in the Matanuska Valley (fig. 109).

89.5. Enter Anchorage D-4 Quadrangle.

89.2. Crossing of Purinton Creek.

88.9. To the right front (northwest) is a small anticline of coal-rich Chickaloon Formation that was folded and faulted by intrusion of the nearby diabase, probably in Eocene time. The field-trip route enters a meltwater



Figure 109. Oblique view (to the west) of the middle Matanuska Valley showing bedrock ridges differentially scoured by glaciation, Anchorage Quadrangle, Alaska. Photograph 88-9 by R.D. Reger, May 21, 1982.

channel of late Naptowne age that is now occupied by Purinton Creek. At the time glacial meltwater occupied this channel, the main glacier was located in a deeper trough about 1 mi (1.6 km) to the south (left). At Mile 88.4, the channel makes an abrupt turn to the southeast and descends about 850 ft (258 m) to the present flood plain of the Matanuska River.

88. Wiener Lake.

87.7 to 85.6. Note the large blocks of diabase that form the colluvial apron along the south slope of the linear ridge to the right (north). This glacier-molded ridge is composed of the diabase intrusive previously described (fig. 109) and extends east-west for a distance of at least 5 mi (8 km). The intrusive is probably the subsurface equivalent of the Eocene volcanics that cap Castle Mountain.

87.1. Chickaloon Formation crops out in the roadcuts along the grade down to Long Lake. Linear ridges of the Matanuska and Chickaloon Formations form an irregular valley floor across the lake to the south (left).

86.7. Above the road, large blocks of diabase rest unstably in the thin blanket of colluvium that covers the glacially steepened surface of the Chickaloon Formation. These blocks (rounded by spheroidal weathering) pose a serious hazard in the spring and during or after heavy rains, when they break loose and roll onto the Glenn Highway. Long Lake occupies a deep trough plucked and abraded into the Chickaloon Formation by glacial ice.

84.9 STOP 35. OPTIONAL PHOTO STOP. Bedrock here is the Matanuska Formation. Lake Naptowne till and stratified drift that overlie bedrock are capped by discontinuous colluvium with a well-developed podzol (spodosol) soil. The B horizon in this post-Naptowne weathering profile is 4 to 6 in. (10.2 to 15.2 cm) thick. The view upvalley includes outstanding examples of the effects of glacial scouring.

Archeological excavations in the vicinity of Long Lake have recovered projectile points, core tablets and fragments, biface implements, scrapers, retouched flakes, and waste flakes that have close affinities with the Denali Complex in the Tangle Lakes area.

The braided flood plain of the Matanuska River, which is 450 ft (136 m) below this location, results from of an overload of rock debris from Matanuska Glacier and numerous smaller ice masses at the heads of many tributaries of the river. This reach of the flood plain is generally covered by a thick stream icing each winter, as are braided reaches of other streams in interior and northern Alaska.

To the south across the Matanuska River is the structurally complex terrane of the northern Chugach Mountains, which is dominated by the Border Ranges fault system. This major structural discontinuity extends for more than 621 mi (1,000 km) from western Kodiak Island in an arc north and east along the western and northern flanks of the Kenai and Chugach Mountains, respectively, to the St. Elias Mountains. In this part of the northern Chugach Mountains, where it is mapped as the Knik fault, the Border Ranges fault separates metavolcanic, metasedimentary, and granitic plutonic rocks of Jurassic to Tertiary age, including Paleozoic-Mesozoic ophiolite assemblages,

from weakly metamorphosed upper Mesozoic sedimentary and volcanic rocks of the McHugh and Valdez Groups to the south. The Border Ranges fault system is interpreted as a plate boundary that developed in latest Mesozoic or early Tertiary time and was the contact between an upper Paleozoic island arc (now on the north) and a subducting block of deep-water sediments and oceanic crust (now on the south). Activity along the fault system apparently waned after early Tertiary time, although Holocene fault scarps occur locally.

83.7 to 82.7. Conglomerate of the Matanuska Formation is exposed in the roadcuts to the right. These rocks formed as channel fillings in a turbidite sequence.

82.7. Kings Mountain, the pyramid-shaped mountain to the left front (west-southwest), is a prominent landmark in the central Matanuska Valley. It was named after Al King, a late-19th-century prospector with a cabin at the confluence of the Matanuska and Kings Rivers. The mountain is composed of a resistant Tertiary intrusive along the contact between the Chickaloon Formation on the south and the Matanuska Formation on the north. Periglacial features of Holocene age that are evident around Kings Mountain include landslides, talus cones and aprons, and rock glaciers; an especially large landslide of Chickaloon Formation occurs on the southwest side of Kings Mountain. The Border Ranges fault crosses south of Kings Mountain.

80.8. Note the calcium-carbonate zone associated with the weathering profile in Naptowne till in the roadcut to the right. The weathering zone is 2 to 3 ft (0.6 to 0.9 m) deep and is capped by 2 ft (0.6 m) of loess containing volcanic-ash layers.

80.4. The 200-ft-thick (61 m) section of maroon-black Eocene volcanic rocks over the 3,000-ft (909 m) section of Eocene Wishbone Formation is visible on Castle Mountain to the right front (northwest) (fig. 110).

79.7. Begin descent into canyon of the Chickaloon River, which has incised 200 to 400 ft (61 to 121 m) into the Chickaloon Formation since the retreat of the late Naptowne glacier about 10,000 yr B.P. Across the Matanuska River to the left (south) near the mouth of Coal Creek, a small coal mine was excavated into the Chickaloon Formation in 1921 and 1922. This mine was operated by the Navy Alaska Coal Commission and consisted of two adits that were cut to prospect three 3- to 6-ft-thick (0.9 to 1.8 m) beds of sub-bituminous coal. The mine closed because faults and Tertiary sills limited the reserves. Between 1925 and 1930, farther up Coal Creek, a private concern extracted coking coal that was used by the Alaska Railroad. To the left front (southwest), ice-scoured bedrock benches form subtle steps from the base of Kings Mountain nearly to tree line.

77.9. Crossing of the Chickaloon River, a major north tributary of the Matanuska River.

77.7. Till and well-rounded glaciofluvial gravel are exposed in the roadcut.

77.6 to 74.9. The Glenn Highway traverses discontinuous treads of Holocene fluvial terraces that are 30 to 50 ft (9.1 to 15 m) above the Matanuska River.



Figure 110. Aerial view (to the north) of Castle Mountain, Anchorage D-4 and D-5 Quadrangles, Alaska. Tw, Eocene Wishbone Formation; Tv, Eocene volcanic rocks. Chickaloon No. 1 test well was drilled (1926-1930) through Chickaloon Formation (with some gas shows reported) and into igneous rock; total depth is 1,465 ft (444 m). Photograph 88-7 by R.D. Reger, May 21, 1982.

76. Enter Anchorage D-5 Quadrangle. Felsic dikes and sills of Tertiary age intrude the Chickaloon and Matanuska Formations, as seen in the roadcuts and across the Matanuska River. Slope icings develop by ground-water seepage in these rock cuts each winter.

75.1. Large blocks of Matanuska Formation on the terrace tread are probably remnants of rock falls and slides from the northwest flank of Kings Mountain.

74.3 to 72.9. The road winds through a maze of esker ridges that formed in the vicinity of Thirtymile Lake when the late Naptowne glacier stagnated about 10,000 yr B.P. Thirtymile, Fish, Drill, and Harrison Lakes occupy a 5-mi-long (8.1 km) drift-filled former valley of the Chickaloon River.

72.9 to 71.8. Glenn Highway crosses the tread of a Holocene terrace that is 10 to 15 ft (3 to 4.6 m) above the Matanuska River.

71.7. Fragments of ammonites and pelecypods (Inoceramus) occur in the

Matanuska Formation in the rock wall on the right (northwest) side of the road. Slope instability is caused by unfavorable orientation of joints in the bedrock.

71.4. Enter Anchorage C-5 Quadrangle.

71.4 to 69.6. Route crosses tread of 10- to 15-ft-high (3 to 4.6 m) terrace of the Matanuska River. On the south side of the river, note the stream terraces that were cut as the river rapidly incised the valley fill following deglaciation in late Naptowne time. The braided flood plain of the Matanuska River is typical of wider reaches of the stream.

68.7 to 68.1. Roadcuts expose stratified stream gravel in terraces equivalent in height to fluvial terraces on the south side of the Matanuska River.

67.3. Descent onto high terrace of the Matanuska River.

67. From here to Sutton, the Glenn Highway follows the route of a branch of the Alaska Railroad (then called the Alaska Engineering Commission Railroad) that was built in 1917 and abandoned in 1933; this short spur extended 19 mi (30.6 km) from Sutton east to Chickaloon, then the center for coal prospecting, mining, and related activities in the central Matanuska Valley. The Matanuska River at this location crosses through a glacier-molded ridge of intensely faulted Matanuska Formation.

66.8 to 66.2. Traverse of terrace that formed at the confluence of the Kings and Matanuska Rivers.

66.5. Crossing of the Kings River.

66.2. Descent down scarp of terrace formed at the confluence of the Kings and Matanuska Rivers and beginning of the Matanuska River terrace at a height of about 15 ft (4.6 m) above river level. Bedrock on the south side of the Matanuska River to the left is Matanuska Formation. Bedrock to the right (north) of the highway is Chickaloon Formation, which is buried beneath ice-contact deposits.

63.6. Roadcut exposes late Naptowne stratified glaciofluvial sand and gravel.

63 to 62.2. Crossing the large gravel fan of Granite Creek (fig. 111).

62.4. Crossing of Granite Creek. Along the stream channel, note the numerous granitic and gneissic boulders that are derived from the Talkeetna batholith in the Talkeetna Mountains to the north (right). These boulders, like those on other coarse-grained alluvial fans, are moved and deposited during periodic floods. The last major flood of Granite Creek occurred between August 8 and 11, 1971, in response to the abrupt drainage of an unnamed, moraine-dammed lake at 3,352 ft (1,016 m) elevation near the head of a west tributary of Granite Creek, 15 mi (24.2 km) upstream from the Glenn Highway bridge. This lake initially contained an estimated 1,645 acre-ft (2,035,690 m³) of water and drained through a shallow channel across the crest of a small end moraine. Accelerated stream erosion during a period of heavy

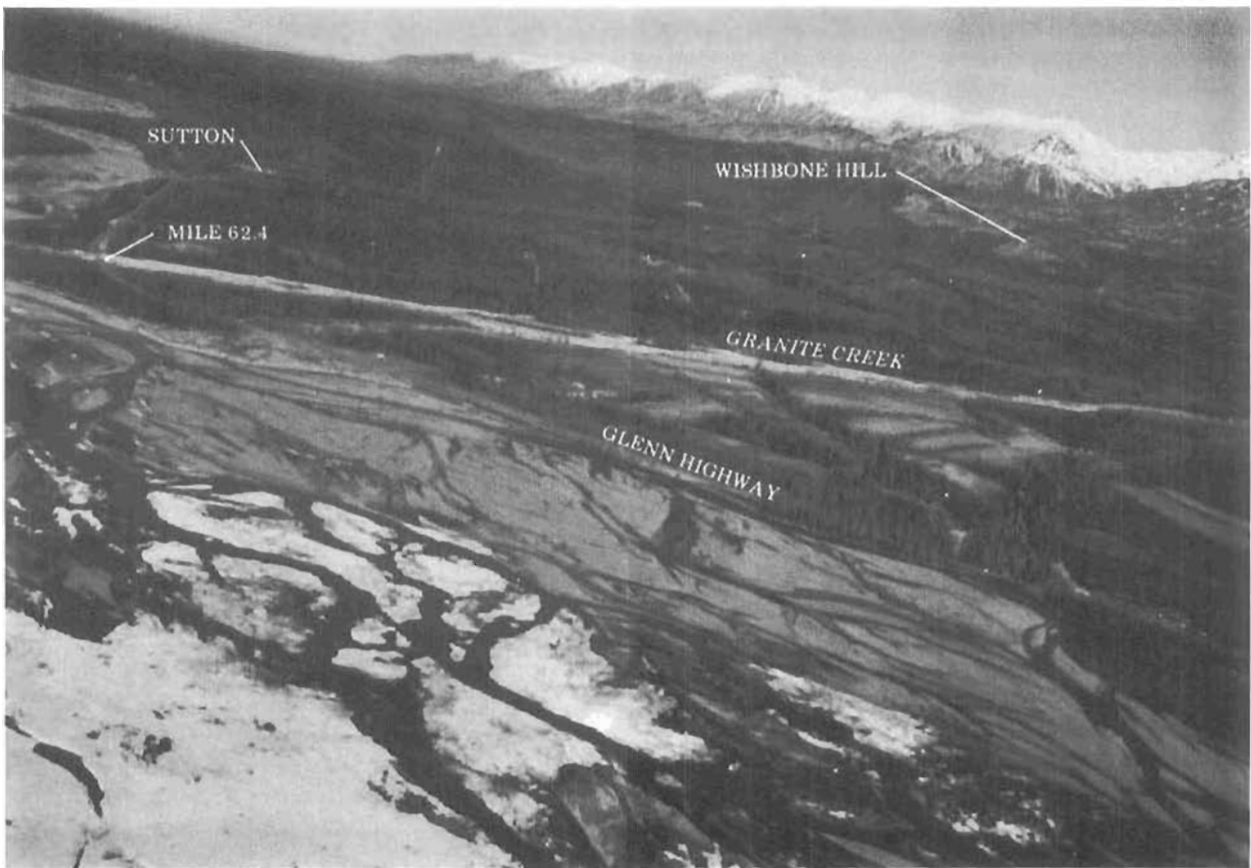


Figure 111. Oblique aerial view (to the west) of Granite Creek fan, Anchorage Quadrangle, Alaska. Photograph 88-6 by R.D. Reger, May 21, 1982.

precipitation, when 3 to 6 in. (7.6 to 15.2 cm) of rain fell in the Palmer-Talkeetna area, rapidly lowered the drainage channel to the level of the lake and released over 400,000,000 gals (1,519,270 m³) of lake water within a few hours. Peak flow during the resulting flood is estimated at 58,600 ft³ per s (1,666 m³ per s); during peak discharge, boulders weighing up to several tons were flushed hundreds of yards downstream and left on the flood plain. Floodwaters washed out the Glenn Highway in several places where the highway crosses the Granite Creek fan.

62.2 to 60.8. Continue traverse across 15-ft-high (4.6 m) terrace of the Matanuska River.

61.7. Enter Anchorage C-6 Quadrangle.

61.3. Wishbone Hill (fig. 111) and huge tailings mounds of the Evan Jones Coal Mine are visible to the right front (northwest). Wishbone Hill is named after the topographic form produced by ice-scouring of a faulted, doubly plunging syncline, termed the Wishbone Hill Syncline, that is capped by the very resistant, cliff-forming Wishbone Formation. The much less resistant Chickaloon Formation forms the gentler slopes beneath the Wishbone Formation. Movable coal occurs only in the upper 1,400 ft (424 m) of the Chickaloon Formation, where 13 beds form three groups separated by thick, generally barren

intervals. The coal-mining district, named after Wishbone Hill, includes an eastern part around Eska and Jonesville in the drainage of Eska Creek and a western part in the drainage of Moose Creek, 4 mi (6.4 km) to the west on the opposite end of Wishbone Hill.

Coal extraction began in the eastern part of the Wishbone Hill district in 1917, when the Eska No. 1 Mine opened 2 mi (3.2 km) up Eska Creek from the modern settlement of Sutton. Coal was initially sledged from the mine several miles to the head of the Chickaloon spur of the Alaska Railroad, which was then located at the mouth of Moose Creek. Later that year, the spur was extended to the Eska No. 1 Mine. Although it opened in 1920, the nearby Evan Jones Mine did not begin production until it was connected to the railroad spur up Eska Creek in October 1921. The Evans Jones Mine was the major coal mine in the Wishbone Hill district, and produced about 67 percent of the district's coal. Except for a temporary shutdown after October 26, 1937, when a methane explosion claimed 14 lives, the mine operated almost without interruption until 1968. Before 1950, all production at the Evan Jones Mine was from subsurface workings. In 1933, the lower levels flooded and were never reclaimed. After 1950, surface stripping began along the limbs of the Wishbone Hill Syncline.

In 1947, the Knob Creek Coal Company began serious prospecting for coal near Knob Creek, about 0.8 mi (1.3 km) northeast of Eska. Two short [(100- and 130-ft-long (30.3 and 39.4 m)] adits were unsuccessfully driven. In mid-1953, surface stripping began, but the mine closed a few years later.

The Wishbone Hill district gradually increased production after 1935, the first year that reliable production figures were kept. From 1935 through 1940, an average of 55,000 short tons (49,929 metric tons) of bituminous coal were produced annually, primarily for the Alaska Railroad, which used it for heating, power, and locomotion. The heating values of raw coal from Wishbone Hill range from 10,400 to 12,500 Btu (10,972 to 13,188 kJ). In response to World War II, when large military establishments were constructed in the Anchorage area, yearly coal production doubled in 1941 and maintained an annual average of 163,100 short tons (148,062 metric tons) through 1951. The impetus of the Korean War boosted production in the district to 243,000 short tons per yr (220,595 metric tons per yr), a level that was generally maintained through 1959, the last year for which figures are published. In 1956, estimates of coal remaining in the district were 6.6 million short tons (6 million metric tons) of measured reserves, 57.3 million short tons (52 million metric tons) of inferred reserves, and probable additional reserves of 48.6 million short tons (44.1 million metric tons). The closure of the Evan Jones Mine and the general collapse of the coal-mining industry in the district, except for supplying small, local needs, was due to loss of the military market. This loss resulted from conversion of fuel for boilers and generators from coal to cheaper natural gas in 1967.

61. Town of Sutton. A short road extends from the right (north) to the defunct Evan Jones and Eska Coal Mines.

60.9. Crossing of Eska Creek. This small stream reworked gravel and sand of the kame-esker complex in this area and constructed the gravel fan on which Sutton is built. Eska Creek floods periodically.

60.7. Road ascends through a series of six late Naptowne fluvial terraces that are capped by about 3 ft (0.9 m) of loess.

59.7 to 56. Traverse across kame-esker deposits and pitted outwash formed between 8,000 and about 10,000 yr B.P. in the Granite Creek-Moose Creek area in response to stagnation of the trunk glacier in the central Matanuska Valley. This surface is 260 to 470 ft (79 to 142 m) above the Matanuska River. A water-well log near Mile 58 penetrated about 33 ft (10 m) of fluvial gravel over 85 ft (25.8 m) of late Naptowne till (well 256 in Trainer, 1960; pl. 1 and app. A).

58.8. Roadcuts reveal ice-stagnation sand and gravel.

57.7. Branch road to right to Palmer Correction Center.

56. Begin descent into Moose Creek drainage that is incised 200 to 350 ft (61 to 106 m) into esker deposits and Tertiary bedrock.

55.4. Leave ice-contact deposits and begin traverse of terrace tread of late Naptowne age. This tread is about 120 ft (36.4 m) above the flood plain of the Matanuska River.

54.6. Begin descent from terrace tread to Moose Creek. Roadside cuts expose sandstone of the Chickaloon Formation. Mining in the western part of the Wishbone Hill coal field has been less productive and more sporadic than in the eastern part. Commercial production at the west end of Wishbone Hill began in 1916 with the completion of the Chickaloon branch of the Alaska Railroad to Moose Creek. In 1916, the Doherty Mine commenced extraction of coking coal for blacksmithing from the Chickaloon Formation at the present crossing of Moose Creek by the Glenn Highway. This small venture lasted only 2 yr. The mine reopened for a short time in 1928, and brief, sporadic attempts to mine coal continued as late as 1953.

In 1917, the nearby Baxter Mine began episodic excavation of an 11-ft-thick (3.3 m) coal seam in the Chickaloon Formation. This effort lasted about 1 yr, but ceased until 1921 when the mine reopened for another 5 yr. Coal was sledged to the railroad at the mouth of Moose Creek until 1923, when a spur of narrow-gauge tracks was laid to the mine. The Baxter Mine closed for the last time in 1925 because of lack of capital and because faulting limited the reserves.

In 1922, the Premier Mine was opened in a 90- to 100-ft-thick (27.3 to 30.3 m) coal-rich section of the Chickaloon Formation 3 mi (4.8 km) up Moose Creek from the present Glenn Highway. This mine was the major source of coal in the western Wishbone Hill district for many years. Lower levels were flooded in 1933 because of improper mining methods, and mining operations stopped except for small-scale attempts in the middle to late 1950s.

In 1939, development work began on the Buffalo Mine, about 5 mi (8 km) up Moose Creek. Serious production did not begin until 1942 and continued to the end of World War II. After severe flooding permanently washed out the standard-gauge railroad tracks connecting this mine with the Chickaloon branch in September 1942, the coal was hauled to market by truck. The Buffalo Mine has operated periodically since 1952 and currently mines a very small quantity

of bituminous coal to satisfy local demand for furnace fuel.

54.4. Crossing of Moose Creek and beginning of ascent through glaciofluvial sand and gravel.

53.4. Top of grade. For the next 4.8 mi (7.7 km), the Glenn Highway crosses an extensive, locally pitted outwash surface 270 to 400 ft (82 to 121 m) above the flood plain of the Matanuska River (fig. 112). To the right (north), eskers provide local relief; these ice-stagnation features are a continuation of the complex that begins 8 mi (12.9 km) east of here near Granite Creek and continues west to north of Palmer (pl. 1). These eskers formed in ice tunnels about 10,000 yr B.P. and closely predate the outwash traversed by the highway. Across the Matanuska River to the left (south) is the Wolverine Complex, a part of the Chugach terrane that contains some of the most highly mineralized rocks in the Chugach Mountains and is currently mined for placer gold, silver, and minor amounts of metallic sulfides.

52.6. Junction of the Glenn Highway and Moose Creek Road to the Buffalo Mine.

51.3 to 51.1. Irregular kettles were formed in the high-level terrace surface by the melting of dead-ice masses that were buried by outwash alluvium about 10,000 yr B.P. Water-well logs in the vicinity of Mile 51.3 indicate that the glaciofluvial gravel underlying this terrace varies in thickness from 36 to 96 ft (10.9 to 29.1 m) and overlies 12 to 15 ft (3.6 to 5.5 m) of late Naptowne till.

50.4. Junction of the Glenn Highway and Farm Loop Road. Surface pitting here results from melting of stagnant and buried glacial ice. From here, poorly integrated, former stream channels extend northwest into a complex terrain initially formed as a broad, thick, sandy outwash fan deposited by the Matanuska River over stagnant glacial ice north and west of Palmer; the original fan was later deformed into a gently irregular surface when the underlying ice melted.

50. The east end of a 1.3-mi-long (2.1 km) series of cliff-head sand dunes starts at the top of the 150- to 170-ft-high (45.5 to 51.5 m) steep bluff of the Matanuska River to the left (east) of the Glenn Highway.

49. Junction of the Glenn Highway and Fishhook Road, which extends for several miles north into the historic Willow Creek and Hatcher Pass gold-mining area in the southwestern Talkeetna Mountains. The recent increase in the price of gold has stimulated renewal of hard-rock and placer mining in the area. The glaciofluvial terrace gravel is about 76 ft (23 m) thick in this area.

48.9. The Glenn Highway passes through a series of vegetated and stabilized cliff-head sand dunes. Cuts expose large-scale eolian cross-bedding and buried humic zones. In the Palmer area, windblown sand occurs in thin beds and thicker blankets, and locally piles up as dunes. The 30-ft-high (9.1 m) cliff-head dunes at this locality overlie 36 ft (10.9 m) of horizontally bedded eolian sand (fig. 113, loc. 5), and comprise the thickest eolian deposits in the Palmer area (fig. 114). These dunes were built primarily by winds blowing down the Matanuska Valley from the northeast. These winds pick up grains of sand and small pebbles from the underlying sandy outwash alluvium



Figure 112. Oblique aerial view (to the southwest) of the high-level outwash terrace and esker complex west of Moose Creek, Anchorage C-6 Quadrangle, Alaska. Photograph 91-9 by R.D. Reger, May 23, 1982.

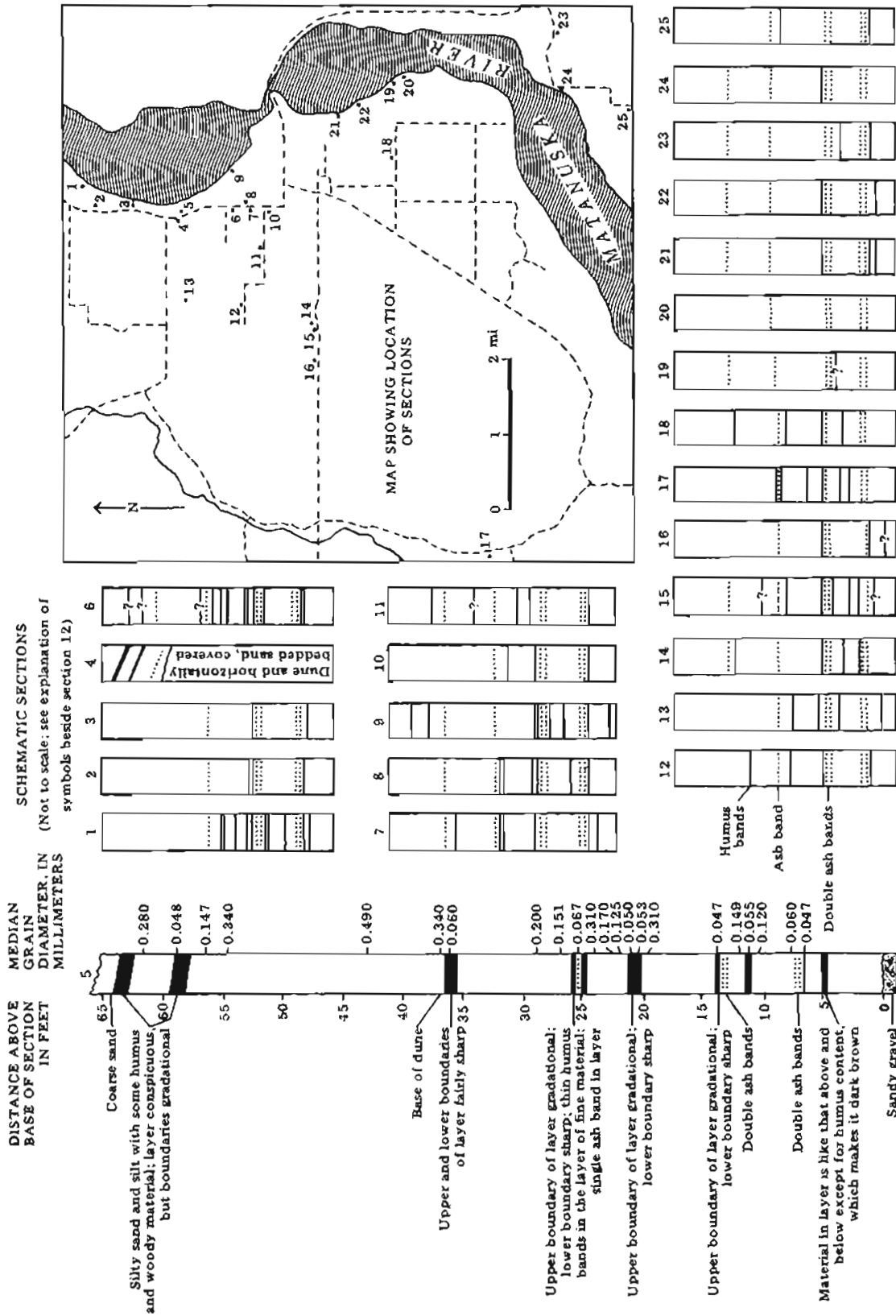


Figure 113. Stratigraphic sections of eolian deposits in the Palmer area, Alaska. Schematic sections 1-4 and 6-25 are not drawn to scale, but show number and relative positions of humus zones and layers of volcanic ash. Section 5 shows stratigraphic details at Mile 48.9 (from Trainer, 1961, fig. 6).

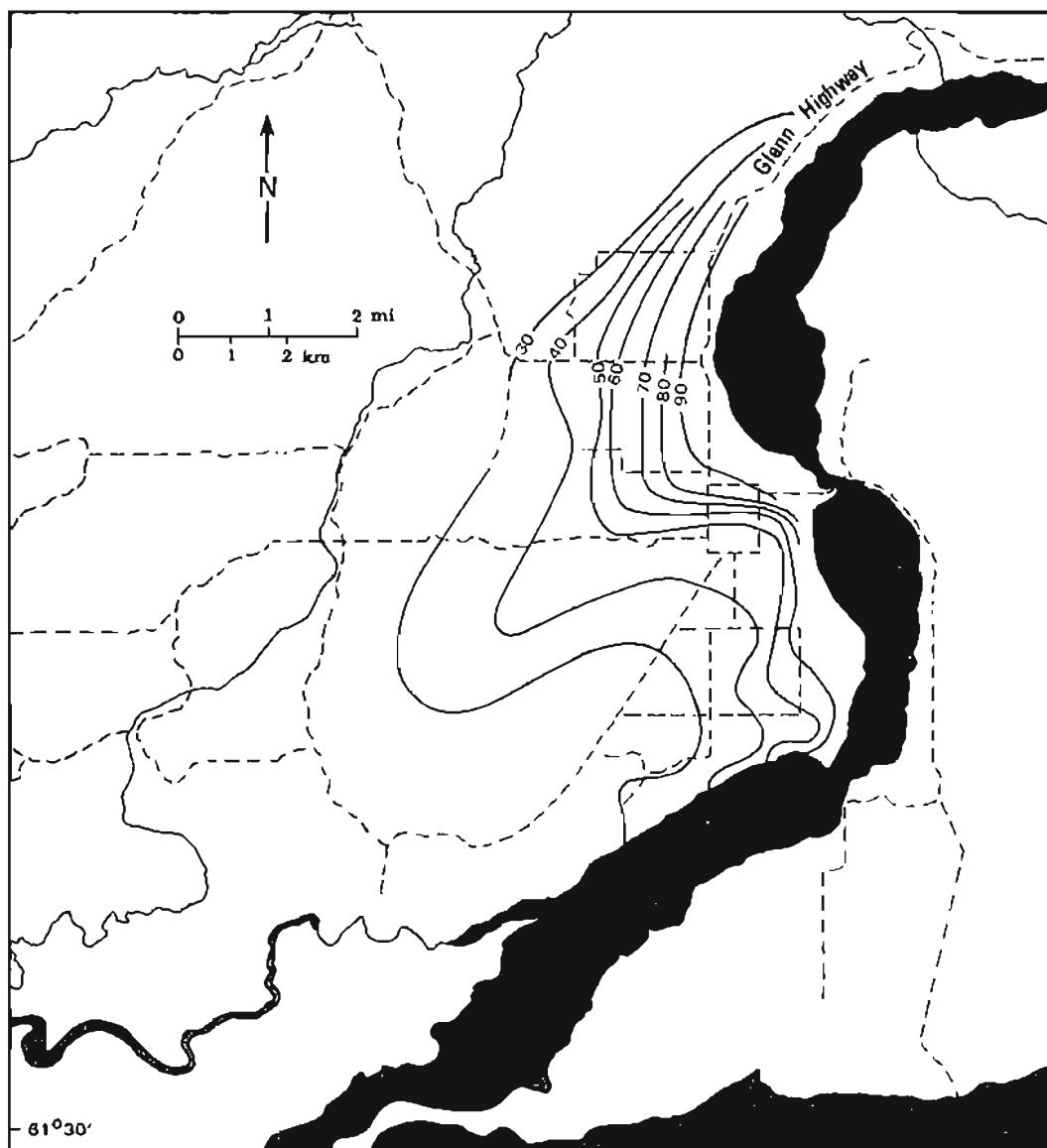


Figure 114. Isopach map of the eolian silt and sand blanket in the Palmer area, Alaska. Contour interval is 10 in. (25.4 cm), and dashed lines are local roads (from Trainer, 1961, fig. 4).

and the thick eolian-sand blanket and carry them upslope; they are deposited where wind velocity decreases and wind vortices develop near the top of the bluff. Sand and dust on modern vegetation that covers the dunes indicate that these low hills are still growing slowly; they will continue to grow as long as sandy sediments downslope are exposed to deflation. Calcareous shells of the air-breathing gastropod *Succinea avara* are locally common in the dune sand, especially in the more organic zones. The component of sand in eolian surface deposits decreases west and southwest away from the Matanuska River (fig. 115).

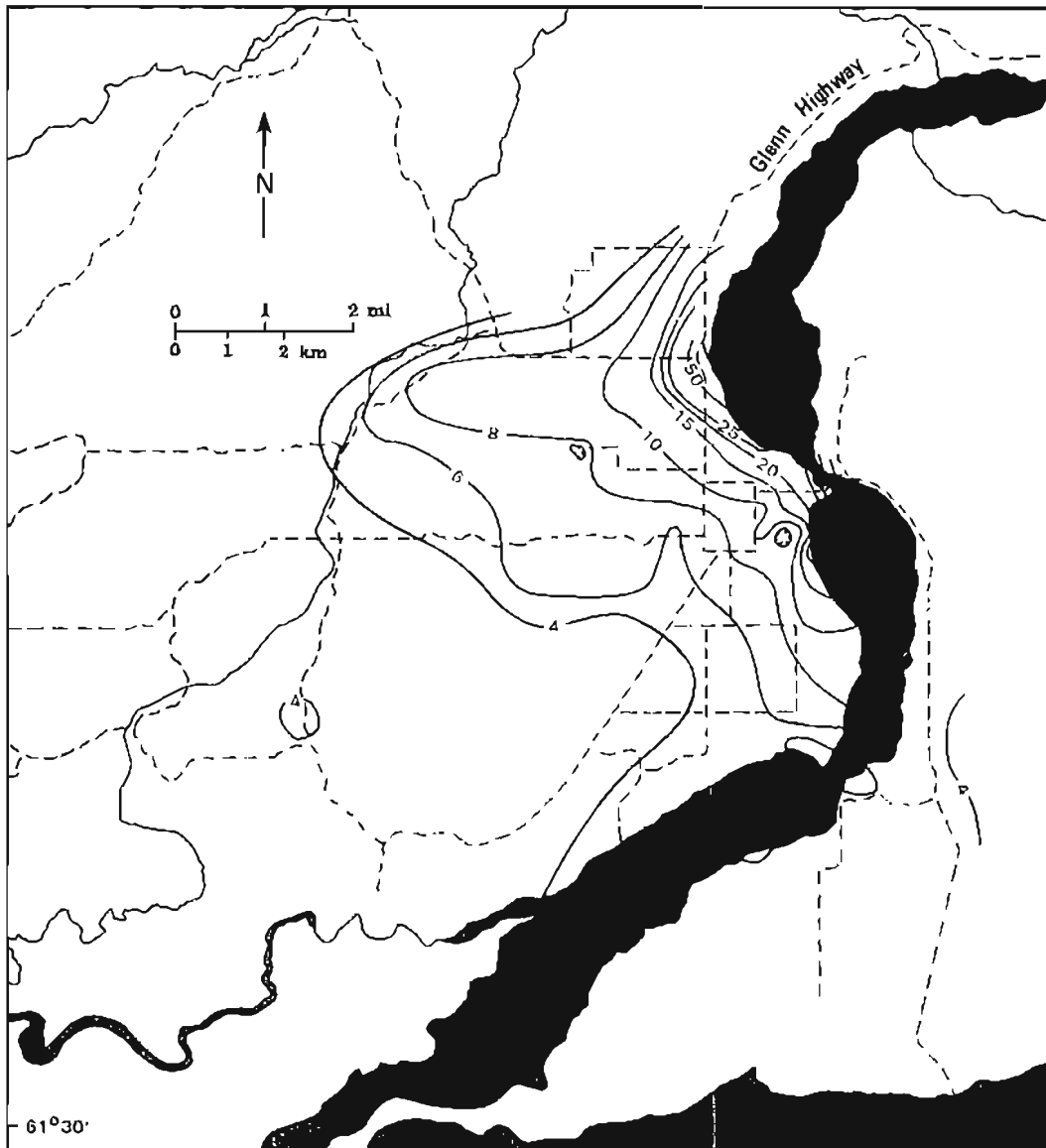


Figure 115. Component of sand in eolian deposits of the Palmer area, Alaska. Contour intervals are 2, 5, and 25 percent, and dashed lines are local roads (from Stump and others, 1959, fig. 7).

Begin descent down a series of five 20- to 95-ft-high (6.1 to 28.8 m) terrace scarps that were cut when the Matanuska River rapidly incised valley fill about 10,000 yr B.P. To the southwest, these terraces grade into complex ice-stagnation deposits northwest and west of Palmer (pl. 1). The generally uniform thickness of the eolian blanket on the five terraces indicates that downcutting was very rapid or predated eolian deposition in the area.

48. In 1929, the lower Matanuska Valley began its growth into the most important agricultural center in southern Alaska, when the Alaska Railroad initiated a program of farm development. The railroad advertised in the contiguous states for farmers to homestead in Alaska in return for lower pas-

senger and freight rates. Fifty-five farm families from the Pacific Northwest came north to settle in the Palmer area. As part of President Franklin Roosevelt's New Deal Program, the Alaska Rural Rehabilitation Corporation was later organized and, in 1935, brought some 200 indigent families, including a few with farming backgrounds, into the lower valley from Minnesota, Wisconsin, and Michigan to bolster the fledgling farm industry.

Palmer has a very favorable climate for producing grains, hay, vegetables, and dairy products. The mean annual temperature is 35.5°F (1.9°C) and the July temperature averages 57.6°F (14.2°C). Average annual precipitation is 16 in. (40.6 cm). The growing season averages 125 days per year. Dominant winds blow from the northeast in winter ('Matanuska wind') and from the southeast in spring and summer ('Knik wind').

Silt loam of eolian origin provides an excellent soil for crops. Loess blankets upland surfaces in the Palmer area up to about 2,000 ft (606 m) elevation on nearby mountain slopes. Thickness of the windblown silt decreases (more or less logarithmically with distance) from a maximum of 15 to 25 ft (4.6 to 7.6 m) adjacent to the western margin of the Matanuska River flood plain in a general west-southwest direction (fig. 116). The percentage of clay in the eolian mantle increases in the same direction (fig. 117). Although the loess is sandy near the base of a typical section, it is generally well sorted, and the degree of sorting increases to the west-southwest (fig. 118). Loess has 50 to 60 percent pore spaces by volume, but is less permeable than eolian sand. Silt grains are dominantly metamorphic-rock fragments, quartz, and feldspar, and the chief clay minerals are chlorite and illite. Many sections exhibit buried humus and volcanic-ash layers (fig. 113). Shells of several pulmonate snails are preserved in zones that are rich in plant material in the upper part of the sandy, coarse silt close to the Matanuska River, including Succinea avara, Discus cronkhietii, D. shimeki, Vallonia gracilicosta?, Euconulus fulvus, Vertigo tridentata, V. modesta, Pupilla muscorum, Retinella electrina, and Columella?³¹ These gastropods indicate that the loess accumulated on a well-vegetated landscape much like the present surface. In general, organic content decreases with depth in the loess due in part to oxidation of older plant remains.

The eolian origin of the upland silt in the Palmer area is evident because deposition of the silt is still very active. Although the mountain scenery around Palmer is spectacular on relatively calm days (fig. 119), on windy days it is partially or completely obscured by a curtain of dust from the unvegetated, braided flood plains of the Knik and Matanuska Rivers (fig. 120). After strong winds, fresh sand and silt coat leaves, branches, and trunks of trees and bushes for several hundred yards downwind from the margins of active flood plains, and fresh air-fall silt has been observed on leaves several miles downwind from the nearest source. Survey markers placed near the Matanuska River in 1913 were buried by several inches of eolian sediment during the following 22 yr. Other conditions that demonstrate that the bare flood plains of the Knik and Matanuska Rivers are the source of the loess blanket include the decrease in thickness, sand content, and grain size coincident with an increase in the degree of sorting away from the flood plains in the dominant downwind direction. The substantial thickness of the

³¹These mollusks are listed in Stump and others (1959, p. 15).

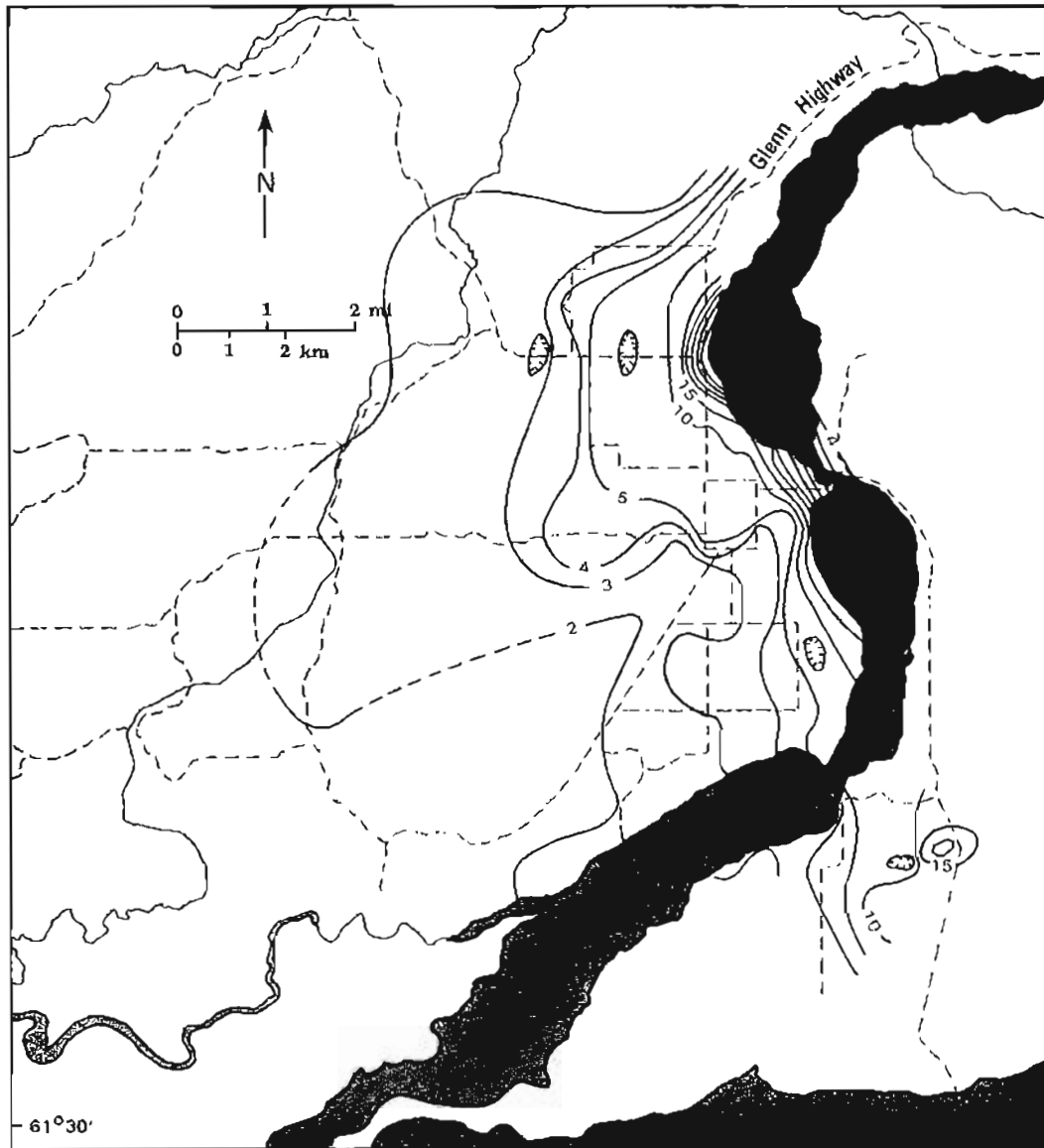


Figure 116. Isopach map of loess in the vicinity of Palmer, Alaska. Contour intervals are 1, 5, and 10 ft (0.3, 1.5, and 3 m) and dashed lines are local roads (from Stump and others, 1959, fig. 4).

loess blanket adjacent to but west of the Matanuska River (figs. 114 and 116) indicates that loess in the immediate vicinity of Palmer was derived primarily from the local, braided flood plain of the Matanuska River. Wind deflation of cultivated fields is a serious problem in the Palmer area, where up to 3 in. (7.6 cm) of soil has been removed in a single series of windstorms (J.R. Williams, written commun., February 10, 1983).

Buried humic zones in the loess probably document several short periods of slower eolian deposition, when organic components of the accumulating surface sediment became important relative to inorganic components and when soil-forming processes produced immature weathering profiles. These brief inter-

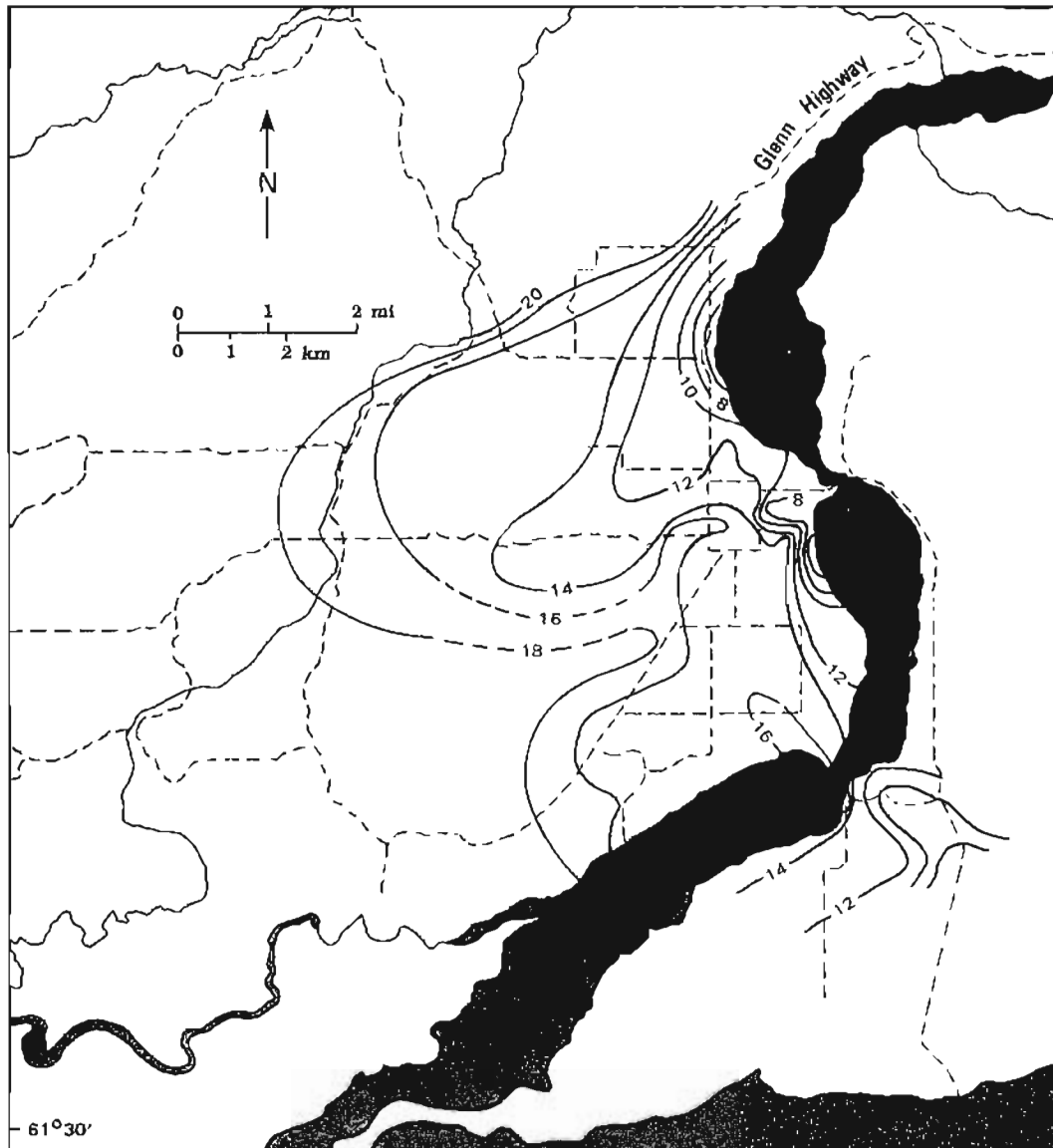


Figure 117. Component of clay in loess in the vicinity of Palmer, Alaska. Contour interval is 2 percent and dashed lines are local roads (from Stump and others, 1959, fig. 8).

vals of slower silt buildup probably resulted from changes in the character of the local flood plains rather than in wind velocity or direction. Causes of flood-plain changes may include: a) growth and recession of glaciers at the heads of the Matanuska and Knik Rivers, b) changes in sea level, and c) changes in the locations of unvegetated flood-plain surfaces due to the positioning of large, seasonal stream icings. Karlstrom (1965, p. 127) concluded that loess in the lower Matanuska Valley was deposited during and after Altithermal time (about 4,000 to 6,000 yr B.P.), which he correlated with his Kasilofian Transgression. Because of Palmer's location near the head of Knik Arm (pl. 1), he speculated that local flood-plain activity is controlled by

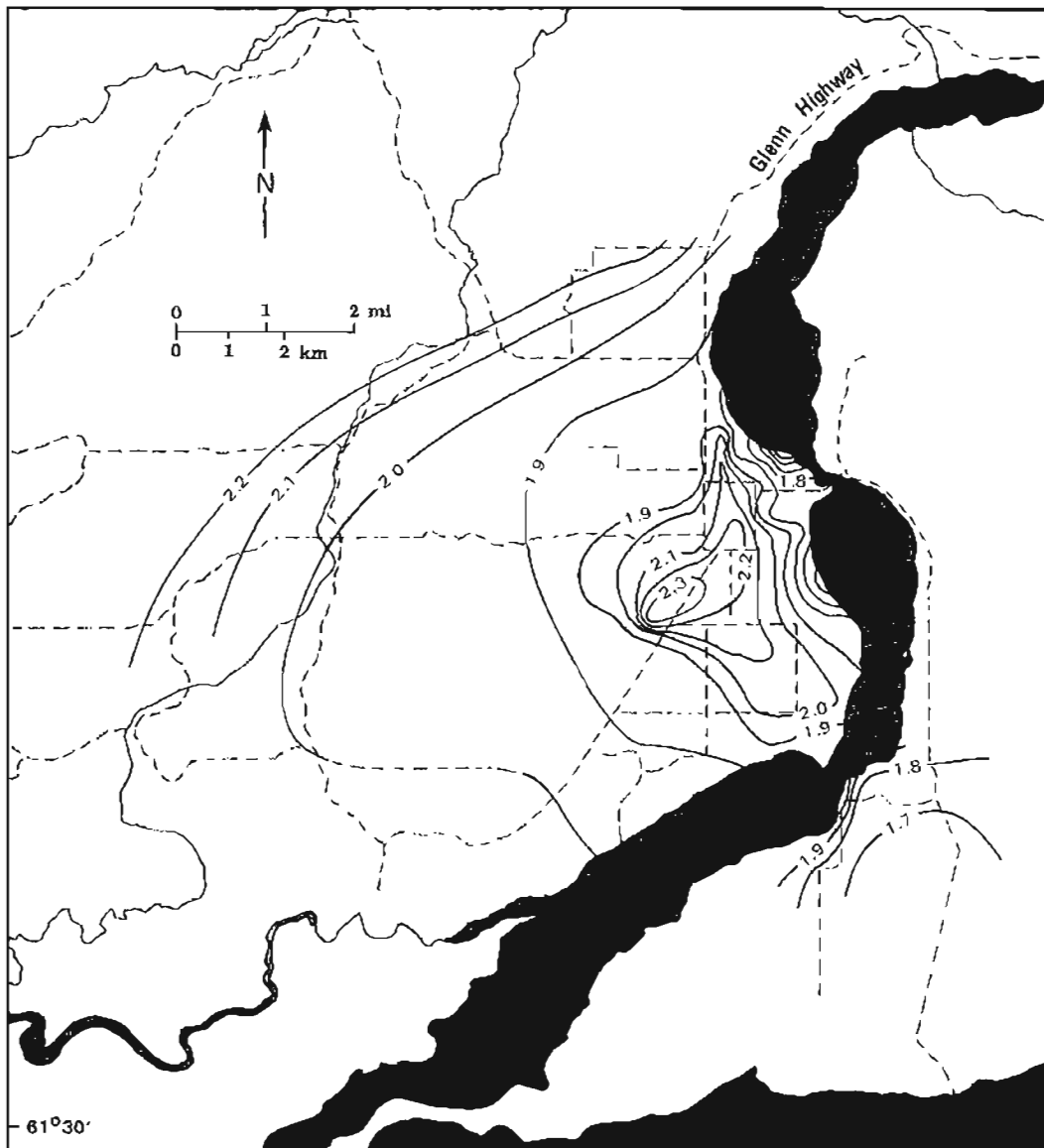


Figure 118. Variation of the sorting coefficient for loess in the vicinity of Palmer, Alaska. Dashed lines are local roads (from Stump and others, 1959, fig. 9).

sea-level changes, so that stream aggradation and accelerated eolian deposition coincidentally occurred during periods of rising sea level. Convincing evidence to confirm this speculation is not available. Geomorphic evidence indicates that loess in the lower Matanuska Valley is less than 10,000 yr old. Radiocarbon samples (in process) will provide more precise dating of the loess.

47.6. Junction of the Glenn Highway and Palmer-Wasilla Road. End of mileposts for the old Glenn Highway and beginning of new mileage (41.8) resulting from changes in highway alignments and routes.

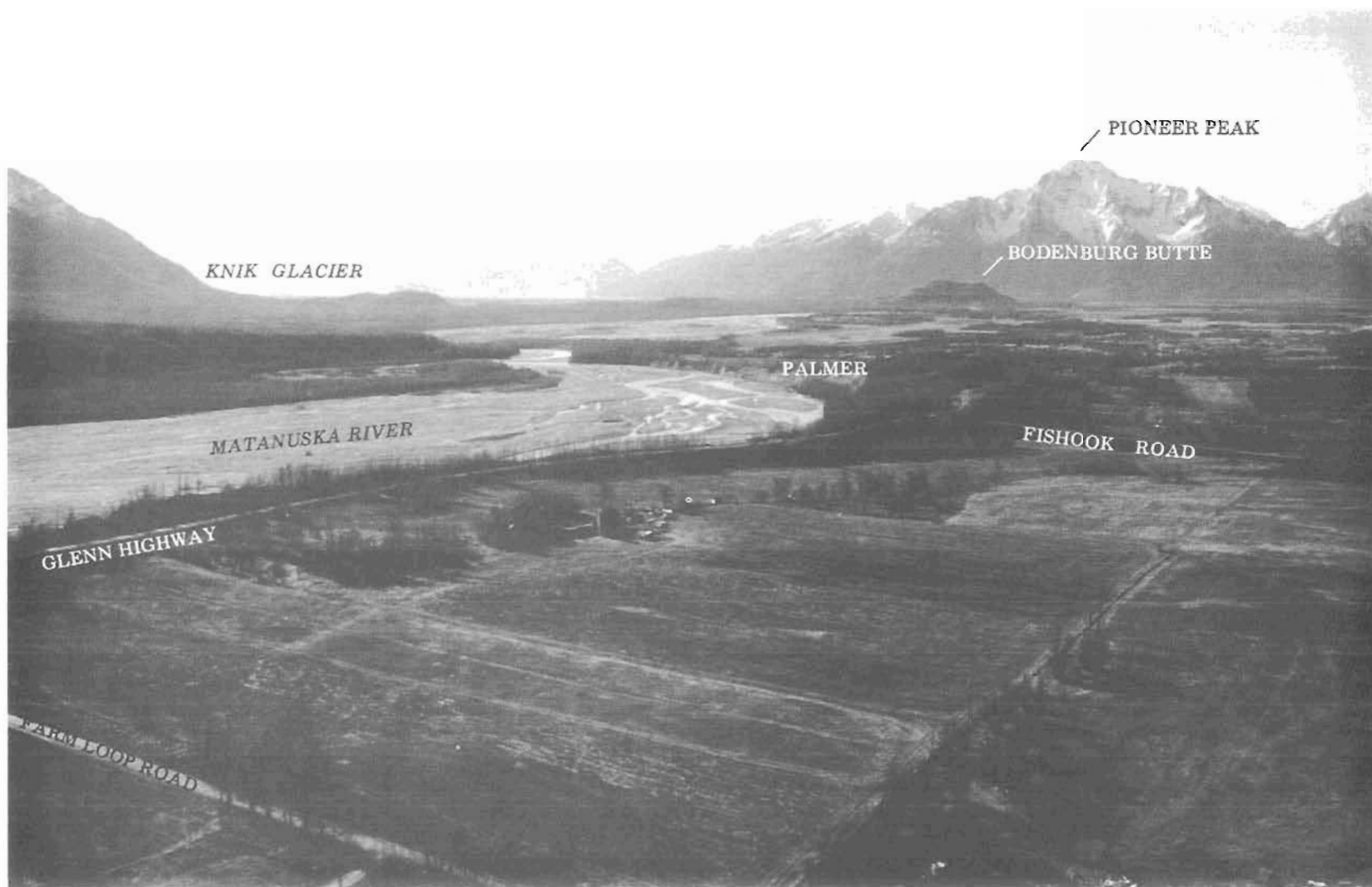


Figure 119. Oblique aerial view (to the southeast) of the Palmer area on a calm day when no loess is deflating from the flood plain of the Knik River, Anchorage Quadrangle, Alaska. Photograph 88-5 by R.D. Reger, May 21, 1982.



Figure 120. Oblique aerial view (to the south) of loess being deflated by the 'Knik wind' from the Knik River flood plain, Anchorage Quadrangle, Alaska. Photograph 91-10 by R.D. Reger, May 23, 1981.

41.6. Begin ascent through late Naptowne glaciofluvial deposits that thinly cover bedrock.

41. Knobs to the right (north) are composed of metasedimentary rocks of Permian or Jurassic age, or both.

40.9. Descent onto the 'Palmer terrace.' The high peak to the south-southeast (left front) is 6,398-ft-high (1,939 m) Pioneer Peak, a well-known, scenic landmark in the Palmer area. During dry weather in March 1949, a rock-fall on the northwest face of Pioneer Peak scattered rock debris to the vicinity of the old Glenn Highway with a rumble that could be heard throughout the valley (J.R. Williams, written commun.,³ January 10, 1983). Following almost a week of heavy rain, about 4,570 yd³ (3,494 m³) of water-saturated till and vegetation debris slid down the glacially steepened and smoothed northeast flank of Pioneer Peak on November 30, 1976, crashed into a house at the base of the mountain, and killed one person. To the southeast (left) is Bodenbug Butte, a roche moutonnée of quartz diorite (Jurassic in age) that stands about 750 ft (227 m) above a pitted surface that is equivalent to the 'Palmer terrace' across the Matanuska River.

The 'Palmer terrace' is fan-shaped, with its apex just north of Palmer. The terrace surface slopes about 35 ft per mi (6.7 m per km), which is intermediate between the shallower slope of the modern flood plain of the Matanuska River (about 26 ft per mi or 4.9 m per km) and the steeper gradient of the higher, slightly older terraces northwest of Palmer (about 40 ft per mi or 7.6 m per km). The 'Palmer terrace' formed by dissection of the former alluvial fan by the Matanuska River. The terrace tread is 30 to 75 ft (9.1 to 22.7 m) above the modern flood plain and is higher north of Palmer and lower to the south. Shallow, braided channels of former streams lace the gravel surface of the 'Palmer terrace,' but are obliterated by the thick loess blanket. The tread of the terrace is locally stepped by three discontinuous, 10- to 15-ft-high (3 to 4.6 m) scarps.

Several kettles that indent the 'Palmer terrace' as deep as 60 ft (18.2 m) are up to 0.2 mi (0.3 km) in diameter. Many kettles contain lakes, like McLeod Lake. Along the southwestern margin of the terrace, modern alluvium of the Matanuska River is filling one kettle that was formerly deeper than the level of the modern flood plain. Thickness of sediment in kettles varies considerably and does not seem to be directly related to the thickness of the eolian cover on the surrounding terrace tread; thicknesses range from little or nothing in the distal parts of the terraced fan to almost 7.5 ft (2.3 m) in the proximal area. Some fillings consist of silt without evidence of inwashing, and other pits are floored with interlayered silt, sand, and gravel that were obviously retransported. Trainer (1960, p. 23) reports a rare occurrence of permafrost in peat on the 'Palmer terrace' 0.75 mi (1.2 km) south of Palmer. This permafrost must be Holocene in age.

Because of irregularities in the bedrock surface beneath the 'Palmer terrace,' the thickness of terrace alluvium varies considerably. In the vicinity of Palmer, bedrock locally crops out on the terrace tread, and wells penetrate up to 30 to 65 ft (9.1 to 19.7 m) of sand and gravel before reaching till and then bedrock. Farther south, near the center of the 'Palmer terrace,' gravel alluvium is over 175 to 200 ft (53 to 60.6 m) thick. In the vicinity of Bodenbug Butte, sandy gravel alluvium is more than 110 ft (33.3 m) thick.

Based on his interpretation of water-well logs, Trainer (1960) reported the presence of as many as three tills (a surface till and two deeper tills) in the Palmer area.

40. The pitted terrace about 35 ft (10.6 m) above the 'Palmer terrace' to the right (northwest) slightly predates the 'Palmer terrace.'

39.2. A 39.6-ft-deep (12 m) kettle pits the 'Palmer terrace' to the right (northwest).

39. Junction of the Glenn Highway and Inner Springer Loop Road.

38.3. To the left (southeast), across the tracks of the Alaska Railroad, are the computer-monitored facilities for loading gravel aggregate onto railroad cars for transport to Anchorage, where much of the aggregate is made into concrete building products. The conveyor belt, which passes beneath the Glenn Highway through a large culvert, carries aggregate from a large pit in the 'Palmer terrace' about 0.1 mi (0.2 km) west of the Glenn Highway.

38.1. A similar gravel-mining operation extracts aggregate from the 'Palmer terrace' 0.1 mi (0.2 km) east of the Glenn Highway (fig. 121). From May through mid-October 1982, the Alaska Railroad hauled 2,753,755 tons (2,499,859 metric tons) of gravel aggregate in open hopper cars from the Palmer area to Anchorage at a cost of \$1.65 per ton (\$1.82 per metric ton). During the busiest periods, four 80-car trains made the 50 mi (80.5 km) trip each day; each hopper car carries 80 tons (72.6 metric tons) of aggregate. Hauling is suspended from mid-October to May, when the aggregate freezes in the hopper cars and is difficult to unload and when the demand for aggregate is greatly reduced. During this time, the cars are used to haul coal.

38. To the left (southeast) is a ridge of glaciofluvial gravel that is situated near the southeastern limit of a crevasse-fill complex that closely predates the 'Palmer terrace.' For the next 0.8 mi (1.3 km), the route of the field trip continues across fill of the 'Palmer terrace' between ridges of this crevasse-fill complex.

37.3. Begin ascent into the crevasse-fill-ridge complex in the vicinity of Bradley Lake. Roadcuts expose sandy gravel that was deposited in open channels between vertical walls of glacial ice about 10,000 yr B.P. These former ice canyons followed the arcuate pattern of subparallel crevasses that developed in stagnant ice of the Knik lobe. Steep-sided ridges of the complex are as high as 150 ft (45.5 m) and grade northeast into a complicated, coeval esker system that formed beneath thick dead ice of the Knik lobe west of Palmer (fig. 122). To the west, they grade into pitted outwash at a higher level than the 'Palmer terrace.' The crevasse-fill-ridge complex is mined for sand and gravel in the vicinity of Canoe and Irene Lakes, 0.3 mi (0.5 km) north of the Glenn Highway (fig. 123).

36.7. Kepler Lake is on the left (south).

36.6. Echo Lake is on the right (north). These lakes are part of a cluster of lakes that occupy oval to arcuate depressions between crevasse-fill ridges. The sites of the lakes were formerly occupied by dead-ice masses that were separated by meltwater streams depositing sandy gravel in channels that were open to the sky.



Figure 121. Oblique aerial view (to the north) of large gravel-extraction operation in pitted 'Palmer terrace' near McLeod Lake, Anchorage C-6 SW Quadrangle, Alaska. Photograph 87-12 by R.D. Reger, May 16, 1982.



Figure 122. Oblique aerial view (to the south-southwest) of esker and crevasse-fill-ridge complex west of Palmer, Anchorage Quadrangle, Alaska. Photograph 91-32 by R.D. Reger, May 26, 1982.



Figure 123. Oblique aerial view (to the southwest) of gravel-mining operation in crevasse-fill-ridge complex near Canoe and Irene Lakes, Anchorage C-6 SW Quadrangle, Alaska. Photograph 91-6 by R.D. Reger, May 23, 1981.

35.6. Begin descent from crevasse-fill complex.

35.5. Leave the crevasse-fill complex and traverse a low terrace of the Matanuska River.

35. Turn right on the Parks Highway and drive toward Wasilla.

35.2 (Parks Highway). Enter crevasse-fill complex.

35.5 (Parks Highway). Enter Anchorage C-7 Quadrangle.

35.4 (Parks Highway). STOP 36. TYPICAL CROSS SECTION THROUGH A CREVASSE-FILL RIDGE. The gently concave upward coarse bedding of the sandy gravel is a result of the progressive filling of an open channel through dead glacial ice (fig. 124). Dip reversal near the sides of the ridge is due to



Figure 124. View (to the southwest) of cross sections through crevasse filling of late Elmendorf (Naptowne) age, Anchorage C-7 SE Quadrangle, Alaska. Photograph 87-3 by R.D. Reger, May 15, 1982.

collapse caused by melting of the ice walls. Holocene loess forms a 1-ft-thick (0.3 m) blanket that is draped over the ridge.

The late Wisconsin glacial history of the Palmer-Wasilla area is very complicated because of the interactions of two large glacier systems and because of sudden climatic changes, but a broad array of intriguing evidence permits at least a general deciphering of the sequence of events.

Geomorphic and stratigraphic evidence in the western Matanuska Valley-Knik Arm area records a strong resurgence of the Knik lobe about 12,000 yr B.P., during a period when the Matanuska lobe was relatively stable but active. The Knik lobe advanced at least 13 mi (20.9 km) to the position of the Elmendorf Moraine just north of Anchorage (pl. 1), overriding a slightly irregular lowland in the lower parts of which the glaciomarine Bootlegger Cove Formation had been deposited. Bluff exposures and hundreds of boreholes in the Anchorage area prove that till and related outwash deposited during the Elmendorf readvance overlie the Bootlegger Cove Formation. Although slightly older moraines were notched (pl. 1), the Elmendorf Moraine was not notched (by waves) by the marine waters in which the Bootlegger Cove Formation was deposited. Outwash graded to the Elmendorf Moraine buried wave-cut scarps and dead ice west of Knik Arm. Lakes occupy some pits that remained after these ice masses melted.

Physiographic evidence for the difference in behavior of the Matanuska and Knik lobes is illustrated on plate 1. First, rock-cored drumlins east of Palmer that were clearly fashioned by ice flowing out of the Knik River valley cut across the trend of similar drumlins formed by ice flowing down the Matanuska Valley. Second, the orientations of drumlins in drumlin fields west and southwest of Palmer demonstrate an arcuate ice flow from west of Palmer to the Elmendorf Moraine. Third, the orientation of Rogen moraines south of the Little Susitna River documents compressive flow produced within the relatively slow-moving Matanuska lobe by the shoving Knik lobe. The debris-rich zone of crushing and fracture between the lobes was the focus for later intense englacial and subglacial meltwater activity and is the site of an extensive, linear network of eskers and chains of kettle lakes. Fourth, in the Big Lake area west of Knik Arm, a strong angular discordance between moraines of the Matanuska and Knik lobes is evident. The junction of the respective moraines coincides with the western end of the interlobate esker complex just mentioned.

Before stagnation of the Matanuska and Knik lobes (about 10,000 to 11,000 yr B.P.), classic de Geer moraines (not shown on pl. 1) formed on top of older Rogen moraines south of the Little Susitna River. Hundreds of these 6.6-ft-high (2 m), annual end moraines, which are commonly constructed of well-washed gravelly alluvium, are uniformly spaced 215 to 248 ft (65 to 75 m) apart across the Rogen moraine field. They are generally subparallel, although some cut across others, and they trend roughly north-south. The de Geer moraines are generally concave to the east in the upglacier direction and record a period of time (after culmination of the Elmendorf resurgence about 12,000 yr B.P.) during which most of the Matanuska lobe maintained a weak flow regimen, although the ice front was retreating. Relationships of de Geer moraines to the belt of eskers between the Matanuska and Knik lobes indicate that the debris-rich medial zone stagnated while at least weak flow continued in most of the Matanuska lobe. When the terminus of the Matanuska lobe had retreated

to just east of the Rogen-moraine field, flow within the lobe became sluggish and eventually ceased, and ice-stagnation features began to form. This stagnation occurred before 9,155 yr B.P. (pl. 1 and app. A, loc. C), probably about 10,000 yr B.P., as documented in the northern Talkeetna Mountains and north-central Alaska Range (fig. 106, cols. 4 and 6). That the lower 38 mi (61.2 km) of the Matanuska Glacier system collapsed about the same time is indicated by the presence of ice-stagnation deposits from the vicinity of Chickaloon to the east end of the Rogen-moraine field.

A similar history is postulated for the Knik lobe, although we have not found de Geer moraines in that lobe, and we suspect that both lobes did not behave similarly between 12,000 and 10,000 yr B.P., just as they did not behave similarly during the Elmendorf readvance. Apparently ice was higher or remained active slightly longer in the Knik lobe at the confluence of the Matanuska and Knik glaciers so that north of Palmer, the Matanuska River was initially diverted westward and deposited a thick, broad, complex, sandy fan over lower, dead ice of the Matanuska lobe. This fan undoubtedly took several years, and perhaps several decades or more, to build. Once the Knik lobe stagnated and began to thin, the Matanuska River began to change direction and character just north of Palmer. Trends and elevations of eskers west and northwest of Palmer and their relations to glaciofluvial terraces north of Palmer demonstrate that the river later flowed west-southwest into tunnels beneath stagnant ice of the Knik lobe to form the esker complex west and northwest of Palmer. A short time later, perhaps a few decades or so, after the Knik lobe had further thinned and the glacier terminus was situated close to Stop 36, the course of the Matanuska River was more southwest. About 3 mi (4.8 km) west of the present location of Palmer, subglacial streams emerged from tunnels and entered ice-walled, arcuate canyons to form the crevasse-fill complex we drove through between Miles 35.6 and 37.3. The heights of ridges in the crevasse-fill complex demonstrate that dead ice was over 150 ft (45.5 m) thick in the vicinity of Stop 36. Pitted-outwash terraces west of here are evidence that sand- and gravel-transporting streams built fans over thinner dead ice to the west.

The heights of terrace scarps north of Palmer and the uniform loess cover on terrace treads record rapid thinning of the Knik lobe and coincident down-cutting by the Matanuska River. The course of the Matanuska River concurrently changed to the south and southeast, and a broad fan was built in the Palmer-Bodenburg Butte area when small dead-ice masses were still present in the valley to levels below the modern flood plain of the Matanuska River. Later, dissection of the fan by the Matanuska River formed the 'Palmer terrace.' We do not know how deeply the Matanuska River was incised, but the period of major stream incision probably ended with the readvance of the Matanuska Glacier in the upper valley and the corresponding alluviation before 8,000 yr B.P.

During Holocene time, the dominant processes in the Palmer-Wasilla area have been eolian deposition and at least intermittent alluviation by glacier-derived streams, perhaps due to rising sea level or minor glacier advances.

Return to the Glenn Highway.

35.5 (Parks Highway). Enter Anchorage C-6 Quadrangle.

35. Turn right on the Glenn Highway and proceed toward Anchorage across a low terrace of the Matanuska and Knik Rivers.

34.6. Crossing of the Alaska Railroad.

33.6. Enter Anchorage C-7 Quadrangle.

33.2. The transition between terrace deposits and dominantly estuarine sediments is to the right (west), where there are numerous dead spruce trees that were killed by saltwater invasion after the March 27, 1964 earthquake. During that event, as a result of regional tilting and sediment compaction induced by intense ground shaking and associated soil liquefaction, this area settled 2 ft (0.6 m).

32.9. To the right (west) is an excellent view of 4,396-ft-high (1,332 m) Mount Susitna, the type locality of the Mount Susitna Glaciation. Beyond it is 11,100-ft-high (3,364 m) Mount Spurr, an active, andesitic, composite volcano. Fresh cirques of Knik and Naptowne age that are carved into the glacially rounded east and west flanks of Mount Susitna form classic biscuit-board topography (pl. 1). Mount Spurr erupted violently on July 9, 1953, propelling an ash cloud to 70,000 ft (21,212 m) elevation. West winds carried the cloud eastward across Anchorage, 80 mi (129 km) away. The 0.1 to 0.3 in. (0.3 to 0.8 cm) of volcanic ash that fell on Anchorage damaged internal combustion engines and was a nuisance to clean up. Ash from this eruption was reported as far east as 200 mi (332 km). Explosive activity ceased on July 16, 1953.

31.7. Enter Anchorage C-6 Quadrangle.

31.6. Crossing of the Matanuska River near its confluence with the Knik River. The Matanuska and Knik Rivers are building a compound estuarine delta at the head of Knik Arm (pl. 1). This reach of the Matanuska River is affected by daily tidal action.

The Matanuska River drains about 2,100 mi² (5,439 km²) of the northern Chugach and southern Talkeetna Mountains. Summer discharges range from 6,000 to 21,000 ft³ per s (170 to 594 m³ per s) and average about 10,000 ft³ per s (283 m³ per s). As an average, the typical, wide, braided reaches of the Matanuska River slope about 26 ft per mi (4.9 m per km), and channels shift radically and rapidly each summer, especially during short-term floods. The Matanuska River is transporting medium to coarse sand and gravel as bed-load material.

31.2. Enter Anchorage B-6 Quadrangle.

30.9. Crossing the north channel of the Knik River.

30.7. Crossing the middle channel of the Knik River.

30.3. STOP 37. VIEW OF WESTERN CHUGACH MOUNTAINS FRONT IN THE TWIN PEAKS AREA. Three mountain peaks are visible to the southeast of this location. On the left is 6,398-ft-high (1,939 m) Pioneer Peak, which is composed chiefly of metavolcanic and metasedimentary rocks of the McHugh Group. To the right are the Twin Peaks, which are made up of the McHugh Group in contact

downslope with ultramafic rocks (dominantly clinopyroxenites and dunites). The boundary between ultramafic rocks and the McHugh Group is the high-angle Border Ranges fault zone. Recent bedrock mapping has delineated a series of active faults that offset Holocene moraines and rock-glacier deposits upslope from the Border Ranges fault (fig. 125). Thus, the Border Ranges fault system is a potential seismic hazard for regional design and planning purposes.

On the slopes below Twin Peaks are lateral moraines deposited by Naptowne- and Knik-age advances of the Knik glacial lobe (fig. 125). The uppermost Naptowne lateral moraine forms a prominent bench near tree line. In addition, at least two more lower lateral moraines of the Naptowne Glaciation are evident. Above tree line, two subdued lateral moraines of Knik age are continuous along the mountain front. Along the skyline to the right is a gently sloping ridge that extends westward (to the right) and that appears to be flat topped. This ridge is composed of ultrabasic bedrock that is capped by scattered patches of till and numerous erratics. This surface was scoured by ice during a pre-Knik glaciation, perhaps during the Eklutna or Caribou Hills Glaciations. Holocene glaciers developed in the cirques on the northwest face of Twin Peaks and flowed generally northwest toward us. Five episodes of Holocene cirque glaciation and two periods of late Holocene rock-glacier activity are recorded in the cirques, but no active rock glaciers occur in the Twin Peaks area. On lower cirque walls, periglacial processes produced talus cones and aprons and small protalus ramparts and lobes. Extensive solifluction lobes and benches (many of which are active) are present on less rugged, tundra-covered alpine slopes.

The tide-influenced flood plain of the Knik River at Stop 37 is underlain by stratified silt, sand, and gravel that accumulated in the transition zone between a riverine environment upstream and an estuarine environment downstream. The combination of loose silt and sand, shallow ground water, and nearby active faults raises concern for earthquake-induced liquefaction of soils beneath this flood plain. Of particular concern are performances of bridges and roadways of the Glenn Highway and Alaska Railroad, because they constitute the only ground-transportation links between Anchorage and interior Alaska. The liquefaction potential of sediments in this area is being analyzed under seismic-loading conditions utilizing geotechnical borehole logs and electric cone-penetration tests (fig. 126) in conjunction with theoretical response models.

The Knik River drains about $1,200 \text{ mi}^2$ ($3,108 \text{ km}^2$) of the northern Chugach Mountains. Since 1966, summer flows have ranged from 8,000 to 31,000 ft^3 per s (226 to 877 m^3 per s) and have averaged about 20,000 ft^3 per s (566 m^3 per s). The slope of the lower, narrow reach of the Knik River near Stop 37 is 3 ft per mi (0.6 m per km), which is about half the slope of the upstream segment that is not restricted by the fan of the Matanuska River.

For several decades prior to 1967, except for 1963, the Knik River was subject to sudden, large-magnitude summer floods that were produced by the abrupt release of waters impounded in Lake George by the Knik Glacier, about 30 mi (48.3 km) southeast of Stop 37 (fig. 127). Between 1914 and 1963 and from 1964 through 1966, these floods occurred between mid-June and late August and lasted 12 to 15 days. Large-magnitude flooding of the Knik River is reported to have destroyed native villages as early as 1899 and reportedly occurred in 15- to 20-yr cycles prior to 1914.



Figure 125. Aerial view (to the south) of the Twin Peaks area, western Chugach Mountains front, Anchorage B-6 Quadrangle, Alaska, showing highest levels of Eklutna, Knik, and Naptowne Glaciations. The active Twin Peaks fault displaces Pleistocene and Holocene deposits and bedrock of the McHugh Group. Photograph by R.G. Updike, April 10, 1981.

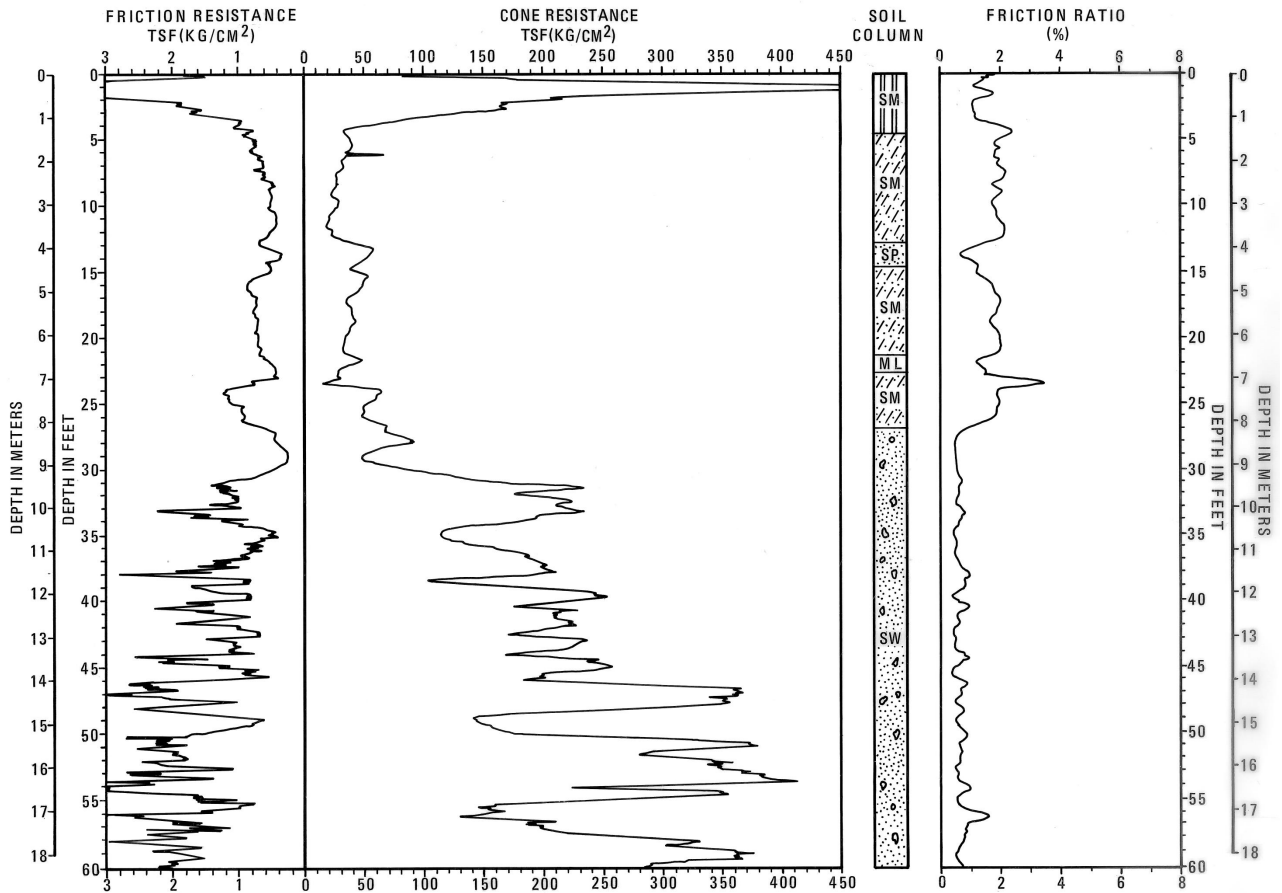


Figure 126. A representative electric cone-penetration test (CPT) through sediments at Stop 37. Uniform Soil Classification symbols: SM, sandy silt; SP, well-sorted sand; ML, inorganic silt; and SW, well-graded gravelly sand. The upper 4 ft (1.3 m) of sandy silt was seasonally frozen at the time of the test (April 9, 1982) (Ertec Western, 1980, probe DR-C-04).

The Lake George basin was formed in late Holocene time by partial deglaciation of the lowland on the south side of the terminus of the Knik Glacier. The basin collects runoff from about 350 mi² (907 km²) of the surrounding mountainous terrain. During the winter prior to each outburst flood, the Lake George basin was closed when the 25-mi-long (40.3 km) Knik Glacier advanced against the northeast flank of Mt. Palmer and formed an ice barrier 250 to 400 ft (75.8 to 121 m) high. The lake basin began filling the following spring and eventually the water level rose to as high as 160 ft (48.5 m) above the level of the drained lake (fig. 128A). At its fullest, the surface area of Lake George was about 28 mi² (73 km²). Depending on the thickness of the glacier dam, lake waters eventually reached a critical level at which they developed sufficient hydraulic head to force flow along the base of Knik Glacier where it pressed against Mt. Palmer. Several hours after lake waters began flowing beneath the southern margin of Knik Glacier, they reached

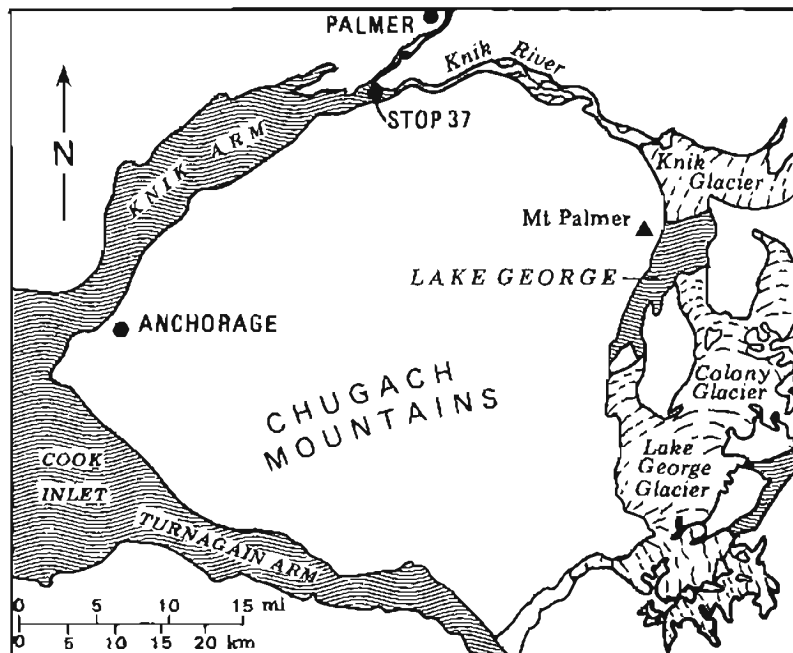
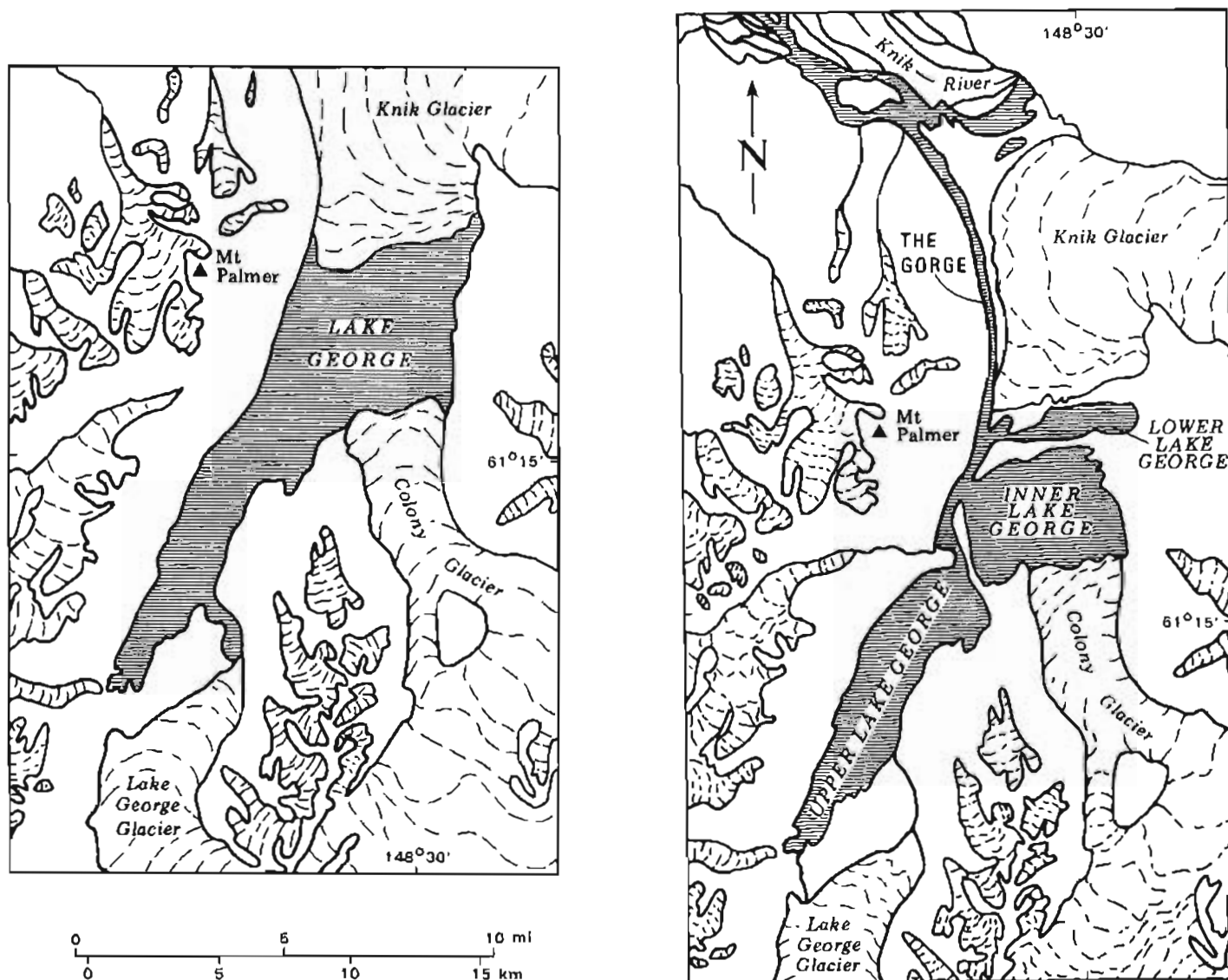


Figure 127. Location of the former Lake George, Knik Glacier, and the Knik River relative to Stop 37 (from U.S. Geological Survey, 1969).

the Knik River. Once a subglacial course was established, the rate of flow through the tunnel increased rapidly, and the undermined glacier terminus collapsed to form 'The Gorge', a deep moat between the glacier and Mt. Palmer (fig. 128B).

The effects of the outbreak of Lake George on the Knik River were dramatic. Within less than a week, initial discharges of 5,000 to 6,000 ft³ per s (142 to 170 m³ per s) in the Knik River were boosted by outburst waters to rates as high as 355,000 ft³ per s (10,047 m³ per s) (fig. 129). Flood waters passing the old Glenn Highway bridge 17.5 mi (28.2 km) downstream from Knik Glacier measured 560,000 to 1,800,000 acre-ft (693,000,000 to 2,227,500,000 m³) per year. During floods, the Knik River generally transported sand and fine gravel and numerous ice masses. 'The Gorge' grew in size by thunderous collapse of the ice (east) wall and reached widths of 100 to 400 ft (30.3 to 121.2 m). A complete, 300-ft-thick (90.9 m) section through lower Knik Glacier was revealed in the east wall of 'The Gorge.' Upon completion of the drainage cycle, former Lake George was reduced to three small remnant lakes separated by late Holocene moraines: Lower Lake George at 228 ft (69 m) elevation, Inner Lake George at 261 ft (79 m) elevation, and Upper Lake George at 254 ft (77 m) elevation (fig. 128B).

Flow dynamics of the Knik Glacier control the outburst cycle of Lake George. Recent thinning of Knik Glacier has slowed ice flow in the terminal zone so that the glacier no longer closes 'The Gorge.' As a result, Lake George has not filled since 1966, and the former spectacular outburst floods no longer occur. A long-term, cooperative program between DGGS and the U.S.



A. Filled condition in early summer. During winter, Knik Glacier pressed against the northeast flank of Mt. Palmer to form a 250- to 400-ft-thick (75.8 to 121.2) ice dam and seal the lake basin. The impounded basin began to fill during breakup the following spring.

B. Drained condition the following fall. Soon after flow commenced through the ice dam along the base of Mt. Palmer later each summer, Lake George drained abruptly. In the drained state, the Lake George basin is divided into three small lake basins by late Holocene moraines.

Figure 128. Annual outburst cycle of Lake George from 1918 through 1966, except 1963 (from U.S. Geological Survey, 1969).

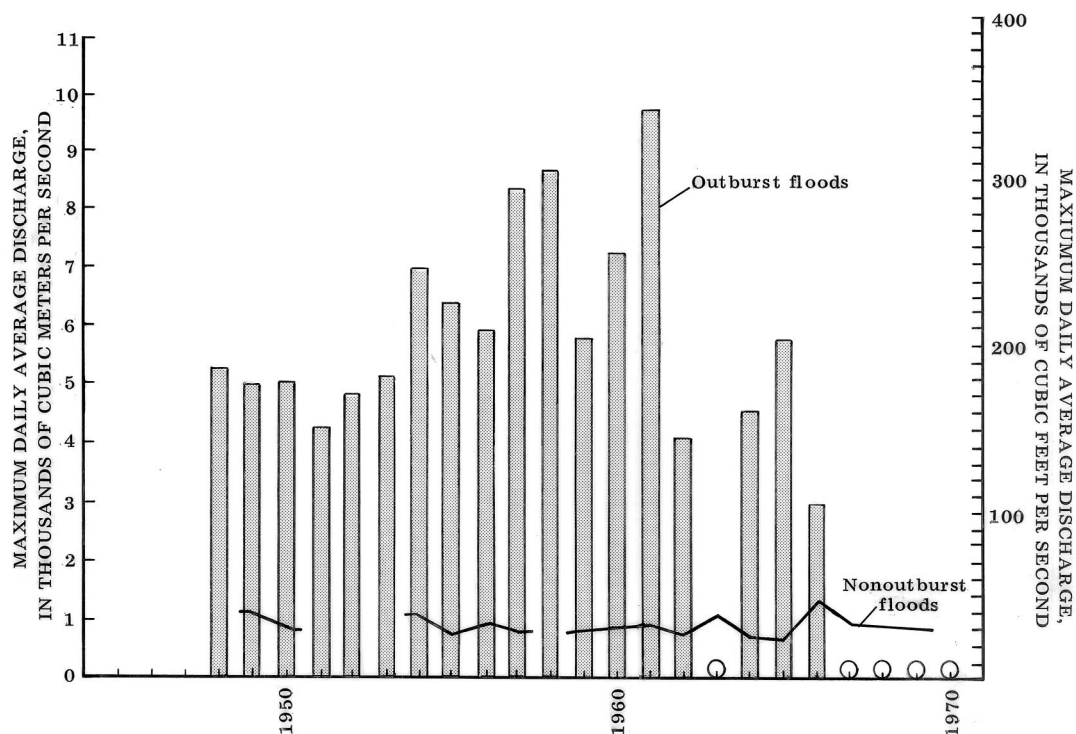


Figure 129. Prior to 1967, the abrupt draining of Lake George caused outburst floods with discharges in excess of nonoutburst floods in the Knik River. The lake failed to refill (open circles) in 1963 and after 1966 (from Post and Mayo, 1971, sheet 1).

Geological Survey monitors the mass balance of Knik Glacier in an attempt to forecast future outburst cycles.

29.9. Crossing the south channel of the Knik River. Enter Anchorage B-7 Quadrangle.

29.7. To the left (southeast) is an outcrop of late Paleozoic-Mesozoic(?) metasedimentary and metavolcanic rocks that was overridden and scoured by ice of the Knik lobe during the Naptowne Glaciation.

25.7. Exit to Eklutna Village to the right (northwest). The Glenn Highway traverses a broad alluvial fan built by the Eklutna River at the mouth of a steep-walled gorge cut in bedrock in the lower Eklutna valley. This fan postdates the recession of ice from the Elmendorf Moraine after 12,000 yr B.P. and is a gravel source for the Peters Creek area.

25. Crossing of the Eklutna River. Flow in this stream is regulated by a dam at the lower end of Eklutna Lake, 8.4 mi (13.5 km) east of the Glenn Highway. Water from Eklutna Lake drains through a tunnel beneath East Twin Peak to the Eklutna Powerhouse at the northern base of the Chugach Mountains along the old Glenn Highway 7.6 mi (12.2 km) east of here. The feasibility of carrying tailrace water from the powerhouse through a pipeline to the Anchorage area (where there is a water shortage) is under study.

The type section of the Eklutna Glaciation, as designated by Karlstrom (1964; 1965), is exposed in the lower walls of the Eklutna River valley about 5.5 mi (8.9 km) east of the Glenn Highway. At the top of the section is 50 to 60 ft (15 to 18 m) of fresh, medium-gray Naptowne till, which in part relates to three end moraines on the valley floor (pl. 1). Underlying the Naptowne till is a thin, discontinuous, sandy, advance outwash gravel that was laid down over an angular unconformity that cuts across mottled grayish-yellowish-buff-colored, bouldery bedded sand. The cliff-forming bouldery sand unit is about 50 ft (15 m) thick, dips gently downvalley, and interfingers downsection and downvalley with a 50- to 60-ft-thick (15 to 18 m) sequence of subaqueous-flow diamictons that are intensely deformed near the mouth of the Eklutna valley. The boulder-rich sand is a fan-delta deposit that prograded into an ice-dammed lake of late Knik or possibly early Naptowne age; the lake was impounded by the Knik lobe in the main valley at a time when the lower Eklutna valley was free of glacial ice. Numerous boulders represent dropstones dumped from melting icebergs into the fan-delta sequence, and the subaqueous diamictons were deposited in the deeper part of the lake basin closer to, and even against, the ice dam at the mouth of the valley. Later, melting of the ice barrier deformed the diamictons near the main valley. The distinctive, yellowish-buff staining of the unit is attributed to discoloration induced by iron-bearing ground water moving through the unit and not to deep weathering as interpreted by Karlstrom (1964; 1965). This reinterpretation of the section shows that deposits of Eklutna age, if present, are not exposed.

24.5. Begin 8-mi (12.9 km) traverse through a drumlin field formed during resurgence of the Knik lobe to the Elmendorf Moraine.

22.8. Mirror Lake is on the left (southeast). The steep, deeply gullied rock wall across the lake exposes metasedimentary and metavolcanic rocks of Paleozoic-Mesozoic(?) age. This wall was scoured by ice during the Eklutna, Knik, and Naptowne Glaciations to present elevations of 2,800, 1,800, and 1,400 ft (848, 545, and 424 m), respectively. Above 3,100 ft (939 m) elevation and bevelled at a sharp angle to the steep, younger valley wall is a bedrock surface that was probably scoured by ice of the Caribou Hills Glaciation (fig. 130). Very little remains of the former glacial deposits on that upland surface, although remnants of ice-marginal drainage channels are preserved. Another part of the same highly dissected, glaciated surface is visible to the left front (south-southwest) at 2,600 to 3,300 ft (788 to 1,000 m) elevation south of Peters Creek.

20.5. Crossing of Peters Creek, one of several major tributary valleys that trends northwest to west to the front of the Chugach Mountains. The valley of Peters Creek supplied ice to the trunk glacier in the main valley during the Eklutna, Knik, and Naptowne Glaciations. The Peters Creek drainage contains several recessional moraines of late Naptowne age.

19.6. Note the ice-scoured knobs of Paleozoic-Mesozoic(?) metasedimentary and metavolcanic rocks to the left (southeast). To the right (northwest) are 12,000-yr-old drumlins formed during the late Naptowne readvance to the Elmendorf Moraine. Lowland depressions contain peat fillings with occasional permafrost.



Figure 130. Oblique aerial view (to the east) of high-level surface west of Mount Eklutna glaciated in Caribou Hills time, Anchorage B-7 Quadrangle, Alaska. Photograph 91-34 by R.D. Reger, May 26, 1982.

The distribution and character of permafrost in the Anchorage area are not well known. This area is near the extreme southern limit of permafrost, where the coldest ground temperatures are very close to 32°F (0°C). The frozen state is very unstable, and minor site differences strongly control the distribution of permafrost. Perennially frozen ground occurs in exceptionally favorable circumstances, such as beneath black-spruce 'islands' that have an insulating ground cover of *Sphagnum* and feather mosses 10 to 12 in. (25.4 to 30.5 cm) thick and that develop on raised bogs growing on thick peat. Depression fillings of peat that probably contain permafrost are commonly 5 to 8 ft (1.5 to 2.4 m) thick and locally reach thicknesses up to 30 ft (9 m).

The presence of considerable moisture generally precludes the preservation of permafrost, especially if the water is flowing. Ground water in the Anchorage area commonly ranges from 36° to 39°F (2.2° to 3.9°C) and averages 37°F (2.8°C). Thus, permafrost does not generally occur near springs or beneath surfaces that receive ground-water seepage from higher, nearby slopes.

Lee (1977) estimated that permafrost underlies 2 to 5 percent of the Anchorage area. Deleterious thawing of ice-rich permafrost has caused the destruction or relocation of several structures, including many single-family dwellings and some large commercial buildings. The largest known masses of

permafrost measure about 30 acres (121,410 m²) in area, and numerous isolated pods with areas of 500 to 600 ft² (46.5 to 55.7 m²) are present. These masses of perennially frozen ground invariably occur at depths of 15 and 35 ft (4.5 to 10.6 m). Ice is present in the form of coatings on clasts, pore ice, irregular masses typically up to 1 ft (0.3 m) in diameter, and massive lenses and layers as thick as several inches to several feet. In 1956, excavations in Spenard in the central Anchorage area exposed a ground-ice lens that measured several tens of feet across and was more than 10 ft (3 m) below the ground surface in the Bootlegger Cove Formation. The presence of ice-rich permafrost in this 13,000 ± yr-old glaciomarine deposit indicates that permafrost in the Anchorage area is latest Wisconsinan or younger in age and could have developed beneath the emerging estuarine plain under exceptionally cold climatic conditions during the Elmendorf readvance. The uniform great depth to permafrost in the Anchorage lowland is evidence that perennially frozen ground is relict and not a product of the modern climate.

Active rock glaciers at higher elevations in the Chugach Mountains east of Anchorage document the presence of Holocene permafrost.

16.7. Overpass. The drumlin on the left (southeast) is cored by Paleozoic-Mesozoic(?) metasedimentary and metavolcanic rocks that are highly faulted and sheared. Springs along bedrock joints in the cuts form hillside icings that pose serious maintenance problems each winter.

15.7. To the left (east), Lower Fire Lake occupies a shallow glacial trough cut into bedrock. Lateral moraines on the slope east of the lake document former ice levels: 2,650 ft (803 m) during the Eklutna Glaciation; 1,800 ft (545 m) during the Knik Glaciation; and 1,400 ft (424 m) during the Naptowne Glaciation. Upper Fire Lake (not visible) occupies a former sideglacial stream channel of late Naptowne age 0.6 mi (1 km) east of the Glenn Highway.

12.9. Good view to the east-northeast (left) of part of the dissected, high-level (3,300 ft or 1,000 m) surface of Caribou Hills age; this bedrock surface was scoured by ice flowing transverse to the tributary valleys. The upper part of the former valley wall is at about 4,000 ft (1,212 m) elevation.

12.2. Crossing of Eagle River. The valley of Eagle River was blocked by the Knik lobe during the resurgence (in late Naptowne time) to the Elmendorf Moraine. At that time, much of lower Eagle River valley was apparently free of ice, and a lake was at least temporarily impounded. The lack of adequate water in the thick sequence of fine-grained lacustrine deposits and inter-layered silty till in the rapidly populating lower valley of Eagle River is causing serious water-shortage problems.

Overflow waters from the ice-dammed lake and ice-marginal streams drained through a complex network of spillways cut in ice-contact deposits in the Fossil Creek-Qtter Lake-Sixmile Lake area. These meltwater courses closely postdate the 12,000-yr-old Elmendorf Moraine.

Another serious problem related to recent development in Eagle River valley is snow avalanching. As population pressures increase in the valley, homes are built near the base of steep mountain slopes in the paths of dangerous snow avalanches.

A very large rock slide that probably moved on a cushion of trapped air covers most of the floor of Eagle River valley 13 mi (20.9 km) east of the Glenn Highway (pl. 1). This feature is typical of several large slides in the higher Chugach Mountains in this area. The landslides appear to be post-Naptowne in age, and many were probably released from glacially oversteepened slopes by the loss of support during deglaciation.

Weakly consolidated, fine-grained, clastic sedimentary rocks of Tertiary age crop out along the south bank of Eagle River just downstream (right) from the bridge.

11.3. The Glenn Highway cuts through gravelly ice-contact deposits just east of the ancient spillway now occupied by Fossil Creek.

10.6. Roadcut through 12,000-yr-old Elmendorf Moraine.

10.4. Crossing outwash gravel fan graded to the Elmendorf Moraine and sloping to the southwest to form the surface upon which Anchorage is constructed.

9.3. Enter Anchorage B-8 Quadrangle.

7.2. The Glenn Highway leaves the outwash surface graded to the Elmendorf Moraine and for 1.5 mi (0.9 km) passes between two parallel discontinuous drumlin belts.

6.7. Enter Anchorage A-8 Quadrangle.

6.1 to 5.3. Leave drumlin belts and cross the alluvial fan of Ship Creek, which laps onto the 12,000-yr-old outwash surface graded to the Elmendorf Moraine.

5.6. Crossing of Ship Creek.

4.8 to 4. The Glenn Highway passes between two parallel, discontinuous belts of drumlins that are continuations of the belts between Miles 7.2 and 6.1. Individual drumlins are elongate north to north-northeast, which indicates that they formed by extending ice flow from the north (pl. 1). The discrete, southwest-trending arcs of the belts on either side of the Glenn Highway are but two of a series of discontinuous, arcuate drumlin belts in the eastern and southeastern Anchorage lowland. These drumlins were previously attributed to the Knik Glaciation (Miller and Dobrovolsky, 1959, p. 25), but evidence encourages another interpretation. The drumlins contain two tills: a) a 3-ft-thick (0.9 m), upper, platy till with horizontal partings, and b) a 4-ft-thick (1.2 m), compact, lower till. In our opinion, these two tills and the arcuate forms of the belts are evidence for two Naptowne glaciations of the Anchorage lowland. A glaciation from the north, probably of early Naptowne or perhaps early late Naptowne age, initially deposited a series of nested, arcuate, recessional end moraines across the lowland. These end moraines were overridden and remolded into drumlins during a later glacier expansion (perhaps about 18,000 to 20,000 yr B.P.) when ice of the Knik lobe advanced to an extended position south of Fire Island (pl. 1).

3.5 to 2.7. The Glenn Highway crosses a former distributary or diversionary channel of Ship Creek that is 0.8 to 1.5 mi (1.3 to 2.4 km) south of and subparallel to the present course of Ship Creek. The alternate courses of Ship Creek split 0.6 mi (1 km) downstream from the toe of the Ship Creek fan, which we crossed at Miles 6.1 to 5.3. These courses are graded to a sea level below modern sea level and their lower valleys are filled by high-level tidal-flat silty clay that was deposited during a rise in sea level in the past 3,000 to 5,000 yr (Kasilofian Transgression of Karlstrom, 1965) (pl. 1). The present (west) gradient of Ship Creek between the toe of its fan and Knik Arm is 43 ft per mi (8.2 m per km). By comparison, the Elmendorf outwash surface slopes west-southwest at 31 ft per mi (5.9 m per km). The former course of Ship Creek that we are traversing descends at an average slope of 36 ft per mi (6.8 m per km) from near the level of the Elmendorf outwash surface in the east near the Ship Creek fan; in the west, near the mouth of the incised valley, it is cut 70 ft (21.2 m) below the level of the Elmendorf outwash surface. The western half of the valley is presently occupied by Chester Creek.

2.7. Turn right onto McCarrey Street and drive up the scarp cut into the Elmendorf outwash onto the outwash plain.

0.2.³² McCarrey Street curves to the left (west) and becomes Mountain View Drive. Beyond two traffic lights, Mountain View Drive becomes Commercial Drive; continue west on Commercial Drive. Between Miles 0.2 and 2.3, the route traverses the outwash plain related to the Elmendorf Moraine. This surface is actually terraced into four closely spaced levels. The highest and oldest level is situated close to the Elmendorf Moraine near Knik Arm and is pitted (pl. 1), indicating that it is coeval with the moraine. The two intermediate levels are small and probably closely postdate the Elmendorf Moraine. The lowest, youngest terrace is the most widespread and underlies most of the Anchorage area ('Anchorage plain'). H.R. Schmoll (personal commun., 1979) believes this surface is considerably younger than the oldest terrace and traces it up into the Eagle River drainage.

Because mining for gravel and sand in the outwash has depleted most of the available aggregate in the Anchorage area, aggregate is delivered by railcar from the Palmer area. The sandy gravel and silty sand of the Elmendorf outwash overlie the Bootlegger Cove Formation and are in turn overlain by thin organic silt and discontinuous peat layers of Holocene age. A post-Naptowne podzol (spodosol) that is 3.8 to 8.9 in. (9.6 to 22.6 cm) thick has developed beneath the present surface.

2.3. Begin descent from the surface of the Elmendorf outwash plain on an old landslide scarp. Note the breaks in the roadway, which suggest that the slide is still creeping. The scarp that forms the bluff to the left (south) predates 1964, although the landslide below the scarp was reactivated during the great earthquake of March 27, 1964. After 1964, heavy construction began on this landslide.

2.6. Intersection of Post Road and Commercial Drive (traffic light); continue straight ahead (west) on 3rd Avenue.

³²Route mileage is reset to 0.0 at the traffic light at the junction of Glenn Highway and McCarrey Street.

2.9. Begin ascent of pre-1964 landslide scarp onto Elmendorf outwash surface.

3. On the right (north) is the Alaska Native Hospital, which was built several years prior to 1964 and survived the earthquake of March 27, 1964. Directly north, beyond the hospital, is a large landslide that occurred on March 27, 1964, along the south bluff of Ship Creek as a result of failure of the Bootlegger Cove Formation. Other large, preexisting landslides that were documented along the bluff in this area were partially reactivated in 1964.

3.3. Descent down a low, pre-1964 slide scarp. The tall, pink building on the left (south) that straddles the slide scarp was severely damaged during the earthquake of March 27, 1964, but was later repaired and reoccupied.

3.6. Turn right at 'A' Street and cross Ship Creek overpass. The valley of Ship Creek is eroded deeply into the Bootlegger Cove Formation and the overlying glaciofluvial deposits and is partially filled with up to 15 to 20 ft (4.6 to 6.1 m) of Holocene fluvial silt, sand, and gravel. The valley-fill alluvium grades west into high-level, tidal-flat deposits. Geotechnical borehole logs for the 'A' Street overpass indicate that the sediments in Ship Creek valley become coarser with depth, varying from silty sand and silt with lenses of sandy gravel near the surface to sandy gravel with sand lenses at depth. Most alluvium has been buried by artificial fill during the past 50 yr. Holocene sediments are loosely to moderately packed and are at or near saturation, which makes them susceptible to limited liquefaction during strong earthquakes.

3.8. Take Port Exit to the right. Pass over 'A' Street and veer left onto Ocean Dock Road.

4.3. Turn left onto Whitney Road and cross the Alaska Railroad tracks.

4.4. Turn left and proceed through the Alaska Railroad complex, under the 'A' Street overpass, past the large railroad maintenance and repair building to the toe of the 1964 Government Hill School landslide.

5.1. STOP 38. GOVERNMENT HILL SCHOOL LANDSLIDE. Among sites in the vicinity of Anchorage that exhibited multiple ground failures during the 1964 Prince William Sound earthquake, the Government Hill area in north Anchorage attracted particular attention because of the great variety of local earthquake-induced damage and the critical role of the area in Alaska's ground-transportation network. With the exception of studies immediately after the 1964 earthquake, very little work was conducted in the area until recently.

In addition to the Government Hill School landslide, which was the focus of most post-1964 geotechnical studies, another large landslide occurred along the bluff to the north, and numerous ground cracks were produced in fill and in tidal-flat deposits adjacent to Government Hill. The entire bluff in this area was also involved in massive landslides before 1964. Several structures have been built on these older slides or on the upland at the heads of the slides. After the 1964 earthquake, several instances of soil instability beneath or adjacent to structures erected on these features demonstrate the

need for a better understanding of the local geology and engineering properties of the subsurface materials.

The Quaternary section here is probably several hundred feet thick. Late Pleistocene deposits consist of two stratified, glaciofluvial sand and gravel units that are separated by the Bootlegger Cove Formation,³³ perhaps the best-known geologic unit in south-central Alaska.

In-situ exposures of the Bootlegger Cove Formation in the Anchorage area are limited by the accumulation of colluvium, including widespread landslide deposits on bluff faces. The thickness of this formation in the Government Hill area ranges from less than 100 ft (30 m) to greater than 215 ft (65 m), reflecting the irregular floor of the depositional basin and differences in the elevation at the top of the formation.

The Bootlegger Cove Formation consists of seven distinctive facies that range from finely laminated silt and clay to thin-bedded, fine to medium sand to massive, clayey silt with random gravel (diamicton) (table 5). These

Table 5. Mean values for physical parameters of engineering-geologic facies in the Bootlegger Cove Formation, Government Hill area, Anchorage, Alaska, based on analyses of several hundred samples.

Characteristic	Engineering geologic facies						
	I	II	III	IV	V	VI	VII
General composition	Clay with minor silt and sand	Silty clay or clayey silt	Dynamically sensitive silty clay or clayey silt	Silty clay or clayey silt with silt and sand lenses	Silty clay or clayey silt with diamicton	Silty fine sand with silt and clay layers	Fine to medium sand with traces of silt and gravel
Mean grain size (mm)	0.0014	0.004	0.004	0.015	0.006	0.15	0.37
Moisture content (%)	29.8	28.4	29.8	28.0	28.5	25.0	29.1
Plastic limit (% moisture)	23.0	22.1	22.0	20.5	22.2	Nonplastic	Nonplastic
Liquid limit (% moisture)	39.0	37.2	28.3	34.8	36.9	Nonviscous	Nonviscous
Plasticity index (% moisture)	16.0	15.1	7.0	16.0	14.7	Nonplastic	Nonplastic
Liquidity index	0.43	0.42	1.10	0.47	0.42	Nonviscous	Nonviscous
Shear strength (tons/ft ²)	0.49	0.79	0.52	0.69	1.09	0.61	No data available
Compressive strength (tons/ft ²)	1.69	1.45	0.92	1.16	1.91	1.32	No data available
Sensitivity ratio	8.9	2.8	14.2	6.1	4.1	Non-sensitive	Non-sensitive

³³This complex unit of late Naptowne age (fig. 106) was originally named the Bootlegger Cove Clay (Miller and Dobrovlny, 1959) for typical sections exposed at Bootlegger Cove in southwest Anchorage. Because the unit varies in composition and because clay is commonly only a secondary constituent, the name was changed (Updike, 1983).

facies are products of subaerial glaciofluvial, glaciomarine, and glaciolacustrine environments, but the dominant environment of deposition was glaciomarine. Occasional abrupt transitions occur between facies, but facies also grade gradually into each other in vertical and horizontal directions. Each facies has particular physical characteristics that together with post-depositional influences like over-consolidation, permafrost, and ground-water leaching, determine the behavior of the facies under static and dynamic conditions (table 5). In the Anchorage area, most of the Bootlegger Cove Formation is a moderately reliable foundation material, but the presence of even minor amounts of certain facies may produce slope and foundation instability. For example, facies III is generally highly sensitive to dynamic loading, and facies IV and V, where they occur at appropriate depths and with sufficient moisture, pose potential liquefaction hazards.

After deposition of the Elmendorf outwash about 12,000 yr B.P., relative sea level in the Anchorage area lowered, probably in response to isostatic rebound and vertical crustal movements of tectonic origin. Ship Creek responded by eroding deep into both the outwash and the Bootlegger Cove Formation. In this area, stream erosion and mass wasting have removed the upper 100 ft (30 m) of the section along Knik Arm and Ship Creek. Tidal-flat deposits partially filled lower Ship Creek valley during the late Holocene rise in sea level, and landslides accumulated along the base of the retreating valley walls.

The 1964 Government Hill School landslide, like most other major failures in the Anchorage area, was directly caused by failure in the Bootlegger Cove Formation. These massive failures resulted from seismic loading, oversteepened slopes, undercutting of the toe of slopes, ground-water piping, induced loading at the heads of former slides or directly on free-face slopes, and lateral spreading due to removal of support. The landslides are composed of material from the Bootlegger Cove Formation and overlying glaciofluvial alluvium, but the stratigraphy is chaotic and the material is broken into detached blocks. Thus, exposures at Stop 38 range from clay to coarse gravel, and silt and sand are the dominant grain-size classes. Surface and groundwater characteristics in the vicinity of the landslides are also quite variable, primarily due to the development of hummocky topography that interferes with surface drainage and disrupts subsurface water-bearing strata. Several springs occur along the toe of this slide. Elsewhere in Anchorage, artesian ground-water conditions exist in large slides, but tilt-block ridges are usually better drained. Surface runoff quickly retransports the poorly consolidated material downslope in landslide ridges that round and smooth slide topography in a few years. This process has already modified the morphology of the 1964 Government Hill School landslide.

Selected References

- Bacon, Glenn, 1975, Preliminary testing at the Long Lake archeological site: Alaskan Anthropology Conference, 2nd, Fairbanks, March 15, 1975, 24 p.
- Barnes, F.F., and Payne, T.G., 1956, The Wishbone Hill district, Matanuska coal field, Alaska: U.S. Geological Survey Bulletin 1016, 87 p.
- Barnwell, W.W., George, R.S., Dearborn, L.L., Weeks, J.B., and Zenone, Chester, 1972, Water for Anchorage, an atlas of the water resources of the Anchorage area, Alaska: City of Anchorage and the Greater Anchorage Area Borough, 77 p.

- Benninghoff, W.S., 1957, Recent contributions to Quaternary vegetation history in Alaska [abs.]: Alaskan Science Conference, 5th, Anchorage, 1954, Proceedings, p. 28.
- Bradley, W.C., Fahnestock, R.K., and Rowekamp, E.T., 1972, Coarse sediment transport by flood flows on Knik River, Alaska: Geological Society of America Bulletin, v. 83, no. 5, p. 1261-1284.
- Broecker, W.S., Kulp, J.L., and Tucek, C.S., 1956, Lamont natural radiocarbon measurements III: Science, v. 124, no. 3213, p. 154-165.
- Capps, S.R., 1927, Geology of the upper Matanuska Valley, Alaska: U.S. Geological Survey Bulletin 791, 92 p.
- Cederstrom, D.J., Trainer, F.W., and Waller, R.M., 1964, Geology and ground-water resources of the Anchorage area, Alaska: U.S. Geological Survey Water Supply Paper 1773, 108 p.
- Clardy, B.I., Hanley, P.T., and LaBelle, Joe, 1982, Field trip guidebook: Anchorage to Matanuska Glacier: Anchorage, Alaska Geological Society, 38 p.
- Clark, S.H.B., 1973, The McHugh Complex of south-central Alaska: U.S. Geological Survey Bulletin 1372-D, 11 p.
- Collins, S.G., 1975, Glaciers of the Talkeetna Mountains, Alaska, in Field, W.O., ed., Mountain glaciers of the Northern Hemisphere: U.S. Army Cold Regions Research and Engineering Laboratory report, v. 2, p. 543-548.
- Conwell, C.N., Triplehorn, D.M., and Ferrell, V.M., 1982, Coals of the Anchorage Quadrangle, Alaska: Alaska Division of Geological and Geophysical Surveys Special Report 17, 8 p., 4 sheets
- Daniels, C.L., 1981a, Geologic and materials maps of the Anchorage (C-7 SE) Quadrangle, Alaska: Alaska Division of Geological and Geophysical Surveys Geologic Report 67, scale 1:25,000, 2 sheets.
- _____, 1981b, Geologic and materials map of the Anchorage (C-7 SW) Quadrangle, Alaska: Alaska Division of Geological and Geophysical Surveys Geologic Report 71, scale 1:25,000, 2 sheets.
- Denton, G.H., 1974, Quaternary glaciations of the White River valley, Alaska, with a regional synthesis for the northern St. Elias Mountains, Alaska and Yukon Territory: Geological Society of America Bulletin, v. 85, no. 6, p. 871-892.
- Detterman, R.L., Hudson, Travis, Plafker, George, Tysdal, R.G., and Hoare, J.M., 1976, Reconnaissance geologic map along Bruin Bay and Lake Clark faults in Kenai and Tyonek Quadrangles, Alaska: U.S. Geological Survey Open-file Map 76-477, scale 1:250,000, 1 sheet.
- Detterman, R.L., Plafker, George, Hudson, Travis, Tysdal, R.G., and Pavoni, Nazario, 1974, Surface geology and Holocene breaks along the Susitna segment of the Castle Mountain fault, Alaska: U.S. Geological Survey Miscellaneous Field Studies Map MF-618, scale 1:24,000, 1 sheet.
- Detterman, R.L., Plafker, George, Tysdal, R.G., and Hudson, Travis, 1976, Geology and surface features along part of the Talkeetna segment of the Castle Mountain-Caribou fault system, Alaska: U.S. Geological Survey Miscellaneous Field Studies Map MF-738, scale 1:63,360, 1 sheet.
- Eckel, E.B., 1967, Effects of the earthquake of March 27, 1964, on air and water transport, communications, and utilities systems in south-central Alaska: U.S. Geological Survey Professional Paper 545-B, 27 p.
- Ertec Western, 1982, Cone penetrometer testing investigation and analyses, Anchorage, Alaska: Long Beach, Ertec Western, Inc., 10 p.
- Fahnestock, R.K., and Bradley, W.C., 1973, Knik and Matanuska Rivers, Alaska: A contrast in braiding, in Morisawa, Marie, ed., Fluvial geomorphology: Publications in geomorphology, Binghamton, State University of New York, p. 220-250.

- Ferrians, O.J., Jr., 1965, Permafrost map of Alaska: U.S. Geological Survey Miscellaneous Geologic Investigations Map I-445, scale 1:2,500,000, 1 sheet.
- Field, W.O., 1975a, Glaciers of the Chugach Mountains, *in* Field, W.O., ed., Mountain glaciers of the Northern Hemisphere: U.S. Army Cold Regions Research and Engineering Laboratory report, v. 2, p. 299-492.
- _____, 1975b, Glaciers of the Kenai Mountains, Alaska, *in* Field, W.O., ed., Mountain glaciers of the Northern Hemisphere: U.S. Army Cold Regions Research and Engineering Laboratory report, v. 2, p. 493-541.
- Freethy, G.W., and Scully, D.R., 1980, Water resources of the Cook Inlet basin, Alaska: U.S. Geological Survey Hydrologic Investigations Atlas HA-620, scale 1:1,000,000, 4 sheets.
- Fuchs, W.A., 1980, Tertiary tectonic history of the Castle Mountain-Caribou fault system in the Talkeetna Mountains, Alaska: Salt Lake City, University of Utah, Ph.D. thesis, 150 p.
- Grant, U.S., and Higgins, D.F., 1913, Coastal glaciers of Prince William Sound and Kenai Peninsula, Alaska: U.S. Geological Survey Bulletin 526, 75 p.
- Grantz, Arthur, 1966, Strike-slip faults in Alaska: U.S. Geological Survey Open-file Report 66-53, 82 p.
- Hamilton, T.D., Stuckenrath, R., and Stuiver, M., 1980, Itkillik Glaciation in the central Brooks Range: Radiocarbon dates and stratigraphic record [abs.]: Geological Society of America Abstracts with Programs, v. 12, no. 3, p. 109.
- Hansen, W.R., 1965, Effects of the earthquake of March 27, 1964, at Anchorage, Alaska: U.S. Geological Survey Professional Paper 542-A, 68 p.
- Hopkins, D.M., 1975, Time-stratigraphic nomenclature for the Holocene Epoch: *Geology*, v. 3, no. 1, p. 10.
- Hopkins, D.M., Karlstrom, T.N.V., and others, 1955, Permafrost and ground water in Alaska: U.S. Geological Survey Professional Paper 264-F, p. 113-146.
- Johnson, P.R., and Hartman, C.W., 1969, Environmental atlas of Alaska: Fairbanks, University of Alaska Institute of Water Resources, 111 p.
- Kachadoorian, Reuben, Ovenshine, A.T., and Bartsch-Winkler, Susan, 1977, Late Wisconsin history of the south shore of Turnagain Arm, Alaska, *in* Blean, K.M., ed., The United States Geological Survey in Alaska: Accomplishments during 1976: U.S. Geological Survey Circular 751-B, p. B49-B50.
- Karlstrom, T.N.V., 1953, Upper Cook Inlet region, Alaska, *in* Péwé, T.L., and others, Multiple glaciation in Alaska: A progress report: U.S. Geological Survey Circular 289, p. 3-5.
- _____, 1955, Late Pleistocene and Recent glacial chronology of south-central Alaska [abs.]: Geological Society of America Bulletin, v. 66, no. 12, pt. 2, p. 1581-1582.
- _____, 1957, Tentative correlation of Alaskan sequences, 1956: *Science*, v. 125, no. 3237, p. 73-74.
- _____, 1964, Quaternary geology of the Kenai Lowland and glacial history of the Cook Inlet region, Alaska: U.S. Geological Survey Professional Paper 443, 69 p.
- _____, 1965, Upper Cook Inlet area and Matanuska River Valley, *in* Péwé, T.L., Ferrians, O.J., Jr., Nichols, D.R., and Karlstrom, T.N.V., Guidebook for field conference F, central and south-central Alaska, International Association for Quaternary Research, 7th Congress, Fairbanks, 1965: Lincoln, Nebraska Academy of Sciences, p. 114-141 (reprinted 1977, College, Alaska Division of Geological and Geophysical Surveys).

- Karlstrom, T.N.V., 1968, The Quaternary time scale---a current problem of correlation and radiometric dating, *in* Morrison, R.B., and Wright, H.E., Jr., eds., Means of correlation of Quaternary successions: Salt Lake City, University of Utah Press, p. 121-150.
- Kelly, T.E., 1963, Geology and hydrocarbons in Cook Inlet basin, Alaska: American Association of Petroleum Geologists Memoir 2, p. 278-296.
- Krinsley, D.B., 1953, Southwest Kenai Peninsula, Alaska, *in* Pêwé, T.L., and others, Multiple glaciation in Alaska: A progress report: U.S. Geological Survey Circular 289, p. 5-6.
- Kulp, J.L., Feely, H.W., and Tryon, L.E., 1951, Lamont natural radiocarbon measurements I: Science, v. 114, no. 2970, p. 565-568.
- Kulp, J.L., Tryon, L.E., Eckelman, W.R., and Snell, W.A., 1952, Lamont natural radiocarbon measurements II: Science, v. 116, no. 3016, p. 409-414.
- Lee, H.R., 1977, Permafrost in Anchorage: International Symposium on Cold Regions Engineering, 2nd, Fairbanks, 1976, Proceedings, University of Alaska Department of Civil Engineering, p. 283-289.
- MacKevett, E.M., Jr., and Plafker, George, 1974, The Border Ranges fault in south-central Alaska: U.S. Geological Survey Journal of Research, v. 2, no. 3, p. 323-329.
- Magoon, L.B., Adkison, W.L., and Egbert, R.M., 1976, Map showing geology, wildcat wells, Tertiary plant fossil localities, K-Ar age dates, and petroleum operations, Cook Inlet area, Alaska: U.S. Geological Survey Miscellaneous Geologic Investigations Map I-1019, scale 1:250,000, 3 sheets.
- Marsters, Beverly, Spiker, Elliot, and Rubin, Meyer, 1969, U.S. Geological Survey radiocarbon dates X: Radiocarbon, v. 11, no. 1, p. 210-227.
- Martin, G.C., 1926, The Mesozoic stratigraphy of Alaska: U.S. Geological Survey Bulletin 776, 493 p.
- Martin, G.C., and Katz, F.J., 1912, Geology and coal fields of the lower Matanuska Valley, Alaska: U.S. Geological Survey Bulletin 500, 98 p.
- Mayo, L.R., Zenone, Chester, and Trabant, D.C., 1977, Reconnaissance hydrology of Portage Glacier basin, Alaska: U.S. Geological Survey Hydrologic Investigations Atlas HA-583, 2 sheets.
- McCulloch, D.S., and Bonilla, M.G., 1970, Effects of the earthquake of March 27, 1964, on the Alaska Railroad: U.S. Geological Survey Professional Paper 545-D, 161 p.
- Meier, M.F., Tangborn, W.V., Mayo, L.R., and Post, Austin, 1971, Combined ice and water balances of Gulkana and Wolverine Glaciers, Alaska, and South Cascade Glacier, Washington, 1965 and 1966 hydrologic years: U.S. Geological Survey Professional Paper 715-A, 23 p.
- Miller, R.D., and Dobrovolsky, Ernest, 1959, Surficial geology of Anchorage and vicinity, Alaska: U.S. Geological Survey Bulletin 1093, 128 p.
- Mörner, Nils-Axel, 1971, The position of the ocean level during the interstadial at about 30,000 B.P.---A discussion from a climatic-glaciologic point of view: Canadian Journal of Earth Sciences, v. 8, no. 1, p. 132-143.
- Olson, E.A., and Broecker, W.S., 1959, Lamont natural radiocarbon measurements V: American Journal of Science, v. 257, no. 1, p. 1-28.
- Pêwé, T.L., 1975, Quaternary geology of Alaska: U.S. Geological Survey Professional Paper 835, 145 p.
- Pêwé, T.L., and Reger, R.D., 1972, Modern and Wisconsinan snowlines in Alaska: International Geological Congress, 24th, Montreal, 1972, Proceedings, v. 12, p. 187-197.

- Plafker, George, 1969, Tectonics of the March 27, 1964, Alaska earthquake: U.S. Geological Survey Professional Paper 543-I, 174 p.
- Post, Austin, 1975, Preliminary hydrology and historic terminal changes of Columbia Glacier: U.S. Geological Survey Hydrologic Investigations Atlas HA-559, scale 1:10,000, 3 sheets.
- Post, Austin, and Mayo, L.R., 1971, Glacier-dammed lakes and outburst floods in Alaska: U.S. Geological Survey Hydrologic Investigations Atlas HA-455, scale 1:1,000,000, 10 p., 3 sheets.
- Powell, R.D., 1981, A model for sedimentation by tidewater glaciers: *Annals of Glaciology*, v. 2, p. 129-134.
- R and M Consultants, Inc., 1981, Geological and geotechnical investigations, Glenn Highway realignment study, Palmer to Mile 135: Anchorage, 146 p.
- Reger, R.D., 1978, Reconnaissance geology of the new capital site and vicinity, Anchorage Quadrangle, Alaska: Alaska Division of Geological and Geophysical Surveys Open-file Report 113A, scale 1:63,360, 1 sheet.
- _____, 1981a, Geologic and materials maps of the Anchorage (C-8 SE) Quadrangle, Alaska: Alaska Division of Geological and Geophysical Surveys Geologic Report 65, scale 1:25,000, 2 sheets.
- _____, 1981b, Geologic and materials maps of the Anchorage (C-8 SW) Quadrangle, Alaska: Alaska Division of Geological and Geophysical Surveys Geologic Report 68, scale 1:25,000, 2 sheets.
- _____, 1981c, Geologic and materials maps of the Anchorage (B-8 NE) Quadrangle, Alaska: Alaska Division of Geological and Geophysical Surveys Geologic Report 69, scale 1:25,000, 2 sheets.
- _____, 1981d, Geologic and materials maps of the Anchorage (B-8 NW) Quadrangle, Alaska: Alaska Division of Geological and Geophysical Surveys Geologic Report 70, scale 1:25,000, 2 sheets.
- Rieger, Samuel, and Juve, R.L., 1961, Soil development in recent loess in the Matanuska Valley, Alaska: *Soil Science Society of America Proceedings*, v. 25, no. 3, p. 243-248.
- Rieger, Samuel, Schoephorster, D.B., and Furbush, C.E., 1979, Exploratory soil survey of Alaska: U.S. Department of Agriculture Soil Conservation Service report, 213 p.
- Rubin, Meyer, and Alexander, Corrine, 1958, U.S. Geological Survey radiocarbon dates IV: *Science*, v. 127, no. 3313, p. 1476-1487.
- _____, 1960, U.S. Geological Survey radiocarbon dates V: *American Journal of Science Radiocarbon Supplement*, v. 2, p. 129-185.
- Rubin, Meyer, and Suess, H.E., 1955, U.S. Geological Survey radiocarbon dates II: *Science*, v. 121, no. 3145, p. 481-488.
- Schmidt, R.A.M., 1961, Recession of Portage Glacier, Alaska, in *Short papers in the geologic and hydrologic sciences 1961*: U.S. Geological Survey Professional Paper 424-D, p. D202-D203.
- Schmoll, H.R., and Dobrovolny, Ernest, 1972, Generalized geologic map of Anchorage and vicinity, Alaska: U.S. Geological Survey Miscellaneous Geologic Investigations Map I-787A, scale 1:24,000, 1 sheet.
- Schmoll, H.R., Dobrovolny, Ernest, and Gardner, C.A., 1980, Preliminary geologic map of the middle part of the Eagle River valley, Municipality of Anchorage, Alaska: U.S. Geological Survey Open-file Report 80-890, scale 1:25,000, 1 sheet.
- _____, 1981, Preliminary geologic map of Fire Island, Municipality of Anchorage, Alaska: U.S. Geological Survey Open-file Report 81-552, 4 p., scale 1:25,000, 1 sheet.

- Schmoll, H.R., and Gardner, C.D., 1982, Diamicton of subglacial or subaqueous origin, Fire Island, Anchorage, Alaska [abs.]: International Union for Quaternary Research Congress, 11th, Moscow, 1982, Proceedings, v. 1, p. 282.
- Schmoll, H.R., Szabo, B.J., Rubin, Meyer, and Dobrovolsky, Ernest, 1972, Radiometric dating of marine shells from the Bootlegger Cove Clay, Anchorage area, Alaska: Geological Society of America Bulletin, v. 83, no. 4, p. 1107-1114.
- Schmoll, H.R., and Yehle, L.A., 1978, Generalized physiography and geology of the Beluga coal field and vicinity, south-central Alaska, in Johnson, K.M., ed., The United States Geological Survey in Alaska: Accomplishments during 1977: U.S. Geological Survey Circular 772-B, p. B73-B76.
- _____, 1983, Glaciation in upper Cook Inlet: A preliminary reexamination based on geologic mapping in progress [abs.]: Workshop on Glaciation in Alaska, Chena Hot Springs, March 18-19, 6 p.
- Schoephorster, D.B., 1968, Soil survey of Matanuska Valley area, Alaska: U.S. Department of Agriculture Soil Conservation Service report, 67 p.
- Schoephorster, D.B., and Hinton, R.B., 1973, Soil survey of Susitna Valley area, Alaska: U.S. Department of Agriculture Soil Conservation Service report, 71 p.
- Scott, K.M., 1982, Erosion and sedimentation in the Kenai River, Alaska: U.S. Geological Survey Professional Paper 1235, 35 p.
- Shackleton, N.J., and Opdyke, N.D., 1973, Oxygen isotope and paleomagnetic stratigraphy of equatorial Pacific core V28-238: Oxygen isotope temperatures and ice volumes on a 10^5 year and 10^6 year scale: Quaternary Research, v. 3, no. 1, p. 39-55.
- Shannon and Wilson, Inc., 1964, Report on Anchorage area soil studies, Alaska: Seattle, 109 p.
- Spiker, Elliott, Kelley, Lea, Oman, Charles, and Rubin, Meyer, 1977, U.S. Geological Survey radiocarbon dates XII: Radiocarbon, v. 19, no. 2, p. 332-353.
- Stone, K.H., 1963, The annual emptying of Lake George, Alaska: Arctic, v. 16, no. 1, p. 26-40.
- Stump, R.W., Handy, R.L., Davidson, D.T., Roy, C.J., and Thomas, L.A., 1959, Silt deposits in the Matanuska Valley, in Davidson, D.T., Roy, C.J., and others, The geology and engineering characteristics of some Alaskan soils: Ames, The Iowa State University Bulletin, v. 57, no. 29, p. 3-32.
- Suess, H.E., 1954, U.S. Geological Survey radiocarbon dates I: Science, v. 120, no. 3117, p. 467-473.
- Sullivan, B.M., Spiker, Elliott, and Rubin, Meyer, 1970, U.S. Geological Survey radiocarbon dates XI: Radiocarbon, v. 12, no. 1, p. 319-334.
- Tarr, R.S., and Martin, Lawrence, 1914, Alaskan glacier studies of the National Geographic Society in the Yakutat Bay, Prince William Sound, and lower Copper River regions: Washington, National Geographic Society, 498 p.
- Ten Brink, N.W., and Ritter, D.F., 1980, Glacial chronology of the north-central Alaska Range and implications for discovery of early-man sites [abs.]: Geological Society of America Abstracts with Programs, v. 12, no. 7, p. 534.
- Ten Brink, N.W., and Waythomas, C.F., 1982, Late Wisconsin glacial chronology of the north-central Alaska Range---A regional synthesis and its implications for early human settlements: National Geographic Society and National Park Service unpublished report.

- Thorson, R.M., Dixon, E.J., Jr., Smith, G.S., and Batten, A.R., 1981, Interstadial proboscidean from south-central Alaska: Implications for biogeography, geology, and archaeology: *Quaternary Research*, v. 16, no. 3, p. 404-417.
- Trainer, F.W., 1960, Geology and ground-water resources of the Matanuska Valley agricultural area, Alaska: U.S. Geological Survey Water Supply Paper 1494, 116 p.
- _____, 1961, Eolian deposits of the Matanuska Valley agricultural area, Alaska: U.S. Geological Survey Bulletin 1121-C, 35 p.
- Trainer, F.W., and Waller, R.M., 1965, Subsurface stratigraphy of glacial drift at Anchorage, Alaska, *in* Geological Survey Research 1965: U.S. Geological Survey Professional Paper 525-D, p. D167-D174.
- Tuck, Ralph, 1938, The loess of the Matanuska Valley, Alaska: *Journal of Geology*, v. 46, p. 647-653.
- Ulery, C.A., and Updike, R.G., 1983, Subsurface structure of the Bootlegger Cove Formation, southwest Anchorage, Alaska: Alaska Division of Geological and Geophysical Surveys Professional Report, 2 sheets [in press].
- U.S. Army, Alaska District Corps of Engineers, 1979, Anchorage area soil survey: Metropolitan Anchorage urban study, v. 7, 124 p.
- U.S. Geological Survey, 1969, The breakout of Lake George: U.S. Geological Survey pamphlet, 15 p.
- Updike, R.G., 1982, Engineering-geologic facies of the Bootlegger Cove Formation, Anchorage, Alaska [abs.]: *Geological Society of America Abstracts with Programs*, v. 14, no. 7, p. 636.
- _____, 1983, Engineering geologic maps, Government Hill area, Alaska: U.S. Geological Survey Miscellaneous Geologic Investigations Map [in press].
- Updike, R.G., and Carpenter, B.A., 1983, Engineering geology of the Government Hill area, Anchorage, Alaska: U.S. Geological Survey Bulletin [in press].
- Updike, R.G., Cole, D.A., and Ulery, Cathy, 1982, Shear moduli and dampening ratios for the Bootlegger Cove Formation as determined by resonant-column testing, *in* Short notes on Alaskan geology 1981: Alaska Division of Geological and Geophysical Surveys Geologic Report 73, p. 7-12.
- Updike, R.G., and Ulery, C.A., 1983a, Engineering geology of southwest Anchorage: Alaska Division of Geological and Geophysical Surveys Professional Report [in press].
- _____, 1983b, Geology of the Anchorage (B-6 NW) Quadrangle, Alaska: Alaska Division of Geological and Geophysical Surveys Report of Investigations 83-8, scale 1:10,000, 2 sheets.
- Varnes, D.J., 1969, Stability of the west slope of Government Hill, port area of Anchorage, Alaska: U.S. Geological Survey Bulletin 1258-D, 61 p.
- Viereck, L.A., 1967, Botanical dating of recent glacial activity in western North America, *in* Wright, H.E., Jr., and Osburn, W.H., eds., *Arctic and alpine environments*: Bloomington, Indiana University Press, p. 189-204.
- Viereck, L.A., and Little, E.L., Jr., 1972, Alaska trees and shrubs: U.S. Forest Service Agriculture Handbook 410, 265 p.
- Wahrhaftig, Clyde, 1965, Physiographic divisions of Alaska: U.S. Geological Survey Professional Paper 482, 52 p.
- Warfield, R.S., 1962, Bituminous coal deposits of the Matanuska coal field, Alaska: Central and western parts, Wishbone Hill district: U.S. Bureau of Mines Report of Investigations 5950, 190 p.

- Watson, C.E., 1959, Climate of Alaska, in Climate of the states: Washington, D.C., U.S. Weather Bureau Climatography of the United States 60-49, 24 p.
- Welsch, Dennis, Goodwin, Robert, and Ten Brink, Norman, 1982, Late Quaternary glaciations of the Talkeetna Mountains, Alaska [abs.]: Geological Society of America Abstracts with Programs, v. 14, no. 6, p. 353-354.
- Wilcox, R.E., 1976, Mount Spurr, in Henning, R.A., Rosenthal, C.H., Olds, Barbara, and Reading, Ed, eds., Alaska's volcanoes---Northern link in the ring of fire: Alaska Geographic, v. 4, no. 1, p. 59-65.
- Williams, J.R., and Ferrians, O.J., Jr., 1961, Late Wisconsin and Recent history of the Matanuska Glacier, Alaska: Arctic, v. 14, no. 2, p. 82-90.

APPENDIX A

Radiocarbon Dates Related to Late Quaternary Events
in the Upper Cook Inlet Region, Alaska

Sample ^a locality	Sample number	Material and stratigraphic context	Chronological significance	Radiocarbon age (¹⁴ C yr B.P.)	Reference
A	W-2152	Peat from lower part of 4-ft-thick (1.2 m) sand underlain by 4 ft (1.2 m) of gravel and 42 ft (12.7 m) of interbedded sand and till, all of Naptowne age.	Provides distant minimum date for recession of Naptowne-age glacier near Potter (Potter Hill railroad cut).	7,890 ± 250	Sullivan and others, 1970, p. 332.
See references	W-431	Peat from basal 1 in. (2.5 cm) of 4-ft-thick (1.2 m) bed overlying 2.5 ft (0.8 m) of fossiliferous pond silt on top of late Naptowne or early Holocene till.	Provides minimum date for latest Naptowne or early Holocene readvance of Macanuka Glacier 2.5 to 5 mi (4 to 8 km) beyond present terminus.	8,000 ± 300	Rubin and Alexander, 1958, p. 1481; Williams and Ferrigno, 1961, fig. 1; Karlstrom, 1964, pl. 1, loc. V.
B	W-2306	Peat overlying glacio-deltaic deposits that probably correlate with similar deposits interfingering with Bootlegger Cove Formation near Point Woronzof.	Provides minimum date for glacio-deltaic deposits on Fire Island.	8,290 ± 250	Schnoll and others, 1981, loc. 3.
See references	L-163B	Wood and organic silt from near base of lower, 4-ft-thick (1.2 m) peat unconformably overlying sequence of thinly laminated silt and clay with some sand and gravel; this sequence is deformed by advance of Naptowne glacier from west.	Provides minimum date for eastward expansion of Naptowne-age glacier from Alaska Peninsula across Cook Inlet to Boulder Point.	8,650 ± 450	Gleason and Broecker, 1959, p. 6; Karlstrom, 1964, pls. 4 and 6, loc. B-1.
C	GK-5019	Silty peat with scattered wood fragments at base of 2.9-ft-thick (0.9 m) silty peat layer underlying 4-ft-thick (1.2 m) silty alluvial-fan sand and overlying gravelly sand deposited in ice-marginal channel.	Provides minimum date for lowering of Naptowne glacier damming mouth of Little Susitna River canyon.	9,155 ± 215	Unpublished ¹⁴ C date.
D	L-163D	Organic silt underlying 30 ft (9.1 m) of post-Naptowne eolian sand and silt and overlying weathered loess capping till weathered to depths of 3 to 5 ft (0.9 to 1.5 m).	Dates first development of cliffhead dunes on Knik moraine and approach of bluff close to present position. Distant minimum age for Knik-age glaciation of Turnagain Arm as far as Point Possession.	9,200 ± 600	Broecker and others, 1956, p. 156; Karlstrom, 1964.
E	W-536	Peat from base of 5-ft-thick (1.5 m) bed overlying pond deposits on top of diamicton thought to overlie and interfinger with extensive deltaic deposits that interfinger with the Bootlegger Cove Formation.	Provides minimum date for till and deltaic deposits on Fire Island at mouth of Turnagain Arm.	9,300 ± 250	Miller and Dobrovolsky, 1959, p. 32; Rubin and Alexander, 1960, p. 165; Karlstrom, 1964, pl. 6, loc. C-2.
F	L-137C	Compressed and deformed peat beneath 15 ft (4.6 m) of post-Naptowne eolian sand and silt and overlying organic silt (loess) capping diamicton.	Provides close maximum age for beginning of cliffhead-dune formation on Knik moraine and approach of cliff to present position. Distant minimum age for Knik Glaciation in Turnagain Arm.	9,500 ± 650	Broecker and others, 1956, p. 156; Karlstrom, 1964, pls. 4 and 6, loc. D-3.
G	W-336	Twigs and wood fragments from base of 7- to 8-ft-thick (2.1- to 2.4 m) bog filling of kettle in most extensive terminal moraine of Naptowne age.	Provides minimum date for most extensive Naptowne advance in Willow Creek valley.	9,870 ± 250	Rubin and Alexander, 1958, p. 1483.
H	W-474	Organic silt from near base of bog deposit buried beneath eolian sand and overlying diamicton.	Provides close maximum age for beginning of cliff-head dune formation on Knik moraine and approach of cliff to present position. Distant minimum age for Knik Glaciation in Turnagain Arm.	10,370 ± 350	Rubin and Alexander, 1958, p. 1479; Karlstrom, 1964, pls. 4 and 6, loc. D-1.

^aSee plate 1 for locations of sample localities in the upper Cook Inlet region.

Sample ^a Locality	Sample number	Material and stratigraphic context	Chronological significance	Radiocarbon age (¹⁴ C yr B.P.)	Reference
I	GX-604)	Organic silt from 0.3 to 0.5 ft (0.1 to 0.2 m) below top of 3.3-ft-thick (1 m) silty and sandy peat that underlies a 2.1-ft-thick (0.6 m) woody <i>Sphagnum</i> peat and overlies a 1.3-ft-thick (0.4 m) layer of organic silt on top of sandy gravel at base of scarp cut during latest Naptowne marine transgression of lower Susitna River valley.	Provides minimum age for regression of marine waters in which Bootlegger Cove Formation was deposited in lower Susitna River valley.	10,720 ± 460	Unpublished ¹⁴ C date.
J	W-540	Peat from base of 8-ft-thick (2.4 m) bed overlying 10 ft (3 m) of sand that overlies 6 to 10 ft (1.8 to 3 m) of Bootlegger Cove Formation.	Provides minimum age for regression of marine waters in which Bootlegger Cove Formation was deposited in Anchorage area.	11,600 ± 300	Rubin and Alexander, 1960, p. 165; Miller and Dobrovolsky, 1959, p. 68 and pl. 9; Schmoll and others, 1972, loc. 8.
K	W-2375	Peat from beneath colluvium overlying till of the Elmendorf Moraine of late Naptowne age.	Postdates Bootlegger Cove Formation and provides close minimum date for Elmendorf Moraine in vicinity of Anchorage.	11,690 ± 300	Schmoll and others, 1972, loc. F; Spiker and others, 1977, p. 346.
L	W-360	Organic pond silt from base of box on Knik-age lateral moraine.	Provides minimum date for Knik (late early Naptowne) Glaciation in area of proposed capital site.	11,930 ± 250	Rubin and Alexander, 1958, p. 1483; Karlstrom, 1964, pl. 1, loc. T.
See references	W-416	Peat from base of 3- to 5-ft-thick (0.9 to 1.5 m) section of organic-rich lacustrine clay, silt, and sand folded during late Naptowne (Skilak) advance.	Close maximum date for late Naptowne (Skilak) glacier advance in East Foreland area.	12,900 ± 300	Rubin and Alexander, 1958, p. 1479; Karlstrom, 1964, pls. 4 and 6, loc. P-2.
M	W-2151	Mollusk shells from macrofossil-rich zone of Bootlegger Cove Formation.	Dates possible middle or upper sublittoral environment of late-Naptowne-age marine transgression in Anchorage area.	13,690 ± 400	Sullivan and others, 1970, p. 333; Schmoll and others, 1972, loc. A.
K	W-2389	Mollusk shells from macrofossil-rich zone of Bootlegger Cove Formation.	Dates possible middle or upper sublittoral environment of late-Naptowne-age marine transgression in Anchorage area.	13,750 ± 500	Schmoll and others, 1972, loc. D; Spiker and others, 1977, p. 346.
N	W-2367	Mollusk shells from macrofossil-rich zone of Bootlegger Cove Formation.	Dates possible middle or upper sublittoral environment of late-Naptowne-age marine transgression in Anchorage area.	14,300 ± 350	Schmoll and others, 1972, loc. C; Spiker and others, 1977, p. 346.
N	W-2369	Mollusk shells from macrofossil-rich zone of Bootlegger Cove Formation.	Dates possible middle or upper sublittoral environment of late-Naptowne-age marine transgression in Anchorage area.	14,900 ± 350	Schmoll and others, 1972, loc. E; Spiker and others, 1977, p. 346.
O	W-1804	Wood from organic zone overlain by silt, gravel, sand, and till of Naptowne age.	Provides maximum date for latest Naptowne advance out of Turnagain Arm and dates inter-Naptowne nonglacial interval in Potter area.	34,000 ± 2,000	Marsters and others, 1969, p. 220.
See references	L-163A	Residual after removal of humic acid from iron-oxide-stained, lignitized log in glaciofluvial-glaciolacustrine silt, sand, and gravel traceable northward to and beneath Naptowne-age till at East Foreland.	Dates advancing phase of early Naptowne glacier expansion from Alaska Peninsula eastward across Cook Inlet to East Foreland.	39,000 ± 2,600 (39,000 ± 2,000 on humic acid fraction)	Olson and Broecker, 1959, p. 5-6; Karlstrom, 1964, pls. 4 and 6, loc. 5.
P	W-1806	Wood fragments in silt overlain by gravel presumably of Naptowne age and underlain by oxidized sand of Knik(?) age.	Provides maximum date for overlying Naptowne-age outwash deposits in Eagle River area.	38,000±	Marsters and others, 1969, p. 221.
Q	W-335 ^b	Very thin peat from beneath Naptowne-age till and outwash and overlying gravel that may be pre-Naptowne in age.	Provides maximum date for Naptowne Glaciation in Eagle River area.	38,000±	Rubin and Alexander, 1960, p. 164-165; Miller and Dobrovolsky, 1959, p. 16 and pl. 9.
R	W-644	Wood from base of advance outwash of Naptowne age overlain by Naptowne-age till and overlying compressed and lignitized peat layer that overlies Knik-age till.	Provides minimum date for nonglacial interval between Naptowne and Knik Glaciations in Goose Bay area.	40,000±	Rubin and Alexander, 1960, p. 169; Karlstrom, 1964, pl. 6, loc. 1.

^aSee plate 1 for locations of sample localities in the upper Cook Inlet region.

^bReanalysis of sample L-101B dated by solid-carbon method at 14,300 ± 600 yr B.P., (Kuip and others, 1951, p. 568).

Sample ^a locality	Sample number	Material and stratigraphic context	Chronological significance	Radjoocarbon age (¹⁴ C yr B.P.)	Reference
S	W-2366	Organic fragments in 2-in.-thick (5 cm) brown sand underlying Bootlegger Cove Formation.	Provides maximum date for Bootlegger Cove Formation in Point MacKenzie area.	40,000+	Spiker and others, 1977, p. 346.
R	I-11,949	Wood from upper 4 in. (10 cm) of 3- to 6-ft-thick (0.9 to 1.8 m), highly compressed and partially lignitized peat overlying 10 ft (3 m) of outwash(?) gravel of late Knik age and underlying 15 to 28 ft (4.6 to 8.5 m) of advance outwash sand and gravel that in turn underlie 20 to 25 ft (6.1 to 7.6 m) of till of latest Naptowne (Elmendorf) advance.	Provides maximum date for Naptowne Glaciation and minimum date for Knik Glaciation in Goose Bay area.	40,000+	Unpublished ¹⁴ C date.
R	I-11,950	Compressed peat from center of 3- to 6-ft-thick (0.9 to 1.8 m) bed lying on 10 ft (3 m) of outwash (?) gravel of late Knik age and underlying 15 to 28 ft (4.6 to 8.5 m) of advance outwash sand and gravel that in turn underlie 20 to 25 ft (6.1 to 7.6 m) of till of latest Naptowne (Elmendorf) advance.	Provides maximum date for Naptowne Glaciation and minimum date for Knik Glaciation in Goose Bay area.	40,000+	Unpublished ¹⁴ C date.
See references	L-1171	Abraded, lignitized log from lowest 1 ft (0.3 m) of post-Naptowne organic lake silt that unconformably overlies Knik-age gravel deformed by Naptowne-age advance.	Probably reworked from Knik-age gravel and dates Knik Glaciation in East Foreland area.	44,000+	Olson and Broecker, 1959, p. 5; Karlstrom, 1964, pls. 4 and 6, loc. 4.
T	W-2154	Peat overlain by 9 ft (2.7 m) of Naptowne-age fluvial gravel and overlying 2 ft (0.6 m) of gray silty clay till(?) of Knik(?) age.	Provides maximum date for Naptowne Glaciation and minimum date for Knik(?) Glaciation in vicinity of Chugink.	45,000+	Sullivan and others, 1970, p. 328.

^aSee plate 1 for locations of sample localities in the upper Cook Inlet region.